The University of Nottingham

# Riboregulation in *Pseudomonas aeruginosa*

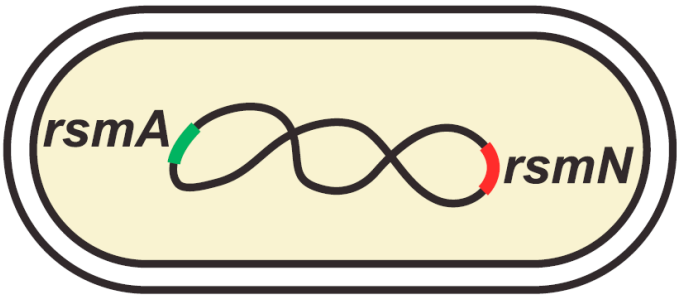


Hazel Silistre

BSc

Thesis submitted to the University of Nottingham
for the degree of Doctor of Philosophy

July 2016

## Declaration

Unless otherwise acknowledged, the work presented in this thesis is my own. No part has been submitted for another degree at the University of Nottingham or any other educational institution.

Hazel Silistre



# Abstract

The opportunistic human pathogen *Pseudomonas aeruginosa* controls virulence, production of secondary metabolites, motility, biofilm formation, growth in anaerobic conditions, intracellular and intercellular signalling and the switch from an acute to a chronic mode of infection at the transcriptional and post-transcriptional levels by modulation of the Gac/Rsm system. Cell density-dependent signal accumulation and environmental stimulators such as pH changes and ion limitation activate the GacS/GacA two-component system which in turn triggers transcription of the small regulatory RNAs RsmY and RsmZ. These sRNAs sequester multiple copies of the RNA-binding protein RsmA, antagonising its function. The RsmA/CsrA proteins act as translational repressors by binding to the GGA-motifs in the untranslated region of target mRNAs and blocking ribosome binding. In this study, the biological function of RsmN, an RsmA homologue with a conserved RNA-binding pocket but a distinct protein folding, the predicted autoregulatory mechanism of RsmN, the nature of target transcripts of RsmN, and the cross-regulation between the two Rsm proteins were investigated.

The positive control of proteolytic and elastinolytic activities and swarming motility by RsmN has been demonstrated using single and inducible double deletion mutants of *rsmN*. Furthermore, *rsmN* deletion increased microcolony formation during biofilm formation. Regulation by RsmN was most apparent in the absence of RsmA, when *rsmN* expression was induced via a multicopy plasmid and at temperatures lower than 37°C. The double deletion of *rsmA* and *rsmN* affected growth, diminished proteolytic and elastinolytic activities, triggered autolysis and led to the increased secretion of the type VI secretion system protein Hcp1. Moreover, the double deletion of *rsmA* and *rsmN* altered the colony morphology of *P. aeruginosa*. Mutagenesis of the functionally critical, conserved RNA-binding residue which is identified as $Arg_{44}$ in RsmA and $Arg_{62}$ in RsmN resulted in the loss of RsmN function.

In a genome-wide analysis by RNASeq, target transcripts were co-purified with RsmN from 37°C and 34°C cultures of a wild-type strain expressing *rsmN* in multicopy numbers. RNASeq results indicated that small regulatory RNAs such as CrcZ, RsmY

and RgsA are common targets of RsmN and RsmA, whereas PhrS is a target of RsmN only. Other common RsmA and RsmN targets included transcriptional regulators, heat shock proteins, proteases, starvation response proteins, components of the denitrification pathway, outer membrane proteins required for pore formation, type III and type VI secretion system proteins and RsmA. Transcripts of heat shock proteins, the *tss* operon genes and *rsmA* were enriched by RsmN at 37°C but not at 34°C whereas the *lasB* transcript was enriched by RsmN at 34°C but not at 37°C.

Based on the list of common targets of RsmA and RsmN and the results obtained from phenotypic assays, induction of the lytic *Pf4* prophage, accumulation of alkyl quinolone or c-di-GMP signalling molecules, imbalanced redox state, carbon starvation, increased membrane permeability, and aggregation of misfolded proteins are suggested as possible mechanisms triggering the excessive autolysis of the $rsmN_{ind}$ Δ*rsmA* mutant under uninducing conditions.

The data gathered so far suggests that *rsmN* is differentially expressed, with increased RsmN activity at temperatures below 37°C in comparison with RsmA, and, RsmA and RsmN collectively contribute to the regulation of secondary metabolite production, motility and microcolony formation in *P. aeruginosa*.

## Publications

Some results presented in this thesis appeared in the following publication:

**Structural Rearrangement in an RsmA/CsrA Ortholog of *Pseudomonas aeruginosa* Creates a Dimeric RNA-binding Protein, RsmN.** Morris, E. R., Hall, G., Li, C., Heeb, S., Kulkarni, R. V., Lovelock, L., Silistre, H., Messina, M., Camara, M., Emsley, J., Williams, P., and Searle, M. S. (2013) *Structure* **21**, 1659-1671.

## Acknowledgements

I should start the list of "thank you"s with Prof. Kendra Rumbaugh who accepted me to her laboratory in Lubbock, Texas as an intern five years ago. I got fascinated by *Pseudomonas aeruginosa* biofilms in her lab and wanted to continue examining this versatile multidrug-resistant bacterium. I would like to express my gratitude to Prof. Paul Williams for replying to my emails personally and guiding me through the application steps for a PhD. I am grateful that I was lucky enough to get a scholarship from the University of Nottingham to cover my tuition fees and a stipend from the former School of Medical Sciences, current School of Life Sciences for my living costs.

I would like to thank all my supervisors; Prof. Paul Williams, Prof. Miguel Cámara, Dr. Stephan Heeb and Dr. Manuel Romero for their support and excitement in my supervision meetings. I especially thank my postdoc Manuel who joined me to work on this long project, the story of which has started during Marco Messina's PhD, continued with Laura Lovelock's and ended up in my hands. Without Manuel's expertise in molecular cloning, this project would have progressed much slower.

I would like to thank everyone in my group for helping me with a method I was new to, sharing protocols with me, giving me a hand when I needed to fix clamps on a shaker or when I struggled to remove the stuck lid from the C0650 centrifuge rotor. I thank Eric who taught me how to perform swarming assays which I ended up loving. I thank Monica for all the cloning suggestions, Matt and Steven for their guidance on how to use the Bioflux to get good biofilms, and Mahmoud for telling me all the details I needed to know to get done with protein work in one go. I thank Josie for sharing her Bunsen burner with me and not even complaining once (also for convincing me to believe that pyocyanin assay is not so bad!). I thank Matt, Robyn, and Daniella for proofreading my reports. I also thank Robyn, Josie and Eliza for always encouraging me not to quit.

I send a huge hug to Ivan, Katrin, Alina, Daniella, Osman, Paolo, Christine and Alexey who have been a great support during tough times. On another note, I thank Margarida,

Jeena, Murhaf and Anne, my friends from the UoN volleyball club for the great moments we shared. I send my gratitude to all of the lovely ladies; Emma, Vivialyn, Winnie, Catherine, Amanda, Natalie, Marina and Sonia who made me feel so loved and appreciated in my A Cappella group that I decided to stay in the U.K. during my thesis-writing period. I am very happy that during the final year of my PhD, I managed to find a very nice landlord, Alan, and adorable flatmates, Clarice, Vitor, Sophia, Miguel and Salvatore, who made the last year of my stay in Nottingham the best. I thank them all for making my stay at 102 Abbey Road such a pleasant one (and never telling me to shut up when I was singing out loud in my room!).

I would like to acknowledge Sunir and Victoria from the DeepSeq facility for their support in sample preparation for RNASeq and Dr. Chan Kok Gan at the University of Malaya for carrying out the sequencing for our RNASeq experiments. I would also like to acknowledge the Protein Nucleic Acid Chemistry Laboratory at the University of Leicester where protein identification was carried out and Prof. Kendra Rumbaugh at Texas Tech University Health Sciences Centre for testing my strains in a chronic infection model of *P. aeruginosa*.

I dedicate this thesis to my Mom and Dad who let me follow my dreams since high school even though it meant leaving them at the age of 14. I am extremely grateful for their unconditional love, support and sacrifices. My strength is the outcome of their love and dedication for my well-being.

*Bu tezi liseden beri hayallerimin pesinden gitmem icin ellerinden ne geliyorsa yapan anne ve babama adiyorum, sizi cok seviyorum.*

# Table of Contents

**DECLARATION** I

**ABSTRACT** II

**PUBLICATIONS** IV

**ACKNOWLEDGEMENTS** V

**LIST OF FIGURES** X

**LIST OF TABLES** XVI

**ABBREVIATIONS & SYMBOLS** XVII

**1 INTRODUCTION** 1

**1.1 Bacterial gene regulation at the post-transcriptional level** 2
1.1.1 Small regulatory RNAs 2
1.1.2 Riboswitches 6
1.1.2.1 Thermosensors 6
1.1.3 RNA-binding proteins 7
1.1.3.1 CsrA 8
1.1.3.2 Hfq 10
1.1.3.3 Crc 11

**1.2 Two-component systems in bacteria** 13
1.2.1 *Escherichia coli* BarA/UvrY 14
1.2.2 *Pseudomonas aeruginosa* CbrA/CbrB 15
1.2.3 *Pseudomonas fluorescens* GacS/GacA 17

**1.3 Regulatory systems of *Pseudomonas aeruginosa*** 18
1.3.1 Adaptation mechanisms that facilitate the versatility of *P. aeruginosa* 19
1.3.2 Virulence determinants of *P. aeruginosa* 22
1.3.3 Secretion of *P. aeruginosa* virulence determinants 23
1.3.4 Regulation of *P. aeruginosa* virulence 25
1.3.4.1 QS circuitry 25
1.3.4.2 The Gac/Rsm system of P. aeruginosa 30
1.3.5 Discovery of RsmN in *P. aeruginosa* 32
1.3.5.1 Sequence and structure comparisons of RsmN and RsmA 33

**1.4 Project Overview** 35

**2 MATERIALS AND METHODS 36**

**2.1 Bacterial strains, plasmids, oligonucleotides and growth conditions 36**

**2.2 Antibiotics and inducers 43**

**2.3 Plasmid and strain construction 44**
2.3.1 Construction of PALT16, PALT13 and PAMR1 strains 44
2.3.2 Construction of pHS2, a multicopy *rsmN* expression plasmid 44
2.3.3 Arginine to alanine substitution in pHS2 to get pHS2R62A 46
2.3.4 Construction of pHS4 and pHS5 (no antisense ideal RsmN: NasIrsmN) 46

**2.4 Protocols 50**
2.4.1 Preparation of the electrocompetent cells 50
2.4.2 Transformation of the electrocompetent/$CaCl_2$-competent cells 51
2.4.3 Molecular cloning procedures 51
2.4.3.1 Plasmid DNA purification 51
2.4.3.2 Ligation 52
2.4.3.3 Polymerase chain reaction (PCR) amplification 52
2.4.4 Blue/white selection 53
2.4.5 DNA sequencing 53
2.4.6 Quantification of DNA, RNA and protein concentrations 53
2.4.7 Complementation of the Δ*rsmA*, Δ*csrA*, $rsmA_{ind}$ Δ*rsmN* and $rsmN_{ind}$ Δ*rsmA* phenotypes by *rsmN* expression 54
2.4.7.1 Motility assays 54
2.4.7.2 Kornberg assay 55
2.4.7.3 Pyocyanin assay 55
2.4.7.4 Protease assays 56
2.4.7.4.1 Total protease assay 56
2.4.7.4.2 Elastase assay 56
2.4.7.5 Biofilm assays 57
2.4.7.5.1 Bioflux 57
2.4.7.5.2 Colony biofilms 57
2.4.7.5.3 Imaging of biofilms 58
2.4.7.6 Phage plaque assay 58
2.4.8 Protein Methods 59
2.4.8.1 Trichloroacetic acid (TCAa) precipitation 59
2.4.8.2 SDS-polyacrylamide gel electrophoresis (SDS-PAGE) 59
2.4.8.3 Coomassie blue staining 60
2.4.8.4 Western blotting 60
2.4.8.5 Protein purification 61
2.4.9 RNA work 62
2.4.9.1 Total RNA extraction 62
2.4.9.2 Purification of RNAs that are bound to the $His_6$-tagged RsmN 63
2.4.9.3 DNase treatment 63
2.4.10 RNA sequencing (RNAseq) 63
2.4.10.1 Analysis of the RNASeq results 64

**2.5 Chronic infection mouse model 65**

**3 THE BIOLOGICAL ROLE OF RSMN 66**

**3.1 Introduction 66**

**3.2 Results 70**
3.2.1 The influence of RsmA and RsmN on the growth of *P. aeruginosa* at 37°C and 34°C 70
3.2.2 The *P. aeruginosa* Δ*rsmA* mutant but not the Δ*rsmN* mutant clumps 72
3.2.3 Regulation of motility by RsmA and RsmN 73
3.2.3.1 Swarming motilities of the single and inducible Δ*rsmA* and Δ*rsmN* double deletion mutants 74
3.2.3.2 Swimming motilities of the single and inducible Δ*rsmA* and Δ*rsmN* double deletion mutants 79
3.2.3.3 Twitching motilities of the single and inducible Δ*rsmA* and Δ*rsmN* double deletion mutants 81
3.2.4 Regulation of pyocyanin production by RsmA and RsmN 82
3.2.5 The impact of RsmA and RsmN on total proteolytic and elastinolytic activities 86
3.2.6 The influence of *rsmA* and *rsmN* deletions on biofilm formation 90
3.2.7 Colony morphologies of the single and double Δ*rsmA* and Δ*rsmN* deletion mutants 94
3.2.8 *P. aeruginosa* undergoes autolysis in the absence of both RsmA and RsmN 97
3.2.9 Repression of glycogen accumulation in *E. coli* TR1-5 cells by RsmA but not RsmN 107
3.2.10 The contribution of RsmA and RsmN to virulence in a mouse chronic infection model 108
3.2.11 The contribution of expression from the $P_{rsmN}$, $P_{rsmF}$ and $P_{nmsR}$ promoters on the regulation of swarming motility and production of secondary metabolites 109

**3.3 Discussion 122**

**4 GENOME-WIDE IDENTIFICATION OF RSMN TARGETS 131**

**4.1 Introduction 131**

**4.2 Results 134**
4.2.1 Raw data analysis 136
4.2.1.1 Ribosomal RNA read removal 137
4.2.2 RsmN-only targets and targets in common with RsmA 140
4.2.3 RsmA and RsmN both regulate CrcZ 145
4.2.4 The double deletion of *rsmA* and *rsmN* might lead to carbon starvation 146
4.2.5 RsmN-RNA interaction at 34°C 150

**4.3 Discussion 152**

**5 GENERAL CONCLUSIONS AND FUTURE DIRECTIONS 163**

**SUPPLEMENTARY FIGURES 169**

**REFERENCES 177**

## List of Figures

Figure 1.1 Possible sRNA base-pairing regions on target transcripts.....3

Figure 1.2 Amino acid sequence alignments of the CsrA/RsmA proteins.....10

Figure 1.3 Sequestration of the Crc proteins by CrcZ in the high abundance of less-preferred carbon sources.....13

Figure 1.4 Modulation of the histidine and arginine degradation pathways by the CbrA/CbrB TCS.....17

Figure 1.5 The AHL-dependent and AQ-dependent QS systems of *P. aeruginosa* are interconnected and intertwined with transcriptional and post-transcriptional regulators.....29

Figure 1.6 The Gac/Rsm system of *P. aeruginosa*.....31

Figure 1.7 The context of the genomic bank fragments inserted in the four clones that restored the Δ*rsmA* swarming motility.....33

Figure 1.8 X-ray crystallography structures of the RsmA (left) and RsmN (right) proteins (above) and topology maps of the β-strands and α-helices (below).....34

Figure 1.9 Structure-based amino acid sequence alignments of *P. aeruginosa* RsmA and RsmN proteins.....35

Figure 2.1 Diagrammatic representation (in the reverse orientation) of the (a) smallest genomic bank fragment containing the *rsmN* ORF cloned in pMMB-16, (b) insert cloned in pHS1, (c) insert cloned in pHS2.....45

Figure 2.2 The *rsmN* and *NasIrsmN* sequences.....50

Figure 2.3 Diagrammatic depiction of enriched transcripts.....65

Figure 3.1 The genomic context of *rsmN*.....67

Figure 3.2 The nucleotide sequence of the *PA5183-PA5184* intergenic region including the promoter and terminator sequences.....69

Figure 3.3 The influence of *rsmA* and *rsmN* mutations on the growth of *P. aeruginosa* in LB.....71

Figure 3.4 The impact of *rsmA* and *rsmN* mutations on cell clumping.....72

Figure 3.5 Abolished clumping in a Δ*rsmA*/pME6000 deletion mutant by multicopy expression of *rsmN*.....73

Figure 3.6 Swarming motilities of the *P. aeruginosa* cells on nutrient broth agar (0.5% w/v) at 37°C in the absence of RsmA or RsmN.....74

Figure 3.7 The effect of *rsmA* or *rsmN* expression on swarming motilities of the *rsmA*$_{ind}$ Δ*rsmN* and *rsmN*$_{ind}$ Δ*rsmA* mutants at 37°C on nutrient broth agar (0.5% w/v)……74

Figure 3.8 The effect of the multicopy expression of *rsmN* on swarming motility of the Δ*rsmA*/pME6000 strain in comparison with swarming of the WT/pME6000 and Δ*rsmN*/pME6000 strains on nutrient broth agar (0.5% w/v) at different temperatures.....76

Figure 3.9 The effect of the multicopy expression of *rsmN* or *rsmN*R62A on swarming motilities of the WT/pME6000, Δ*rsmA*/pME6000 and Δ*rsmN*/pME6000 strains on nutrient broth agar (0.5% w/v) at 37°C and 34°C……78

Figure 3.10 Motilities of the *P. aeruginosa* WT, Δ*rsmA*, Δ*rsmN*, *rsmA*$_{ind}$ Δ*rsmN* and *rsmN*$_{ind}$ Δ*rsmA* strains on nutrient broth agar (0.3% w/v) at 37°C.....80

Figure 3.11 Swimming and swarming intermediate motility of *P. aeruginosa* observed at 37°C on nutrient broth agar (0.3% w/v).....81

Figure 3.12 Twitching motilities of the PAO1-N WT strain and the isogenic Δ*rsmA,* Δ*rsmN*, *rsmA*$_{ind}$ Δ*rsmN*, and *rsmN*$_{ind}$ Δ*rsmA* mutants on the surface of a petri dish over 48 h at 37°C……82

Figure 3.13 PYO production of *P. aeruginosa* in LB at 37°C in the absence of RsmA, RsmN or both.....83

Figure 3.14 PYO production of *P. aeruginosa* in LB at 34°C in the absence of RsmA, RsmN or both.....84

Figure 3.15 The effect of the multicopy expression of *rsmN* or *rsmN*R62A on PYO production of the Δ*rsmA*/pME6000 strain in comparison with the WT/pME6000 and Δ*rsmN*/pME6000 strains in LB at 37°C.....85

Figure 3.16 The effect of the multicopy expression of *rsmN* on the appearance of the Δ*rsmA*/pME6000 strain on PIA agar at 37°C.....86

Figure 3.17 The impact of *rsmA* and/or *rsmN* deletions (panel a) and *rsmN* or *rsmN*R62A expression (panel b) on total proteolytic activity at 37°C.....88

Figure 3.18 The impact of *rsmA* and/or *rsmN* deletions (panel a) and *rsmN* or *rsmN*R62A expression (panel b) on elastinolytic activity at 37°C……...89

Figure 3.19 Z-stack images demonstrating the effect of *rsmA* and/or *rsmN* deletions on the biofilm formation of *P. aeruginosa* PAO1 cultivated in 10% LB under continuous shear flow (0.5 dyn/cm$^2$) at 37°C.....91

Figure 3.20 2D images (14 h post-inoculation) of the WT, Δ*rsmA*, Δ*rsmN* and *rsmN*$_{ind}$ Δ*rsmA* biofilms cultivated in 10% LB under continuous shear flow (0.5 dyn/cm$^2$) at 37°C……92

Figure 3.21 Microscopic images 4 h (panel a), 8 h (panel b), and 12 h (panel c) post-inoculation of WT and Δ*rsmA* biofilms cultivated in 10% LB under continuous shear flow (0.5 dyn/cm$^2$) at 37°C…….....93

Figure 3.22 The effect of the multicopy expression of *rsmN* or *rsmN*R62A on the biofilm formation of the Δ*rsmA*/pME6000 strain in comparison with WT/pME6000 and Δ*rsmN*/pME6000 biofilms cultivated in 10% LB under continuous shear flow (0.5 dyn/cm$^2$) at 37°C.....95

Figure 3.23 Colony morphologies of the WT, Δ*rsmA*, Δ*rsmN*, *rsmA*$_{ind}$ Δ*rsmN* and *rsmN*$_{ind}$ Δ*rsmA* strains during 2-6 days incubation on Congo red-tryptone agar at room temperature.....96

Figure 3.24 Investigation of phage-induced lysis on the surface of PAO1B1 and PAO1B1Δ*Pf4* soft top agar lawns after spreading culture supernatants of the PAO1B1, PAO1B1Δ*Pf4*, Δ*pqsL*, PAO1-N, Δ*rsmA*, Δ*rsmN* and *rsmN*$_{ind}$ Δ*rsmA* strains.....98

Figure 3.25 Supernatant protein profiling of the WT, Δ*rsmA*, Δ*rsmN*, *rsmA*$_{ind}$ Δ*rsmN*, and *rsmN*$_{ind}$ Δ*rsmA* strains (the latter two grown with/without IPTG) at 37°C and 34°C.....100

Figure 3.26 Investigation of cell lysis in the WT, Δ*rsmA*, Δ*rsmN*, *rsmA*$_{ind}$ Δ*rsmN* and *rsmN*$_{ind}$ Δ*rsmA* strains (the latter two grown with/without IPTG) by detection of the cytosolic protein IscS (47 kDa) among secreted proteins.....101

Figure 3.27 Exogenous addition of HHQ but not PQS results in a lytic colony morphology of the Δ*rsmA* mutant grown on Congo red-tryptone agar at room temperature for 3 days……..……104

Figure 3.28 Colony morphologies of the WT PAO1-N (a), *rsmN*$_{ind}$ Δ*rsmA* (b), Δ*pqsH* Δ*pqsL* (c), Δ*pqsH* (d), and Δ*pqsL* (e) strains on Congo red-tryptone agar at room temperature 2 days (top panel) and 6 days post-inoculation (bottom panel)….....105

Figure 3.29 Snapshot of the percent coverages of probable proteins (identified in the 17 kDa region) released to the culture supernatants of the *rsmA*$_{ind}$ Δ*rsmN* and *rsmN*$_{ind}$ Δ*rsmA* strains….....106

Figure 3.30 Repression of glycogen accumulation in the *E. coli* Δ*csrA* mutant TR1-5 by *P. aeruginosa* RsmA but not RsmN or RsmNR62A.....107

Figure 3.31 Diagrammatic representation of TSSs and promoter sequences in the pHS2 derivatives.....110

Figure 3.32 Transcription of the predicted *nmsR* RNA does not influence the growth of the *rsmN*$_{ind}$ Δ*rsmA*/pME6000 double mutant in LB at 37°C.....111

Figure 3.33 Investigating the influence of *nmsR* transcription on the swarming motility of the *rsmN*$_{ind}$ Δ*rsmA*/pME6000 double mutant on nutrient broth agar (0.5% w/v) at 37°C.....112

Figure 3.34 The effect of the multicopy expression of *rsmN* with or without *nmsR* transcription on the exoprotease (panel a), elastase (panel b) and PYO (panel c) levels of the *rsmN*$_{ind}$ Δ*rsmA*/pME6000 mutant grown in LB at 37°C.....113

Figure 3.35 Colony morphologies of the *rsmN*$_{ind}$ Δ*rsmA*/pME6000, *rsmN*$_{ind}$ Δ*rsmA*/pHS2, *rsmN*$_{ind}$ Δ*rsmA*/pMR1, *rsmN*$_{ind}$ Δ*rsmA*/pMR11 and *rsmN*$_{ind}$ Δ*rsmA*/pMR12 strains on Congo red-tryptone agar up to 4 days post-inoculation at room temperature.....114

Figure 3.36 The impact of the multicopy expression of *rsmN* in the presence or absence of the *nmsR* transcript on swarming motilities of the WT, Δ*rsmA* and Δ*rsmN* strains at 37°C and 34°C on nutrient broth agar (0.5% w/v).....116

Figure 3.37 Depiction of the hairpin loop formation between the *rsmN* TSS and translation start site.....118

Figure 3.38 The influence of the hairpin loop located near the *rsmN* TSS on the suppression of WT and Δ*rsmN* swarming motilities and complementation of Δ*rsmA* swarming on nutrient broth agar (0.5% w/v) at 37°C.....120

Figure 3.39 Investigation of cell lysis in the WT/pME6000, Δ*rsmA*/pME6000 and Δ*rsmN*/pME6000 strains upon *rsmN* expression by detection of the cytosolic protein IscS (47 kDa) among secreted proteins.....121

Figure 3.40 Colony morphologies of a *P. aeruginosa wspF10* mutant grown on swimming agar (left) and an *rsmA*$_{ind}$ Δ*rsmN* mutant grown on Congo red-tryptone agar (right) after 2 days of incubation at room temperature.....128

Figure 4.1 RNASeq workflow.....133

Figure 4.2 Raw data and replicate robustness.....136

Figure 4.3 RsmN-enrichment, indicated by an enrichment index greater than 2.0, of PhrS at 37°C……..139

Figure 4.4 The double deletion of *rsmA* and *rsmN*, like the deletion of *crcZ*, prevents the growth of PAO1 on acetamide supplemented BSM agar (a), none of the strains grow on BSM agar without any acetamide (b) at 37°C.....145

Figure 4.5 The influence of *rsmA* and *rsmN* mutations on the growth of *P. aeruginosa* in chemically defined minimal medium (CDM) supplemented with citrate (A), malate (B), fumarate (C) and succinate (D) at 37°C.....148

Figure 4.6 The influence of *rsmA* and *rsmN* mutations on the growth of *P. aeruginosa* on basal salts minimal agar supplemented with citrate, malate, fumarate and succinate.....149

Figure 4.7 Protein profiles of each fraction during purification of RsmN from the 34°C (left) and 37°C (right) cultures of the PAO1-L/pMR4 strain.....151

Figure 4.8 The *tss* operon as an RsmN target only at 37°C (A) and *lasB* as an RsmN target only at 34°C (B).....152

Figure 4.9 Predicted regulatory roles of the Rsm proteins on the T6SS of *P. aeruginosa* ……...156

Figure 5.1 A cellular diagram illustrating (left panel) the proposed negative regulation of T6SS, positive regulation of protease/chaperone levels, *crcZ* and *lasB* translation and the denitrification pathway by RsmA and RsmN, and the negative control by RsmA on *rsmN* in the WT strain characterised by a smooth colony morphology and flat undifferentiated biofilm phenotype, and (right panel) the possible mechanisms behind the excessive autolysis of the *rsmN*$_{ind}$ Δ*rsmA* mutant (-IPTG) characterised by a rough colony morphology and microcolony biofilm phenotype……167

Supplementary Figure 1 Genomic DNA removal from the RNA samples using Turbo DNase……169

Supplementary Figure 2 Agilent bioanalyzer electrograms of the total RNA purified from the PAO1-L/pMR4 strain cultured at 37°C (top panel) and 34°C (bottom panel)…….170

Supplementary Figure 3 Agilent bioanalyzer electrograms of the RsmN-bound RNAs purified from the PAO1-L/pMR4 strain cultured at 37°C (top panel) and 34°C (bottom panel)……..171

Supplementary Figure 4 *P. aeruginosa* strains used in this study and their characteristics……172

Supplementary Figure 5 Swarming motilities of the WT and Δ*rsmN* strains on nutrient broth agar (0.5% w/v) monitored in a time-dependent manner at 37°C……173

Supplementary Figure 6 Surface of the soft top agar after spreading undiluted cell-free supernatants from the WT PAO1-N, Δ*rsmA*, Δ*rsmN*, *rsmN*$_{ind}$ Δ*rsmA* and Δ*pqsL* strains……174

Supplementary Figure 7 The effect of *rsmN* or *rsmN*R62A expression induced in the presence (a) or absence (b) of the $P_{rsmN}$ and $P_{nmsR}$ promoters on total proteolytic (top) and elastinolytic (bottom) activities of the Δ*rsmA*/pME6000 mutant at 37°C.....175

Supplementary Figure 8 The effect of *rsmN* expression induced in the presence of the $P_{lac}$, $P_{rsmN}$ and $P_{nmsR}$ promoters (via pHS2) or the $P_{lac}$ promoter (pMR1) on PYO production of the Δ*rsmA*/pME6000 mutant in LB at 37°C……176

## List of Tables

Table 2.1 Bacterial strains used in this study.....38

Table 2.2 Plasmids used in this study.....39

Table 2.3 Primers used for the construction of plasmids used in this study, TSS detection and checking expression levels from the $P_{rsmN,}$ $P_{rsmF}$ and $P_{nmsR}$ promoters....40

Table 2.4 Codon usage table listing synonymous codons with the two highest RSCU values ($RSCU_{max}$ and RSCU) in *P. aeruginosa* PAO1.....46

Table 2.5 Codon selection of RsmN (third column) and NasIrsmN (last column).....48

Table 3.1 $OD_{600}$ of bacterial strains during supernatant collection for supernatant protein profiling.....99

Table 3.2 Quantification of cell lysis in the WT, Δ*rsmA*, Δ*rsmN*, $rsmN_{ind}$ Δ*rsmA* and Δ*pqsL* strains by c.f.u. count.....102

Table 3.3 Bacterial loads, calculated as the ratio of the c.f.u. and weight gain (g), of the WT PAO1-N and $rsmN_{ind}$ Δ*rsmA* strains in mouse chronic wound infections 4 days post-infection.....108

Table 4.1 Strand-specific RNASeq starting files processed in this study.....135

Table 4.2 Exclusion boundaries for reads corresponding to ribosomal RNAs.....137

Table 4.3 Changes in the RNASeq data after excluding rRNAs.....138

Table 4.4 RsmN-enriched targets at 37°C.....141

Table 4.5 RsmN-RsmA common targets.....143

Table 4.6 RsmN-enriched targets only at 34°C.....151

# Abbreviations & Symbols

| | |
|---|---|
| °C | Celcius degrees |
| σ | sigma factor |
| µg | microgram |
| µL | microlitre |
| µm | micrometer |
| µM | micromolar |
| 3D | three-dimensional |
| 3O-C12-HSL | *N*-(3-oxododecanoyl)-L-homoserine lactone |
| aa | amino acid |
| ACP | acyl carrier protein |
| AHL | *N*-acyl-homoserine lactone |
| AI | autoinducer |
| AIDS | acquired immune deficiency syndrome |
| Amp | ampicillin |
| APEC | avian pathogenic *Escherichia coli* |
| Apr | alkaline protease |
| APS | ammonium persulfate |
| AQ | 2-alkyl-4(1H)-quinolone |
| ARF-TSS | adaptor and radioactivity free transcription start site detection |
| Arg | arginine |
| asRNA | antisense ribonucleic acid |
| *B. subtilis* | *Bacillus subtilis* |
| bp | base pair |
| BSM | basal salts medium |
| C4-HSL | *N*-butanoyl-L-homoserine lactone |
| c-di-GMP | bis-(3'-5')-cyclic-dimeric guanosine monophosphate |
| cAMP | cyclic adenosine monophosphate |
| CAP | catabolite gene activator protein |
| Cb | carbenicillin |
| Cbr | catabolic regulation |
| CCR | carbon catabolite repression |
| CDM | chemically defined medium |
| cDNA | complementary deoxyribonucleic acid |
| CF | cystic fibrosis |
| c.f.u. | colony forming unit(s) |
| cm | centimeter |
| $Cm^R$ | chloramphenicol resistant |
| Crc | catabolite repression control protein |
| CRP | cyclic adenosine monophosphate-dependent catabolite repression protein |
| Csr | carbon storage regulator |
| $dH_2O$ | distilled water |
| DMSO | dimethyl sulphoxide |
| DNase | deoxyribonuclease |
| dNTP | deoxyribonucleotide triphosphate |
| dsRNA | double-stranded ribonucleic acid |
| dsRBM | double-stranded ribonucleic acid binding motif |
| DTT | dithiothreitol |
| *E. coli* | *Escherichia coli* |

| | |
|---|---|
| eDNA | extracellular deoxyribonucleic acid |
| EDTA | ethylenediamine tetraacetic acid |
| eGFP | enhanced green fluorescent protein |
| EMSA | electrophoretic mobility shift assay |
| EPM | extracellular polymeric matrix |
| EPS | extracellular polysaccharide |
| EtOH | ethanol |
| $FeSO_4*7H_2O$ | iron sulfate heptahydrate |
| g | gram |
| *g* | relative centrifugal force |
| Gac | global activator of antibiotic and cyanide production |
| GCI | genome codon index |
| Gm | gentamicin |
| GTP | guanosine-5'-triphosphate |
| H-bond | hydrogen bond |
| $H_2O_2$ | hydrogen peroxide |
| HAA | 3-(3-hydroxyalkanoyloxy) alkanoic acid |
| HCl | hydrochloric acid |
| HCN | hydrogen cyanide |
| Hfq | host factor protein |
| HHQ | 2-heptyl-4(1H)-quinolone |
| $His_6$ | hexahistidine tag |
| HK | histidine kinase |
| hnRNP | heterogeneous nuclear ribonucleoprotein |
| H-NS | histone-like nucleoid structuring protein |
| h | hour(s) |
| HPLC | high pressure liquid chromatography |
| Hsp | heat shock protein |
| $I_2$ | iodine |
| IDT | Integrated DNA Technologies |
| IHF | integration host factor |
| IF | initiation factor |
| IPTG | isopropyl-thio-β-D-galactopyranoside |
| Ile | isoleucine |
| $K_2HPO_4$ | dipotassium phosphate |
| Kan | kanamycin |
| kb | kilo base pair |
| KCl | potassium chloride |
| kDa | kilo Dalton |
| KH | K-homology |
| $KH_2PO_4$ | monopotassium phosphate |
| KI | potassium iodide |
| kV | kilovolts |
| L | litre |
| LasA | staphylolysin or LasA protease |
| LasB | pseudolysin or elastase |
| LadS | lost adherence sensor |
| LB | Luria Bertani (broth) |
| LC-MS | liquid chromatography-mass spectrometry |
| Leu | leucine |
| Lys | lysine |
| M | molarity |
| mA | milliampere |
| Mb | megabase pair |
| MDR | multidrug-resistant |

| | |
|---|---|
| MES | 2-(*N*-morpholino)-ethane sulfonic acid |
| mg | milligram |
| $Mg^{2+}$ | magnesium |
| $MgCl_2$ | magnesium chloride |
| $MgSO_4$ | magnesium sulfate |
| min. | minute |
| mL | millilitre |
| mM | millimolar |
| MOPS | 3-(*N*-morpholino)-propane sulfonic acid |
| mRNA | messenger ribonucleic acid |
| N | any nucleotide |
| NaCl | sodium chloride |
| $NADH/NAD^+$ | reduced and oxidised forms of nicotinamide adenine dinucleotide |
| NaOAc | sodium acetate |
| NaOH | sodium hydroxide |
| NB | nutrient broth |
| ncRNA | non-coding ribonucleic acid |
| $(NH_4)_2SO_4$ | ammonium sulfate |
| Ni-NTA | nickel-nitrilotriacetic acid |
| nm | nanometer |
| No. | number |
| $NO_3$ | nitrate |
| nt | nucleotide |
| Ntr | nitrogen assimilation |
| OD | optical density |
| o/n | overnight |
| Opr | outer membrane protein |
| ORF | open reading frame |
| P | peptidyl site of the ribosome |
| *P. aeruginosa* | *Pseudomonas aeruginosa* |
| *P. fluorescens* | *Pseudomonas fluorescens* |
| *P. syringae* | *Pseudomonas syringae* |
| PA | *P. aeruginosa* |
| PAGE | polyacrylamide gel electrophoresis |
| PBS | phosphate-buffered saline |
| $P_{BAD}$ | promoter of the *araBAD* operon |
| $P_{lac}$ | *lac* promoter |
| $P_{nmsR}$ | *rsmN* antisense promoter |
| $P_{rsmN}$ | *rsmN* sense promoter |
| $P_{tac}$ | isopropyl-thio-β-D-galactopyranoside inducible *tac* promoter |
| PBS | phosphate buffered saline |
| PCR | polymerase chain reaction |
| PIA | *Pseudomonas* isolation agar |
| pM | picomolar |
| PQS | *Pseudomonas* quinolone signal |
| p.s.i. | per square inch |
| pv. | pathovar |
| PYO | pyocyanin |
| qRT-PCR | quantitative real-time polymerase chain reaction |
| QS | quorum sensing |
| QscR | quorum sensing control repressor |
| r.p.m | revolutions per minute |
| RACE | rapid amplification of cDNA ends |

| | |
|---|---|
| RBP | ribosome binding protein |
| RBS | ribosome binding site |
| RetS | regulator of exopolysaccharide and type III secretion |
| rhl | rhamnolipid |
| RIN | ribonuclease integrity number |
| RNA | ribonucleic acid |
| RNAP | ribonucleic acid polymerase |
| RNase | ribonuclease |
| RNASeq | ribonuclease sequencing |
| ROSE | repression of heat shock gene expression |
| RR | response regulator |
| RRM | ribonucleic acid recognition motif |
| rRNA | ribosomal ribonucleic acid |
| RSCU | relative synonymous codon usage |
| Rsm | regulator of secondary metabolism |
| s | second |
| *S. aureus* | *Staphylococcus aureus* |
| SAM | S-adenosylmethionine |
| SD | Shine-Dalgarno |
| SDS | sodium dodecyl sulphate |
| Sm/Sp | streptomycin/spectinomycin |
| spp. | species |
| sRNA | small ribonucleic acid |
| ssDNA | single-stranded deoxyribonucleic acid |
| sv. | serovar |
| T1SS | type I secretion system |
| T2SS | type II secretion system |
| T3SS | type III secretion system |
| T6SS | type VI secretion system |
| TAE | tris-acetate/ethylenediamine tetraacetic acid |
| TCA | tricarboxylic acid |
| TCAa | trichloroacetic acid |
| TCS | two-component system |
| TEMED | N,N,N',N'-tetramethylethylenediamine |
| Tc | tetracycline |
| tmRNA | transfer messenger RNA |
| TRAP | *trp* ribonucleic acid-binding attenuation protein |
| Tris·Cl | tris chloride |
| Tris-HCl | tris-hydrochloric acid |
| tRNA | transfer ribonucleic acid |
| UPEC | uropathogenic *Escherichia coli* |
| UTR | untranslated region |
| UV | ultraviolet |
| V | volts |
| Vfr | virulence factor regulator |
| VqsR | virulence and quorum sensing regulator |
| v/v | volume per volume |
| w/v | weight per volume |
| X-gal | 5-bromo-4-chloro-3-indolyl β-D-galactopyranoside |
| WT | wild-type |

# 1 Introduction

In the 21st century that we live in, infections by multidrug-resistant (MDR) bacteria are posing a challenge to the health care systems. Over the last few decades, the resistance of pathogenic bacteria against antimicrobials has been increasing in parallel with the advances in vaccine production and treatment. As traditional antibiotics which usually kill bacteria or inhibit their growth become ineffective, alternative methods are needed to treat bacterial infectious diseases [1]. Bacterial cells secrete virulence factors that aid in their entry to and multiplication within the host cell to establish a successful infection. Downregulating the production of these factors or interfering with their secretion led to a decrease in bacterial fitness and reduced the damage on the host [2-4]. For this reason, identifying ways to prevent the dissemination of virulence factors represents a promising approach to alter the pathogenicity of bacteria that cause infectious diseases.

A significant portion of a bacterial pathogen's genome is dedicated to regulatory genes to ensure a tight control of the production and secretion of virulence factors, and to thrive under different environmental conditions such as scarce nutrient availability or elevated temperatures by providing cells physiological and metabolic flexibility. Surmounting host defense mechanisms requires the reprogramming of bacterial gene expression and this can be achieved by transcriptional regulators. Examples of the pleiotropic transcriptional regulators are the sigma (σ) factors, integration host factor (IHF), histone-like nucleoid structuring protein (H-NS), and second messenger molecules like cyclic adenosine monophosphate (cAMP) and bis-(3'-5')-cyclic-dimeric guanosine monophosphate (c-di-GMP) [5, 6].

Gene regulation can also take place at the post-transcriptional (see below) and post-translational levels by modification or degradation of mRNAs and proteins after synthesis. In bacteria, post-transcriptional regulators typically modulate transcript elongation, mRNA (messenger RNA) stability, and translation initiation [7, 8]. Proteases and chaperones have been shown to coordinately regulate protein levels [9].

## 1.1 Bacterial gene regulation at the post-transcriptional level

Studies on bacterial gene regulation at the post-transcriptional level have mainly focused on processes involving mRNA transcripts after they have been synthesised. Post-transcriptional regulators such as RNA-binding proteins (RBPs), small regulatory RNAs (sRNAs) -the majority of which do not encode proteins thus, the term small RNA is interchangeably used with non-coding RNA (ncRNA)-, riboswitches, and ribonucleases (RNases) modulate the elongation or decay of transcripts, alter RNA secondary structures or interfere with ribosome binding/translation initiation and hence, affect the abundance of proteins made [8, 10].

Translation initiation is the rate-limiting step of protein synthesis; therefore, it is the most tightly regulated step. It requires the mRNA, the 30S and 50S ribosomal subunits, initiating transfer RNA (tRNA) carrying the methionine amino acid (aa), initiation factors (IFs) 1, 2, and 3, guanosine-5'-triphosphate (GTP) and magnesium ($Mg^{2+}$). Recognition of mRNA by the ribosome involves ribosomal RNA (rRNA)-mRNA base-pairing. More specifically, the pyrimidine-rich sequence, close to the 3'-end of the 16S rRNA from the 30S ribosomal subunit, base-pairs with the purine-rich Shine-Dalgarno (SD) sequence of the mRNA. This base-pairing positions the start codon AUG on the mRNA to the peptidyl (P) site of the ribosome where the transfer (tRNA) carrying the *N*-formylmethionine residue binds. The anticodon of this tRNA pairs up with the start codon of the mRNA. The 30S ribosomal subunit then combines with the 50S ribosomal subunit to form an initiation complex (70S). The dependence of protein synthesis on the formation of this initiation complex makes these RNA interactions a pivotal point for regulation. Small RNAs and riboswitches are examples of regulatory RNA elements which target these interactions [11, 12].

### 1.1.1 Small regulatory RNAs

Shimoni *et al*. [13] studied the dynamics of transcriptional regulation and post-transcriptional regulation by regulatory RNAs and regulation by protein-protein interactions at the post-translational level and concluded that RNA-mediated regulation is the fastest way to drive gene expression under stress conditions when fast responses are required. For this reason, sRNAs are starting to be recognised as major players in the regulatory pathways that govern cellular processes to allow bacteria to adjust their metabolism, activate coordinated gene expression in a population-

dependent manner via quorum sensing (QS), control stress responses, reorganise surface proteins and regulate virulence [14, 15].

Regulatory sRNAs are transcripts of 50-500 nucleotides (nt) that modulate transcription, translation, mRNA stability, and DNA maintenance. Even though sRNAs are also termed non-coding, there are exceptions such as RNAIII in *Staphylococcus aureus* (*S. aureus*), SgrS in *Escherichia coli* (*E. coli*) and PhrS in *Pseudomonas aeruginosa* (*P. aeruginosa*) which encode small polypeptides in addition to their regulatory RNA roles [16, 17]. They usually bind to their target mRNAs in the close vicinity of or at the ribosome binding site (RBS) and hinder ribosome binding (Figure 1.1). Some might bind at distant locations and alter secondary structures and/or affect mRNA stability by accelerating cleavage by RNases [18].

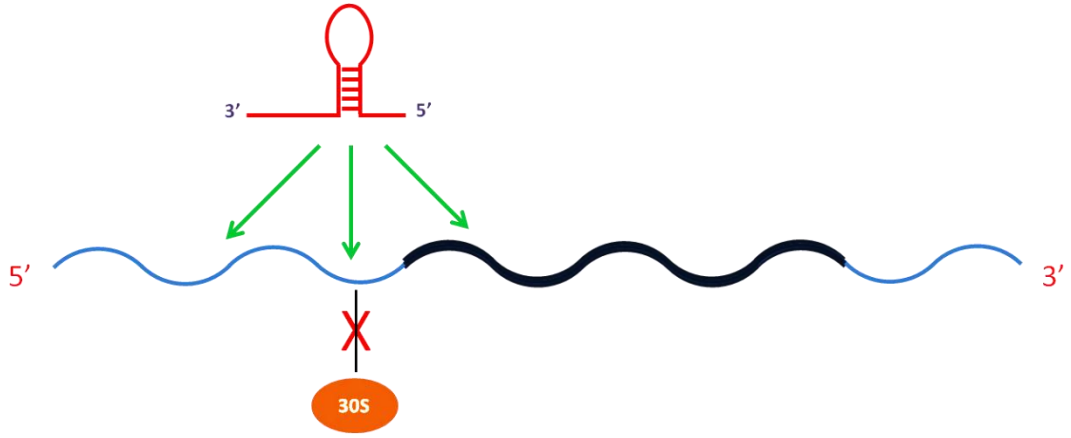


**Figure 1.1. Possible sRNA base-pairing regions on target transcripts**
Base-pairing between a sRNA and the target mRNA might occur upstream/downstream of the RBS or might overlap the RBS (pointed by green arrows) and the translation is blocked. The sRNA is depicted in red, the orange circle represents the 30S subunit of the ribosome, and the target transcript as a whole is shown in blue. The translated region of the transcript is illustrated in darker blue. The figure is modified from Storz *et al*. [18].

The majority of sRNAs act antagonistically. Although positive regulation by sRNAs appears to be less common, transcript activation is possible via melting of the secondary structures which mask the RBS [16]. Additionally, sRNAs can silence or enhance the translation of target mRNAs indirectly by altering the translation of nearby open reading frames (ORFs) to which the target is translationally coupled. For example, anaerobically induced sRNA, PhrS, of *P. aeruginosa* upregulates the

translation of the transcriptional regulator PqsR indirectly by triggering the translation of an upstream ORF which terminates at an adjacent region to the translation initiation site of the *pqsR* gene [14, 19].

Transcription of sRNAs is dependent on environmental cues such as iron and oxygen availability, osmotic balance and pH. A conserved secondary structure is common to most sRNAs: stem-loop structures with repeated motifs such as ANGGA motifs or CA-rich sites. For example, the RsmY sRNA of *P. aeruginosa* possesses multiple GGA motifs which are the recognition sites of the RsmA (regulator of secondary metabolism) protein [17, 20, 21].

Based on their genomic position, sRNAs can be classified into two categories: *cis*- and *trans*-encoded. *Cis*-encoded sRNAs are encoded on the opposite DNA strand to their target mRNAs therefore they have high complementarity whereas *trans*-encoded sRNAs are encoded at a different genomic location than their target mRNAs and have partial complementarity. Most *trans*-encoded sRNAs require the chaperone protein Hfq to facilitate binding. *Trans*-encoded sRNAs, in conjunction with Hfq, might regulate more than one target mRNA as their partial target complementarity allows flexibility. Furthermore, an mRNA might be regulated by a few sRNAs [22]. There are also protein-binding sRNAs besides these mRNA base-pairing (antisense) sRNAs. Regulatory sRNAs usually associated with two-component regulatory systems (TCS) act as direct competitors to the target mRNAs of RNA-binding proteins and sequester RBPs. Moreover, some sRNAs such as the *E. coli* 6S RNA modulate enzymatic activity [18].

Naturally occurring antisense sRNAs (asRNAs) are found in all three domains of life and first studied examples were of phage, transposon, and plasmid origin. Later, prokaryotic chromosomal asRNAs taking part in the regulation of stress responses and virulence were also discovered. Plasmid, transposon or phage origin asRNAs are mostly *cis*-encoded whereas chromosomal asRNAs are mostly *trans*-encoded [23, 24].

The interaction of an asRNA with its target mRNA results in the alteration of the secondary structures present leading to the formation of a double-stranded RNA (dsRNA) and, in most cases, both RNAs get degraded by RNases. However,

modification of the secondary structures can sometimes activate a translationally inert mRNA. Generation of a specific processing site as a result of dsRNA formation such as during the GadY-*gadX* binding in the acid response system of *E. coli* is an example of this [25]. Moreover, asRNAs can provide protection against RNase E-dependent decay by overlapping the 5'-region of a target mRNA. This protection mechanism has been suggested to have a role in the phage-host interplay [26]. Some asRNAs are employed in toxin-antitoxin mechanisms (where the cell synthesises a stable toxin under specific conditions and the corresponding antitoxin is expressed from a plasmid) such as the *hok* (host killing)*/sok* (suppression of killing) system of the *E. coli* R1 plasmid. Usually, toxin-antitoxin pairs are both proteins but sometimes, like the Sok RNA in the *hok/sok* system of the R1 plasmid in *E. coli*, the antitoxin is an asRNA, inhibiting the translation of the toxin mRNA [27, 28].

The main similarities between the bacterial *cis*- and *trans*-encoded sRNAs are that both, (a) form Watson-Crick H-bonds with complementary bases of the mRNA target, (b) interact with the target stoichiometrically, and (c) get co-degraded with the target. The differences are, (a) *cis*-encoded sRNAs have complete complementarity with their target which leads to the formation of a more stable dsRNA and the interaction does not require Hfq as a chaperone, (b) transcription of *cis*-encoded sRNAs and their target mRNAs in close proximity might enhance their interactions, eliminating the need to increase genome size, and (c) *cis*-encoded sRNAs are highly structured (1-4 stem loops rich in GC-motifs) [24, 26].

It is presumed that sRNAs play a key role in the regulation of bacterial metabolism because they provide regulatory plasticity and can be processed (synthesised/degraded) much faster and at a reduced metabolic cost compared with proteins [21, 29]. For example, asRNAs can be used to adjust mRNA levels of individual genes within an operon via specific processing of the polycistronic message or by alternative termination. The use of asRNAs to fine-tune expression in this way provides great advantages in comparison with protein regulators which control regulons as a whole [11, 26].

### 1.1.2 Riboswitches

Riboswitches are other bacterial *cis*-acting elements which are part of the mRNA they regulate, usually found within the 5'-untranslated region (UTR) and are activated upon binding of a metabolite or through temperature changes. Riboswitches represent one of the oldest mechanisms to control the expression of the genes that code metabolic proteins, ion transporters, vitamins or purine bases [30]. The first riboswitches discovered were regulators of vitamin biosynthesis operons in *E. coli* and *Bacillus subtilis* (*B. subtilis*) [31, 32].

Riboswitches have high-affinity receptors for small organic molecules such as sugars or amino acids which can be collectively termed as 'ligands'. Their main role is to maintain the homoeostasis of these ligands by altering the levels of proteins synthesizing or transporting these molecules [32].

Based on their structure and the type of signal they recognise, several classes of riboswitches have been defined, 1) small molecule-binding riboswitches with two separate domains for gene expression and ligand-binding, 2) small molecule-binding riboswitches with a gene expression domain which participates in ligand-binding, 3) tRNA-binding riboswitches, and 4) RNA thermosensors [33]. The most common type of bacterial riboswitches has gene expression and aptamer domains. The gene expression domain is usually located downstream of the aptamer domain. Upon ligand binding, the riboswitch undergoes a conformational change that results in the sequestration of a portion of RNA. Usually, a helix that functions as an intrinsic terminator to attenuate transcription is formed or the SD sequence is sequestered and ribosome binding is blocked. Moreover, some mRNAs might undergo autocleavage due to the ribozyme activity of the riboswitch. A small number of riboswitch RNAs have also been found to regulate the synthesis of antisense transcripts [30, 34].

#### 1.1.2.1 Thermosensors

RNA thermosensors are single domain riboswitches which exert a regulatory control in response to the temperature changes instead of ligand binding thus, eliminating the need for a ligand recognition domain. In most cases, the SD sequence of the mRNA is inaccessible by ribosomes to start translation at environmental temperatures.

Increasing the temperature melts the RNA helix and the SD sequence becomes accessible [35].

Virulence genes of pathogenic bacteria are generally expressed more at higher temperatures. An increase in temperature leads to the formation of unstable secondary structures and allows access to the RBS, enabling ribosomes to translate the required genes. At lower temperatures, RNA thermosensors block ribosome binding [36, 37]. A few examples of the thermosensors found in pathogenic bacteria include the secondary structures present in the *prfA*-UTR of *Listeria monocytogenesis* [38], intergenic RNA thermosensor of *Yersinia pseudotuberculosis* controlling the synthesis of the LcrF transcription factor [39], and the ROSE (repression of heat shock gene expression)-like element located in the 5'-UTR of *P. aeruginosa rhlA* [37].

ROSE-like elements are one of the best-studied RNA thermosensors comprising three-four stem loops and generally found in the transcripts of genes encoding heat shock proteins (Hsp). Recently, Grosso-Becerra *et al*. [37] showed that the translation of *rhlA* and *lasI*, components of the AHL (*N*-acyl-homoserine lactone)-dependent QS system of *P. aeruginosa* was regulated by the ROSE-like elements found in the 5'-UTR of gene transcripts, demonstrating the thermoregulation of virulence for the first time.

### 1.1.3 RNA-binding proteins

Bacterial RBPs regulate the stability and elongation of target mRNA molecules and modulate translation initiation via different mechanisms, for instance, by i) altering the susceptibility towards RNase treatment, ii) changing the accessibility of the RBS, iii) acting as a chaperone between the mRNA target and effector molecules, and iv) modulating the formation of terminator/antiterminator structures [8].

RNA-binding proteins can modulate RNA stability directly by preventing RNase binding, and indirectly by triggering changes in the secondary structures which confer stability to the RNA. Regulatory RBPs such as the CsrA (carbon storage regulator)/RsmA proteins can prevent ribosome binding to the RBS through competitive binding or alteration of the secondary structures near the RBS of the mRNA targets. In this kind of regulation, in addition to translation initiation, the

lifetime of the targeted transcript is also affected, mostly due to the decay of the ribosome unbound mRNAs by RNases such as RNase E [8].

The RNA recognition sites of the RBPs can be grouped based on the structural motifs such as the 1) arginine (Arg) and lysine (Lys)-rich motifs which aid in the recognition of the major groove of RNA for binding, and 2) α/β motifs that are present in the RNA recognition motifs (RRM), dsRNA-binding motifs (dsRBM), and K-homology (KH) and zinc finger domains [40-42].

The majority of RBPs possess an RRM which consists of a $\beta_1\alpha_1\beta_2\beta_3\alpha_2\beta_4$ fold composed of 90 amino acids with a few conserved residues. The first and third β-strands make up an antiparallel sheet [43]. RBPs with a role in transcriptional and translational gene regulation have a heterogeneous nuclear ribonucleoprotein complex (hnRNP) KH domain which is similar to the RNA-binding domain of protein K from the human hnRNP that binds to single-stranded DNA (ssDNA) or RNA. KH domains have several conserved motifs: a GxxG motif (G is glycine and x is any aa), a variable loop, three β-strands and α-helices and either isoleucine (Ile) or leucine (Leu) as a hydrophobic residue [40].

#### 1.1.3.1 CsrA

One of the well-studied RBPs is the CsrA protein. It was discovered by Romeo and co-workers [44] while searching for novel factors that regulate glycogen biosynthesis in *E. coli*. It is a global post-transcriptional regulator of carbon metabolism (positive regulator of glycolysis and negative regulator of gluconeogenesis), QS, peptide uptake, oxidative stress response, motility, c-di-GMP accumulation and biofilm formation [45]. CsrA represses the expression of numerous genes which are induced upon entry into the stationary phase and activates genes required for growth. Upon the discovery of four CsrA binding sites upstream of the *csrA* translation start codon, and analysis of protein binding to these sites, it was concluded that *E. coli* CsrA can regulate its own translation [46].

CsrA is a 61 amino acid protein containing a GxxG motif, a structural characteristic of the KH domains of some RBPs, and present in the cell as a homodimer. Structural analysis of a CsrA monomer revealed five β-strands and an α-helix just before the C-

terminus (see Figure 1.2). In the dimer, the β1 and β5 strands of one monomer connect to the β4' and β2' strands of the other monomer via H-bonds and create an antiparallel β-sheet which forms the core of the CsrA protein [47]. CsrA homologues with roles in metabolism, biofilm formation, motility, host cell invasion and virulence were identified in other bacterial species [48-50]. In 1995, a CsrA homologue repressing the production of secondary metabolites was discovered in *Pectobacterium carotovarum*. Hence, this RBP was named as the regulator of secondary metabolism A, RsmA [51]. In *Pseudomonas fluorescens* (*P. fluorescens*) CHA0, CsrA homologues RsmE and RsmA were found to repress processes regulated by the global activator of antibiotic and cyanide production (Gac) TCS [52]. Amino acid sequence comparison of CsrA and RsmA proteins (Figure 1.2) shows that the GxxG motif is conserved in some *Pseudomonas* species [53].

The CsrA/RsmA family proteins mostly act as translational repressors by binding to the 5'-UTR region (5'-$^{A}/_{U}$CANGGANG$^{U}/_{A}$-3' consensus sequence which is very similar to the ideal SD sequence 5'-AAGGAGGU-3' complementary to the 16S rRNA of the 30S ribosomal subunit) in the near vicinity of the SD sequence of mRNAs and blocking ribosome binding. Furthermore, it has been demonstrated that CsrA binding could stop transcription prematurely. For example, CsrA binding upstream of the 5'-UTR of the *E. coli pgaA* mRNA, which codes a polysaccharide adhesin export protein involved in biofilm formation, stopped transcription prematurely by altering the secondary structure which sequesters an entry site for the Rho-dependent transcription termination factor [54]. The CsrA/RsmA proteins might also act as positive regulators of translation by protecting mRNAs from degradation by RNases [9, 49].

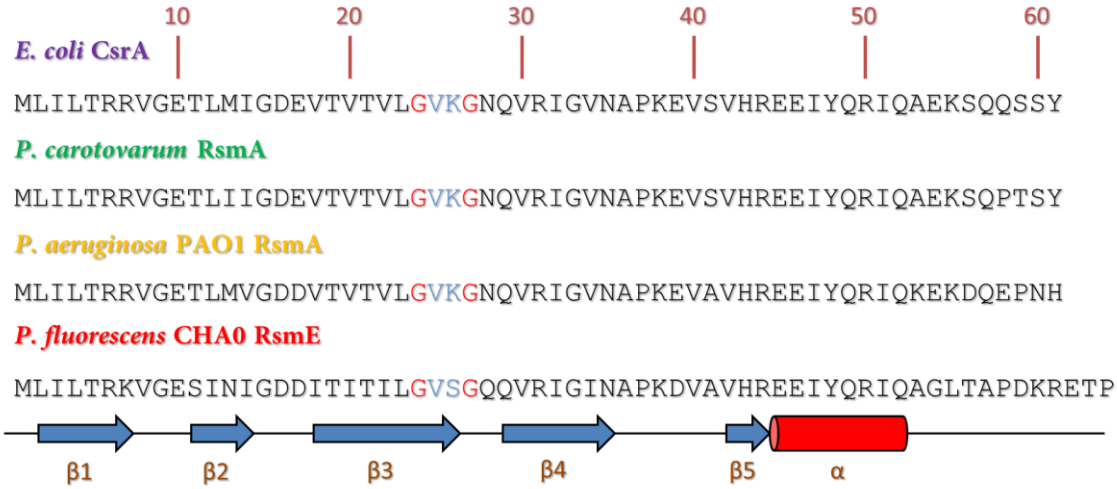


**Figure 1.2. Amino acid sequence alignments of the CsrA/RsmA proteins**
Homologues of the *E. coli* CsrA protein are aligned from the top to the bottom on the basis of amino acid similarity. The glycine residues flanking the GxxG motif are highlighted in red and the amino acids in between are highlighted in blue. The locations of β-strands and α-helix are represented by arrows and the cylinder at the bottom of the figure. The amino acid number is depicted as intervals of 10 at the top of the figure. The figure is adapted from Schubert *et al*. [55].

The CsrA activity in *E. coli* is controlled by two non-coding sRNAs (CsrB and CsrC) that contain multiple binding sites enabling them to sequester and antagonise CsrA. In particular, CsrB and CsrC possess 18 and 9 potential CsrA binding sites respectively. The CsrA binding sites of CsrB and CsrC resemble those of target mRNAs and the affinity of CsrA for the CsrB/CsrC sRNAs is higher than its affinity for the mRNA targets [45]. CsrA regulates CsrB/CsrC turnover through BarA/UvrY TCS (see section 1.2.1) and CsrD, a member of the GGDEF-EAL domain family of proteins [56].

#### 1.1.3.2 Hfq

Base pairing of *trans*-encoded sRNAs to target mRNAs is mediated by the chaperone Hfq from the Sm/LSm (named after Sm antibodies of the immune system/Sm-like) family of proteins which include components of the mRNA splicing machinery, scaffold proteins of the RNA-decapping assembly and rRNAs, sRNAs or tRNA chaperones [57]. Hfq also called the host factor 1 (HF-1) due to its discovery as an essential host factor of the bacteriophage Qβ, is a highly conserved RBP found in 50% of all bacterial species. Deletion of *hfq* in pathogenic bacteria, including *Vibrio cholera, Salmonella typhimurium, Brucella abortus, Yersinia enterolitica* and *P. aeruginosa* resulted in attenuated virulence which might be related to the pleiotropic

changes observed such as decreased growth rate, increased cell length, osmosensitivity and ultraviolet (UV) light sensitivity [58, 59].

Hfq binds to the AU-rich sequences of the sRNAs and mRNAs and facilitates their interaction through alteration of the secondary structures which results in an enhanced base pairing. According to the current data, the sRNA-mRNA duplex seems to be the regulatory element. The formation of this duplex can inhibit translation by masking the RBS of a target mRNA or activate translation by exposing a previously masked RBS [57]. Hfq binding can also protect unpaired sRNAs against degradation by RNase E or trigger polyadenylation of a target mRNA [29, 60].

The ring-like quaternary structure of Hfq provides two sides for interaction; the 'proximal face' which is the side exposing the amino-terminal α-helix and the 'distal face' on the opposite side. The quaternary architecture exposing distinct binding sites enables Hfq to bind to multiple RNA molecules at the same time [61].

Hfq binding sRNAs were found to fold into stem-loop structures extending out of the proximal and distal faces in crystallography studies. Homologous sRNAs have a 5'-region that is highly conserved, a common stem-loop structure at the 3'-end and a short poly-U sequence that constitutes a part of the Rho-independent transcription terminator. Hfq-binding mRNAs generally possess a poly-A sequence, disrupted by other nucleic acids in their 5'-UTR [57].

#### 1.1.3.3 Crc

When more than one carbon source is present in the growth medium, bacterial cells go through diauxic growth. Diauxie can be defined as the sequential use of nutrients represented by two growth curves distinguished by a lag phase in between. Carbon catabolite repression (CCR) is a regulatory system that controls the expression of 5-10% of the total number of genes in most heterotrophic bacteria and provides a competitive advantage in natural habitats. The reduced expression of certain genes and operons which control the rate of growth and virulence in pathogenic bacteria is a common result of CCR in different species, however, the regulatory network and factors involved can be diverse. Furthermore, some bacteria such as the pathogens *Chlamydia trachomatis* and *Mycoplasma pneumonia* lack a CCR mechanism [62, 63].

One of the most intensively studied examples of CCR is that of *E. coli* glucose-lactose diauxie where transcriptional activation of the catabolic genes is prevented in the presence of glucose by the catabolite gene activator protein (CAP), adenylate cyclase and signal metabolite cAMP [63]. In the opportunistic human pathogen *P. aeruginosa*, CCR takes place in the presence of the tricarboxylic acid (TCA) cycle intermediates and carbohydrates, glucose is only a secondary substrate. Organic acids are preferentially utilised first, thus, translation of enzymes required for the catabolism of carbohydrates is switched off whilst organic acids are being used up [64].

The gene (*crc*, catabolite repression control) modulating CCR was discovered and its protein product (Crc) was purified from *P. aeruginosa*. Various operons and enzymes regulated by Crc were identified. These included the *hex* regulon, a glucose transporter, gluconate, mannitol and fructose regulons and enzymes from the nitrogen metabolic pathway like amidase, histidase, urocanase [65, 66]. Crc is a post-transcriptional regulator of carbon metabolism in *Pseudomonas* species. Like RsmA, Crc is also a global regulator modulating expression/repression of a variety of genes and its activity is modulated by the CrcZ sRNA whose expression is mediated by the CbrA/CbrB (catabolic regulation) TCS (see section 1.2.2 for a more detailed description) [67, 68]. CrcZ has five CA-rich motifs which are binding sites for Crc. The high abundance of secondary carbon sources induces *crcZ* expression via the CbrA/CbrB TCS so that the Crc proteins get titrated out by CrcZ and translation of the enzymes utilizing less-preferred carbon sources can take place (Figure 1.3) [68].

In 2000, O'Toole *et al.* [69] demonstrated that Δ*crc* mutants are defective in twitching motility which is modulated by the type IV pili and biofilm formation. Linares *et al.* [67] demonstrated the contribution of Crc to virulence and antibiotic resistance in *P. aeruginosa*. Crc regulation of amino acid and nitrogen metabolisms, QS-regulated virulence (e.g. *hcnB*, hydrogen cyanide), type III secretion system (T3SS), and motility of *P. aeruginosa* were also reported [67].

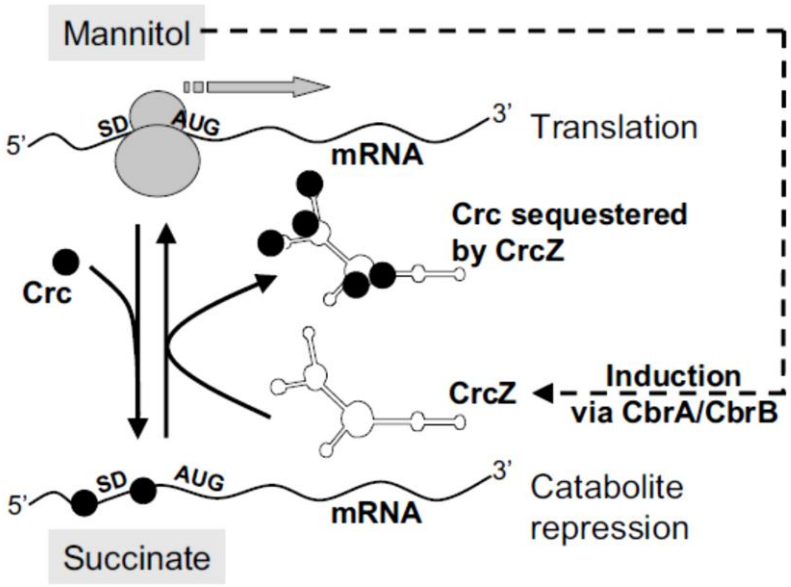


**Figure 1.3. Sequestration of the Crc proteins by CrcZ in the high abundance of less-preferred carbon sources**

The presence of less-preferred carbon sources such as mannitol activates the CbrA/CbrB TCS and triggers *crcZ* transcription. Multiple copies of the Crc protein which block the translation of the catabolic enzymes required to utilise less-preferred carbon sources by binding near the SD sequence are sequestered by CrcZ. As a result, catabolite repression by Crc is relieved. The figure is taken from Sonnleitner *et al*. [68].

## 1.2 Two-component systems in bacteria

Bacteria are constantly exposed to environmental stress such as changes in osmolarity, pH, and temperature. To trigger quick adaptive responses, they use multiple TCS consisting of a sensor protein which is generally a histidine kinase (HK) and a response regulator (RR) protein [70]. A few examples of TCS-regulated responses are antibiotic resistance, motility, nitrogen fixation and virulence [71, 72]. Genes coding TCS proteins are detected in the genomes of almost all sequenced bacteria but most abundantly in the genomes of gram-negative bacteria and cyanobacteria. Rodrigue *et al.* [73] reported that the *P. aeruginosa* genome has the largest number of putative genes, 63 encoding HKs and 64 encoding RRs, dedicated to TCSs among all bacterial genomes sequenced to date. TCSs are also found in yeast, fungi, slime molds, and plants, but higher eukaryotes lack these regulatory mechanisms. The absence of the TCS proteins in humans led scientists to target these systems for antimicrobial treatment against infections by pathogenic bacteria [74, 75].

Two highly conserved domains, the dimerization/histidine phosphotransfer domain, and the catalytic/ATP-binding domain are common to all HKs. In classical TCSs, the phosphotransfer domain is at the carboxyl terminus of the protein. HKs usually contain at least one more domain such as a sensor domain placed in an extracellular loop N-terminal to the dimerization/histidine phosphotransfer domain. 'Hybrid' proteins sometimes contain additional histidine phosphorylation sites [75, 76].

After an environmental signal is received, a reversible phosphorylation reaction takes place on a conserved histidine residue of the HK. In the majority of TCSs, this phosphoryl group is directly transferred to a conserved aspartate residue on the RR protein. In hybrid systems, the phosphoryl group is transferred to an aspartate residue in another domain of the histidine kinase and alternatively to a second histidine residue. Afterwards, the phosphoryl group is carried to the aspartate residue of the RR via a histidine phosphotransferase. Phosphorylated RR undergoes conformational changes which trigger changes in gene expression. In the inactive state (when not stimulated by a signal) of the HK, the initial reversible phosphorylation reaction takes place in the opposite direction and kinases act as phosphatases of their cognate RRs [75]. One advantage of such a global regulatory system is that it allows the simultaneous expression of unlinked genes in response to an environmental stimulus [77].

The abundance of TCS genes in bacteria is found to correlate with the variability of the niche bacterial cells inhabit. Bacteria that change the environment they live in frequently tend to expand the set of TCS genes in comparison with bacteria which do not change their habitats so much [78].

### 1.2.1 *Escherichia coli* BarA/UvrY

*E. coli* BarA (bacterial adaptive response)/UvrY(ultraviolet light-induced DNA repair response) two-component system is one of the conserved TCSs and a common feature with its homologues such as the BarA/SirA of *Salmonella*, ExpS/ExpA of *Erwinia*, VarS/VarA of *Vibrio*, and GacS/GacA of *Pseudomonas* spp. is the activation of ncRNA expression [79].

The hybrid sensor kinase BarA is from the family of tripartite sensor kinases and it consists of three domains: the main transmitter domain, the receiver domain, and a phosphotransfer domain at the C-terminus. A mutation in *barA* renders *E. coli* cells sensitive to oxidative stress due to a defect in catalase expression [80, 81]. Pernestig *et al*. [82] showed that BarA is the cognate kinase for the UvrY response regulator belonging to the FixJ family of proteins. Despite its nomenclature, the deletion of *uvrY* did not interfere with the UV-light induced DNA repair system; however the deletion of *barA* or *uvrY* affected CrsA function. Furthermore, the deletion of *barA* or *uvrY* had a negative influence on the growth of *E. coli* cells depending on the carbon source provided in the medium. When a glycolytic substrate such as glucose was used, the Δ*uvrY* mutant was outgrown by the wild-type (WT) strain; whereas in the presence of gluconeogenic substrates, the Δ*uvrY* mutant dominated the growth culture.

The physiological signals/conditions that trigger the Bar system are products of carbon metabolism such as formate and acetate, short chain fatty acids, and TCA cycle intermediates in some species [48, 83]. In the uropathogenic *E. coli* (UPEC), transcription of *barA* is induced after bacterial contact with the uroepithelial cell surface [84]. On the other hand, low pH (<5.5) is found to block the kinase activity of BarA, hence, the Bar system is not active under low pH growth conditions [79].

Studies indicate a link between the CsrB/CsrC sRNAs and the BarA/UvrY TCS in *E. coli*. Alterations to the Bar TCS downregulated the expression of *csrB*, and a Δ*csrB* mutant displayed a phenotype which is reminiscent of the Δ*barA* or Δ*uvrY* mutant phenotype [85, 86].

BarA/UvrY homologues in gram-negative pathogenic bacteria such as *Erwinia* and *Pseudomonas* spp. were found to regulate the expression of virulence genes. Furthermore, mutation of *varA* (coding the RR) resulted in attenuated virulence in *Vibrio* spp. It has been shown that the Bar TCS also regulates virulence in the avian pathogenic *E. coli* (APEC) serotype O78:K80:H9 and UPEC CFT073 [80, 87].

### 1.2.2 *Pseudomonas aeruginosa* CbrA/CbrB

*P. aeruginosa* CbrA/CbrB TCS was discovered by Nishijyo *et al.* [88]. This system consists of the NtrB/NtrC (nitrogen assimilation) family proteins: CbrA, the sensor

kinase and CbrB, the RR protein. In the mentioned study, Nishijyo and colleagues found that the CbrA/CbrB system controls the utilization of nitrogenous compounds. Further analysis of nutrient utilization in the Δ*cbrA* Δ*cbrB* and Δ*ntrB* Δ*ntrC* mutants by Li and Lu [89] supported these findings. Li and Lu demonstrated that the utilization of numerous organic compounds was abolished in a Δ*cbrA* Δ*cbrB* double deletion mutant and the CbrA/CbrB system monitored the carbon to nitrogen ratio in a coordinative manner with the NtrB/NtrC system. It has been found that the *P. aeruginosa* Δ*cbrB* and Δ*crcZ* mutants display similar phenotypes, suggesting that CrcZ governs some activities of the CbrA/CbrB system [68, 90]. The CbrA/CbrB and Crc systems also control swarming motility, cytotoxicity, resistance to antimicrobials and biofilm development in *P. aeruginosa* [91].

Glucose is not among the highly preferred carbon sources for the growth of *P. aeruginosa*. The presence of C4-dicarboxylates of the TCA cycle, especially of succinate, together with glucose triggers CCR and drives cells to the diauxic mode of growth. CCR of *P. aeruginosa* requires the CbrA/CbrB TCS, the sRNA CrcZ and the RBP Crc [90]. During the growth of *P. aeruginosa* cells on succinate rather than less-preferred substrates such as glucose or mannitol, levels of CrcZ are lowered due to the reduced activity of the CbrA/CbrB TCS. On the other hand, in the high abundance of less-preferred carbon sources, CbrB binds to an upstream activating sequence within the promoter region of *crcZ* and increases *crcZ* transcription, resulting in the titration of Crc proteins by CrcZ (Figure 1.3). As a result, high CbrA/CbrB activity allows the expression of degradative pathways of less-preferred carbon sources via Crc sequestration [68].

It was discovered that mutations in the *cbrA* and *cbrB* genes also affected histidine and arginine degradation pathways [88, 92]. Histidine and arginine are both good carbon and nitrogen sources for *P. aeruginosa* and their utilization requires enzymes encoded by the *hutCUHIG* and *aruCFGDBE* operons respectively [93, 94]. Activation of the *hut* and *aru* operons requires the binding of $\sigma^{54}$, encoded by the *rpoN* gene, to the RNA polymerase. It is presumed that CbrB upregulates the production of $\sigma^{54}$. Increased levels of the $\sigma^{54}$-bound RNA polymerase activate the *aotJQMP* operon coding the ABC family of transporter proteins for arginine uptake and triggers the transcription

of *argR* [89]. Gene expression from the *aru* operon can also be induced by the transcriptional regulator ArgR [94] (Figure 1.4).

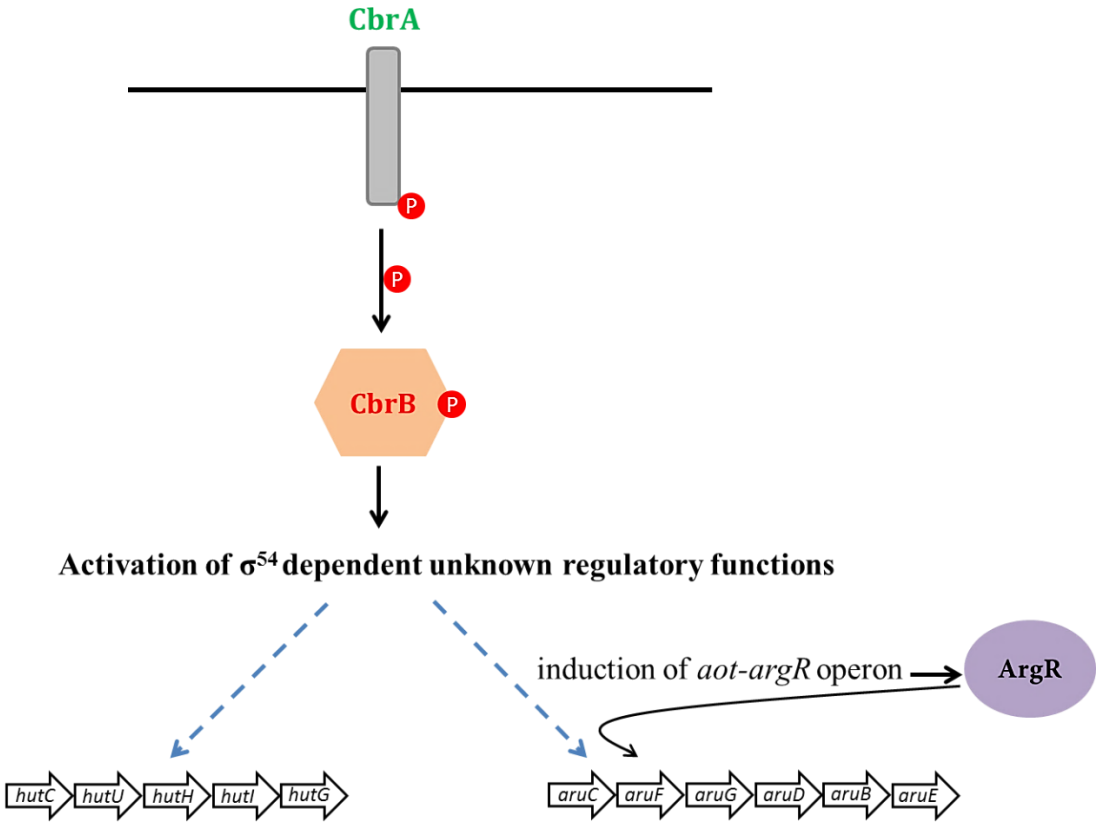


**Figure 1.4. Modulation of the histidine and arginine degradation pathways by the CbrA/CbrB TCS**
After activation by a stimulus (signals reflecting the C:N ratio), CbrA HK undergoes autophosphorylation and transfers the phosphoryl group to the CbrB RR protein. Phosphorylated CbrB activates expression of the *aot-argR* genes, *aru* and *hut* operons. Expression of the *aru* genes is also induced by the ArgR transcriptional regulator [88].

Sonnleitner *et al*. [91] identified a few targets of the CbrA/CbrB TCS with a role in the uptake and degradation of less-preferred carbon substrates in *P. aeruginosa*: *estA* (secreted esterase), *acsA* (acetyl-CoA synthetase), *bkdR* (regulator of branched-chain aa catabolism) and *aroP2* (aromatic aa uptake protein).

### 1.2.3 *Pseudomonas fluorescens* GacS/GacA

The *P. fluorescens* CHA0 strain colonises the rhizosphere of crop plants and benefits the plant by antagonizing plant-pathogenic fungi and nematodes. *P. fluorescens* CHA0 cells secrete lytic exoenzymes and other compounds with antibiotic properties [95].

All of these extracellular products are termed 'biological control factors' and the GacS/GacA TCS has been shown to play a key role in the biosynthesis of these factors [96].

The GacS/GacA TCS of *P. fluorescens* CHA0 controls the motility and synthesis of extracellular metabolites that function as antimicrobial agents such as pyoluteorin, hydrogen cyanide (HCN) and lytic enzymes such as phospholipase C and AprA (alkaline protease A) [97]. The regulatory mechanism usually follows an indirect route; activation of this TCS leads to the increased levels of ncRNAs and the translational interference by RBPs is reverted. Upon receiving a signal, the GacS kinase undergoes autophosphorylation and via the transfer of a phosphoryl group activates the RR GacA. The activated GacA protein enhances expression of the RsmX, RsmY and RsmZ sRNAs which sequester RsmA and RsmE RBPs. Both RsmA and RsmE repress the translation of genes coding biocontrol factors. For example, at low bacterial population densities, expression of the *hcnABC* operon is repressed by RsmA and RsmE and HCN is not produced [85, 98]. Heeb *et al.* [97] demonstrated that signals activating the Gac system were unrelated to AHLs and were released by *P. fluorescens* CHA0 at the end of the exponential growth. Later, Takeuchi *et al.* [99] demonstrated that TCA cycle intermediates can trigger expression of the GacA-dependent sRNAs in *P. fluorescens* CHA0.

Seaton *et al*. [100] demonstrated that mixed populations of $Gac^+$ and $Gac^-$ cells prevail in the environment. A major advantage of having an active GacS/GacA system is to have a better survival rate compared with other organisms due to the antimicrobial characteristics of the produced biocontrol factors. However, $Gac^-$ cells might benefit from better motility, faster proliferation and a reduced metabolic load in soil. This phenomenon is a good example of diversification within species for a better survival in changing environmental conditions.

## 1.3 Regulatory systems of *Pseudomonas aeruginosa*

*P. aeruginosa* is a gram-negative, rod-shaped bacterium that inhabits a wide range of environments such as soil, water, plant leaves and surfaces of the hospital equipment [101]. It has been extensively investigated as a human opportunistic pathogen associated with the infections of immunocompromised individuals such as those with

acquired immune deficiency syndrome (AIDS) and cancer, acute and chronic wounds, and the lungs of CF patients [102, 103]. *P. aeruginosa* cultures are characterised by a blue/green color and a grape-like odor. *P. aeruginosa* grows well aerobically but it is also adapted to grow under microaerobic or anaerobic conditions using alternative electron receptors such as nitrate, nitrite, and nitrous oxide [104]. Reduction of nitrate to dinitrogen generates the motive force driving ATP synthesis and allows growth under anaerobic conditions. Alternatively, *P. aeruginosa* can acquire the energy required for anaerobic growth from arginine catabolism by substrate-level phosphorylation [105, 106].

### 1.3.1 Adaptation mechanisms that facilitate the versatility of *P. aeruginosa*

*P. aeruginosa* is also a major contributor to the hospital-acquired infections [107, 108]. Sequencing results showed that the genome of the PAO1-UW reference strain is 6.3 Mb with around 10% of its genes coding regulators of gene expression [109, 110]. This large and complex genome provides *P. aeruginosa* with great versatility for utilizing a large array of organic compounds and growing at a broad temperature range [110]. Adaptation mechanisms of *P. aeruginosa* include (i) formation of biofilms, (ii) antibiotic resistance, (iii) motility, (iv) physiological flexibility (formation of the outer capsule, control over membrane permeability), and (v) morphological changes [111, 112].

Biofilm formation is a group behaviour that contributes to the pathogenesis of *P. aeruginosa* [113]. Biofilms can be defined as communities of bacterial cells that are encased in an extracellular polymeric matrix (EPM) made up of polysaccharides, proteins, lipids and extracellular DNA (eDNA), of their own secretion. Sessile (surface-attached) bacteria differ from planktonic (free-swimming) bacteria in many aspects. Sessile bacteria are at least 1000-fold more resistant towards antibiotics, detergents, and hydrogen peroxide ($H_2O_2$). Up to 40% of all cellular proteins are differentially expressed during biofilm growth and bacteria in biofilms survive much longer under changing environmental conditions (pH, ion concentration, osmolarity, viscosity, nutrient availability, gas exchange) [69, 114].

Biofilm formation involves changes in the expression of motility genes as bacteria stop floating around and adhere to a substratum or to each other. Several steps of biofilm

formation include 1) initial adherence of the planktonic cells onto a solid surface, 2) irreversible attachment of the bacterial cells onto a surface via the type IV pili, 3) cell division and growth of bacteria, 4) EPM synthesis, 5) formation of microcolonies with void spaces structuring the complex three-dimensional (3D) architecture of biofilms [115].

Schleheck and colleagues [115] reported that *P. aeruginosa* PAO1 cells grow as aggregates when they are grown as standard liquid cultures; in a medium with sufficient nutrients and moderate shaking. Upon examination of these aggregates under the microscope, they found out that bacteria were submerged in an EPM of which the major constituent was eDNA. Formation of these aggregates was reversible and their dispersal seemed to be triggered after entering the stationary phase of growth when substrates required for cell division such as oxygen and carbon became limited. Other studies showed that nitric oxide, unsaturated fatty acids, cyclic di-GMP (c-di-GMP) levels and bacteriophage Pf4 of *P. aeruginosa* also have roles in biofilm dispersal. Cell death as a consequence of superinfection by the filamentous, Pf1-like prophage designated Pf4 within *P. aeruginosa* microcolonies was demonstrated by Webb *et al.* [116]. With the development of a *Pf4* deletion mutant (PAO1B1Δ*Pf4*), the study of phage release from different strains was rendered possible as strains such as the WT PAO1 which possesses prophages naturally are resistant to re-infection whereas the Δ*Pf4* mutant is susceptible to phage killing [116, 117].

Many bacteria translocate until an environment with the most favourable conditions is found [118]. *P. aeruginosa* displays various types of motility to translocate: swimming, swarming, twitching, gliding, sliding and surfing [113, 119, 120]. The single flagellum of *P. aeruginosa* enables swimming and adherence to surfaces. Type IV pili-mediated twitching allows bacterial cells to move on solid surfaces. On the other hand, *P. aeruginosa* swarming is mediated by the flagellum and type IV pili. Swarming motility requires a) rhamnolipids (rhl) or the rhamnolipid precursor 3-(3-hydroxyalkanoyloxy) alkanoic acid (HAA) to surmount the surface tension of water and b) cell-cell interactions as it is the result of a collective behaviour [107, 108, 113, 121]. Gliding uses focal adhesion complexes instead of relying on the flagellum or pili. Sliding is hard to differentiate from swarming as it is also dependent on surface

surfactants and cells spread outwards from an origin as they grow. It is possible that cells that lost the ability to swarm spread across a surface by sliding [120].

The morphologies of *P. aeruginosa* strains isolated from acute and chronic wounds differ greatly. One way to distinguish colonies from chronic wounds is to look for a mucoidy appearance which is the outcome of alginate overproduction. Furthermore, chronic infection isolates are usually non-motile as they tend to aggregate and develop biofilms that provide protection from the host immune system and antimicrobials [122]. Yoon *et al*. [123] discovered that alterations in oxygen levels promote morphological changes which eventually influence characteristics of *P. aeruginosa* biofilms. When grown in LB with enough aeration, PAO1 cells were rod-shaped whereas cells that grew under anaerobic conditions in the presence of nitrate ($NO_3$) ions were elongated and formed thicker biofilms.

The high mortality rate of *P. aeruginosa* infections is mostly due to the intrinsic and acquired antibiotic resistance of this nosocomial pathogen. The intrinsic resistance of *P. aeruginosa* to most β-lactams, tetracycline, chloramphenicol and fluoroquinolones was initially attributed to the low permeability of the outer membrane. The contribution of the efflux pumps to the MDR of *P. aeruginosa* was discovered later [124]. In addition to the efflux pumps, the resistance mechanisms of *P. aeruginosa* include cleavage by β-lactamases and aminoglycoside-modifying enzymes, modification of lipopolysaccharides, and mutations in gyrase and/or topoisomerase genes [104]. Mutational changes and horizontal gene transfer (exchange of plasmids and transposons) lead to the establishment of these resistance mechanisms [125].

Mutational changes resulting in the upregulation of *P. aeruginosa* MDR efflux pumps, mainly MexAB-OprM, MexCD-OprJ, MexEF-OprN, and MexXY, have a big impact on the development of resistance to most antimicrobials [67, 126]. The best-characterised efflux pump MexAB-OprM removes β-lactams, chloramphenicol, fluoroquinolones, macrolides, sulphonamides, trimethoprim, tetracycline, novobiocin, detergents and some dyes. β-lactam-inducible AmpC (ampicillin) β-lactamase contributes to the development of resistance against cephalothin and ampicillin [127]. Additionally, the contribution of MexAB-OprM and MexEF-OprN to the export of QS signalling molecules have been demonstrated [128, 129].

### 1.3.2 Virulence determinants of *P. aeruginosa*

Apart from the adaptation mechanisms listed in 1.3.1, *P. aeruginosa* produces a variety of virulence factors like pyocyanin (PYO), AprA, elastase, PA-IL lectin and exotoxin A to establish a successful infection [111, 130]. Expression of genes coding these virulence factors, the determinants of biofilm formation, and secondary metabolites were found to be controlled by AHL and 2-alkyl-4(1H)-quinolone (AQ)-dependent QS systems in *P. aeruginosa* [111, 131]. However, it should be noted that the gene regulation cascade of *P. aeruginosa* is not limited to QS systems but that QS systems are integral components of bigger global regulatory networks where they intertwine with many other regulatory elements including TCSs [132].

Phenazines are a group of secondary metabolites that by definition are not essential for the growth of bacteria but required to enhance the virulence of pathogenic pseudomonads. Phenazine compounds are low molecular weight and contain a three-ringed heterocyclic nucleus with a nitrogen substitution at positions 5 and 10. Phenazines produced by *P. aeruginosa* include 5-methyl-1-hydroxy phenazinium betaine (shortly PYO), phenazine-1-carboxamide (PCN), phenazine-1-carboxylic acid (PCA), chlororaphine (oxychlororaphine 5, 10-dihydro derivative), aeruginosin A (5-methyl-7-amino-1-carboxyphenazinium betaine), and aeruginosin B (5-5-methyl-7-amino-1-carboxy-3-sulphophenazinium betaine). Phenazines such as PYO constitute one of the distinctive features of *P. aeruginosa* infections, the blue-green color of PYO can be detected in the pus around the infection sites such as eyes [133].

PYO is a redox-active phenazine compound with antifungal, antibacterial and antiprotozoal antibiotic activity. High cell population densities and suboptimal nutrient conditions favour PYO production [134, 135]. Sorensen and Joseph postulate that phenazines may have an effect on host defense mechanisms in the chronic lung infections of *P. aeruginosa* as it is likely that they escape neutralization by antibodies [133]. Huang *et al*. [134] showed that PYO regulates pyruvate secretion and intracellular NADH/$NAD^+$ ratio and the Crc system controls PYO production. Moreover, Dietrich *et al*. [136] demonstrated that PYO is the physiological signal which upregulates the *mexGHI* (multidrug efflux pump) operon and *opmD* (outer periplasmic membrane) gene via QS.

Extracellular proteases also contribute to the full virulence of *P. aeruginosa*. Bacterial proteases degrade host proteins to remove the physical defense barriers and overcome the host immune system. Seven extracellular proteases, six of which are endopeptidases while the seventh is an aminopeptidase, of *P. aeruginosa* have been reported. These are pseudolysin (LasB protease or elastase), aeruginolysin (alkaline protease), staphylolysin (LasA protease), lysyl endopeptidase (protease IV or PrpL), PASP (*P. aeruginosa* small protease), LepA (large exoprotease A), and PAAP (*P. aeruginosa* aminopeptidase) [137, 138].

Elastase is the most abundant endopeptidase of *P. aeruginosa* and it has the highest proteolytic activity on casein or azocasein among others. Moreover, only elastase can degrade elastin which is highly abundant in the connective tissue. It can also degrade a wide variety of host proteins such as collagen types III and IV, proteoglycans, immunoglobulins A and G, α1-proteinase inhibitor, fibrinogen, cytokines, surfactant proteins A and D and laminin [139-143]. Furthermore, elastase interferes with the T3SS and facilitates epithelial cell invasion [144]. Because of these characteristics, elastase vastly contributes to *P. aeruginosa* pathogenesis.

Ohman *et al*. [145] discovered that the elastinolytic activity of *P. aeruginosa* was also dependent on the product of the *lasA* gene. Later on, Kessler and colleagues [137] studied this newly discovered LasA protease in parallel with the staphylolytic protease (named for the ability to cleave the pentaglycine bonds in the peptidoglycan of *S. aureus*) of *P. aeruginosa* based on the amino acid sequence homology and common physiochemical properties and concluded that LasA protease also has staphylolytic activity. Additionally, LasA enabled *P. aeruginosa* cells to take advantage of the host cell environment by facilitating the shedding of the cell surface molecule syndecan-1 [146].

### 1.3.3 Secretion of *P. aeruginosa* virulence determinants

*P. aeruginosa* exports its virulence determinants across the inner and outer cellular membranes and the periplasmic space in a one or two-step mechanism using secretion tubes [147]. The majority of *P. aeruginosa* virulence factors are translocated via the type II secretion system (T2SS), also called the general secretion pathway.

T2SS is a two-step secretion mechanism involving the Sec, Tat, Xcp and Hxc systems. In the first step, where proteins are transported across the inner membrane and into the periplasm, either the Sec or Tat system can be used. Once in the periplasm and properly folded, proteins are exported across the outer membrane by the Xcp or Hxc system [147]. LasA protease and elastase of *P. aeruginosa* are secreted via the Xcp secretion system [148, 149]. The alkaline phosphatase (PhoA) protein has been shown to be secreted by the Hxc system [150]. On the other hand, AprA is transported via the type I (T1SS) secretion system which uses a one-step mechanism for the translocation of proteins across both membranes [151].

*P. aeruginosa* uses two other secretion systems to translocate proteins directly into the cytosol of the host cell. Type III (T3SS) and type VI (T6SS) secretion systems of *P. aeruginosa* both form a needle-like secretion machinery and play a role in acute and chronic infections respectively. The T3SS of *P. aeruginosa* consists of approximately 20 proteins, 4 of which -ExoS, ExoT, ExoU and ExoY- are linked to the virulence of this organism due to their cytotoxicity [152].

The role of T6SS in protein export was first demonstrated by Bladergroen *et al.* [153] in *Rhizobium leguminosarum*. Mutations in *imp* genes coding the core components of the secretory apparatus influenced the symbiotic host range of the bacterium. Studies conducted in *P. aeruginosa* revealed that a functional T6SS machinery requires the products of around 15 genes that are found in the Hcp secretion island I (HSI-I) [154, 155]. The Hcp1 protein of *P. aeruginosa* is a ring-shaped protein and forms the secretion tube in hexamers whereas the valine-glycine repeat protein G (VgrG) acts as a puncturing device to penetrate through the bacterial cell envelope. Structural studies of Hcp1 and VgrG highlighted the similarity of these proteins to the phage tail proteins, creating an image of T6SS as an inverted phage tail on the surface of bacterial cells [156, 157]. Fha1, a domain associated protein in the T6SS machinery, integrates phosphoregulation into the modulation of the T6SS. Phosphorylation of Fha1 by PpkA (a transmembrane serine-threonine kinase) activates Fha1 and results in the synthesis of Hcp1. PppA phosphatase interferes with the phosphorylation of Fha1 [155, 158-160].

The T6SS machinery of *P. aeruginosa* has been linked to bacterial fitness in a chronic infection model of the rat lung. Mutations of HSI-I genes resulted in decreased fitness of bacterial cells [159, 161].

### 1.3.4 Regulation of *P. aeruginosa* virulence

Research on therapeutic approaches to overcome the antibiotic resistance and virulence of *P. aeruginosa* has been centred on the inhibition of the QS systems as they play a central role in the control of virulence factor production, biofilm formation and antibiotic resistance [162]. Recently, bacteriophages have also started to be considered as alternatives for the treatment of *P. aeruginosa* infections and there have been some promising human trials [163].

It is known that the virulence of *P. aeruginosa* is controlled by multiple signalling systems that are interconnected. In addition to the QS circuitry, TCSs also govern the synthesis of some virulence factors and take part in the transition from an acute to a chronic mode of infection [164, 165]. The Gac/Rsm system has major roles in the virulence and persistence of *P. aeruginosa* [166, 167]. In the following sections, QS systems, external contributors to the QS-mediated regulation and the Gac/Rsm system of *P. aeruginosa* are explained more in detail.

#### 1.3.4.1 QS circuitry

In the last several decades it was discovered that bacteria, as living animals, can communicate with each other both in intraspecies and interspecies manner via 'quorum sensing' [168]. QS-regulated processes include bioluminescence, symbiosis, competence, protein secretion, virulence factor production, biofilm formation and maturation, motility and conjugation in diverse species of bacteria [21, 101, 169, 170]. Moreover, effects of the QS signal molecules on host-pathogen interactions and host immune-modulatory responses were discovered [104, 168].

The AHL and AQ-dependent QS systems of *P. aeruginosa* are one of the best-studied examples of QS systems in gram-negative bacteria [171]. The AHL synthases LasI and RhlI and their cognate regulators LasR and RhlR are homologues of the LuxI/LuxR QS circuitry of *Vibrio fischeri*, and autoinducers (AI) of the *las* and *rhl*

systems are *N*-3-oxododecanoyl-L-homoserine lactone (3O-C12-HSL) and *N*-butyryl-L-homoserine lactone (C4-HSL) molecules [132].

The accumulation of bacterial cells in a confined environment results in increased concentrations of AIs [101]. At high cell populations, when 3O-C12-HSL is synthesised at threshold concentrations by the LasI synthase, binding of LasR to 3O-C12-HSL molecules results in its activation. LasR/3O-C12-HSL complex binds to the palindromic sequences around the promoter regions of target genes such as *lasB, lasA, aprA, toxA, xcpP, xcpR, rsaL, pqsH, pqsR, lasI* and *rhlR* [130, 172-174]. Moreover, it has been demonstrated that the *las* system promotes the maturation of *P. aeruginosa* biofilms [170, 175].

In a similar mechanism, the *rhl* system regulates expression of the *lasB, lasA, aprA, rpoS* genes and *phz* and *hcn* operons [103]. RhlR mediates swarming motility by inducing expression of *rhlAB* genes coding rhamnolipids [113]. Interestingly, the *rhl* system represses expression of the genes linked to the T3SS which plays a key role in the establishment of acute infections [112].

Sequencing of *P. aeruginosa* genome revealed two other LuxR homologue proteins, QscR (quorum sensing control repressor) and VqsR (virulence and quorum sensing regulator) both of which lack an associated LuxI-type protein. Studies on QscR demonstrated that it inhibits *lasI* and *rhlI* transcription by forming heterodimers with LasR and RhlR when AHL concentrations are low. The deletion of *qscR* increased virulence and resulted in premature expression of some genes controlled by the *las* and *rhl* systems [176, 177]. On the other hand, VqsR which was found to be under the control of the *las* system upregulated *lasI* transcription [178]. Juhas *et al.* [179] discovered that VqsR was important for protease and PYO production. Furthermore, a Δ*vqsR* mutant had reduced levels of siderophores [180]. A study conducted by Liang *et al.* [181] demonstrated that VqsR blocks the QscR activity directly and hence, regulates the *las* and *rhl* systems indirectly.

In addition to the control of the *rhl* system by the *las* system both at transcriptional and post-transcriptional levels, and regulation by QscR and VqsR, the AHL-dependent QS system of *P. aeruginosa* is under the control of many other regulators such as the

Gac/Rsm regulatory circuit, AQ-dependent QS system, Vfr (virulence factor regulator), RpoS (stationary phase σ-factor) and MvaT and RsaL transcriptional regulators [21, 182] (Figure 1.5).

The cAMP receptor protein (CRP), Vfr, of *P. aeruginosa* has been considered as one of the master regulators of gene expression due to its control over 100 genes [177]. Vfr responds to the intracellular metabolic status of the cell and modulates type IV pili assembly (twitching is abolished in Δ*vfr* mutants), upregulates *lasR* transcription by binding to a CRP consensus sequence upstream of *lasR* and increases exotoxin A and PYO production [112, 183, 184].

The expression of *rsaL* located between the *lasR* and *lasI* genes is under LasR control. RsaL has been shown to control virulence factor production indirectly by binding to the *lasI* promoter at the same time as the LasR/3O-C12-HSL complex and repressing *lasI* transcription, and directly by binding to the promoters of the *phz* and *hcnAB* operons [162]. It was also demonstrated that a Δ*rsaL* mutant overproduced AHLs [185].

The GacA regulator upregulates *lasR* and *rhlR* transcription directly and *lasI* translation indirectly through sequestration of the RsmA proteins by RsmY and RsmZ sRNAs [186].

*P. aeruginosa* QS is dependent on growth phase and environmental conditions. The stationary phase sigma factor RpoS represses *rhlI* expression [187]. The MvaT transcriptional regulator was found to be important for *lecA* expression and the addition of exogenous AHLs to the growth culture of the *mvaT* strain enhanced *lecA* expression. Hence, it can be suggested that MvaT links the growth phase and QS regulation in *P. aeruginosa* [188].

AQs were first discovered for their antibiotic properties in *P. aeruginosa*, however, their role in QS was overlooked for some time [189]. Major AQ molecules produced by *P. aeruginosa* are 2-heptyl-3-hydroxy-4-quinolone (*Pseudomonas* quinolone signal, PQS), 2-heptyl-4-quinolone (HHQ), 2-nonyl-4-quinolone (NHQ), 2-heptyl-4-quinolone *N*-oxide (HHQNO) and 2-nonyl-4-quinolone *N*-oxide (NHQNO) [182].

Expression of *pqsR* and *pqsH* genes of the AQ-dependent QS system of *P. aeruginosa* is induced by the *las* system. Transcription of *pqsR* is under positive regulation by LasR and negative regulation by RhlR [190]. PqsR activates the *pqsA* promoter region and triggers expression of the *pqsABCDE* operon, adjacent *phnA* and *phnB* genes responsible for anthranilate synthesis, and *pqsR*, creating an autoinduction loop [112, 191, 192]. HHQ is synthesised in a condensation reaction (catalyzed by PqsABCD) of anthranilate and β-keto fatty acids. HHQ to PQS conversion (by the addition of a hydroxyl group) is catalyzed by PqsH, a FAD-dependent monooxygenase. PQS and HHQ are both inducers of PqsR (Figure 1.5) [193]. A mutation in *pqsE* does not affect PQS production but downregulates the production of some exoproducts [194].

The absence of PQS affected elastase, lectin and PYO production which are controlled by the *rhl* system [175]. McKnight *et al*. [195] showed that PQS induces *rhlI* expression. Furthermore, PQS promotes membrane vesicle formation and acts as an iron chelator [196]. D'Argenio *et al*. [197] demonstrated that the deletion of *pqsL* coding a FAD-dependent monooxygenase leads to the increased levels of PQS and a Δ*pqsL* mutant has a lytic colony morphology. The authors speculated that induction of the lytic lifestyle of the filamentous bacteriophage or bacteriocins might trigger autolysis of the Δ*pqsL* mutant.

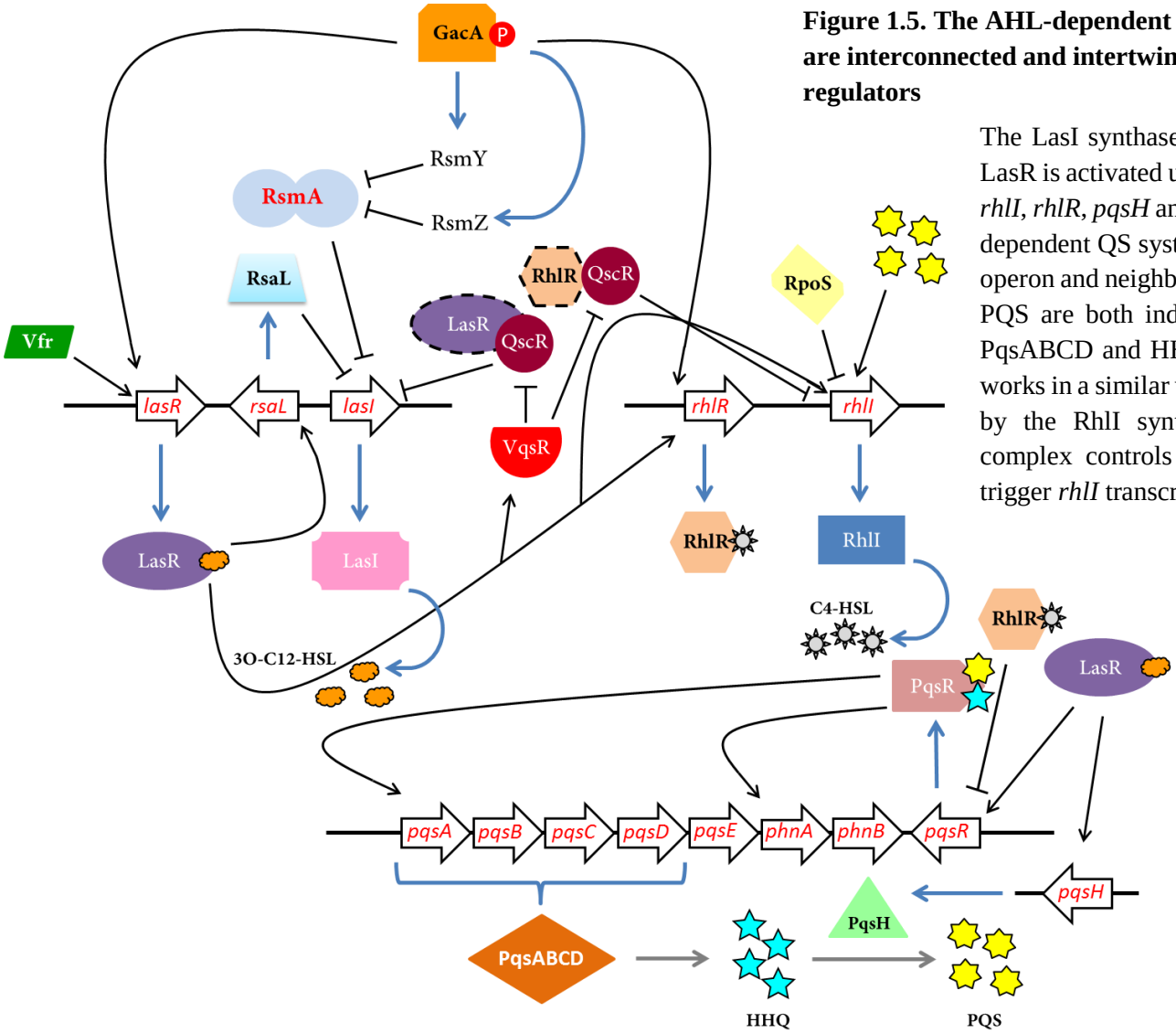


**Figure 1.5. The AHL-dependent and AQ-dependent QS systems of *P. aeruginosa* are interconnected and intertwined with transcriptional and post-transcriptional regulators**

The LasI synthase produces 3O-C12-HSL signalling molecules and LasR is activated upon binding to 3O-C12-HSL triggering *rsaL*, *vqsR*, *rhlI*, *rhlR*, *pqsH* and *pqsR* transcription and activating the *rhl* and AQ-dependent QS systems. PqsR induces transcription of the *pqsABCDE* operon and neighboring *phnAB* genes. Signalling molecules HHQ and PQS are both inducers of PqsR. HHQ production is catalyzed by PqsABCD and HHQ is converted to PQS by PqsH. The *rhl* system works in a similar way to the *las* system; C4-HSL molecules produced by the RhlI synthase activate the RhlR protein. RhlR/C4-HSL complex controls *pqsR* transcription negatively. High PQS levels trigger *rhlI* transcription.

VqsR positively regulates the expression of *lasI* and *rhlI* indirectly by blocking the QscR activity. QscR inhibits *lasI* and *rhlI* transcription by forming heterodimers with the LasR and RhlR regulators (inactive state of proteins is represented by dashed lines). The sigma factor RpoS represses *rhlI* and RsaL represses *lasI* transcription. Phosphorylated hence, active GacA protein upregulates *lasR* and *rhlR* transcription directly, and *lasI* translation indirectly due to the sequestration of the RsmA proteins by the RsmY and RsmZ sRNAs. Vfr also upregulates *lasR* transcription. The figure is modified from Williams *et al*. [170].

#### 1.3.4.2 The Gac/Rsm system of *P. aeruginosa*

The GacS/GacA TCS controls the virulence of *P. aeruginosa* by affecting the production of exoenzymes, secondary metabolites and QS together with the RsmA protein [186, 198]. Upon interaction with biotic and abiotic signals, the GacS sensor kinase is activated and undergoes autophosphorylation, with a phosphate group being transferred from the first histidine residue ($H_1$) to an aspartate (D) and a second histidine ($H_2$) residue respectively. Then the phosphate group is transferred to the aspartate residue of the GacA response regulator. Activated GacA triggers the transcription of *rsmY* and *rsmZ* which sequester RsmA and relieve the translational repression on target mRNAs (Figure 1.6).

Motility and T3SS are important to establish acute infections of *P. aeruginosa* [199] whereas chronic infections are characterised by biofilm formation, mucoidy morphology (a result of alginate overproduction), O-antigen production and active T6SS [200]. Recent studies demonstrate that *P. aeruginosa* coordinates the switch from an acute to a chronic infection through the Gac/Rsm system and RetS (regulator of exopolysaccharide and type III secretion)/LadS (lost adherence sensor) regulators [122, 201]. The GacS/GacA TCS itself is under the control of the LadS and RetS sensors (Figure 1.6) [112]. LadS and RetS are both sensor kinases without a cognate response regulator. LadS functions in parallel to GacS and enhances the transcription of *rsmZ*. RetS exerts its negative control on the GacS/GacA TCS by preventing the autophosphorylation of GacS [202, 203]. Goodman *et al.* [122] reported that inactivation of *retS* resulted in the premature expression of genes related to biofilm formation and attenuated virulence of *P. aeruginosa*. Later, using murine acute infection models, it was proved that the RetS sensor kinase is required for T3SS activation and *P. aeruginosa* colonization [202].

The RsmA protein forms a link between the Gac system and the virulence of *P. aeruginosa*. Direct regulation by RsmA was first demonstrated for the *hcnA* transcript (HCN production) by Pessi *et al*. [204]. A reduction in protease, elastase, PYO, and PA-IL lectin production and the staphylolytic activity as a result of *rsmA* overexpression was also demonstrated in the same study. Furthermore, negative control of RsmA on the synthesis of 3O-C12-HSL and C4-HSL was discovered using *lasI'-'lacZ* and *rhlI'-'lacZ* translational fusions [204]. In another study carried out by

Heurlier *et al*. [121], reduced rhamnolipid production by the Δ*rsmA* mutant was detected and using a *rhlA*'-'*lacZ* translational fusion, positive regulation of *rhlA* by RsmA was confirmed. Increased levels of the *rsmZ* transcript and swarming motility by *rsmA* overexpression was also demonstrated.

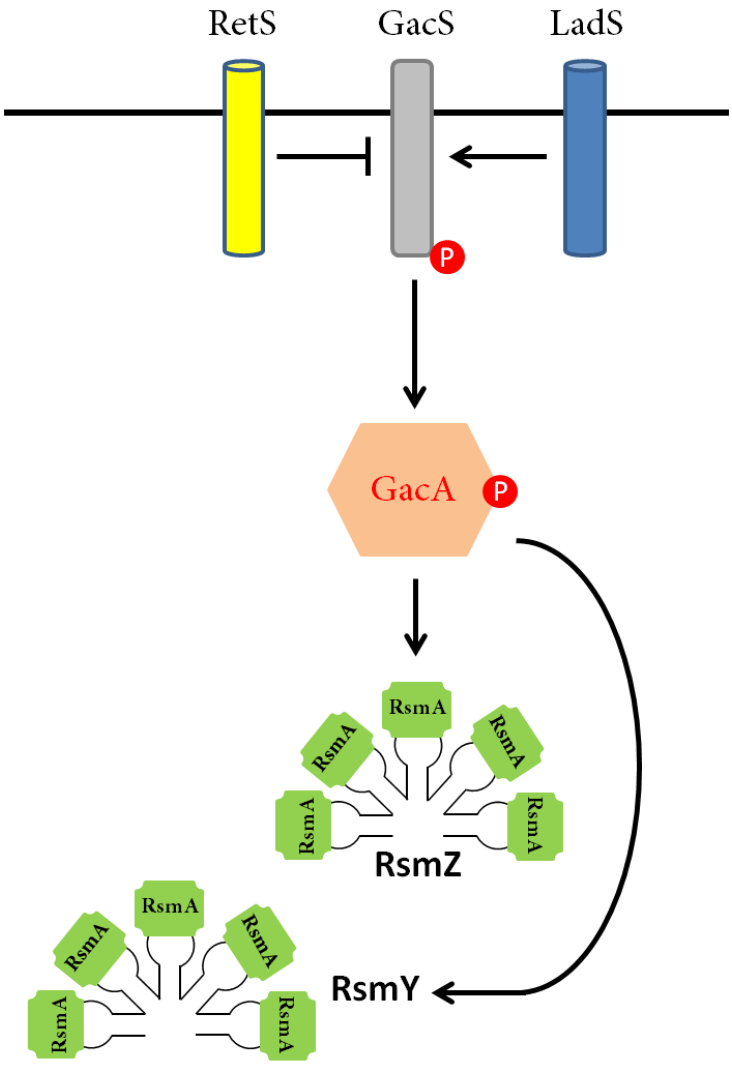


**Figure 1.6. The Gac/Rsm system of *P. aeruginosa***
The GacS kinase, positively controlled by LadS and negatively controlled by RetS activates the GacA protein upon transfer of a phosphoryl group. Phosphorylated GacA triggers the transcription of *rsmY* and *rsmZ*. Rsm sRNAs sequester multiple copies of the RsmA protein. The figure is modified from Jimenez *et al*. [112].

Mulcahy *et al*. [205] demonstrated that *rsmA* deletion prevented secretion of the T3SS effector proteins ExoS and ExoT. Furthermore, the positive control of RsmA on T3SS and negative control on T6SS was verified using *lacZ* reporters of *exsD* (T3SS) and *tssa1* (T6SS) in the Δ*rsmA* mutant. In addition, positive regulation of the type IV pili

genes and negative regulation of exopolysaccharide production by RsmA have been reported [202, 206]. RsmA binds to the mRNA of *psl* which codes one of the major exopolysaccharides that contribute to the EPM structure in biofilms and prevents ribosome binding, downregulating protein translation. Therefore, a Δ*rsmA* mutant develops robust biofilms [207, 208]. These findings altogether indicate the role of RsmA in the switch from an acute to a chronic mode in *P. aeruginosa* infections.

### 1.3.5 Discovery of RsmN in *P. aeruginosa*

In a previous set of experiments, a genomic library of the *P. aeruginosa* PAO1-L strain was introduced into the Δ*rsmA* mutant which is deficient in swarming motility, of the PAO1-N background. Briefly, random 2-4 kb DNA fragments obtained from the partial digestion of the PAO1-L chromosomal DNA with *Sau*3AI were cloned in the multicopy expression vector pME6000 (linearised by *BamH*I). The PAO1-L strain was used instead of PAO1-N due to the 58 kb deletion (between bases 724103 – 780973) and single nucleotide polymorphisms (SNPs) such as *bifA* (*PA4367*) and *mexF* (*PA2494*) identified in the PAO1-N genome. Amongst the genes present in the deleted region are *toxR* (*PA0707*), *hemO* (*PA0672*), *gloA2* (*PA0710*), *cat* (*PA0706*), and *hxc* pseudopilin genes (*PA0677-PA0682*) [209]. The Δ*rsmA* mutant (PAZH13) was transformed with the recombinant plasmids. From this screen, 14 clones were found to restore Δ*rsmA* swarming and 4 of these shared *PA5183* and *PA5184* genes and their intergenic region (Figure 1.7) [210]. *In silico* analysis of this intergenic region identified an ORF that encoded a protein of the CsrA/RsmA family. This protein, named RsmN, was 34% identical and 52% similar to RsmA.

After the discovery of the *rsmN* ORF, searching other available genomes identified homologues of RsmN. Amino acid sequence comparisons of the CsrA homologues found in *Enterobacteriaceae*, RsmA proteins of γ-proteobacteria closely related to *P. aeruginosa*, RsmE from *P. fluorescens, Pseudomonas protegens* and *Pseudomonas syringae* (*P. syringae*), as well as the newly discovered orthologues of *P. aeruginosa* RsmN suggested duplication of a common *csrA* ancestor gene. According to this theory, most *Pseudomonas* species have two alleles of the gene, *rsmA* common to all, and a copy of either *rsmE* (e.g. *P. fluorescens*) or *rsmN* (e.g. *P. aeruginosa*) [211].

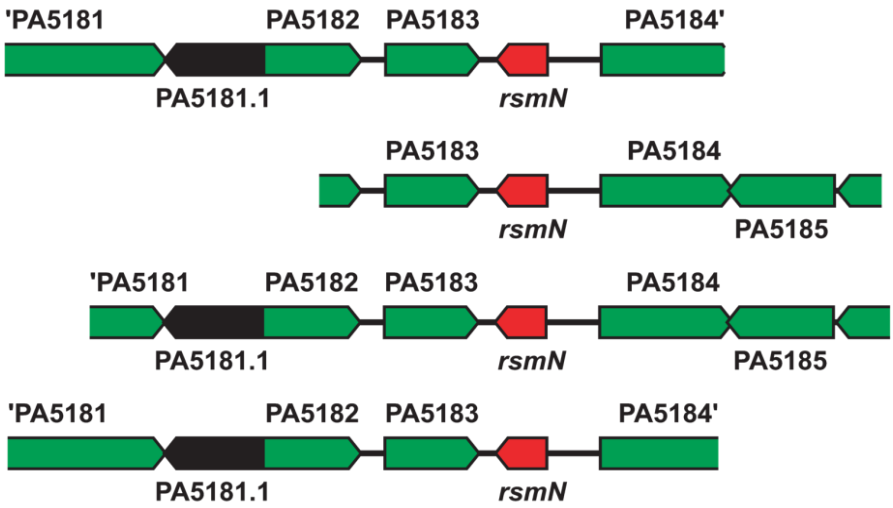


**Figure 1.7. The context of the genomic bank fragments inserted in the four clones that restored the Δ*rsmA* swarming motility**

In this diagram of the genomic bank fragments identified for the restoration of the swarming motility of the Δ*rsmA* mutant, the *rsmN* ORF is depicted in red, genes in the sense direction to *rsmN* are illustrated in black and genes in the antisense direction to *rsmN* are illustrated in green. The shortest genomic bank fragment (inserted in pMMB-16) chosen for further cloning steps in this study is the second from the top.

### 1.3.5.1 Sequence and structure comparisons of RsmN and RsmA

The RsmA/CsrA proteins function as dimers. RsmA monomers consist of five-stranded antiparallel β-sheets and an α-helix each. The β2-β3-β4 strands are connected to each other in the centre via hydrogen bonds (H-bond). The β1 strand of one monomer is H-bonded to the β4, and the β5 strand is H-bonded to the β2 strand of the other monomer. The α-helices project outwards from the C-terminals [53]. It was found that RsmN has 10 more amino acids than RsmA (71 aa vs. 61 aa) and it is slightly larger (7.8 kDa vs. 6.9 kDa) [212]. A comparison of the X-ray crystallography structures, as illustrated in Figure 1.8, revealed that the fundamental structural difference between RsmN and RsmA is the positioning of the α-helices. In RsmN, α-helices are positioned in between the β2 and β3 strands instead of protruding from the C-terminals. Nevertheless, the overall composition of the protein (five β-strands and an α-helix per monomer) and the RNA-binding pocket were conserved [211].

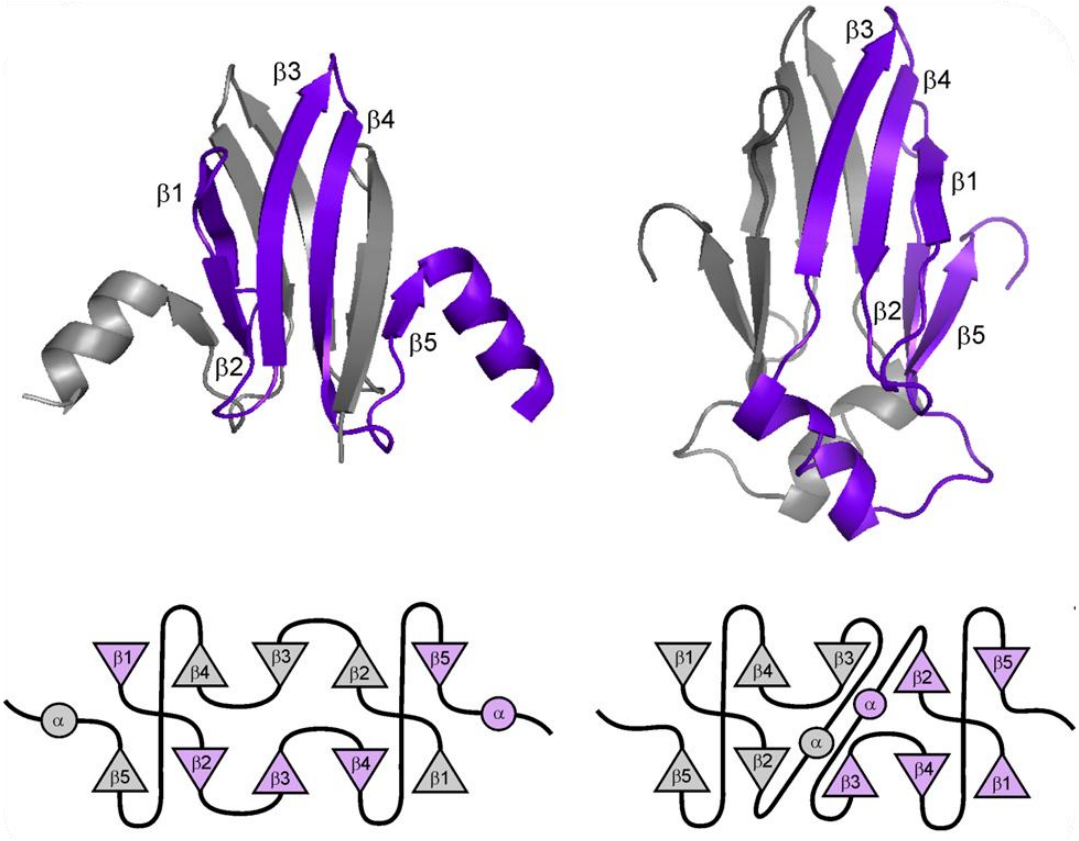


**Figure 1.8. X-ray crystallography structures of the RsmA (left) and RsmN (right) proteins (above) and topology maps of the β-strands and α-helices (below)**
Different positioning of the α-helices changes the shape of the protein. RsmN α-helices (right) are positioned in between the β2 and β3 strands instead of protruding from the C-terminals like RsmA α-helices (left). Protein monomers are colored in purple and gray. The β-strands of each monomer are numbered 1-5. The figure is taken from Morris *et al*. [211].

An amino acid comparison of the RsmA and RsmN proteins revealed conserved residues (Figure 1.9). RsmN $Leu_4$-$Ile_5$-$Leu_6$-$Arg_8$-$Arg_9$-$Gly_{11}$-$Glu_{12}$-$Thr_{15}$-$Leu_{16}$-$Val_{40}$-$Gly_{45}$-$Asn_{46}$-$Gln_{47}$-$Arg_{49}$-$Gly_{51}$-$Ala_{54}$-$Pro_{55}$-$Val_{58}$-$Arg_{62}$-$Glu_{64}$ residues are equivalent to RsmA $Leu_2$-$Ile_3$-$Leu_4$-$Arg_6$-$Arg_7$-$Gly_9$-$Glu_{10}$-$Thr_{11}$-$Leu_{12}$-$Val_{22}$-$Gly_{27}$-$Asn_{28}$-$Gln_{29}$-$Arg_{31}$-$Gly_{33}$-$Ala_{36}$-$Pro_{37}$-$Val_{40}$-$Arg_{44}$-$Glu_{46}$ residues. Some of these conserved residues were found to play structural roles. It has been demonstrated that RsmA $Arg_6$ and $Glu_{46}$ ($Arg_8$ and $Glu_{64}$ in RsmN) formed an interchain salt-bridge. RsmA $Ala_{36}$ and $Pro_{37}$ ($Ala_{54}$ and $Pro_{55}$ in RsmN) located at the end of the β4-strand were presumed to have a role in the formation of H-bonds with other residues on the β5-strand. Furthermore, it was speculated that $Gly_{33}$ ($Gly_{51}$ in RsmN) is present to keep the β4-strand twisted [212]. Moreover, Heeb *et al*. [53] showed that $Arg_{44}$ ($Arg_{62}$ in RsmN) has a role in the RNA-binding and biological function of RsmA.

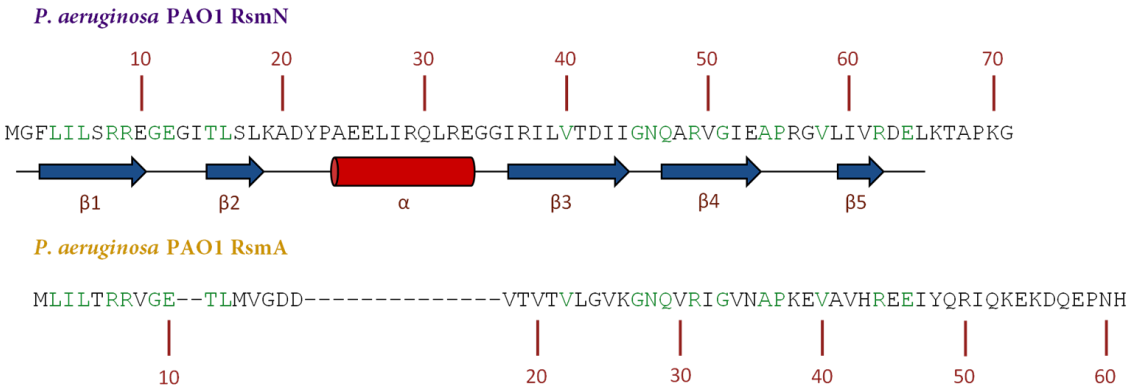


**Figure 1.9. Structure-based amino acid sequence alignments of *P. aeruginosa* RsmA and RsmN proteins**

Conserved amino acid residues of RsmA and RsmN are depicted in green. The absence of the α-helix between β2 and β3 strands is indicated by the dashed lines in the RsmA sequence. Positions of the β-strands and the α-helix are aligned below the amino acid sequence of RsmN. The amino acid number is depicted as intervals of 10 at the top and bottom of the sequences. The figure is adapted from Lovelock L. [212].

During the course of this study, a manuscript demonstrating the identification of an RNA-binding protein, RsmF in *P. aeruginosa* was published online by Marden *et al*. [206]. A comparison of the structural studies and sequence analyses revealed that RsmF is identical to RsmN.

## 1.4 Project Overview

Although RsmN was found to be an RsmA homologue structurally, no *rsmN*-driven phenotypes could be identified in previous studies. Thus, the goals of this project were to:

1. determine the biological function of RsmN

2. identify RsmN targets on a genome-wide basis

3. investigate RsmA-RsmN cross-regulation and RsmN autoregulation

# 2 Materials and Methods

## 2.1 Bacterial strains, plasmids, oligonucleotides and growth conditions

The strains, plasmids and primers used in this study are listed in Tables 2.1, 2.2 and 2.3.

In this study, *E. coli* strains were cultured at 37°C and *P. aeruginosa* strains were cultured at 34°C, 37°C or 42°C on Luria-Bertani (LB) agar or in LB broth [bactotryptone 1% w/v, yeast extract 0.5% w/v, sodium chloride (NaCl) 1% w/v, pH adjusted to 7.0] with or without antibiotics on a rotary shaker at 200 revolutions per minute (r.p.m). All strains were stored at -80°C [750 µL of the bacterial culture grown in LB was mixed with 750 µL 50-100% (v/v) glycerol]. Media for motility assays were prepared as outlined by Rashid and Kornberg [213] using Nutrient Broth (NB) No. 2 (0.8% w/v) from Oxoid and Bacto Agar (0.3% for swimming, 0.5% for swarming, 1% for twitching, w/v) from Difco. *P. aeruginosa* strains were cultured in liquid LB or streaked on Pseudomonas Isolation Agar (PIA) [45 g of the powder (Difco) per litre of distilled water ($dH_2O$), 20 mL of glycerol] plates for PYO assay. Growth curves were plotted from 25 mL bacterial cultures grown in LB and 50 mL bacterial cultures grown in chemically defined medium (CDM) supplemented with TCA cycle intermediates as the single carbon source with 200 r.p.m shaking at 37°C or 34°C. Strains were grown in sterile Erlenmeyer flasks with a 1:10 culture volume:total flask volume ratio to allow enough aeration.

Generation times (in minutes) were calculated from the optical density values measured at 600 nm ($OD_{600}$) plotted on a logarithmic scale after determining two time points between which the growth was exponential using the formula:

$$generation\ time\ (\text{min.}) = \frac{t\ \times \log 2}{[\log b - \log a]} \times 60$$

where *a* is the $OD_{600}$ value at a chosen time point, *b* is the $OD_{600}$ value at a second time point and *t* is the hour (h) difference between two time points [214]. For any of the strains, *t* was 2 hours. The base-10 logarithm was applied. $OD_{600}$ measurements were taken using a BioMate 3 spectrophotometer (Thermo Scientific).

The composition of the Kornberg medium used to check glycogen accumulation was 1.1% dipotassium phosphate ($K_2HPO_4$), 0.85% monopotassium phosphate ($KH_2PO_4$), 0.6% yeast extract and 0.5% glucose (all w/v). 1.5% (w/v) Bacto agar was added when preparing agar plates [44, 215]. Basal salts medium (BSM) [30.8 mM $K_2HPO_4$, 19.3 mM $KH_2PO_4$, 15 mM ammonium sulfate $(NH_4)_2SO_4$, 1 mM magnesium chloride ($MgCl_2$), and 2 µM iron sulfate heptahydrate ($FeSO_4 * 7H_2O$) supplemented with 40 mM acetamide/succinate/fumarate/malate or 20 mM citrate] or CDM [3 mM potassium chloride (KCl), 3 mM NaCl, 25 mM 4-morpholinepropanesulfonic acid (MOPS), 12 mM $(NH_4)_2SO_4$, 6.4 mM magnesium sulfate ($MgSO_4$), 20 µM $FeSO_4 * 7H_2O$, 1.2 mM $K_2HPO_4$, supplemented with 40 mM succinate/fumarate/malate or 20 mM citrate] were used as minimal media to grow *P. aeruginosa* cells [68]. When bacterial strains were streaked on BSM agar plates supplemented with TCA cycle intermediates, overnight (o/n) cultures were adjusted to $OD_{600}$ of 1.0 in LB, pelleted and resuspended in 1 mL $dH_2O$. 2 µL of these bacterial cell suspensions were spread on agar with an inoculation loop. Plates were left at 37°C overnight. When bacterial strains were streaked on BSM agar plates supplemented with acetamide, a loopful of bacteria from each strain streaked on an o/n LB plate was resuspended in 500 µL $dH_2O$.

Colony morphologies of the single and inducible Δ*rsmA*/Δ*rsmN* double mutants were investigated on Congo red-tryptone agar with the following composition: 1% agar (No.3 Oxoid), 1% tryptone (Difco), 20 µg/mL Coomassie Brilliant R-250 (Sigma-Aldrich) and 40 µg/mL Congo red (MP Biomedicals, LLC) [216]. For the phage plaque assay, LB agar was layered with 5 mL of soft top agar (1% tryptone Oxoid, 0.8% agar Oxoid No.1, 0.5% NaCl) seeded with 5 µL of *P. aeruginosa* cells with an adjusted $OD_{600}$ of 1.0.

To investigate biofilm formation, *P. aeruginosa* cells were cultivated in a continuous flow of 10% LB in the Bioflux 200 microfluidics device (Fluxion Biosciences) [217]. For RNA extraction and protein purification, *P. aeruginosa* cells were grown in LB supplemented with respective antibiotics/inducers.

Media were autoclaved using the Omega Media Prestige or Classic Prestige Medical bench top autoclaves at 121°C for 20 min. at 15 pound-force per square inch (p.s.i).

Oligonucleotide primers (Table 2.3) were synthesised by Sigma-Aldrich or Eurofins Genomic Services Ltd. 100 µM stock solutions were diluted 1:10 and 1 µL from the 10 µM solutions were used for PCR reactions.

**Table 2.1. Bacterial strains used in this study**

| Strains | Genotype | Reference |
|---|---|---|
| ***E. coli*** | | |
| DH5α | F$^{-}$, φ80d*lacZ*Δ*M15*, Δ(*lacZYA-argF*)$_{U169}$, *deoR*, *recA1*, *endA1*, *phoA*, *hsdR17* ($r_K^-$, $m_K^+$), *supE44*, *thi-1*, *gyrA96*, *relA1* | Sambrook *et al*. [218] |
| DH10β | F$^-$ *endA1 recA1 galE15 galK16 nupG rpsL* Δ*lacX74 Φ80lacZΔM15 araD139* Δ*(ara,leu)7697 mcrA* Δ*(mrr-hsdRMS-mcrBC) λ*$^-$ | Invitrogen corporation |
| C2987H | *fhuA2*, *Δ(argF-lacZ)$_{U169}$*, *phoA*, *glnV44*, ϕ80Δ*(lacZ)M15*, *gyrA96*, *recA1*, *relA1*, *endA1*, *thi*-1, *hsdR17* | New England Biolabs corporation |
| TR1-5 | Δ*csrA*::Kan$^R$ | Romeo *et al.* [44] |
| ***P. aeruginosa*** | | |
| PAO1-N | WT, Nottingham strain | Lab collection |
| PAO1-L | WT, Lausanne strain | Haas collection |
| PAO1B1 | WT, Australia strain | Rice *et al.* [117] |
| PAO1B1Δ*Pf4* | PAO1, Δ*Pf4*: Gm$^R$ | Rice *et al.* [117] |
| PAZH13 | Δ*rsmA*, in-frame deletion in PAO1-N | Pessi *et al.* [204] |
| PASK10 | *lacI*$^Q$, P$_{tac}$-*rsmA*; inducible *rsmA*, Sm$^R$/Sp$^R$ | Kuehne S. [219] |
| PALT13 | *lacI*$^Q$, P$_{tac}$-*rsmN*/Δ*rsmA* allelic exchange, Sm$^R$/Sp$^R$ | Lovelock L. [212] |
| PALT16 | Δ*rsmN*, in frame deletion in PAO1-N | Lovelock L. [212] |
| PAMR1 | *lacI*$^Q$, P$_{tac}$-*rsmA*/Δ*rsmN* allelic exchange, Sm$^R$/Sp$^R$ | M. Romero, unpublished |
| PAO1Δ*pqsL* | *pqsL* deletion in the PAO1-N chromosome | Lab collection |
| PAO1Δ*pqsH* | *pqsH* deletion in the PAO1-N chromosome | Lab collection |
| PAO1Δ*pqsH* Δ*pqsL* | *pqsH pqsL* double deletion in the PAO1-N chromosome | Lab collection |
| PAO6679 | Δ*crcZ*, 160 bp deletion of the promoter and the 5'-UTR region of *crcZ* | Sonnleitner *et al*. [68] |

**Table 2.2. Plasmids used in this study**

| Plasmids | Description | Reference |
|---|---|---|
| pME6000 | pBBR1MCS-derived, broad host range multicopy cloning vector, $Tc^R$ | Maurhofer *et al*. [220] |
| pME6032 | *lacI*-$P_{tac}$ expression vector; pVS1-p15A shuttle vector, $Tc^R$ | Heeb *et al*. [97] |
| pRsmA | pME6032::*rsmA*, $Tc^R$ | Heeb *et al*. [53] |
| pMMB-16 | pME6000 with a 2.5-kb PAO1-L chromosomal DNA insert spanning *PA5182* (partial) to *PA5186* (partial), $Tc^R$ | Messina M. [210] |
| pHS1 | derivative of pMMB-16 where the insert is reduced to a 1.7-kb fragment lacking downstream of the *rsmN* ORF using *Sph*I-*Pst*I, $Tc^R$ | This study |
| pHS2 | derivative of pMMB-16 where the insert is reduced to the 0.47-kb *Nhe*I-*Sph*I fragment including *rsmN*, $Tc^R$ | This study |
| pHS2R62A | equivalent of pHS2 with a CGC to GCC substitution of the *rsmN* R62 residue (R62A), $Tc^R$ | This study |
| pHS2RBSLac | equivalent of pHS2 where *rsmN* RBS is replaced with *lac* RBS, $Tc^R$ | M. Romero, unpublished |
| pHS4 | ideal *rsmN* obtained by codon optimisation and replacement of the native RBS with the *lac* RBS, cloned in pME6000, $Tc^R$ | This study |
| pHS5 | derivative of pHS4 where ideal *rsmN* is replaced by native *rsmN* by joining the PCR products obtained using rsmNF and rsmNR primers, $Tc^R$ | This study |
| pMR1 | construct to express *rsmN* by the $P_{lac}$ promoter of pME6000, excluding all other promoter sequences, $Tc^R$ | M. Romero, unpublished |
| pMR4 | pME6032-based construct to include a $His_6$-tag at the amino terminus of RsmN for co-purification of the RsmN-bound RNA, $Tc^R$ | M. Romero, unpublished |
| pMR6 | *rsmN* expression vector constructed using the arabinose inducible vector pHERD30t as the plasmid backbone | M. Romero, unpublished |
| pMR7 | equivalent of pMR1 with R62A substitution, $Tc^R$ | M. Romero, unpublished |
| pMR8 | pMR1 derivative with a modified 5'-UTR sequence of *rsmN* to avoid the hairpin loop formation in between the *rsmN* TSS and translation start site, $Tc^R$ | M. Romero, unpublished |
| pMR9 | pMR1 derivative lacking the hairpin loop sequence in between the *rsmN* TSS and translation start site, $Tc^R$ | M. Romero, unpublished |
| pMR11 | *nmsR* transcription vector constructed in pUCP18, $Cb^R$ | M. Romero, unpublished |
| pMR12 | pHS2 derivative including the *rsmF* TSS according to Marden *et al*. [206] | M. Romero, unpublished |

**Table 2.3. Primers used for the construction of plasmids used in this study, TSS detection and checking expression levels from the $P_{rsmN}$, $P_{rsmF}$ and $P_{nmsR}$ promoters**

| Oligonucleotides | Sequence (5' to 3') | Function |
|---|---|---|
| T3 | ATTAACCCTCACTAAAGGG | the forward primer to detect the multicloning site (MCS) in pME6000 |
| T3a | TTCATCATGCCGTTTGTGATGGCTTCCATGTCGG | the forward primer to detect the MCS in pME6000 |
| T7p | TAATACGACTCACTATAGGG | the reverse primer to detect the MCS in pME6000 |
| T7t | TATGCTAGTTATTGCTCAGCGG | the reverse primer to detect the MCS in pME6000 |
| PHS2RBSLacF1 | TATGGTACCCTGGAAATCTCGGATGGAAT, anneals 2PRsmNR forming *Kpn*I/*Eco*RI compatible ends | the forward primer used in the construction of pMR12 and pHS2RBSLac |
| 2PRsmNF | TATAAGCTTTGACCATCCCTCCACACCATTTCATT, anneals 2PRsmNR and PMR7R forming *Hind*III/*EcoR*I compatible ends | the forward primer used in the construction of pMR1 and pMR7 |
| 2PRsmNR | TATGAATTCTCAGCCTTTCGGTGCCGTTTTCAACT, anneals 2PRsmNF, PMR8F, PMR9F and PHS2RBSLacF1 forming *Hind*III/*Eco*RI and *Kpn*I/*Eco*RI compatible ends | the reverse primer used in the construction of pMR1, pMR8, pMR9, pMR12 and pHS2RBSLac |
| PMR4F | TATGAATTCATGCACCATCACCATCACCATGGTTTCC TGATACTCTCCCG, anneals PMR4R forming *EcoR*I/*Cla*I compatible ends | the forward primer used to clone *rsmN*-$His_6$ for protein purification |
| PMR4R | TATATCGATTCAGCCTTTCGGTGCCGTTT, anneals PMR4F forming *EcoR*I/*Cla*I compatible ends | the reverse primer used to clone *rsmN*-$His_6$ for protein purification |
| PMR6F | TATCAGATCTGACGCTTTTTATCGCAACTCTCTACTG TTTCTCCATTGACCATCCCTCCACACCATTTCA, anneals PMR6R | the forward primer used in the construction of pMR6 |
| PMR6R | TATAAGCTTTCAGCCTTTCGGTGCCGTTTT, anneals PMR6F | the reverse primer used in the construction of pMR6 |
| PMR7R | TATGAATTCTCAGCCTTTCGGTGCCGTTTTCAACTCG TCGGCAAC, anneals 2PRsmNF forming *Hind*III/*EcoR*I compatible ends | the reverse primer used in the construction of pMR7 |
| PMR8F | TATAAGCTTTGACCATCCCTCCACACCATTTCATTCA CCAAAGCCGCC, anneals 2PRsmNR forming *Hind*III/*EcoR*I compatible ends | used together with 2PRsmNR to construct pMR8 |

| | | |
|---|---|---|
| PMR9F | TATAAGCTTTGACCATCCCTCCACACCATTTCATTCA CCAAGCTATGACTGGC, anneals 2PRsmNR forming *Hind*III/*EcoR*I compatible ends | used together with 2PRsmNR to construct pMR9 |
| PMR11F | TATACATGTTTTACACTTTATGCTTCCGGCTCGTATGT TGTGTGGGCTTTTACTTTCTACCGTTCGTCA, anneals PMR11R forming *Pci*I/*Sal*I compatible ends | the forward primer used to clone *nmsR* in pUCP18 |
| PMR11R | TATGTCGACTGGCGTGAGGCGAACAGGAAGC, anneals PMR11F forming *Pci*I/*Sal*I compatible ends | the reverse primer used to clone *nmsR* in pUCP18 |
| rsmNF | TACGAATTCATGGGTTTCCTGATACTCTCCCGCC, anneals rsmNR forming *EcoR*I/*Sac*I compatible ends | the forward primer to clone *rsmN* from the pHS2 sequence for the construction of pHS5 |
| rsmNR | TACGAGCTCTCAGCCTTTCGGTGCCGTTTTCAAC, anneals rsmNF forming *EcoR*I/*Sac*I compatible ends | the reverse primer to clone *rsmN* from the pHS2 sequence for the construction of pHS5 |
| 2TSSRsmNR1P | CTACCGTTCGTCAGCCTTTCG, anneals RNA for cDNA synthesis | *rsmN*-specific primer with a phosphorylated 5'-end, used in the reverse transcription step of TSS identification |
| TSSRsmNR2 | GCGGGAGAGTATCAGGAAACC, anneals TSSRsmNF3 | *rsmN*-specific reverse primer to amplify circularised cDNA for TSS detection |
| TSSRsmNF3 | AAGGCATCACCCTGTCCCT, anneals TSSRsmNR2 | *rsmN*-specific forward primer to amplify circularised cDNA for TSS detection |
| 2TSSNmsRR1P | CCGAGAAGGCGAAGGCATCACCCTGT, anneals RNA for cDNA synthesis | *nmsR*-specific TSS detection primer (reverse) with a phosphorylated 5'-end, used in the reverse transcription step of TSS identification |
| 2TSSNmsRR2 | GACGAGTTGAAAACGGCACC, anneals 2TSSNmsRF3 | *nmsR*-specific reverse primer to amplify circularised cDNA for TSS detection |
| 2TSSNmsRF3 | GAACGATCAGGACGCCACGC, anneals 2TSSNmsRR2 | *nmsR*-specific forward primer to amplify circularised cDNA for TSS detection |
| AntPLuxFwEcoRIKpnI | AATTCCCCCGCGTTCGCGGGGCTTTTACACATCAGCT TCGGCAAGCATGCCGAGGTAC, anneals AntPLuxRvEcoRIKpnI | the forward primer to introduce *EcoR*I/*Kpn*I restriction sites in *lux* fusions of the pFLUX dual biosensor |
| AntPLuxRvEcoRIKpnI | CTCGGCATGCTTGCCGAAGCTGATGTGTAAAAGCCC CGCGAACGCGGGGG, anneals AntPLuxFwEcoRIKpnI | the reverse primer to introduce *EcoR*I/*Kpn*I restriction sites in *lux* fusions of the pFLUX dual biosensor |
| MardenPFFwSacI | TATGAGCTCCTGGAAATCTCGGATGGAAT, anneals PFRvSpeI | the forward primer to introduce a *Sac*I site in *rsmF* sense promoter ($P_{rsmF}$) fusions according to Marden *et al*. [206] in the pFLUX dual biosensor |
| ManuPFFwSacI | TATGAGCTCGGCGTGAGGCGAACAGGAAG, anneals PFRvSpeI | the forward primer to introduce a *Sac*I site in *rsmN* sense promoter ($P_{rsmN}$) fusions in the pFLUX dual biosensor |
| PFRvSpeI | ATAACTAGTGAAACCCATGTTCCGTTTCCTGTGCCA, anneals MardenPFFwSacI and ManuPFFwSacI | the reverse primer to introduce a *Spe*I site in $P_{rsmF}$ and $P_{rsmN}$ fusions in the pFLUX dual biosensor |
| AntPFFwSacISpeI | CGCATGCTTGCCGAAGCTGATGTGTAAAAGCCCCGC GAACGCGGGGCTTTTACTTTCTACCGTTCGCACAGGA AACAGAATTCATGA, anneals AntPFRvSacISpeI | the forward primer to introduce *Sac*I/*Spe*I restriction sites in the transcriptional fusion with the *dsRed* operon of the pFLUX dual biosensor |

| | | |
|---|---|---|
| AntPFRvSacISpeI | CTAGTCATGAATTCTGTTTCCTGTGCGAACGGTAGAA AGTAAAAGCCCCGCGTTCGCGGGGCTTTTACACATC AGCTTCGGCAAGCATGCGAGCT, anneals AntPFFwSacISpeI | the reverse primer to introduce *Sac*I/*Spe*I restriction sites in the transcriptional fusion with the *dsRed* operon of the pFLUX dual biosensor |
| MardenPLuxFwKpnI | TATGGTACCCTGGAAATCTCGGATGGAAT, anneals PLuxRvXhoI | the forward primer to introduce a *Kpn*I site in the transcriptional fusion of $P_{rsmF}$ with the *lux* operon according to Marden *et al*. [206] in the pFLUX dual biosensor |
| ManuPLuxFwKpnI | TATGGTACCGGCGTGAGGCGAACAGGAAG, anneals PLuxRvXhoI | the forward primer to introduce a *Kpn*I site in the transcriptional fusion of $P_{rsmN}$ with the *lux* operon of the pFLUX dual biosensor |
| PLuxRvXhoI | ATACTCGAGTGAAATGGTGTGGAGGGATG, anneals MardenPLuxFwKpnI and ManuPLuxFwKpnI | the reverse primer to introduce a *Xho*I site in the transcriptional fusions of $P_{rsmF}$ and $P_{rsmN}$ with the *lux* operon of the pFLUX dual biosensor |

## 2.2 Antibiotics and inducers

Powder antibiotics were purchased from Sigma-Aldrich or AppliChem and stock solutions of antibiotics were prepared according to Sambrook *et al*. [218] as follows: ampicillin (100 mg/mL) in 50% EtOH, carbenicillin (50 mg/mL) in 50% EtOH and tetracycline (50 mg/mL) in 100% MeOH. A ready-made solution of gentamicin (10 mg/mL) was ordered from Sigma-Aldrich. Antibiotics were added to the bacterial cultures at the following concentrations: Tc 25 µg/mL and Cb 100 µg/mL for *E. coli*, Amp 100 µg/mL, Tc 125 µg/mL, and Cb 400 µg/mL for *P. aeruginosa*. *P. aeruginosa* strains transformed with pME6000 and its derivatives were cultivated in LB supplemented with tetracycline only to select for successful transformants due to an increase of cell clumping in bacterial cultures with tetracycline.

1 M stock solution of isopropyl-thio-β-D-galactopyranoside (IPTG, Sigma-Aldrich) was prepared and added to the media at a final concentration of 1 mM to induce gene expression in constructs with $P_{tac}$. L-(+)-arabinose (Sigma-Aldrich) was included in the media at a final concentration of 0.2% to induce the expression of genes under the control of the $P_{BAD}$ promoter.

100 µL of the ChromoMax™ 5-bromo-4-chloro-3-indolyl β-D-galactopyranoside (X-gal, Fischer Scientific) ready-made solution was spread on LB agar for the blue/white selection.

D-glucose was prepared as a 20% (w/v) stock solution and added to the motility media with a final concentration of 0.5% (v/v). BSM and CDM reagents were also prepared as stock solutions at the following concentrations: $K_2HPO_4$ 0.1 M, $KH_2PO_4$ 0.1 M, $(NH_4)_2SO_4$ 1 M, $MgCl_2$ 0.1 M, KCl 0.2 M, $MgSO_4 * 7H_2O$ 1 M, NaCl 0.2 M, MOPS 1 M, $FeSO_4 * 7H_2O$ 2 mM, acetamide 1 M, succinic acid disodium salt 1 M, sodium fumarate dibasic 1 M, and DL-malic acid 1 M. The pH of the carbon solutions was neutralised (pH ~ 7.0), and all reagents were filter sterilised with the 0.22 µm-Sartorius Ministart filter before use.

Synthetic PQS and HHQ molecules were prepared by A. Truman at the School of Life Sciences, University of Nottingham. Compounds were dissolved in MeOH and kept as 10 mM stock solutions at -20°C until further use [221].

## 2.3 Plasmid and strain construction

### 2.3.1 Construction of PALT16, PALT13 and PAMR1 strains

Construction of the single and inducible double deletion mutants involved the use of pDM4-based suicide plasmids pMM33 and pLT10. pDM4 carries a chloramphenicol resistance cassette and the *sacB* gene which encodes levansucrase for converting sucrose to levan, the latter being toxic to cells hence enabling sucrose sensitivity selection [222]. Construction of the pMM33 and pLT10 plasmids and allelic replacement in *P. aeruginosa* are described elsewhere [210, 212].

Plasmid pMM33 was used for the in-frame deletion of *rsmN* in PAO1-N (PALT16 strain). Construction of the *rsmN*$_{ind}$ Δ*rsmA* (PALT13) strain required the use of the pLT10 suicide plasmid in trans conjugation with the Δ*rsmA* (PAZH13) recipient strain. Selection steps are described in the PhD thesis of L. Lovelock [212].

*E. coli* S17-1$\lambda_{pir}$ strain transformed with pMM33 was used as the donor strain in bacterial mating with the *rsmA*$_{ind}$ (PASK10, see Table 2.1) strain to construct an *rsmA*$_{ind}$ Δ*rsmN* strain (PAMR1). Both strains were grown overnight in 5 mL of LB with agitation. The *rsmA*$_{ind}$ strain was grown at 42°C to reduce the restriction enzyme activity against foreign DNA while *E. coli* S17-1$\lambda_{pir}$ strain was grown at 37°C. 1 mL of each culture was centrifuged, washed twice with fresh LB, resuspended in 500 µL LB and mixed. The mixture was pelleted and resuspended in 100 µL LB, plated on LB agar and incubated for 8 h at 37°C. Mating cells were scraped from the agar plate, resuspended in 1 mL LB and plated on PIA agar with 400 µg/mL Cm to select for the *rsmA*$_{ind}$ transconjugants. The suicide plasmid pMM33 was integrated by double-crossover after plating the transconjugants in LB + 10% sucrose. Clones obtained were analysed for *rsmN* deletion by PCR (M. Romero, personal communication).

### 2.3.2 Construction of pHS2, a multicopy *rsmN* expression plasmid

Genes capable of restoring the swarming motility of the Δ*rsmA* mutant were screened from a genomic bank and the pMMB-16 vector with a 2.5-kb chromosomal fragment

was purified from one of the positive clones (section 1.3.5, Figure 1.7) due to its smaller size. To obtain the RsmN coding region without the neighboring genes from this 2.5-kb fragment (Figure 2.1, panel a), the 1.7-kb *Pst*I-(*Sph*I) fragment (Figure 2.1, panel b) was first subcloned in pME6000 digested with *Pst*I and (*Bam*HI) to obtain the pHS1 construct. After confirming the complementation of Δ*rsmA* swarming with the pHS1 construct (data not shown), the 1.25-kb *Pst*I-*Nhe*I fragment was deleted to obtain an insert of 0.47-kb that spans the *rsmN* ORF (depicted in Figure 2.1, panel c). This insert was cloned in pMME6000 to obtain a multicopy *rsmN* expression plasmid (pHS2).

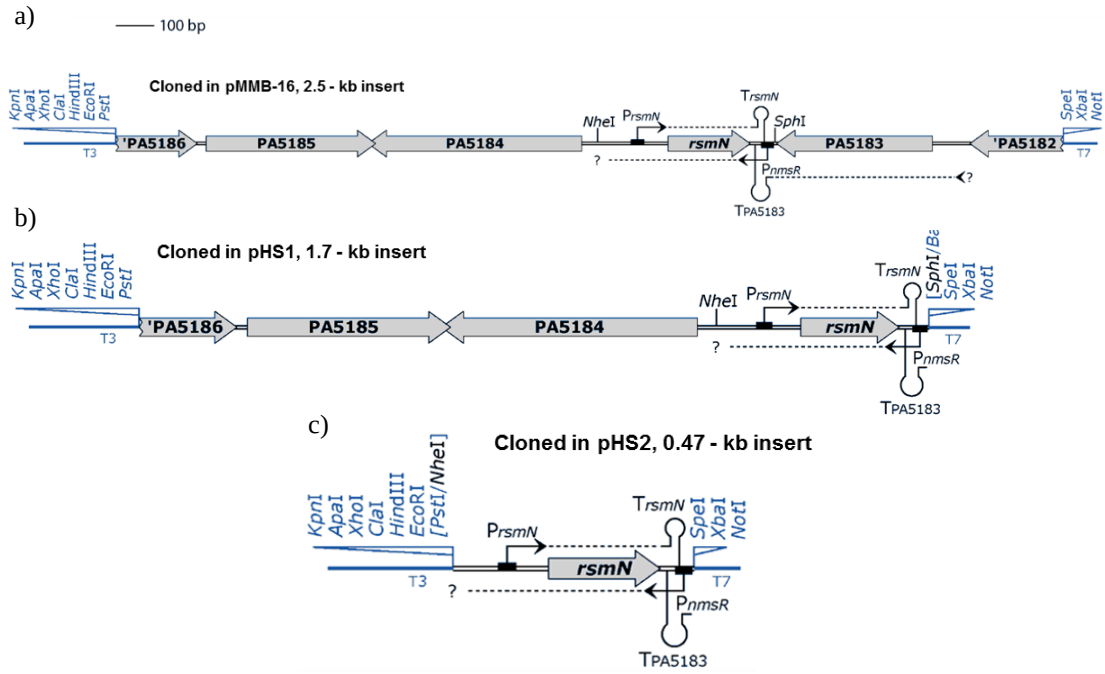


**Figure 2.1. Diagrammatic representation (in the reverse orientation) of the (a) smallest genomic bank fragment containing the *rsmN* ORF cloned in pMMB-16, (b) insert cloned in pHS1, (c) insert cloned in pHS2**

The 2.5-kb PAO1-L chromosomal fragment (a) cloned in the pMMB-16 vector includes two truncated (‘*PA5186* and ‘*PA5182*) and four functional genes including *rsmN*. The 0.47-kb fragment containing the *rsmN* ORF flanked by the *Nhe*I and *Sph*I restriction sites was extracted from the 2.5-kb fragment in two steps. Firstly, the 1.7-kb *Pst*I-(*Sph*I) fragment spanning ‘*PA5186-PA5185-PA5184-rsmN* was subcloned in pME6000 to obtain the pHS1 construct (b), then, the *Pst*I-*Nhe*I fragment was removed from the pHS1 vector to get pHS2 (c). Promoters (illustrated as black boxes) and terminators (illustrated as loops) were detected using Softberry BPROM and TransTermHP programs and diagrams were generated in the latter. The restriction sites and the sequencing primers used are depicted in blue on the left and right sides. Due to the lack of a terminator sequence, expression from the predicted $P_{nmsR}$ promoter is represented by dashed lines and a question mark.

### 2.3.3 Arginine to alanine substitution in pHS2 to get pHS2R62A

The *rsmN*R62A allele was obtained from the Integrated DNA Technologies (IDT) as a 0.49-kb *Eco*RI-*Spe*I fragment (pIDTSmart-AMP, approx. 2 µg DNA) and inserted in pME6000 to generate pHS2R62A. CGC codon was exchanged with GCC for the R62A substitution.

### 2.3.4 Construction of pHS4 and pHS5 (no antisense ideal RsmN: NasIrsmN)

Amino acids are encoded by three nucleotide codes called codons and most amino acids are encoded by several codons. 21 amino acids of *P. aeruginosa* and the corresponding codons with the highest relative synonymous codon usage (RSCU) values which represent ratios of the observed frequencies to the expected codon usage frequencies [223] are outlined in Table 2.4.

**Table 2.4. Codon usage table listing synonymous codons with the two highest RSCU values ($RSCU_{max}$ and RSCU) in *P. aeruginosa* PAO1**

| | Amino acid | Codon | $RSCU_{max}$ | Synonymous Codon | RSCU |
|---|---|---|---|---|---|
| 1 | Ala | GCC | 2.38 | GCG | 1.34 |
| 2 | Arg | CGC | 4.00 | CGG | 1.10 |
| 3 | Asn | AAC | 1.75 | AAT | 0.25 |
| 4 | Asp | GAC | 1.64 | GAT | 0.36 |
| 5 | Cys | TGC | 1.83 | TGT | 0.17 |
| 6 | End | TGA | 2.43 | TAG | 0.33 |
| 7 | Gln | CAG | 1.72 | CAA | 0.28 |
| 8 | Glu | GAG | 1.23 | GAA | 0.77 |
| 9 | Gly | GGC | 3.02 | GGG | 0.45 |
| 10 | His | CAC | 1.44 | CAT | 0.56 |
| 11 | Ile | ATC | 2.78 | ATT | 0.17 |
| 12 | Leu | CTG | 4.07 | CTC | 1.36 |
| 13 | Lys | AAG | 1.78 | AAA | 0.22 |
| 14 | Met | ATG | 1.00 | - | - |
| 15 | Phe | TTC | 1.93 | TTT | 0.07 |
| 16 | Pro | CCG | 2.69 | CCC | 1.03 |
| 17 | Ser | AGC | 2.90 | TCG | 1.44 |
| 18 | Thr | ACC | 3.24 | ACG | 0.57 |
| 19 | Trp | TGG | 1.00 | - | - |
| 20 | Tyr | TAC | 1.62 | TAT | 0.38 |
| 21 | Val | GTG | 1.97 | GTC | 1.69 |

To investigate the influence of codon usage bias on RsmN function, original codons of RsmN were replaced with synonymous codons with the highest RSCU values (codons highlighted in yellow in Table 2.5) which provided the highest possible genome codon index (GCI) for RsmN. GCI provides a comparison of the codon usage of a gene with the codon usage of a genome [224]. During the modification of RsmN codons, when an amino acid was subsequently used, in the second turn, the synonymous codon with the second highest RSCU value was chosen (Table 2.5, codons highlighted in magenta coding the amino acids highlighted in green). This arrangement resulted in an average GCI of 0.914. When three or more codons were not changed subsequently, further modifications were made (Table 2.5, codons highlighted in blue). Even though the codon resulting in the maximum GCI value ($GCI_{max}$) was GAG (highlighted in red) for $Glu_{33}$, it was overlooked and the original codon GAA was kept. Furthermore, codons encoding the native RBS of *rsmN* was replaced with codons encoding the *lac* RBS (pHS2RBSLac construct) according to the RsmA-binding site demonstrated in Marden *et al*. [206] to eliminate RsmA binding to RsmN. Final codon selection is displayed in the very right column of Table 2.5.

This synthetic version of *rsmN* (no antisense ideal RsmN, *NasIrsmN*) flanked by the following restriction sites and having the *lac* RBS, SphI–Plac-35/-10-NcoI-+1rsmN-RsmN5′UTR-***lacRBS***-EcoRI-NasIrsmN-SacI-+1nmsR-PnmsR-SphI (Figure 2.2) was obtained from the IDT in a high-copy plasmid (pIDTSmart-AMP, approx. 4 µg DNA). The pHS4 vector was constructed by the *Sph*I/*Sac*I double digestion of the pIDTSmart vector and cloning of the acquired insert into the pME6000 vector digested with the same enzymes. For the construction of pHS5, pHS4 was midi-prepped from DH5α/pHS4 cells. The synthetic *NasIrsmN* fragment was cut off the pHS4 vector by *EcoR*I/*Sac*I (Thermo Scientific) double digestion (30 min. at 37°C). The native *rsmN* sequence to be replaced with *NasIrsmN* was amplified from pHS2 (1439.7 ng/µL, diluted 1:100 for PCR amplification) using rsmNF and rsmNR primers flanked with the *EcoR*I and *Sac*I restriction sites.

**Table 2.5. Codon selection of RsmN (third column) and NasIrsmN (last column)**
Original codons of RsmN were modified (highlighted in yellow) to obtain the highest possible GCI for RsmN. When the same amino acid was subsequently used, the synonymous codon with the second highest RSCU value was inserted (codons highlighted in magenta coding the amino acids highlighted in green). Furthermore, when three or more codons were left unmodified, a few of these codons (highlighted in blue) were replaced randomly.

| No. | Amino acid | Original codon | $GCI_{max}$ codon | $GCI_{max}$ codon corrected |
|---|---|---|---|---|
| 1 | Met | ATG | ATG | ATG |
| 2 | Gly | GGT | GGC | GGC |
| 3 | Phe | TTC | TTC | TTC |
| 4 | Leu | CTG | CTG | CTG |
| 5 | Ile | ATA | ATC | ATC |
| 6 | Leu | CTC | CTG | CTG |
| 7 | Ser | TCC | AGC | AGC |
| 8 | Arg | CGC | CGC | CGC |
| 9 | Arg | CGA | CGC | CGG |
| 10 | Glu | GAA | GAG | GAG |
| 11 | Gly | GGC | GGC | GGC |
| 12 | Glu | GAA | GAG | GAG |
| 13 | Gly | GGC | GGC | GGC |
| 14 | Ile | ATC | ATC | ATT |
| 15 | Thr | ACC | ACC | ACG |
| 16 | Leu | CTG | CTG | CTG |
| 17 | Ser | TCC | AGC | AGC |
| 18 | Leu | CTC | CTG | CTG |
| 19 | Lys | AAG | AAG | AAG |
| 20 | Ala | GCC | GCC | GCC |
| 21 | Asp | GAC | GAC | GAT |
| 22 | Tyr | TAC | TAC | TAT |
| 23 | Pro | CCG | CCG | CCG |
| 24 | Ala | GCG | GCC | GCC |
| 25 | Glu | GAG | GAG | GAG |
| 26 | Glu | GAA | GAG | GAA |
| 27 | Leu | CTG | CTG | CTG |
| 28 | Ile | ATT | ATC | ATC |
| 29 | Arg | CGG | CGC | CGC |
| 30 | Gln | CAA | CAG | CAG |
| 31 | Leu | TTG | CTG | CTG |
| 32 | Arg | CGC | CGC | CGC |
| 33 | Glu | GAA | GAG | GAA |

| | | | | |
|---|---|---|---|---|
| 34 | Gly | GGC | GGC | GGC |
| 35 | Gly | GGC | GGC | GGG |
| 36 | Ile | ATC | ATC | ATC |
| 37 | Arg | CGG | CGC | CGC |
| 38 | Ile | ATC | ATC | ATC |
| 39 | Leu | CTG | CTG | CTG |
| 40 | Val | GTC | GTG | GTG |
| 41 | Thr | ACC | ACC | ACC |
| 42 | Asp | GAT | GAC | GAC |
| 43 | Ile | ATC | ATC | ATC |
| 44 | Ile | ATC | ATC | ATT |
| 45 | Gly | GGC | GGC | GGC |
| 46 | Asn | AAC | AAC | AAT |
| 47 | Gln | CAG | CAG | CAA |
| 48 | Ala | GCC | GCC | GCC |
| 49 | Arg | CGG | CGC | CGC |
| 50 | Val | GTC | GTG | GTG |
| 51 | Gly | GGG | GGC | GGC |
| 52 | Ile | ATC | ATC | ATC |
| 53 | Glu | GAG | GAG | GAG |
| 54 | Ala | GCG | GCC | GCC |
| 55 | Pro | CCG | CCG | CCG |
| 56 | Arg | CGT | CGC | CGC |
| 57 | Gly | GGC | GGC | GGC |
| 58 | Val | GTC | GTG | GTG |
| 59 | Leu | CTG | CTG | CTG |
| 60 | Ile | ATC | ATC | ATC |
| 61 | Val | GTT | GTG | GTG |
| 62 | Arg | CGC | CGC | CGC |
| 63 | Asp | GAC | GAC | GAT |
| 64 | Glu | GAG | GAG | GAG |
| 65 | Leu | TTG | CTG | CTG |
| 66 | Lys | AAA | AAG | AAG |
| 67 | Thr | ACG | ACC | ACC |
| 68 | Ala | GCA | GCC | GCC |
| 69 | Pro | CCG | CCG | CCG |
| 70 | Lys | AAA | AAG | AAG |
| 71 | Gly | GGC | GGC | GGC |
| 72 | - | TGA | TGA | TGA |

***rsmN***

**ATG**GGTTTCCTGATACTCTCCCGCCGAGAAGGCGAAGGCATCAC
CCTGTCCCTCAAGGCCGACTACCCGGCGGAGGAACTGATTCGGC
AATTGCGCGAAGGCGGCATCCGGATCCTGGTCACCGATATCATC
GGCAACCAGGCCCGGGTCGGGATCGAGGCGCCGCGTGGCGTCCT
GATCGTTCGCGACGAGTTGAAAACGGCACCGAAAGGCTGA

***NasIrsmN***

**ATG**GGCTTCCTGATCCTGAGCCGCCGGGAGGGCGAGGGCATTAC
GCTGAGCCTGAAGGCCGATTATCCGGCCGAGGAACTGATCCGCC
AGCTGCGCGAAGGCGGGATCCGCATCCTGGTGACCGACATCATT
GGCAATCAAGCCCGCGTGGGCATCGAGGCCCCGCGCGGCGTGCT
GATCGTGCGCGATGAGCTGAAGACCGCCCCGAAGGGCTGA

**Figure 2.2. The *rsmN* and *NasIrsmN* sequences**
The nucleotide sequence of *rsmN* (blue) with the native codons (top) and the synthetic *NasIrsmN* sequence with alterations (green) in the nucleotide sequence after codon optimisation (bottom). The start codon ATG is illustrated in bold.

## 2.4 Protocols

### 2.4.1 Preparation of the electrocompetent cells

*E. coli* and *P. aeruginosa* electrocompetent cells were prepared according to standard protocols [218]. For *E. coli* DH5α and TR1-5 electrocompetent cells, 500 µL of the o/n culture was inoculated in 200 mL of LB and incubated for ~ 6 h (until $OD_{600}$ reaches 0.6-0.8). Cells were distributed into four 50 mL falcon tubes and centrifuged at 10,000 r.p.m for 5 min. (all centrifugation steps took place at 4°C). The supernatants were removed and pellets were resuspended in ~ 10 mL ice-cold glycerol (10% v/v). After pooling all in a falcon, centrifugation for 5 min. and removal of the supernatant, the pellet was washed in ~ 20 mL of ice-cold glycerol (10% v/v) twice and resuspended in 1 mL ice-cold glycerol (10% v/v). 50 µL aliquots were stored at -80°C.

A similar protocol was followed for the preparation of *P. aeruginosa* electrocompetent cells. Shortly, 10 mL of an o/n culture was prepared. 1.5 mL aliquots of the o/n culture grown at 42°C were pelleted, washed three times in 1 mL of ice-cold glycerol (10% v/v) and 50 µL aliquots were stored at -80°C.

### 2.4.2 Transformation of the electrocompetent/$CaCl_2$-competent cells

The competent cells (~ 50 µL) were thawed on ice. 2 µL of the plasmid DNA (diluted to ~ 50 ng/µL) was added to the cell mixture and left on ice for a min. The mixture was transferred to the bottom of a precooled electroporation cuvette (BioRad Gene Pulser with a 2 mm electrode gap) avoiding bubbles. An electroporation pulse of 2.5 kV was delivered for 4.5-5.5 s using the BioRad MicroPulser. For transformation into the $CaCl_2$-competent cells, cells were exposed to heat shock (42°C) for 30 s and cooled on ice for 2 min.

After transformation, 950 µL of LB was added and the mixture was left at 37°C for 1 h. 100 µL of the mixture was spread on LB agar supplemented with the appropriate antibiotic. The rest of the mixture was pelleted, the supernatant was decanted, cells were resuspended in the remaining supernatant (80 µL-100 µL) and spread on another LB plate with antibiotic. Transformants were left to grow at 37°C o/n.

### 2.4.3 Molecular cloning procedures

#### 2.4.3.1 Plasmid DNA purification

QIAGEN Plasmid Midi, QIAprep Spin MiniPrep and Sigma GenElute Plasmid Mini-Prep kits were used according to manufacturer's specifications for plasmid extraction. The compositions of the P1, P2, P3, QBT, QC and QF buffers were as follows: Buffer P1, 50 mM Tris·Cl pH 8.0, 10 mM ethylenediaminetetraacetic acid (EDTA), 100 µg/mL RNase A; Buffer P2, 200 mM sodium hydroxide (NaOH), 1% sodium dodecyl sulphate (SDS) (w/v); Buffer P3, 3.0 M potassium acetate pH 5.5; Buffer QBT, 750 mM NaCl, 50 mM MOPS pH 7.0, 15% isopropanol (v/v), 0.15% Triton X-100 (v/v); Buffer QC, 1.0 M NaCl, 50 mM MOPS pH 7.0, 15% isopropanol (v/v); Buffer QF, 1.25 M NaCl, 50 mM Tris · Cl pH 8.5, 15% isopropanol (v/v).

All plasmids used in this study were isolated in large quantities and kept at -20°C for further use. After 18 h of growth in LB + the corresponding antibiotic, 200 mL of the bacterial cultures were centrifuged in an Avanti™ J20-I centrifuge (with rotor JA-14). Plasmid DNA was extracted following the QIAGEN Plasmid Midi Kit protocol for 100 mL bacterial cultures with minor modifications. DNA pellets were dried of EtOH using SpeedVac and resuspended in 20 µL HPLC-grade water.

New England Biolabs (NEB), Promega and Thermo Scientific FastDigest restriction enzymes and buffers were used for restriction digestions. Digests usually contained 1-2 µg DNA, 0.5-1 µL restriction enzyme, 1x volume of the appropriate restriction buffer and were set to a final volume of 20 µL in HPLC-grade water. Digestion mixtures were usually left at 37°C for 1 h. 1 kb and 0.1-10.0 kb Quick-Load 2-Log DNA Ladders (Promega) were used as molecular weight markers. Orange Gel 6x Loading Dye from NEB [1x buffer components; 2.5% Ficoll®-400, 11 mM EDTA, 3.3 mM Tris-HCl, 0.017% sodium dodecyl sulfate (SDS), 0.15% Orange G at pH 8.0] and Blue/Orange 6x Loading Dye from Promega were used during agarose gel electrophoresis in 1x Tris-acetate/ethylenediaminetetraacetic acid (TAE) buffer (50x TAE buffer; 242 g Trisma, 20.81 g EDTA, 57.1 mL glacial acetic acid, up to 1 L with $dH_2O$). Depending on the DNA size, 0.4%, 0.6% or 1.0% (w/v) agarose gels were run as described in Sambrook *et al*. [218] with the addition of 5 µL SYBR® Safe DNA Gel Stain [from a 10,000 concentration in dimethyl sulphoxide (DMSO), Invitrogen]. Agarose gel electrophoresis was performed at 80-120 V using a horizontal gel apparatus (BioRad). Pictures of the agarose gels were taken in the Gel Doc™ XR+ System (BioRad) using Filter 2. Relevant DNA fragments were visualised on a UV transilluminator (UVP) and extracted using the ZymoClean™ Gel DNA Recovery Kit (Cambridge Biosciences) in accordance with the manufacturer's instructions.

#### 2.4.3.2 Ligation

T4 DNA ligase and T4 DNA ligase buffer (10x) from Promega were used for the ligation reactions that took place on melting ice o/n. Ligations were performed using a 1:3 or 1:5 vector to insert ratio. The following day, the electrocompetent cells were transformed with 2 µL of the ligation reaction. The rest of the ligation mixture (~ 10 µL) was precipitated with 0.1 µL of 3 M sodium acetate (NaOAc, pH 5.2) and 100 µL of absolute EtOH and kept at -20°C.

#### 2.4.3.3 Polymerase chain reaction (PCR) amplification

Oligonucleotide primers used in this study are outlined in Table 2.3. PCR reactions were run on Labcycler (SensoQuest) and $T_{3000}$ Thermocycler (Biometra) based on the methods described in Saiki *et al*. [225] and included the following cycle steps: denaturation for 5 min. at 95°C followed by 15 s. at 94°C, annealing for 30 s. at 55°C, and an extension for 1 min. at 72°C. Amplification took place for 35 cycles and the

reaction was completed with a 5 min. step at 72°C. The illustra™ PuReTaq™ Ready-To-Go™ PCR beads (GE Healthcare) which included 1.5 mM $MgCl_2$, 50 mM KCl, and 200 mM dNTP mix in a final volume of 25 µL were used as the master mix in PCR reactions. The GenElute™ PCR Clean-Up kit (Sigma-Aldrich) was used to purify PCR products.

Steps of the PCR reactions run to check genomic DNA contamination in the RNA samples were identical but the amplification took place for 30 cycles.

### 2.4.4 Blue/white selection

Recombinant plasmids containing the *lacZα* multicloning site of *E. coli* were screened by blue/white selection using X-Gal which allows screening of the β-galactosidase activity. Colonies appear blue if there is no insert DNA and β-galactosidase breaks down X-Gal. White colonies lack β-galactosidase activity due to the disruption of the *lacZα* site by the insert DNA. *E. coli* DH5α has a *lacZα* deletion, therefore, when the blue/white selection was used, insert DNA was transformed into C2987H or DH10β cells.

### 2.4.5 DNA sequencing

Sequencing of the pME6000-based constructs took place at the DNA Sequencing Laboratory, Queens Medical Centre, the University of Nottingham using the Applied Biosystems BigDye® Terminator v3.1 Cycle Sequencing Kit and 3130x1 Genetic Analyzer. T3, T3a, T7 and T7t primers (Table 2.3) and 100 ng/µL of DNA were used to run a sequencing reaction.

DNA sequences were analysed using MultAlin established by Florence Corpet [226], the reverse complement function of The Sequence Manipulation Suite at http://www.bioinformatics.org/sms/ and Lasergene 8 Client software package (DNAstar Ltd).

### 2.4.6 Quantification of DNA, RNA and protein concentrations

1.5-2 µL of the sample was applied to the electrode of NanoDrop ND-1000 to measure the concentration and purity of plasmid DNA, total and RsmN-bound RNA and RsmN.

### 2.4.7 Complementation of the Δ*rsmA*, Δ*csrA*, *rsmA*$_{ind}$ Δ*rsmN* and *rsmN*$_{ind}$ Δ*rsmA* phenotypes by *rsmN* expression

#### 2.4.7.1 Motility assays

Swarming, swimming and twitching motilities of *P. aeruginosa* strains were examined as described previously [121, 213, 227]. The protocols followed were similar to the ones described with small modifications. Briefly, 8 g/L Nutrient Broth No.2 (Oxoid) was mixed with 0.5%, 0.3% and 1.0% (w/v) Bacto agar (Difco) for swarming, swimming and twitching motilities respectively. Autoclaved media were cooled down to 50°C and D-glucose was added at a final concentration of 0.5% (v/v) before transferring 25 mL (for swarming and swimming) or 10 mL (for twitching) of the media into each petri dish. Bacterial motility is really sensitive to the water concentration of the medium, if the plates were too wet, swimming might take place instead of swarming and if plates were too dry, bacteria would swarm poorly. Therefore, swarming plates were dried for 45 min. in a laminar flow hood to remove the surface water after settlement whereas swimming plates were used immediately and the interference of condensation on the water concentration of the medium was minimised by replacing the lids of the petri dishes [228].

$OD_{600}$ of the o/n cultures were adjusted to 1.0 in 1 mL of LB and cultures were centrifuged. Pellets were resuspended in 1 mL LB. 3 µL of the o/n cultures were inoculated onto the centre of the swarming and swimming agar. Swimming assay was also set up by inoculation of the bacterial colonies directly from an o/n plate with a toothpick. Moreover, swimming assay was repeated by inoculating 1 µL of the subcultures grown to an $OD_{600}$ of 0.8. The stabbing technique was used to inoculate cells in the twitching assay. Bacterial inocula were obtained from the agar plates left at 37°C o/n with sterile wooden toothpicks and stabbed perpendicularly at the centre of the twitching agar.

Swarming and swimming plates were incubated for 24 h and twitching plates were incubated for 48 h at 37°C or 34°C using a beaker filled with water to sustain the humidity in a Kuhner Shaker Lab-Therm incubator (Scientific Lab Supplies). Pictures were taken immediately using a Nikon D40 camera with indirect light reflected from the bottom.

#### 2.4.7.2 Kornberg assay

The effect of *rsmN* and *rsmN*R62A expression on glycogen production of *E. coli* TR1-5 cells characterised by a Δ*csrA* mutation was assayed by iodine staining as described previously [44]. Iodine stain was prepared as follows: 15 g of potassium iodide (KI) was dissolved in 125 mL $dH_2O$ and 3 g of iodine ($I_2$) crystals were mixed in later. The solution was stirred and diluted to 1 L.
(http://www.flinnsci.com/media/396156/labsolutionprep.pdf). 5 mL of the iodine stain was poured on top of the plates and spread around equally. Iodine solution was poured back and pictures were taken immediately with a Nikon D40 camera.

#### 2.4.7.3 Pyocyanin assay

PYO production was measured based on the assay described in Essar *et al.* [192]. Optical densities of the o/n bacterial cultures were standardised to 1.0 in 1 mL of LB and cultures were pelleted. Pellets were resuspended in 1 mL LB and 250 µL was inoculated in 25 mL of LB. Cultures were grown in 250 mL conical flasks for 18 h with 200 r.p.m shaking at 37°C or 34°C. 7.5 mL aliquots of the culture supernatants were filter sterilised and mixed with 4.5 mL chloroform (Fischer Scientific). It is reported that the decomposition compound of PYO, 1-hydroxyphenazine is found in the supernatants of aged *P. aeruginosa* cultures [133]. To avoid such degradation, filter sterilised supernatants were immediately used.

The mixture was vortexed for 2 x 10 s (color change from green to blue at this point) and centrifuged at 10,000 r.p.m, 4°C for 10 min. 3 mL of the chloroform layer was transferred to a new 5 mL falcon and mixed with 1.5 mL of 0.2 M HCl by vortexing 2 x 10 s (blue color turns to pink upon HCl addition). Samples were centrifuged at 10,000 r.p.m, 4°C for 2 min. 900-1000 µL of the pink layer was transferred to cuvettes, avoiding any chloroform, and the absorbance was read at 520 nm using a BioMate 3 spectrophotometer (Thermo Scientific). 1 mL of 0.2 M HCl was used as blank. PYO levels were calculated as mg per L by multiplying the absorbance value with the ratio of the volume of chloroform added to the volume of chloroform used (4.5 mL/3 mL) and the PYO constant of 17.072 (a constant derived from the extinction coefficient of PYO). The experiment was repeated three times and the average was calculated. Error

bars represent standard error of the mean. Significant differences were determined by ANOVA analysis, followed by Tukey multiple comparison test (GraphPad Prism 6.0).

#### 2.4.7.4 Protease assays

2.4.7.4.1 Total protease assay

Most assays to measure the protease activities are based on the breakdown of modified/unmodified casein. Here, a quantitative assay based on the absorbance measurements at 400 nm was performed to check the total proteolytic activity [229]. Azocasein (Sigma-Aldrich) (final concentration 5 mg/mL) was dissolved in Tris-$CaCl_2$ buffer (100 mM Tris, 1 mM $CaCl_2$, pH 7.5). 1 mL buffer was mixed with 100 µL of the supernatant from an o/n culture grown at 37°C or 34°C, with agitation (200 r.p.m) for 18 h. The reaction took place at 37°C or 34°C for 20 min. with agitation and was stopped by the addition of 500 µL 10% trichloroacetic acid (TCAa, Sigma-Aldrich) which precipitates proteins. Undigested azocasein was pooled at the bottom of the tubes by centrifugation; the supernatant was separated from the insoluble azocasein particles and absorbance was measured at 400 nm using a BioMate 3 spectrophotometer (Thermo Scientific). The experiment was repeated three times and the average was calculated. Error bars represent standard error of the mean. Significant differences were determined by ANOVA analysis, followed by Tukey multiple comparison test (GraphPad Prism 6.0).

2.4.7.4.2 Elastase assay

Fractionated Elastin-Congo red was quantified as a measure of the elastinolytic activity in this study [230, 231]. 5 mg of insoluble Elastin-Congo red (Sigma-Aldrich) was added per mL of the Tris-$CaCl_2$ buffer (100 mM Tris, 1 mM $CaCl_2$, pH 7.5). Identical steps were followed as the total protease assay, but the reaction was stopped after 2 h by adding 100 µL EDTA (120 mM). Absorbance measurements of the supernatants were taken at 495 nm using a BioMate 3 spectrophotometer (Thermo Scientific). The experiment was repeated three times and the average was calculated. Error bars represent standard error of the mean. Significant differences were determined by ANOVA analysis, followed by Tukey multiple comparison test (GraphPad Prism 6.0).

### 2.4.7.5 Biofilm assays

2.4.7.5.1 Bioflux

Bacterial strains were grown o/n at 37°C with agitation (200 r.p.m). $OD_{600}$ of the strains were measured and adjusted to 1.0 in LB. Cells were pelleted and resuspended in 1 mL fresh LB. From these cultures, 150 µL was inoculated in a 5 mL fresh culture of LB for the *rsmN*$_{ind}$ Δ*rsmA* mutant (PALT13). 100 µL was inoculated for the Δ*rsmA* mutant (PAZH13) and 50 µL was inoculated for the WT and Δ*rsmN* (PALT16) strains. Cells were cultivated until $OD_{600}$ values reached 0.8 (it takes a longer time for the *rsmN*$_{ind}$ Δ*rsmA* mutant to reach an $OD_{600}$ of 0.8 due to clumping, therefore it was subcultured first). In the next step, $OD_{600}$ of each strain was standardised to 0.05 in 10% LB (v/v). The microfluidic chamber (BioFlux 48-well, 24 channels plate 70 µ-370 µ, 0-20 dyn/cm$^2$) was primed from the 'in' well with 100 µL of 10% LB (v/v) until the first circle of the 'out' well was filled (takes 2.5 min. with a max shear of 2.00 dyn/cm$^2$). 65 µL of the $OD_{600}$ standardised strains were then added to the 'out' well and the plate was gently tapped to break the water tension. Strains were then pumped from the 'out' chamber for 1 s at a speed of 2 dyn/cm$^2$. After spotting a few zigzagging cells at the inlet of the chamber at 40x objective magnification, cells were left to seed at 37°C for 40 min.-1 h. Afterwards, 1.1 mL of 10% LB + Syto 9® green fluorescent nucleic acid stain (5.5 µL of 1:200 diluted solution from a stock of 5 mM solution in DMSO) was added to the 'in' wells and then pumped through the chamber at a speed of 0.5 dyn/cm$^2$ for approximately 14 h (set to 1.0 dyn/cm$^2$ for the first 20 s to get the flow going then reduced down) on a heating block set to 37°C or 34°C.

2.4.7.5.2 Colony biofilms

Colony morphologies of the Δ*rsmA*/Δ*rsmN* single and inducible double deletion mutants were investigated on Congo red-tryptone agar plates prepared as described in Dietrich *et al*. [216]. Briefly, 1% tryptone (Oxoid) and 1% agar (No. 3 Oxoid) were mixed in 200 mL $dH_2O$ and autoclaved. Media were cooled down to 50°C before the addition of 8 milligrams (mg) of Congo red (MP Biomedicals, LLC) and 4 mg of Coomassie Brilliant R-250 (Sigma-Aldrich). 60 mL of the medium was poured per square plate (Sterilin Petri Plate 100 mm Square 109) and left to settle. Plates were left to dry for 24 h at room temperature before use.

Bacterial cultures that were grown for 12 h were collected, $OD_{600}$ was adjusted to 1.0 in 1 mL LB, cells were pelleted and resuspended in 1 mL of fresh LB. 5 µL of these o/n cultures were spotted onto the agar (supplemented with or without 1 mM IPTG when the inducible *rsmA*$_{ind}$ Δ*rsmN* and *rsmN*$_{ind}$ Δ*rsmA* strains were used). Plates were incubated at room temperature up to 6 days.

2.4.7.5.3 Imaging of biofilms

During the 14 h Bioflux run, time-lapse images were taken once every 10 min. at 10x objective magnification using an EVOS microscope and images were compiled together to generate videos.

The wells of the BioFlux plate were imaged under the confocal microscope (Carl Zeiss AG) at 20x objective magnification using ZEN 2009 computer software. At least 3 (1 at the start, 1 at the end and 1 in the middle) individual Z-stacks of the bottom layer of each chamber were taken using phase contrast setting. Syto 9® excitation and emission wavelengths were set at 483 nm and 500 nm respectively; these are values that are close to the excitation/emission values for eGFP, which was the dye chosen on the ZEN program. The acquisition conditions were set as follows: Laser 488 nm, Averaging 4, Laser power 15.0, Master Gain 600-900, Digital gain 1.0, Digital offset 0, 1 AU optimal pinhole (~ 0.92 µM for full and bottom chamber Z-stacks), Speed 8, and Zoom 1.1.

Colony biofilms were imaged daily with a Nikon D40 camera.

**2.4.7.6 Phage plaque assay**

For phage plaque assays, a modified version of the soft top agar protocol described in Rice *et al.* [117] was followed. LB plates were layered with 5 mL of 0.8% soft top agar seeded with 5 µL of *P. aeruginosa* PAO1B1 or PAO1B1Δ*Pf4* strains. $OD_{600}$ of PAO1B1 and PAO1B1Δ*Pf4* o/n cultures were adjusted to 1.0 in 1 mL of LB, cultures were pelleted and resuspended in fresh LB to get rid of the phages in the o/n cultures. After soft top agar was settled, 10 µL of cell-free supernatants from the WT PAO1-N, Δ*rsmA*, Δ*rsmN*, *rsmN*$_{ind}$ Δ*rsmA* and Δ*pqsL* (used as a positive control) strains were spread on plates. $OD_{600}$ of these cultures were also adjusted to 1.0 in 1 mL of LB. Pictures were taken after 18 h of incubation at 37°C.

Alternatively, serial dilutions from the o/n cultures ($OD_{600}$ standardised to 1.0) of the strains mentioned above were prepared and 5 µL of $10^{-5}$ diluted cultures were seeded in 5 mL of the soft top agar to be able to count colony forming units (c.f.u) as precisely as possible.

## 2.4.8 Protein Methods

### 2.4.8.1 Trichloroacetic acid (TCAa) precipitation

To check the protein profiles of the WT, Δ*rsmA*, Δ*rsmN* and inducible $rsmA_{ind}$ Δ*rsmN*/$rsmN_{ind}$ Δ*rsmA* strains, supernatant proteins were precipitated by trichloroacetic acid addition. 900 µL of the o/n cultures grown at 37°C or 34°C for 18 h at 200 r.p.m were treated with 100 µL 100% TCAa (Sigma-Aldrich) stored at 4°C in the dark according to the protocol described in Luckett *et al.* [232]. Supernatant-TCAa mixture was incubated on ice for 30 min. and centrifuged at 4°C for 15 min. at 13,000 r.p.m. The supernatant was discarded and the resulting protein pellet was resuspended in 500 µL ice-cold acetone (Fischer Scientific). The suspension was centrifuged at 4°C for 5 min. with agitation (13,000 r.p.m). The supernatant was decanted and the pellet was air-dried for 15 min. for the removal of the residual acetone. The pellet was resuspended in a solution of 10 µL 50 mM NaOH, 65 µL $dH_2O$ and 25 µL of the 4x sample buffer (200 mM Tris-Cl pH 6.8, 400 mM DTT, 8% sodium dodecyl sulphate (SDS), 0.4% w/v Bromophenol Blue, 40% v/v glycerol, up to 50 mL with $dH_2O$). Samples were kept at -20°C until further use.

### 2.4.8.2 SDS-polyacrylamide gel electrophoresis (SDS-PAGE)

For the identification of proteins, samples previously prepared and kept at -20°C were boiled for 10 min. at 95°C in a heat block (Grant QBA2, Scientific Laboratory Supplies) and run on 10% SDS gels at 16 milliamperes (mA) for the stacking gel and at 40 mA for the resolving gel until the dye reached the bottom. The resolving gel components were as follows: 1.7 mL 30% w/v acrylamide/bisacrylamide premade solution (Sigma-Aldrich), 1.3 mL 1.5 M Tris (pH 8.8, Fischer Scientific), 50 µL 10% SDS (Sigma-Aldrich), 50 µL 10% ammonium persulfate (APS) (frozen as aliquots at -20°C), 5 µL N,N,N',N'-tetramethylethylenediamine (TEMED) (Sigma-Aldrich, kept at room temperature) and 1.9 mL of $dH_2O$. 3.5 mL of the resolving gel mixture was poured in between glass plates (Mini PROTEAN® System, BioRad) and a thin layer of isopropanol (Fischer Scientific) was immediately transferred on top. When the

resolving gel was polymerised, isopropanol was poured away and ~ 1 mL of the stacking gel (330 µL 30% acrylamide/bisacrylamide mix, 250 µL 1.0 M Tris (pH 6.8), 20 µL 10% SDS, 20 µL 10% APS, 5 µL TEMED, 1.4 mL $dH_2O$) was poured on top. Glycine-SDS gels were run in 1x running buffer (10x running buffer components are 125 mM Tris, 0.96 M glycine, 1% w/v SDS, $dH_2O$ up to 1 L). 5-15 µL of the samples were loaded into the wells. Broad range prestained protein marker (NEB) was used as a molecular weight marker.

Additionally, proteins were run on 4-12% gradient Bis-Tris (1.0 mm thick) and 12% Bis-Tris (1.0 mm thick) NuPAGE gels (NOVEX®) using the XCell SureLock™ Mini-Electrophoresis system (Life Technologies) for proteomics analysis. Trypsin digestion and liquid chromatography-mass spectrometry (LC-MS) steps were performed at the Protein Nucleic Acid Chemistry Laboratory, University of Leicester. The samples to run on NuPAGE gels were mixed with 4x NuPAGE® LDS Sample Buffer at the last step of the TCAa precipitation protocol. SeeBlue® Pre-stained Standard (NOVEX®) was used as the molecular weight marker. Gels were run in 1x 2-(*N*-morpholino) ethane sulfonic acid (MES) buffer (20x stock solution from NOVEX® Invitrogen, 1.0 M MES, 1.0 M Tris base, 69.3 mM SDS, 20.5 mM EDTA free acid, up to 1 L with $dH_2O$) at 120 V for 75 min.

#### 2.4.8.3 Coomassie blue staining

For immediate visualization, proteins were stained with Coomassie Blue solution (0.1% w/v Coomassie Brilliant Blue R250, 10% v/v acetic acid, 40% v/v methanol) for 1 h and destained with 20% methanol (v/v, Fischer Scientific) and 10% acetic acid glacial (v/v, Fischer Scientific) solution in 3 washes. Gel pictures were taken in the Gel Doc™ XR+ System (BioRad) using Filter 1.

#### 2.4.8.4 Western blotting

To inspect the autolysis of the Δ*rsmA*/Δ*rsmN* single and inducible double deletion mutants, supernatant proteins were first transferred to nitrocellulose (0.2 µm, BioRad) or PVDF membranes (Immobilon-P Membrane, PVDF, 0.45 µm, Merck Millipore) using a Mini Trans-Blot cell (BioRad). Protein transfer was carried out in chilled (kept at 4°C) 1x transfer buffer (20 mM Tris base; 150 mM glycine; 20% methanol, $dH_2O$

up to 1 L) at 150 mA for 1 h at room temperature. Membranes and blotting sponges were wetted in the 1x transfer buffer prior to the run.

To block the membrane, 20 mL phosphate buffered saline [PBS, 1x solution composition: NaCl 137 mM, KCl 2.7 mM, sodium phosphate dibasic ($Na_2HPO_4$) 10 mM, $KH_2PO_4$ 1.8 mM] with 0.5% (v/v) Tween 20 (Sigma-Aldrich) and 5% (w/v) non-fat dried skimmed milk powder (AppliChem) was added and left at 4°C (1 h up to o/n). The primary antibody (rabbit) against IscS, a cysteine desulfurase was diluted 1:1000 in 20 mL blocking solution (PBS with 0.5% Tween 20 and 5% non-fat dried skimmed milk powder) and incubated with the membrane for 1 h at room temperature. The membrane was washed 3 × 5 min. in PBS with 0.5% Tween 20. The secondary antibody (α-rabbit IgG) was diluted 1:10000 in the blocking solution and incubated with the membrane for 1 h at room temperature. The membrane was washed 3 × 5 min. and once for 15 min. in PBS with 0.5% Tween 20 before developing the blot. The membrane was dried and Pierce® ECL Western Blotting Substrate (Thermo Scientific) solutions (solution A: luminol, solution B: peroxide, 125 µL from each solution per membrane) were added on top of the membrane. Excess reagent was dried off and the blot was placed inside a plastic shield in an X-ray cassette. Blots were exposed to a Hyperfilm$^{TM}$ chemiluminescence film (GE Healthcare, Amersham Biosciences) with the use of the Carestream® Kodak® autoradiography GBX developer/replenisher and fixer/replenisher solutions (Sigma-Aldrich).

#### 2.4.8.5 Protein purification

The use of affinity tags permits the purification of any protein at high levels following a single standardised affinity chromatography protocol. QIA*express*® Ni-NTA Fast Start System used in this study employs an affinity tag comprising six consecutive histidine residues ($His_6$-tag) which bind to the nickel-nitrilotriacetic acid (Ni-NTA) metal affinity chromatography matrices.

PAO1-L electrocompetent cells were transformed with the pMR4 (pME6032-based, with IPTG-inducible $P_{tac}$ promoter) construct that was cloned using the PMR4F and PMR4R primers (see Table 2.3) to introduce a $His_6$-tag at the amino terminus of RsmN. The expression of *rsmN* was induced in the PAO1-L strain due to the 58 kb deletion in the PAO1-N genome (see section 1.3.5). Overnight cultures of the PAO1-

L/pMR4 strain were grown in 10 mL of LB + 125 µg/mL Tc at 37°C and 34°C with 235 r.p.m agitation for 18 h. QIA*express*® Ni-NTA Fast Start Handbook protocol was followed under native conditions; 1 mM IPTG was added to induce *rsmN* expression at an $OD_{600}$ of ~ 0.6, and cultures were incubated 5 more h ($OD_{600}$ of ~ 2.0).

RsmN was eluted in three fractions (E1, E2 and E3) of 1 mL elution buffer. Protein and RNA obtained in elution fractions were quantified using a NanoDrop ND-1000 Spectrophotometer and concentrated in ~ 100 µL using Amicon Ultra-4 or Ultra-15 (10KMWCOPP – UFC801008) centrifugal filters.

200 mL culture of the PAO1-L/pMR4 strain grown at 34°C yielded less RsmN-bound RNA than the bacterial culture grown at 37°C previously. To obtain enough RsmN-bound RNA for RNASeq, four 200 mL cultures with similar optical densities (start $OD_{600}$ ~ 0.1, $OD_{600}$ at the time of sampling ~ 2.0) were pooled together to give duplicates. The total RNA was extracted from two cultures.

At each step (such as flow-through, wash, elution) of the Ni-NTA Fast Start Kit protocol, 5-10 µL of the sample was mixed with 5-10 µL of 2x NuPAGE® LDS Sample Buffer. In addition, 1 µL of the concentrated RsmN solution was mixed with 9 µL of 2x Sample Buffer. Samples were run on 12% Bis-Tris NuPAGE Gels (1.0 mm) from NOVEX® as described in 2.4.8.2.

### 2.4.9 RNA work

#### 2.4.9.1 Total RNA extraction

For RNASeq, the total RNA was extracted from the PAO1-L/pMR4 cultures grown to an $OD_{600}$ of ~ 2.0 after 5 h of *rsmN* expression at 37°C and 34°C. 600 µL RNAprotect reagent was added to 300 µL of the bacterial culture. The mixture was incubated for 5 min. at room temperature and centrifuged for 10 min. at 5000 x *g*. The total RNA was extracted following Protocols 4 and 7 (excluding DNase digestion step) of the RNeasy Mini Kit (QIAGEN). The RNA samples were treated with Turbo DNase to get rid of the contaminating genomic DNA (see section 2.4.9.3).

#### 2.4.9.2 Purification of RNAs that are bound to the $His_6$-tagged RsmN

RsmN-bound RNA and total RNA were purified from PAO1-L/pMR4 cells for RNASeq analysis. After pooling down and concentrating RsmN in centrifugal filters as described in 2.4.8.5, RsmN-bound RNAs were purified using the RNeasy Mini Kit (QIAGEN) following step 7 of protocol 4 (Enzymatic Lysis and Proteinase K Digestion of Bacteria, reagent volumes adjusted for 1 x $10^8$ – 2.5 x $10^8$ bacteria) and protocol 7 (Purification of Total RNA from Bacterial Lysate Using the RNeasy Mini Kit) excluding the DNase digestion step. 2 mL solution of Proteinase K was ordered from QIAGEN. RNA was eluted in 30 µL RNase-free water.

#### 2.4.9.3 DNase treatment

The genomic DNA was removed using the Turbo DNA-free Kit. In a total volume of 50 µL; 20 µg RNA, 5 µL 10 x TURBO DNase Buffer, 5 µL TURBO DNase, 1 µL SUPERase (inhibitor of RNase activity, Ambion®) and RNase-free water were mixed and incubated at 37°C for 45 min.

The removal of the genomic DNA was confirmed by PCR. The illustra™PuReTaq™ Ready-To-Go™ PCR beads from GE Healthcare were resuspended in 22 µL RNase-free water; 1 µL forward and reverse *rsmA* primers and 1 µL of the digested RNA product were added afterwards. A colony of the WT PAO1-N strain was included as a positive control. The reaction mixture without any RNA template was used as a negative control. 2 µL of the Orange Gel Loading Dye (6x) was added to 25 µL of the reaction mixture and PCR products were run on 1% agarose gel at 100 V for 60 min. Quick-Load 2-Log DNA ladder (NEB) was used for reference. Agarose gel electrophoresis (Supplementary Figure 1) shows that 45 min. of digestion with Turbo DNase was sufficient to clear out the remaining genomic DNA.

### 2.4.10 RNA sequencing (RNAseq)

After the extraction and purification of the total RNA and RsmN-bound RNA from PAO1-L/pMR4 cells, around 5 µg of DNA-free RNA was sent to the Deep Sequencing Facility (School of Life Sciences, Queens Medical Centre) for the preparation of the strand-specific RNASeq libraries using the Illumina sequencing platform. DNase treatment, rRNA depletion, fragmentation, adapter ligation and cDNA synthesis steps were carried out by Sunir Malla. The quality of RNA was checked using the

Prokaryote Total RNA Nano assay on an Agilent 2100 BioAnalyzer LabChip® Caliper prior to rRNA depletion (see Supplementary Figures 2 & 3). The RiboZero kit for gram-negative bacteria was used to remove the rRNA.

The cDNA libraries were constructed using the NEBNext Ultra Directional RNA Library Prep kit (Illumina™, E7420S). 12 cycles of PCR amplifications were run. The cDNA samples were eluted in HPLC-grade water. The yield of the amplified DNA was confirmed by loading 1 µL of the 1:8-1:10 diluted samples on an Agilent 2100 Bioanalyzer.

The size selection, amplification and sequencing steps of RNASeq were carried out at the Institute of Biological Sciences at the University of Malaya in collaboration with Dr. Chan Kok Gan.

To increase the concentration and prevent the loss during size selection, additional adapters were ligated to the cDNA samples in Malaysia. Sample libraries were prepared using the TruSeq® ChIP Sample Preparation Kit (Illumina™) and loaded into the sequencer at a concentration of 10 pM. The sequencing experiment was performed on Illumina MiSeq in 150 cycles cartridge with the v3 chemistry (Workflow → Generate FASTQ; Application → ChIPSeq; Assay → TruSeq LT).

#### 2.4.10.1 Analysis of the RNASeq results

The adapters were removed and the leftover rRNA/tRNA were filtered by Victoria Wright where necessary (Deep Sequencing Facility, School of Life Sciences, Queens Medical Centre).

To be able to compare the RsmN targets with the RsmA targets, results from RsmA RNASeq which was previously performed [212] was reanalysed in the same manner as RsmN data and `.wig` ('wiggle') files that list the number of times each nucleotide on the chromosome has been read were created by Victoria Wright using the bash script in Bedtools (Bam2Wig.sh, https://github.com/arq5x/bedtools2, bedtools v2.17.0). The `.wig` files were processed using a series of dedicated perl scripts written by Stephan Heeb to perform basic operations. Rsm-bound RNAs are a subset of the total RNA extracted at the time of sampling (Figure 2.3). By dividing the read values

of the former by the latter an "enrichment index", in which a value above 1 would correspond to a nucleotide of an RNA bound by RsmN, was generated and enriched targets were assessed by plotting the `.wig` files against the annotated genome of the PAO1-L strain on Artemis annotation tool [233].

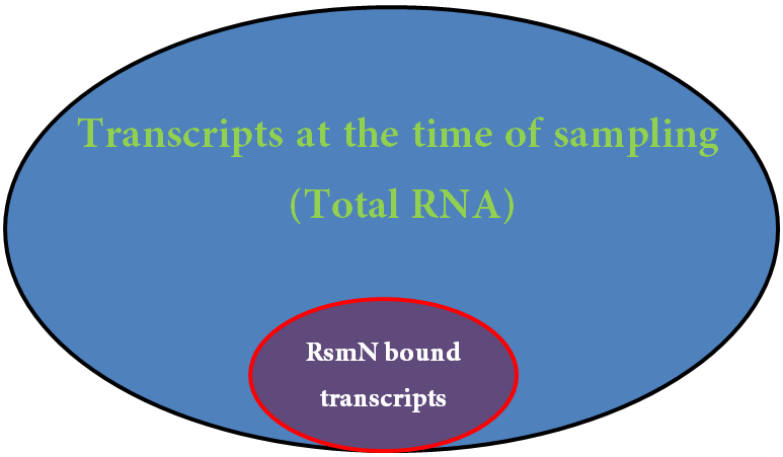


**Figure 2.3. Diagrammatic depiction of enriched transcripts**
The purple region represents RsmN-bound hence 'enriched' transcripts. Enriched transcripts are a subset of the total RNA, however, RNAs that are illustrated as the blue region in the total RNA sample are not bound to the Rsm proteins at the time of sampling.

## 2.5 Chronic infection mouse model

The bacterial loads of the PAO1-N and *rsmN*$_{ind}$ Δ*rsmA* strains in a chronic infection model were investigated in collaboration with Prof. Kendra Rumbaugh (Department of Surgery, Texas Tech Health Sciences Centre, Lubbock, Texas/U.S.A). A murine chronic wound infection was set up as described in Watters *et al*. [234].

# 3 The Biological Role of RsmN

## 3.1 Introduction

*P. aeruginosa* is an opportunistic pathogen able to establish acute as well as chronic infections in humans through the production of a wide variety of virulence determinants such as phenazines, proteases, HCN, motility factors and exotoxins (see section 1.3.2). Production of some of these determinants is governed by the QS systems of *P. aeruginosa* [235]. The negative control on the production of HCN, phenazine pigment PYO, cytotoxic lectin PA-IL, the QS molecules 3O-C12-HSL and C4-HSL, and staphylolytic activity by the RNA-binding protein RsmA has been demonstrated previously [204]. Furthermore, the positive role of RsmA in lipase synthesis, rhamnolipid production and swarming motility has been shown [121, 183]. The deletion of *rsmA* led to robust biofilm formation and coincided with high c-di-GMP levels [207, 210]. In a cell culture model with human bronchial epithelial cells, the Δ*rsmA* mutant displayed increased invasion of the airway epithelial cells whereas it failed to induce actin depolymerisation and cytotoxicity [205]. RsmA repressed the expression of some T6SS genes while it was required for the maximal expression of the T3SS genes [236]. Furthermore, antibiotic resistance profiling indicated increased resistance of the Δ*rsmA* mutant to amikacin, nalidixic acid, trimethoprim, ceftazidime (substrates of the MexEF-OprN pump) and gentamicin (substrate of the MexXY-OprM pump) [205]. RsmA activity was found to be modulated by two sRNAs, RsmY and RsmZ which are transcribed under the control of the Gac TCS and RetS and LadS sensors of *P. aeruginosa* [112]. Testing the protein function after modification of the conserved residues revealed that $Arg_{44}$ is a key residue involved in the target RNA-RsmA interactions and $Arg_{6}$ and $Glu_{46}$ play structural roles in the formation of a stabilising salt bridge [53].

An RsmA homologue, encoded by the *rsmN* gene (Figure 3.1) annotated *PA5183.1* was discovered in *P. aeruginosa* in a previous study [210]. The *rsmN* gene overlaps the *phrX* gene (annotated *PA5183.01*) coding a 151 nt-long sRNA [237] and it is flanked by an intergenic region (depicted in purple) where a LasR binding site is located (*Pseudomonas* Genome Database, [238]). X-ray crystallography and sequence comparison of the RsmA and RsmN proteins revealed that RsmN is 34% identical and

52% similar to RsmA (see section 1.3.5). Whereas some RsmA homologues such as the A1 and A2 proteins in *Pseudomonas entomophila* are functionally redundant, some, for instance the RsmA and RsmE proteins of *P. fluorescens* CHA0, are expressed differentially to provide a tight control of gene regulation at the post-transcriptional level [239, 240]. Therefore, after the discovery of RsmN through phenotypic complementation [210], functional equivalence of the RsmA and RsmN proteins was investigated [212]. A previous study [241] has provided information on the RNA-binding of RsmN, demonstrating the importance of the $Arg_{62}$ residue for target binding in the same way $Arg_{44}$ is required for target binding of RsmA. However, no evidence of RsmN acting as an RsmA homologue in phenotypic assays such as swarming, Kornberg, elastase, protease or pyocyanin could be found [212].




**Figure 3.1. The genomic context of *rsmN***
The *rsmN* gene is adjacent to an intergenic region (purple) and the *phrX* gene (light blue) coding a sRNA and located between the *PA5184* (red) and *PA5183* (yellow) genes.

The biological function of RsmN in relation to RsmA and how the two proteins function in the presence and absence of each other is the focus of this chapter. The initial experimental approach taken to investigate the biological function of RsmN was to use a single deletion mutant of *rsmN* in phenotypic assays where Δ*rsmA* phenotypes were identified and to compare the observed phenotypes with the WT and Δ*rsmA* phenotypes. In addition, the $rsmA_{ind}$ Δ*rsmN* and $rsmN_{ind}$ Δ*rsmA* inducible double deletion mutants were included to evaluate the effect of *rsmN* deletion in a Δ*rsmA* background and *vice versa*. To investigate the influence of the double deletion of *rsmA* and *rsmN*, sometimes only the $rsmN_{ind}$ Δ*rsmA* strain was used due to a leakage from the $rsmA_{ind}$ Δ*rsmN* strain. The Δ*rsmN*, $rsmA_{ind}$ Δ*rsmN* and $rsmN_{ind}$ Δ*rsmA* strains were constructed (see Supplementary Figure 4) in PAO1-N because in this genetic background, the Δ*rsmA* mutant is swarming-deficient and motility could be complemented by providing an intact copy of *rsmN* [210].

In the phenotypic assays tested at 37°C, *rsmN* deletion did not result in striking phenotypic differences compared with the WT PAO1-N strain. Therefore, in an

alternative approach, *rsmN* expression was induced in the Δ*rsmA* and $rsmN_{ind}$ Δ*rsmA* mutants via either a chromosomally inserted $P_{tac}$ promoter or a multicopy plasmid (pME6000 and its derivatives) to determine whether any of the known Δ*rsmA* phenotypes and detected phenotypes of the double mutant could be restored by RsmN. The pME6000 vector is derived from pBBR1MCS which is maintained at 20 to 30 copies per cell and encodes the Rep protein responsible for plasmid maintenance [242].

The effect of *rsmN* expression in the *E. coli* Δ*csrA* mutant which is characterised by excessive glycogen accumulation was also investigated. Heeb *et al*. [53] showed that swarming motility and PYO and lipase production of the Δ*rsmA* mutant could be restored to wild-type levels by inducing *rsmA* via a plasmid. However, none of these phenotypes could be complemented by inducing *rsmA*R44A expression. Similarly, in the Kornberg assay, a plasmid-borne copy of *rsmA* but not *rsmA*R44A restored glycogen overproduction by the *E. coli* Δ*csrA* mutant. As $Arg_{44}$ of RsmA was important for the biological activity, the effect of inducing the *rsmN* equivalent with the same point mutation (Arg→Ala; CGC→GCC), *rsmN*R62A, instead of *rsmN* was also investigated in phenotypic assays.

While carrying out the above investigation, complementation of Δ*rsmA* swarming at temperatures below 37°C, which is the standard temperature used under laboratory conditions for the study of human bacterial pathogens, by RsmN was discovered. The multicopy expression of *rsmN* in the Δ*rsmA* mutant resulted in a different motility phenotype at 34°C and lower temperatures in comparison with 37°C and higher temperatures. For this reason, assays performed at 37°C were also repeated at 34°C.

Sequence analysis of the *rsmN* ORF and surrounding genes using Softberry BPROM (http://linux1.softberry.com/berry.phtml) and TransTermHP [243] programs has allowed the prediction of an antisense promoter, $P_{nmsR}$, near the $T_{rsmN}$ and $T_{PA5183}$ terminator sequences [212] (Figure 3.2). For further analysis of the biological role of RsmN using transcriptional or translational fusions, the transcription start site (TSS) of *rsmN* had to be detected. Furthermore, expression from the predicted antisense promoter $P_{nmsR}$ needed to be confirmed. In a set of experiments run by Manuel Romero, *rsmN* and *nmsR* TSSs were identified (Figure 3.2, T highlighted in red and C highlighted in turquoise respectively, see Table 2.3 for oligonucleotides used)

applying a new technique called ARF-TSS (adaptor and radioactivity-free detection of the transcription start site) that involves self-ligation of the first-strand cDNA, PCR amplification, and sequence analysis steps and eliminates the need to use adaptors or radioactive labelling in TSS detection [244]. In a parallel study, Marden *et al*. [206] detected the TSS of *rsmF* (T highlighted in pink in Figure 3.2), which is another annotation of *rsmN*, by RACE (rapid amplification of cDNA ends) method that is generally used to obtain full-length cDNAs if a part of the gene sequence was already known [245, 246].

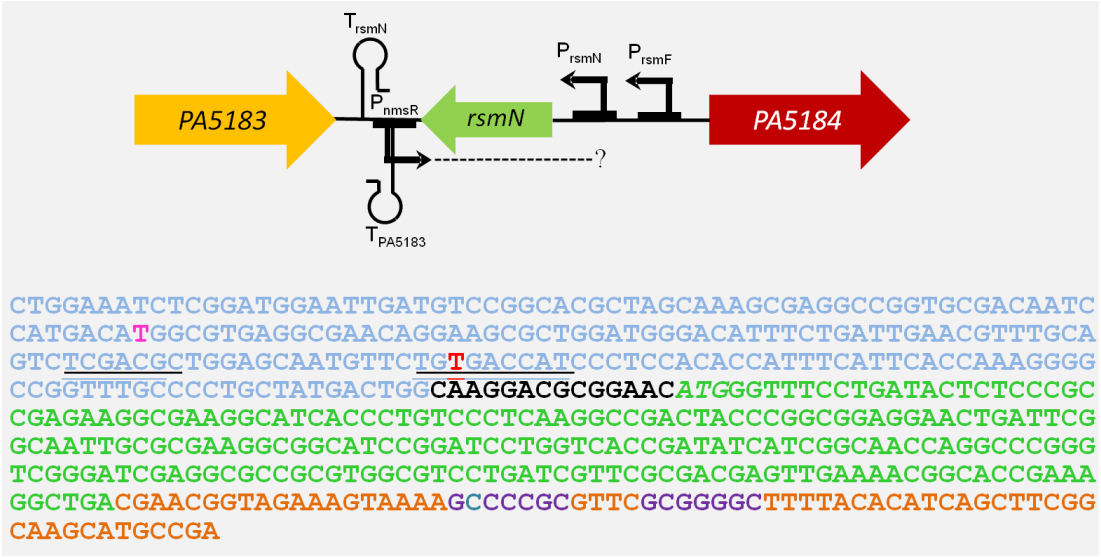


**Figure 3.2. The nucleotide sequence of the *PA5183-PA5184* intergenic region including the promoter and terminator sequences**
The *rsmN* sequence is highlighted in green and the start codon ATG is depicted in italic. The predicted -35 and -10 consensus sequences are underlined. The RBS sequence is highlighted in black and inverted repeats of the Rho-independent $T_{PA5183}$ terminator are highlighted in purple. Transcription start sites of *rsmN*, *rsmF* and *nmsR* are shown in red, pink and turquoise respectively.

In addition, using a dual reporter, pFLUX (where the *dsRed* and *luxCDABE* operons are separated by an omega terminating cassette built in the pMINI-CTX1 backbone) developed by S. Higgins [247], expression levels from the $P_{rsmN}$, $P_{rsmF}$ and $P_{nmsR}$ promoters were investigated by Manuel Romero (primers used in the construction of these fusions are listed in Table 2.3) and it was discovered that all tested promoters were active. Expression from the $P_{nmsR}$ promoter was more prominent when compared to the expression from the $P_{rsmN}$ promoter. These findings led to the speculation that RsmN might have an autoregulatory mechanism where an antisense RNA is

transcribed from the $P_{nmsR}$ promoter to control RsmN activity. This hypothesis was tested using *rsmN* expression plasmids with a different combination of the promoters mentioned above.

## 3.2 Results

### 3.2.1 The influence of RsmA and RsmN on the growth of *P. aeruginosa* at 37°C and 34°C

Initially, to determine whether the deletion of *rsmN* influenced the growth of *P. aeruginosa* in a rich laboratory medium, growth of the WT PAO1-N, Δ*rsmA*, Δ*rsmN* and *rsmN*$_{ind}$ Δ*rsmA* strains cultured in LB without IPTG over 24 h at 37°C and 34°C were compared. $OD_{600}$ measurements were taken every 2 h until 12 h and one last measurement was taken after 24 h.

The growth curves shown in Figure 3.3 suggest that although *rsmN* deletion had no effect, growth was affected by the mutation of *rsmA* alone and most severely in the *rsmN*$_{ind}$ Δ*rsmA* inducible double deletion mutant. Extended lag phases were observed for the Δ*rsmA* and *rsmN*$_{ind}$ Δ*rsmA* mutants (~ 2 h). All four strains reached similar optical densities after 24 h and grew slower at 34°C than at 37°C. Generation times (calculated as outlined in section 2.1) were ~ 41 (WT), 42 (Δ*rsmN*), 57 (Δ*rsmA*), and 72 (*rsmN*$_{ind}$ Δ*rsmA*) min. at 34°C in comparison with ~ 36 (WT), 36 (Δ*rsmN*), 41 (Δ*rsmA*) and 38 (*rsmN*$_{ind}$ Δ*rsmA*) min. at 37°C. Generation time of the *rsmN*$_{ind}$ Δ*rsmA* mutant almost doubled at 34°C compared with 37°C. Population densities of the WT and Δ*rsmN* strains increased faster compared with the Δ*rsmA* and *rsmN*$_{ind}$ Δ*rsmA* strains at 34°C.

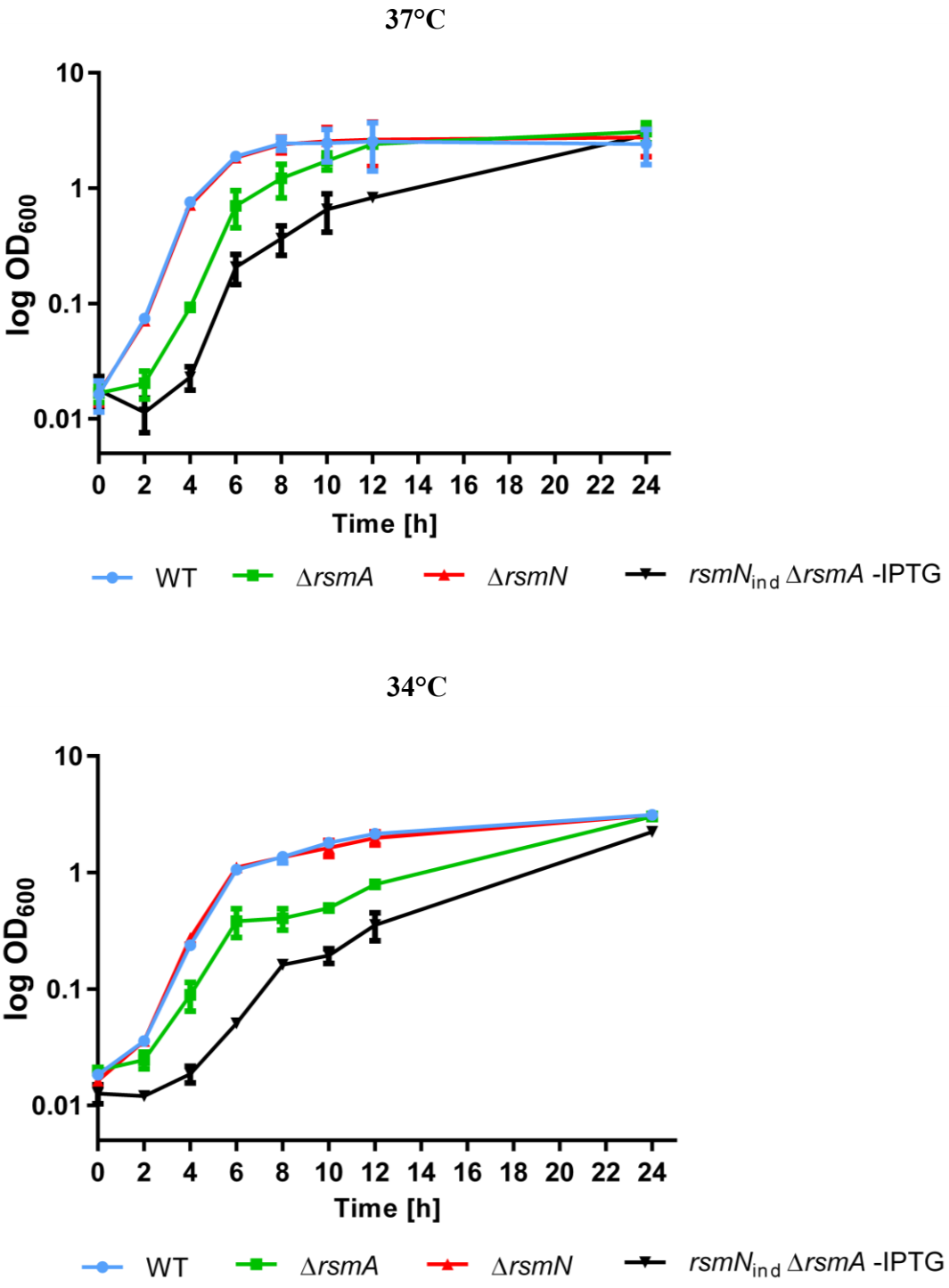


**Figure 3.3. The influence of *rsmA* and *rsmN* mutations on the growth of *P. aeruginosa* in LB**

The single deletion of *rsmA* and subsequent deletion of *rsmN* in the Δ*rsmA* mutant result in extended lag phases of growth both at 37°C and 34°C. The deletion of *rsmN* does not influence the growth of *P. aeruginosa* at both temperatures. All strains grow faster at 37°C (top) compared with 34°C (bottom). Error bars represent the standard deviation from triplicate measurements.

### 3.2.2 The *P. aeruginosa* Δ*rsmA* mutant but not the Δ*rsmN* mutant clumps

Since the deletion of *rsmA* causes the aggregation of *P. aeruginosa* cells [121], cell clumping might be responsible for the longer lag phases observed for the Δ*rsmA* and *rsmN*$_{ind}$ Δ*rsmA* mutants (Figure 3.3). For this reason, clumping phenotype in the Δ*rsmA* and inducible *rsmA*$_{ind}$ Δ*rsmN*/*rsmN*$_{ind}$ Δ*rsmA* mutants and the effect of *rsmA* or *rsmN* expression on the clumping phenotypes of the inducible double deletion mutants were investigated. During sampling for OD measurements, clumped cells did not disperse even after vortexing. Figure 3.4 shows aliquots from the overnight cultures of the WT, Δ*rsmA*, Δ*rsmN* and inducible *rsmA*$_{ind}$ Δ*rsmN*/*rsmN*$_{ind}$ Δ*rsmA* strains (latter two supplemented with or without IPTG) grown in flasks (1:10 ratio of the culture volume to the flask volume).

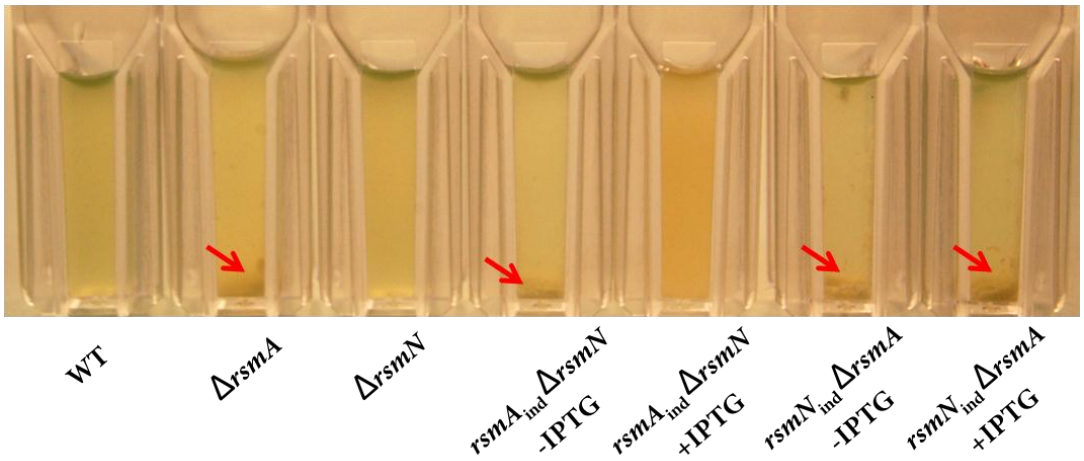


**Figure 3.4. The impact of *rsmA* and *rsmN* mutations on cell clumping**
Cell aggregates in the Δ*rsmA*, *rsmA*$_{ind}$ Δ*rsmN* -IPTG, *rsmN*$_{ind}$ Δ*rsmA* -IPTG and *rsmN*$_{ind}$ Δ*rsmA* +IPTG aliquots are highlighted by red arrows. The single deletion of *rsmA* but not *rsmN* leads to the formation of cell aggregates. Expression of *rsmA* in the *rsmA*$_{ind}$ Δ*rsmN* mutant abolishes clumping whereas *rsmN* expression in the *rsmN*$_{ind}$ Δ*rsmA* mutant does not.

It is clear that Δ*rsmA*, *rsmA*$_{ind}$ Δ*rsmN* and *rsmN*$_{ind}$ Δ*rsmA* mutants but not the WT strain or the Δ*rsmN* mutant aggregate and form clumps as they grow. The addition of IPTG to induce *rsmA* expression abolishes the clumping phenotype of the inducible double deletion mutant, however, *rsmN* expression has no apparent effect.

To determine whether clumping of the Δ*rsmA* mutant could be prevented by *rsmN* expression, the Δ*rsmA* mutant PAZH13 was transformed with pHS2 (Figure 2.1, panel c) which is a multicopy *rsmN* expression plasmid constructed using the pME6000

vector. In addition, the contribution of $Arg_{62}$ which is the RsmN equivalent of RsmA $Arg_{44}$ residue that was demonstrated to be fundamental for target-binding and biological function [53] was investigated in a Δ*rsmA*/pHS2R62A strain where the arginine residue at the 62$^{nd}$ position has been substituted with an alanine residue. WT/pME6000, Δ*rsmA*/pME6000 and Δ*rsmN*/pME6000 strains were included for reference. Figure 3.5 illustrates that whereas multicopy expression of *rsmN* resulted in the dispersal of the aggregates formed by the Δ*rsmA*/pME6000 mutant, R62A substitution in the *rsmN* gene resulted in the loss of this complementary effect.

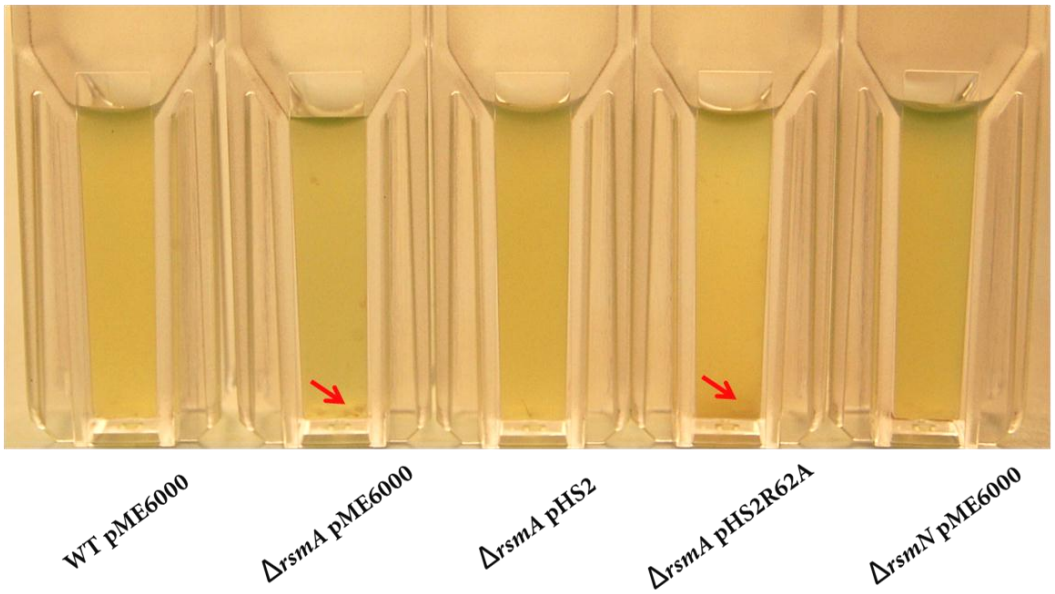


**Figure 3.5. Abolished clumping in a Δ*rsmA*/pME6000 deletion mutant by multicopy expression of *rsmN***

Aggregates of the Δ*rsmA* mutant can be dispersed by *rsmN* expression via pHS2 but not when the $Arg_{62}$ is substituted by an alanine. The wild-type strain PAO1-N and the Δ*rsmN* mutant transformed with the backbone plasmid do not clump. Clumped cells of the Δ*rsmA*/pME6000 and Δ*rsmA*/pHS2R62A strains are highlighted by red arrows.

### 3.2.3 Regulation of motility by RsmA and RsmN

Under laboratory conditions, *P. aeruginosa* swims on glucose supplemented media with low agar concentration (0.3% w/v), swarms on semi-solid agar (0.5% to 0.7% w/v) and twitches at the interface between a more solid agar (1.0% agar w/v) and the plastic base of a petri dish [107, 108]. Heurlier *et al*. [121] showed that the deletion of *rsmA* abolished swarming of the PAO1-N strain. In this study, motility deficiency of the PAO1-N Δ*rsmA* mutant was exploited in swarming, swimming and twitching assays to investigate whether RsmN controlled motility positively.

### 3.2.3.1 Swarming motilities of the single and inducible Δ*rsmA* and Δ*rsmN* double deletion mutants

Figures 3.6 and 3.7 illustrate the impact of *rsmN* on swarming. Figure 3.6 shows that unlike *rsmA* deletion, *rsmN* deletion does not abolish swarming at 37°C. However, swarming of the Δ*rsmN* mutant is decelerated as Δ*rsmN* cells reached to the edges of the plates after 24 h post-inoculation whereas swarmer cells of the WT strain reached to the edges of the plates after ~ 16 h (see Supplementary Figure 5). The *rsmA*$_{ind}$ Δ*rsmN* and *rsmN*$_{ind}$ Δ*rsmA* strains grown without IPTG did not spread from the point of inoculation, resembling the Δ*rsmA* swarming phenotype. Inducing *rsmA* expression in the *rsmA*$_{ind}$ Δ*rsmN* strain restored swarming motility of the inducible double deletion mutant; however, *rsmN* expression in the *rsmN*$_{ind}$ Δ*rsmA* strain did not (Figure 3.7).

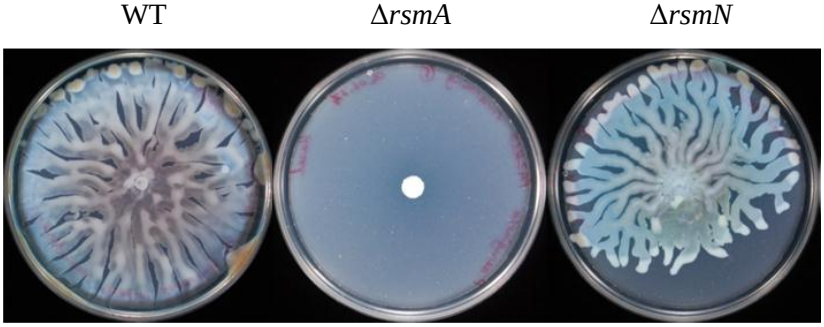


**Figure 3.6. Swarming motilities of the *P. aeruginosa* cells on nutrient broth agar (0.5% w/v) at 37°C in the absence of RsmA or RsmN**
The Δ*rsmA* strain is deficient in swarming motility whereas the WT and Δ*rsmN* strains both swarm, the latter to a lesser extent than the former.

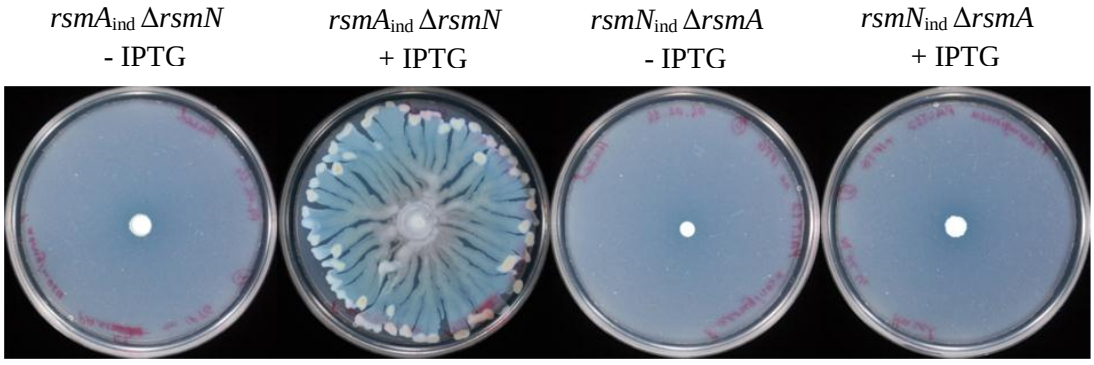


**Figure 3.7. The effect of *rsmA* or *rsmN* expression on swarming motilities of the *rsmA*$_{ind}$ Δ*rsmN* and *rsmN*$_{ind}$ Δ*rsmA* mutants at 37°C on nutrient broth agar (0.5% w/v)**
The expression of *rsmA* but not *rsmN* in a Δ*rsmA* Δ*rsmN* background, mimicked by the *rsmA*$_{ind}$ Δ*rsmN* and *rsmN*$_{ind}$ Δ*rsmA* mutants grown without IPTG, restores swarming motility.

To determine whether the multicopy expression of *rsmN* could restore swarming motility of the Δ*rsmA* mutant, the Δ*rsmA* mutant PAZH13 was transformed with pHS2 (Figure 2.1, panel c) and the swarming assay was repeated with WT, Δ*rsmA* and Δ*rsmN* strains carrying the backbone vector pME6000 and the Δ*rsmA*/pHS2 mutant. The multicopy expression of *rsmN* did not re-establish swarming in the Δ*rsmA* mutant when incubated at 37°C. To determine whether temperature influences the motility control by RsmN, the swarming assay was undertaken at a range of temperatures such as 28°C, 30°C, 32°C, 34°C, 37°C, 39°C and 42°C (Figure 3.8).

Figure 3.8 shows that the WT/pME6000 strain swarmed at all tested temperatures except 42°C whereas the Δ*rsmA*/pME6000 strain did not swarm at any temperature. All strains had reduced motility at 42°C. Swarming motility of the Δ*rsmN*/pME6000 mutant increased directly proportional to the increasing temperature until 42°C. These results indicate that swarming motility is reduced at temperatures below 37°C in the absence of RsmN and it is likely that the Δ*rsmN* mutant does not swarm at temperatures below 28°C. On the other hand, the Δ*rsmA*/pHS2 strain exhibited two different phenotypes: i) swarming at temperatures below 37°C and ii) non-swarming at 37°C and above. Within the 3°C between 34°C and 37°C, the positive impact of *rsmN* on Δ*rsmA* swarming was abolished.

Given the results illustrated in Figure 3.8, phenotypic assays were performed at 37°C and 34°C to investigate the regulatory role of RsmN as a function of temperature. The growth of the WT, Δ*rsmA*, Δ*rsmN* and *rsmN*$_{ind}$ Δ*rsmA* strains was also assessed at 34°C as illustrated in Figure 3.3.

Swarming phenotypes of the WT, Δ*rsmA*, Δ*rsmN*, *rsmA*$_{ind}$ Δ*rsmN* and *rsmN*$_{ind}$ Δ*rsmA* strains at 34°C (data not shown) were similar to the respective phenotypes observed at 37°C (Figures 3.6 and 3.7).

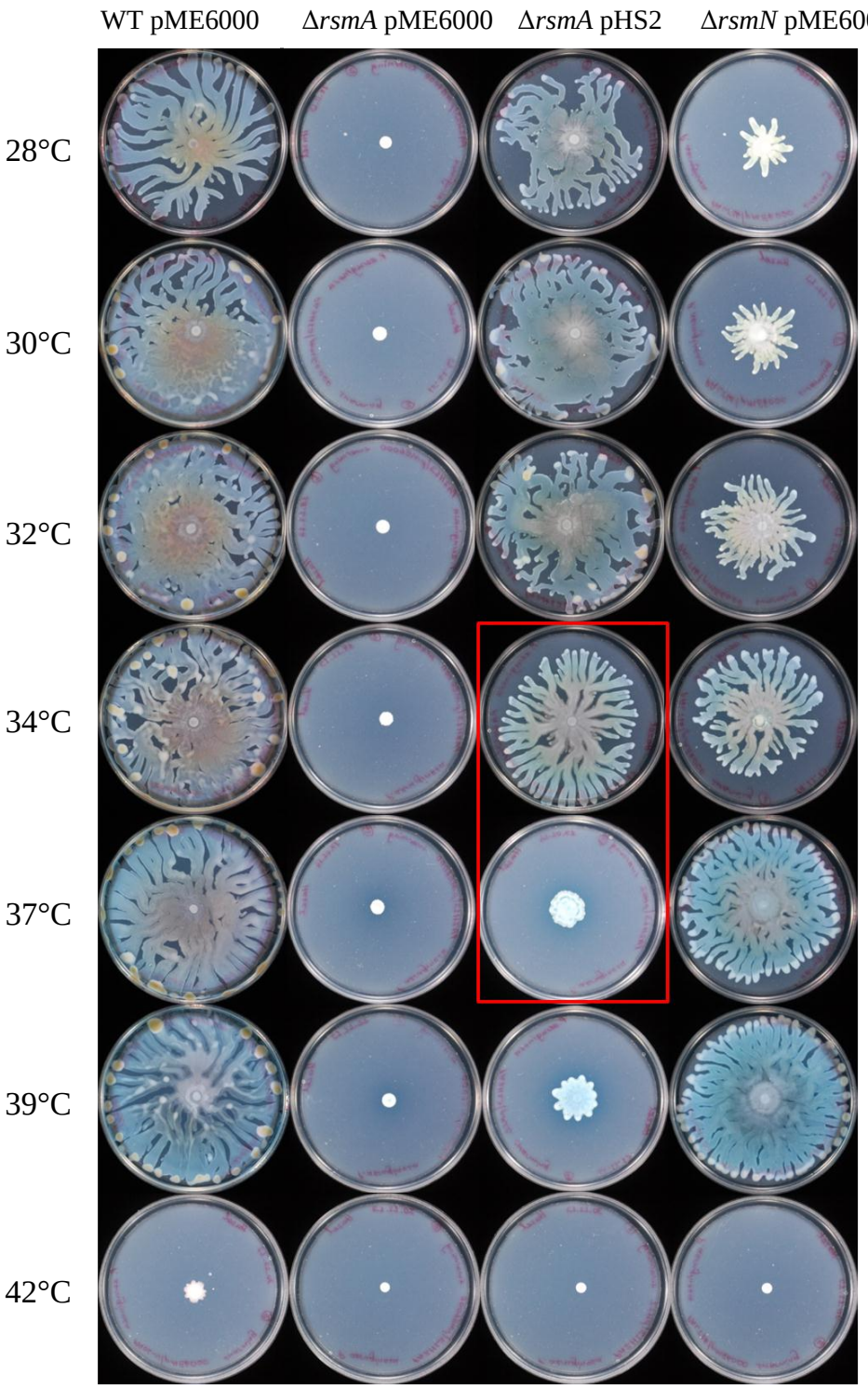


**Figure 3.8. The effect of the multicopy expression of *rsmN* on swarming motility of the Δ*rsmA*/pME6000 strain in comparison with swarming of the WT/pME6000 and Δ*rsmN*/pME6000 strains on nutrient broth agar (0.5% w/v) at different temperatures**
WT/pME6000 and Δ*rsmA*/pME6000 strains display swarming and non-swarming phenotypes respectively across the temperature range except for 42°C. The swarming zone of the Δ*rsmN*/pME6000 strain decreases as the temperature is lowered from 39°C to 28°C. The Δ*rsmA*/pHS2 strain stops swarming as the temperature increases from 34°C to 37°C (highlighted in red box).

Due to numerous possibilities such as conformational changes to the RNA structures or the RBS of RsmN which might be the reason for the non-swarming phenotype of the Δ*rsmA*/pHS2 mutant at 37°C and higher temperatures, swarming motilities of the WT/pHS2 and Δ*rsmN*/pHS2 transformants were also investigated at 37°C and 34°C (Figure 3.9). Furthermore, the effect of R62A mutation (see sections 3.1 and 3.2.2) on the motility control by RsmN was determined.

Figure 3.9 demonstrates that the multicopy expression of *rsmN* cannot complement swarming motility of the Δ*rsmA*/pME6000 mutant and it reduces swarming of the WT/pME6000 and Δ*rsmN*/pME6000 strains at 37°C. The reduction in swarming of the WT/pME6000 strain is to a lesser extent and swarming motility of the Δ*rsmN*/pME6000 mutant is increased as a result of *rsmN* expression at 34°C. Moreover, *rsmN* but not *rsmN*R62A expression restores swarming of the Δ*rsmA*/pME6000 mutant at 34°C. The WT/pHS2R62A and Δ*rsmN*/pHS2R62A transformants have similar phenotypes as the WT/pME6000 and Δ*rsmN*/pME6000 strains at both temperatures. These results suggest that the multicopy expression of *rsmN* increases swarming motility in the absence of RsmA or RsmN whereas there is a reduction in swarming when both proteins are active at 34°C. In contrast, the multicopy expression of *rsmN*R62A does not influence swarming of the WT/pME6000, Δ*rsmA*/pME6000 and Δ*rsmN*/pME6000 strains at either temperature.

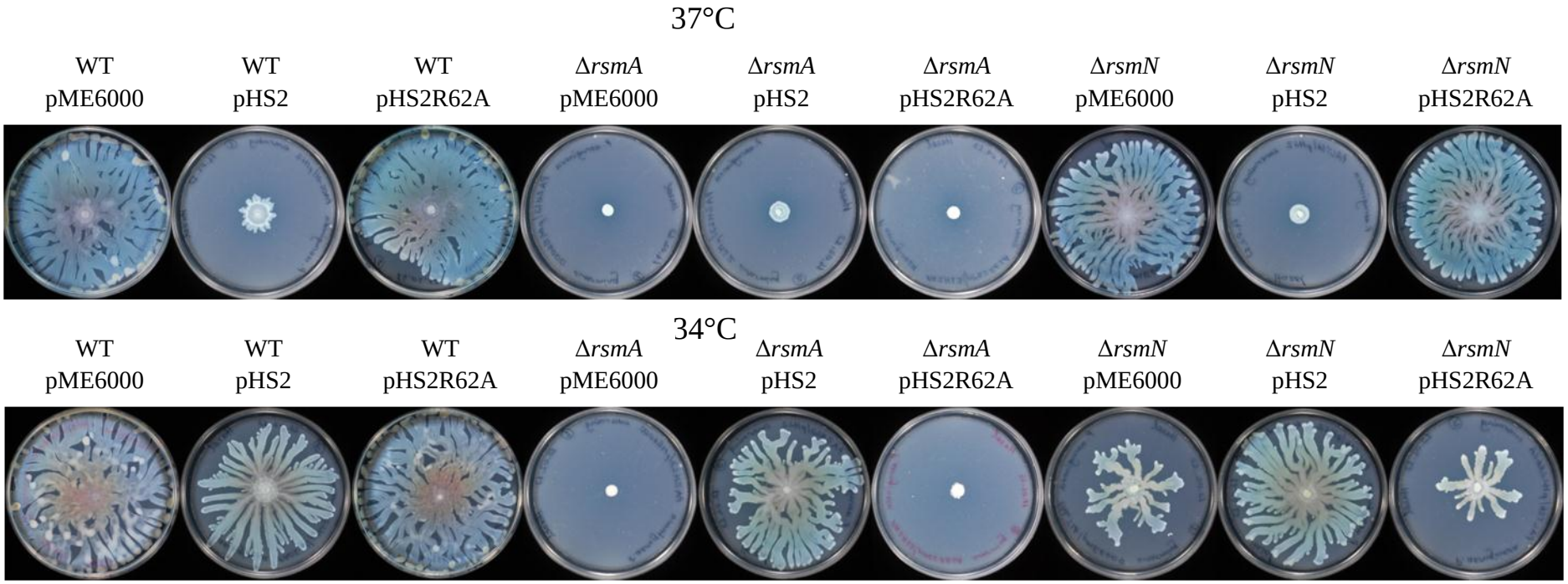


**Figure 3.9. The effect of the multicopy expression of *rsmN* or *rsmN*R62A on swarming motilities of the WT/pME6000, Δ*rsmA*/pME6000 and Δ*rsmN*/pME6000 strains on nutrient broth agar (0.5% w/v) at 37°C and 34°C**

The WT/pME6000, Δ*rsmN*/pME6000, WT/pHS2R62A and Δ*rsmN*/pHS2R62A transformants swarm both at 37°C and 34°C (the Δ*rsmN* strain swarms to a lesser extent than the WT strain). The Δ*rsmA*/pME6000 strain does not swarm at either temperature. The multicopy expression of *rsmN* complements swarming motility of the Δ*rsmA*/pME6000 mutant at 34°C but not at 37°C and reduces swarming of the WT/pME6000 and Δ*rsmN*/pME6000 strains at 37°C greatly. Substitution of $Arg_{62}$ into an alanine residue results in the loss of RsmN function.

### 3.2.3.2 Swimming motilities of the single and inducible Δ*rsmA* and Δ*rsmN* double deletion mutants

Motilities of the WT, Δ*rsmA*, Δ*rsmN* and inducible *rsmA*$_{ind}$ Δ*rsmN* and *rsmN*$_{ind}$ Δ*rsmA* strains were also compared on swim agar. Strains with a functional RsmA protein (WT, Δ*rsmN*, and *rsmA*$_{ind}$ Δ*rsmN* strains grown with IPTG) translocated on swim agar when the swimming assay was set up by either inoculating colonies (Figure 3.10, panel a) or 1 µL of the overnight cultures with an adjusted $OD_{600}$ of 1.0 at the centre of the agar (Figure 3.10, panel b). However, the Δ*rsmN* mutant did not reach to the edges of the plates 24 h post-inoculation. Given that more bacterial cells would be inoculated with a toothpick compared with the number of cells in 1 µL of the overnight culture, the increased motility diameter illustrated in panel a) in comparison with panel b) was expected. However, when 1 µL from the subcultured strains grown to an $OD_{600}$ of 0.8 were inoculated at the centre of the swim agar, results obtained were a bit different than the results depicted in panel a) and panel b) as Δ*rsmA* and *rsmA*$_{ind}$ Δ*rsmN* strains (the latter grown without IPTG) translocated on the swim agar (Figure 3.10, panel c). It is known that swarming motility is promoted by high growth rates [248, 249]. Based on this, one might suggest that cells harvested at the exponential growth stage have more tendency to translocate in comparison with cells harvested at the stationary phase (Figure 3.10, panel c).

Inducing *rsmA* expression in the *rsmA*$_{ind}$ Δ*rsmN* mutant increased motility. Although motility was reduced as a result of *rsmN* deletion, inducing *rsmN* expression in the *rsmN*$_{ind}$ Δ*rsmA* mutant did not have any effect.

A close-up picture of the Δ*rsmN* mutant revealed cells moving in tendrils which are much thinner than those observed during swarming motility on 0.5% (w/v) agar (Figure 3.11). It is possible that instead of swimming, swarming motility took place on the surface of the 0.3% (w/v) swim agar in this experiment.

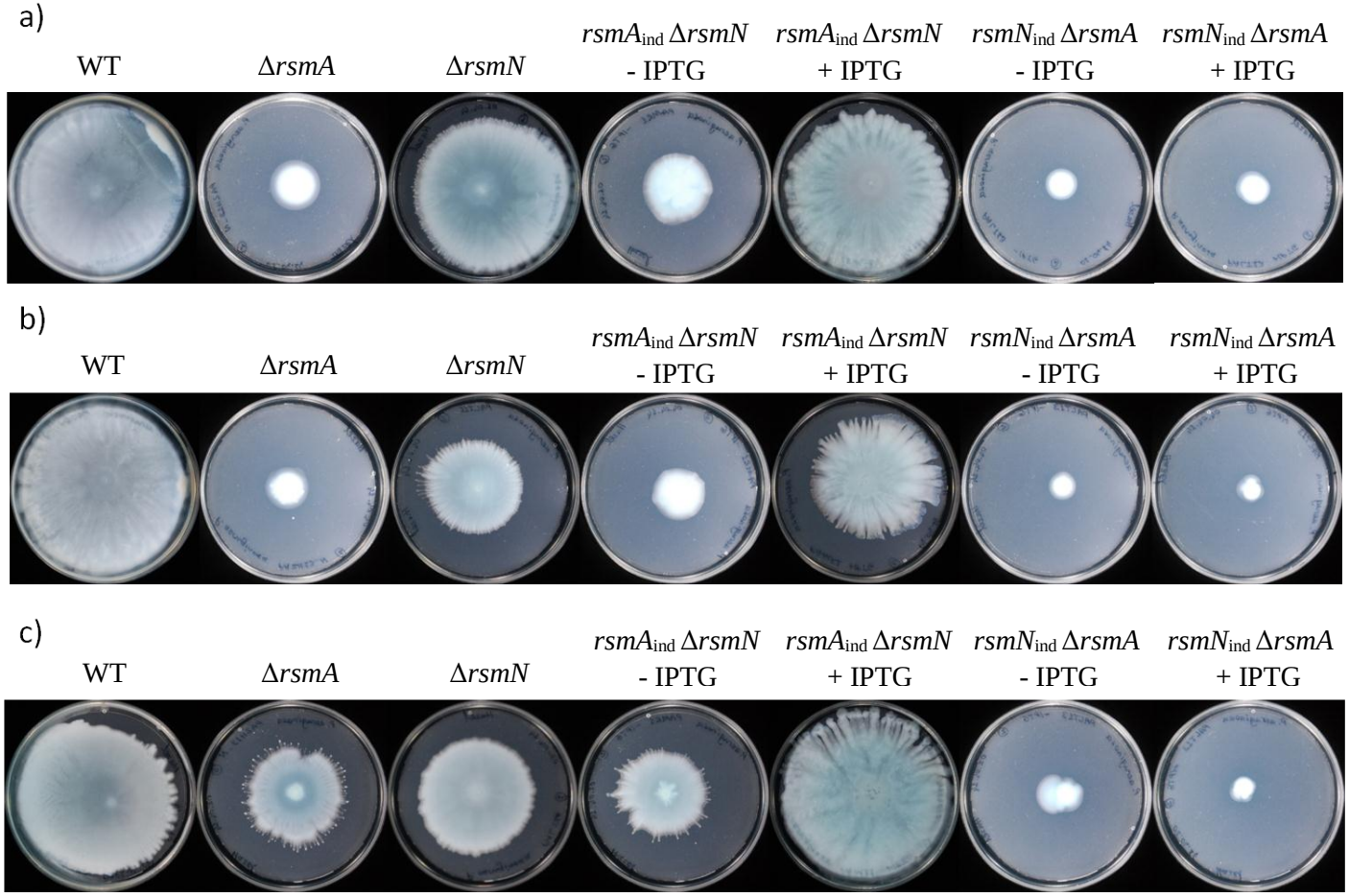


**Figure 3.10. Motilities of the *P. aeruginosa* WT, Δ*rsmA*, Δ*rsmN*, *rsmA*$_{ind}$ Δ*rsmN* and *rsmN*$_{ind}$ Δ*rsmA* strains on nutrient broth agar (0.3% w/v) at 37°C**

Bacterial motilities from inocula of picked colonies, 1 µL of the overnight cultures grown to an $OD_{600}$ of ~ 2.5 and 1 µL of the cultures grown to an $OD_{600}$ of ~ 0.8 on swim top agar are illustrated in panels a), b) and c) respectively. The Δ*rsmA* (when cells are grown to the stationary phase) and inducible *rsmA*$_{ind}$ Δ*rsmN* and *rsmN*$_{ind}$ Δ*rsmA* strains grown without IPTG (except for *rsmA*$_{ind}$ Δ*rsmN* in panel c) are motility-deficient whereas the WT and Δ*rsmN* strains are not. Expression of *rsmA* but not *rsmN* in a double mutant background restores motility.

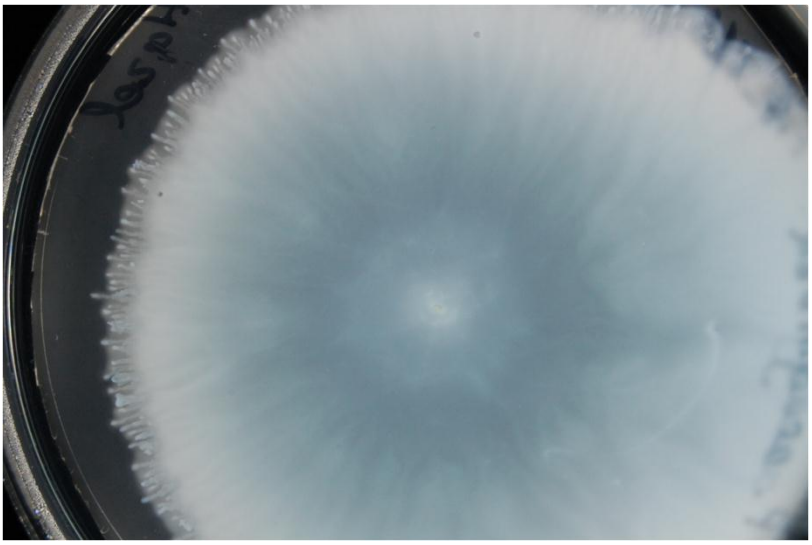

**Figure 3.11. Swimming and swarming intermediate motility of *P. aeruginosa* observed at 37°C on nutrient broth agar (0.3% w/v)**
Bacterial cells moving in thin tendrils can be detected at the forefront of spreading cells. This motility pattern reveals a phenotype intermediate of swarming and swimming.

### 3.2.3.3 Twitching motilities of the single and inducible Δ*rsmA* and Δ*rsmN* double deletion mutants

Twitching assays were performed with minor modifications to the twitching stab assay protocol described in Lazenby *et al.* [227]. Instead of LB, nutrient broth (NB) agar supplemented with 0.5% glucose was used as the growth medium. The nutrient source in swarming, swimming and twitching assays was standardised in this way. Twitching plates were incubated for 48 h as there was rarely any change after 24 h. 10 mL of NB agar (1.0% w/v) was poured into each petri dish and bacterial colonies were stabbed to the very bottom of the petri dishes. After 48 h, the agar was discarded carefully, the twitching zone was stained with 1% crystal violet and washed with $dH_2O$ prior to imaging.

As it can be seen from Figure 3.12, twitching zones turned out to be small even after 48 h of incubation, therefore, no diameter measurements were taken. Results were proved to be unreliable, even triplicate inocula from the same strain had twitching zones with different sizes.

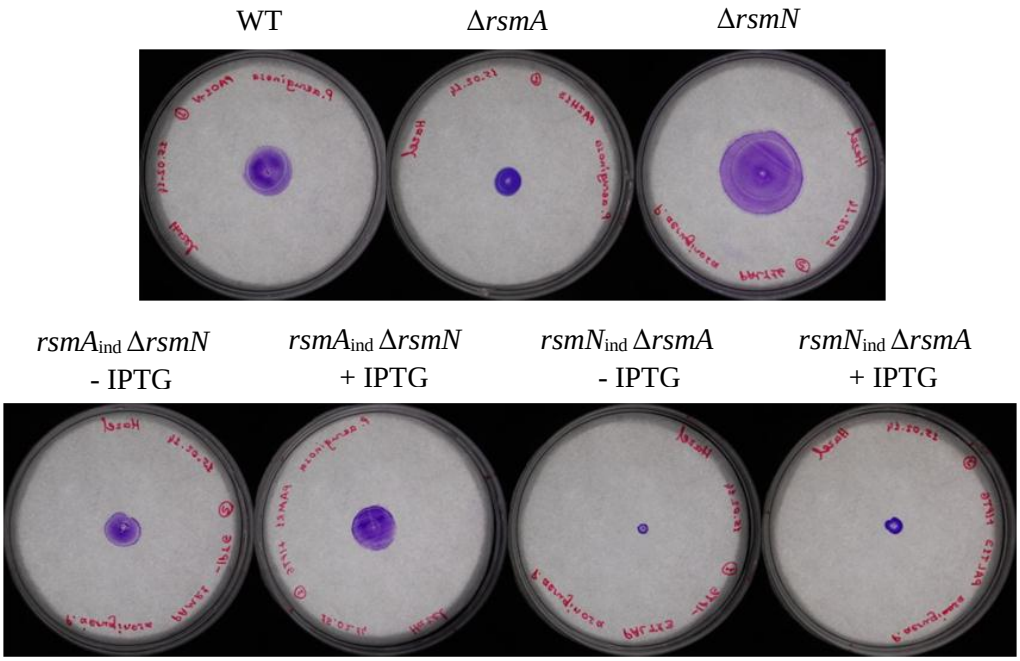


**Figure 3.12. Twitching motilities of the PAO1-N WT strain and the isogenic Δ*rsmA*, Δ*rsmN*, *rsmA*$_{ind}$ Δ*rsmN*, and *rsmN*$_{ind}$ Δ*rsmA* mutants on the surface of a petri dish over 48 h at 37°C**

The effect of the single and double deletions of *rsmA* and *rsmN* on twitching motility was investigated (in the absence and presence of 1 mM IPTG for the inducible strains), however, illustrated results could not be reproduced.

### 3.2.4 Regulation of pyocyanin production by RsmA and RsmN

Pessi *et al*. [204] reported that a Δ*rsmA* mutant produces five-fold more PYO in the late exponential phase in a glycerol-alanine medium than the WT PAO1 strain. To check if the deletion of *rsmN* influenced PYO production, PYO in culture supernatants of the Δ*rsmN* and *rsmN*$_{ind}$ Δ*rsmA* strains were quantified and compared with PYO produced by the WT, Δ*rsmA* and *rsmA*$_{ind}$ Δ*rsmN* strains after growing cells for 18 h ($OD_{600}$ 2.5 - 3.0) at 37°C and 34°C in LB medium with agitation (Figures 3.13 and 3.14). Inducible strains were supplemented with 1 mM IPTG at the time of inoculation.

Figure 3.13 demonstrates that neither *rsmA* nor *rsmN* deletion nor their double deletion (mimicked by the *rsmN*$_{ind}$ Δ*rsmA* and *rsmA*$_{ind}$ Δ*rsmN* strains grown without IPTG) changes PYO production significantly at 37°C. Chromosomally induced *rsmA* (*rsmA*$_{ind}$ Δ*rsmN* +IPTG) but not *rsmN* expression (*rsmN*$_{ind}$ Δ*rsmA* +IPTG) in the inducible double deletion mutants reduces PYO production significantly.

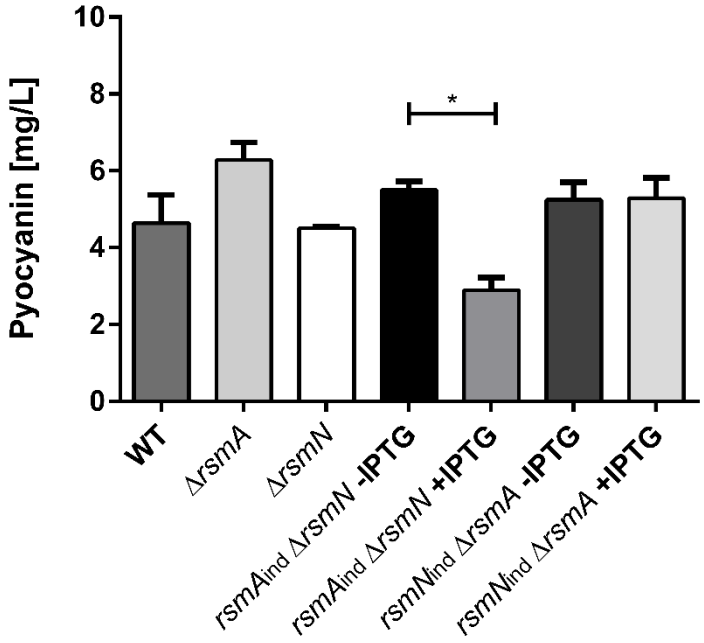


**Figure 3.13. PYO production of *P. aeruginosa* in LB at 37°C in the absence of RsmA, RsmN or both**

The deletion of *rsmA*, *rsmN* or both (mimicked by the $rsmA_{ind}$ Δ*rsmN* and $rsmN_{ind}$ Δ*rsmA* strains grown without IPTG) does not result in significant changes in PYO production compared with the wild-type strain at 37°C. Inducing *rsmA* in the $rsmA_{ind}$ Δ*rsmN* strain reduces PYO production significantly whereas *rsmN* expression in the $rsmN_{ind}$ Δ*rsmA* strain does not. Data represents averages of three independent extractions from cultures grown in LB for 18 h. Error bars represent standard error of the mean. Statistical differences were determined by ANOVA analysis, followed by Tukey multiple comparisons test; * $p < 0.05$.

PYO production by each of these strains was slightly decreased at 34°C (Figure 3.14). Figure 3.14 depicts that WT and Δ*rsmN* strains produced similar levels of PYO. PYO production in the Δ*rsmA*, $rsmA_{ind}$ Δ*rsmN* and $rsmN_{ind}$ Δ*rsmA* strains grown without IPTG was increased ~ 2-fold at 34°C in comparison with the WT strain. Inducing *rsmA* expression in the $rsmA_{ind}$ Δ*rsmN* strain decreased PYO levels significantly.

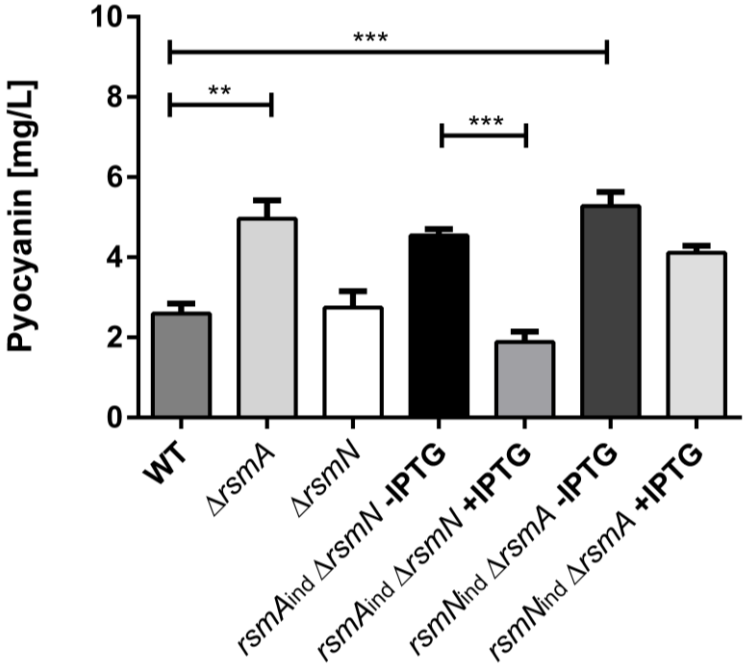


**Figure 3.14. PYO production of *P. aeruginosa* in LB at 34°C in the absence of RsmA, RsmN or both**

The deletion of *rsmN* does not affect PYO production, however, PYO production by the Δ*rsmA* and inducible $rsmA_{ind}$ Δ*rsmN* and $rsmN_{ind}$ Δ*rsmA* strains grown without IPTG increases ~ 2-fold compared with the WT and Δ*rsmN* strains at 34°C. Expression of *rsmA* in the inducible double deletion mutant decreases PYO levels significantly whereas *rsmN* expression does not. Data represents averages of three independent extractions from cultures grown in LB for 18 h. Error bars represent standard error of the mean. Statistical differences were determined by ANOVA analysis, followed by Tukey multiple comparisons test; ** $p < 0.01$, *** $p < 0.001$.

PYO production at 37°C (Figure 3.15) and 34°C (data not shown) by the Δ*rsmA* mutant transformed with either the empty vector pME6000, *rsmN* expression plasmid pHS2 or *rsmN*R62A expression plasmid pHS2R62A in comparison with the WT and Δ*rsmN* strains transformed with pME6000 was also quantified to eliminate the possibility that the multicopy expression of *rsmN* is required to detect a phenotypic difference. There was not a significant difference between PYO production by the WT/pME6000, Δ*rsmA*/pME6000 and Δ*rsmN*/pME6000 transformants. Expression of *rsmN* did not affect PYO production by the Δ*rsmA*/pME6000 strain significantly while expression of *rsmN*R62A resulted in a significant decrease.

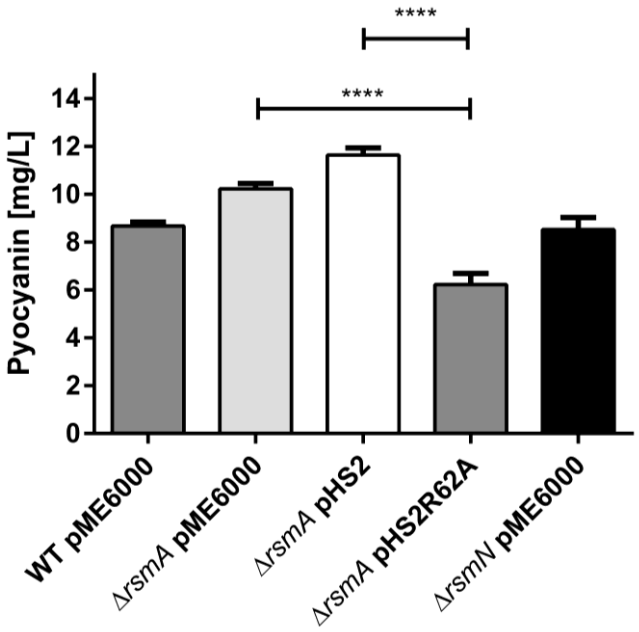


**Figure 3.15. The effect of the multicopy expression of *rsmN* or *rsmN*R62A on PYO production of the Δ*rsmA*/pME6000 strain in comparison with the WT/pME6000 and Δ*rsmN*/pME6000 strains in LB at 37°C**

The deletion of *rsmA* or *rsmN* does not influence PYO production at 37°C. Furthermore, the multicopy expression of *rsmN* does not affect PYO production by the Δ*rsmA*/pME6000 strain. On the other hand, expression of *rsmN*R62A reduces PYO production by the Δ*rsmA*/pME6000 strain significantly. Data represents averages of three independent extractions from cultures grown in LB for 18 h. Error bars represent standard error of the mean. Statistical differences were determined by ANOVA analysis, followed by Tukey multiple comparisons test; **** $p < 0.0001$.

Results of the PYO assay performed with the WT/pME6000, Δ*rsmA*/pME6000, Δ*rsmA*/pHS2, Δ*rsmA*/pHS2R62A and Δ*rsmN*/pME6000 strains at 34°C (data not shown) did not show significant differences in PYO production due to the overall reduction in PYO production at 34°C.

Based on these findings, it can be concluded that RsmN does not control PYO production. However, when grown on solid PIA agar, the Δ*rsmA*/pHS2 strain has a colour intermediate of the Δ*rsmA*/pME6000 and WT/pME6000 strains (Figure 3.16) suggesting a negative regulation of PYO production.

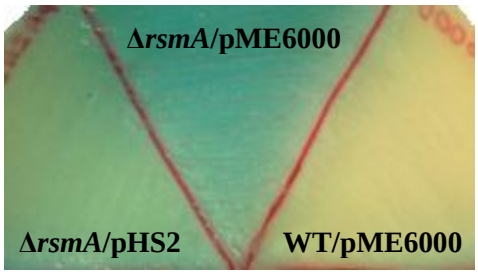


**Figure 3.16. The effect of the multicopy expression of *rsmN* on the appearance of the Δ*rsmA*/pME6000 strain on PIA agar at 37°C**
Blue/green pigmentation of strains grown on PIA agar is associated with PYO production. The deletion of *rsmA* results in increased PYO production (indicated by the turquoise color of Δ*rsmA*/pME6000 cells in comparison with the yellow color of WT/pME6000 cells). The green color indicates that the multicopy expression of *rsmN* reduces PYO production, although not to the wild-type levels, by the Δ*rsmA*/pME6000 strain when grown on PIA agar.

### 3.2.5 The impact of RsmA and RsmN on total proteolytic and elastinolytic activities

Pessi *et al.* [204] demonstrated that overexpression of *rsmA* leads to a reduction in proteolytic and elastinolytic activities of the PAO1 strain and concluded that protease and elastase production is negatively regulated by RsmA. To investigate the role of RsmN, in comparison with RsmA, on the synthesis of these extracellular products, initially, supernatants from the WT strain and the *rsmA*/*rsmN* single and inducible double deletion mutants were used in assays (described in section 2.4.7.4) which employ azocasein (protease) and Elastin-Congo red (elastase) as substrates. To check the effect of *rsmN* and *rsmN*R62A (see section 3.1) expression at multicopy levels on proteolytic and elastinolytic activities, pME6000-based pHS2 and pHS2R62A expression plasmids were transformed into the Δ*rsmA* strain and assays were repeated.

Figure 3.17 illustrates that the single deletion of *rsmA* but not *rsmN* results in reduced total proteolytic activity while an almost complete lack of activity is observed for both of the inducible $rsmA_{ind}$ Δ*rsmN* and $rsmN_{ind}$ Δ*rsmA* double mutants grown without IPTG at 34°C and 37°C (panel a). The expression of *rsmA* in the $rsmA_{ind}$ Δ*rsmN* mutant led to a significant increase in total proteolytic activity at 34°C and 37°C but did not reach wild-type levels. On the other hand, *rsmN* expression partially restored total proteolytic activity in the $rsmN_{ind}$ Δ*rsmA* mutant only at 34°C (panel a). A comparison of the left and right sides of the panel a) in Figure 3.17 reveals that total proteolytic activities of all strains were elevated at 34°C compared with 37°C.

The panel b) of Figure 3.17 illustrates total proteolytic activities of the Δ*rsmA* strain transformed with either the pME6000, pHS2 or pHS2R62A vectors in reference to the WT/pME6000 and Δ*rsmN*/pME6000 strains. The single deletion of *rsmA* reduced total proteolytic activity significantly at both 37°C and 34°C whereas *rsmN* deletion reduced total proteolytic activity significantly only at 34°C. The multicopy expression of *rsmN* increased the proteolytic activity in the Δ*rsmA*/pME6000 mutant partially at 37°C but not at 34°C due to the overall increase in proteolytic activity at 34°C compared with 37°C. The expression of *rsmN*R62A failed to restore proteolytic activity in the Δ*rsmA*/pME6000 mutant at both temperatures. Interestingly, the Δ*rsmA*/pME6000 transformant had reduced proteolytic activity at 37°C than the Δ*rsmA* mutant without the plasmid.

As illustrated in Figure 3.18, the deletion of *rsmA* led to a significant reduction in elastinolytic activity at 37°C and 34°C (panels a and b) while there was no change in activity in the Δ*rsmN* mutant (panel a). Elastinolytic activity of the Δ*rsmN*/pME6000 transformant was slightly reduced at 34°C in comparison with the WT/pME6000 strain (panel b). In contrast to the WT, Δ*rsmA* and Δ*rsmN* strains, the inducible $rsmA_{ind}$ Δ*rsmN* and $rsmN_{ind}$ Δ*rsmA* double deletion mutants demonstrated very little elastinolytic activity at 37°C and 34°C (panel a). Induction of either *rsmA* or *rsmN* expression restored elastinolytic activity in the inducible double deletion mutants, although not completely (panel a). The expression of *rsmA* in the inducible double deletion mutant restored elastinolytic activity to Δ*rsmN* levels whereas expression of *rsmN* increased the activity to Δ*rsmA* levels both at 37°C and 34°C. The expression of *rsmN* but not *rsmN*R62A partially restored the elastinolytic activity in the Δ*rsmA*/pME6000 mutant at 37°C and 34°C (Figure 3.18, panel b).

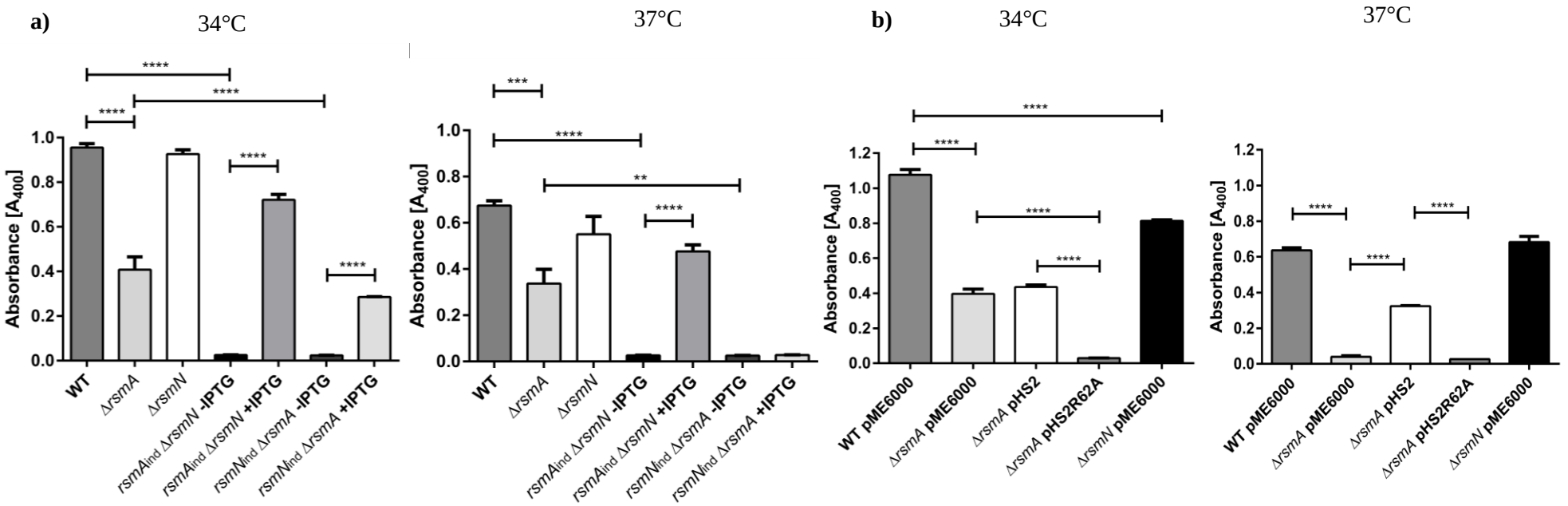


**Figure 3.17. The impact of *rsmA* and/or *rsmN* deletions (panel a) and *rsmN* or *rsmN*R62A expression (panel b) on total proteolytic activity at 37°C**
The WT and Δ*rsmN* strains have similar levels of total proteolytic activity and significantly higher than the Δ*rsmA* mutant at both temperatures. In the absence of both Rsm proteins, proteolytic activity is greatly reduced. Expression of *rsmA* at 37°C and 34°C; *rsmN* only at 34°C partially restore the activity in the inducible double deletion mutants grown without IPTG (panel a). The WT/pME6000 and Δ*rsmN*/pME6000 strains have similar levels of total proteolytic activity at 37°C, but *rsmN* deletion reduces the activity at 34°C (panel b). The multicopy expression of *rsmN* increases (at 37°C) but *rsmN*R62A decreases (at 34°C) the total proteolytic activity in the Δ*rsmA*/pME6000 mutant. Total proteolytic activities of all strains are elevated at 34°C compared with 37°C. Data represents averages of three independent absorbance measurements of the reaction buffer containing fractionated azocasein and culture (grown in LB for 18 h) supernatant. Error bars represent standard error of the mean. Statistical differences were determined by ANOVA analysis, followed by Tukey multiple comparisons test; ** $p < 0.01$, *** $p < 0.001$, **** $p < 0.0001$.

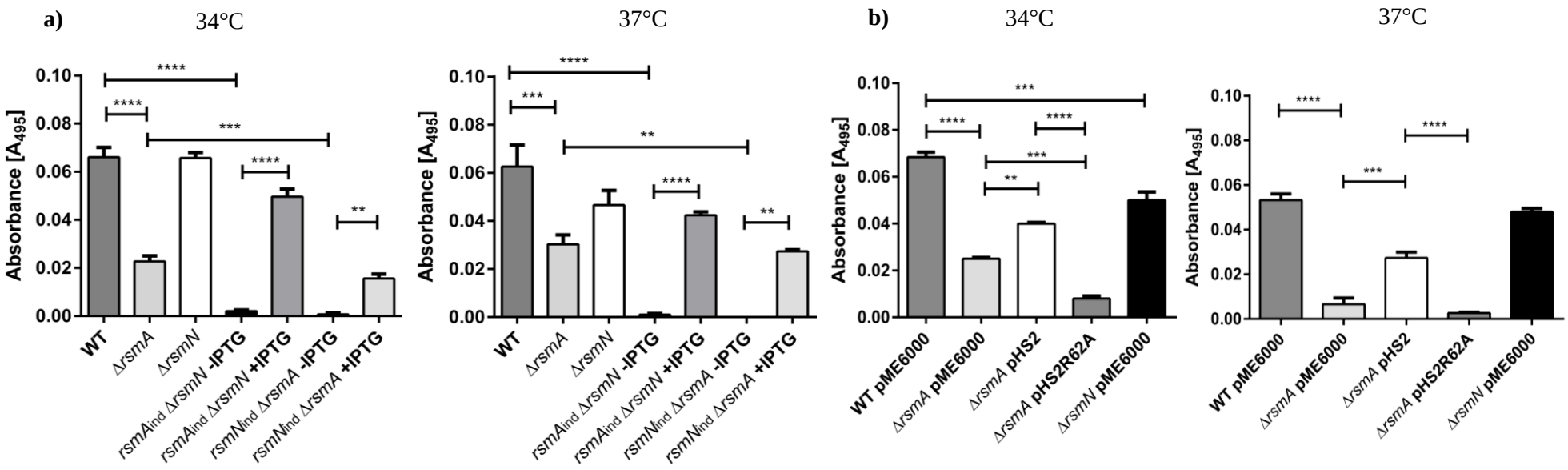


**Figure 3.18. The impact of *rsmA* and/or *rsmN* deletions (panel a) and *rsmN* or *rsmN*R62A expression (panel b) on elastinolytic activity at 37°C**

The WT and Δ*rsmN* strains have similar levels of elastinolytic activity, which is 3-fold higher than the Δ*rsmA* mutant at 34°C. Elastinolytic activity is also reduced at 37°C as a result of *rsmA* deletion. In the absence of both Rsm proteins, elastinolytic activity is greatly reduced. Expression of *rsmA* and *rsmN* at 37°C and 34°C increases elastinolytic activity significantly in the $rsmA_{ind}$ Δ*rsmN* and $rsmN_{ind}$ Δ*rsmA* strains respectively (panel a). The WT/pME6000 and Δ*rsmN*/pME6000 strains have similar levels of elastinolytic activity at 37°C, but *rsmN* deletion reduces the activity significantly at 34°C. The multicopy expression of *rsmN* but not *rsmN*R62A increases elastinolytic activity in the Δ*rsmA*/pME6000 mutant at 37°C and 34°C. Expression of *rsmN*R62A reduces the elastinolytic activity in the Δ*rsmA*/pME6000 mutant at 34°C (panel b). Data represents averages of three independent absorbance measurements of the reaction buffer containing fractionated Elastin-Congo red and culture (grown in LB for 18 h) supernatant. Error bars represent standard error of the mean. Statistical differences were determined by ANOVA analysis, followed by Tukey multiple comparisons test; ** $p < 0.01$, *** $p < 0.001$, **** $p < 0.0001$.

### 3.2.6 The influence of *rsmA* and *rsmN* deletions on biofilm formation

The *P. aeruginosa* Δ*rsmA* mutant is known to make robust biofilms [207] (see section 1.3.4.2). To determine whether RsmN influences biofilm development, both Δ*rsmN* and *rsmN*$_{ind}$ Δ*rsmA* mutants were grown (the latter without any IPTG supplementation) in comparison with the WT and Δ*rsmA* strains in a microfluidics flow cell as described in 2.4.7.5.1. Figure 3.19 illustrates robust microcolony formation by the Δ*rsmA* and *rsmN*$_{ind}$ Δ*rsmA* mutants. The *rsmN*$_{ind}$ Δ*rsmA* mutant forms smaller microcolonies than the Δ*rsmA* mutant. The WT strain forms a few microcolonies and WT biofilms look flat and undifferentiated. Interestingly, the Δ*rsmN* mutant has a biofilm phenotype that is intermediate to the Δ*rsmA* and WT biofilms. Both the Δ*rsmA* and Δ*rsmN* single deletion mutants and the inducible double deletion mutant form more microcolonies than the WT strain.

Imaging of the microfluidic flow cells under light microscope shows that both WT and Δ*rsmN* cells accumulated on the outer walls of the chamber (Figure 3.20, panels a and c) whereas Δ*rsmA* and *rsmN*$_{ind}$ Δ*rsmA* mutants grew entirely as microcolonies and void spaces were detectable between microcolonies (Figure 3.19, Figure 3.20, panels b and d). In addition, time-lapse images show that the Δ*rsmA* mutant started to form microcolonies within the first 4 h of growth in a microfluidic chamber (Figure 3.21, panel a). After 8 h, larger Δ*rsmA* microcolonies were clearly visible while WT cells just started to cover the well surface. After 12 h, there was robust microcolony formation by the Δ*rsmA* mutant whereas microcolonies of the WT strain just started to become visible. Microcolonies of the Δ*rsmN* mutant also became apparent after ~ 12 h (data not shown). Time-lapse videos of biofilm formation by the Δ*rsmA* and Δ*rsmN* mutants in comparison with the WT strain over 14 h can be found at https://youtu.be/afGLWsmYy9c and https://youtu.be/SCb-bQP1X3E.

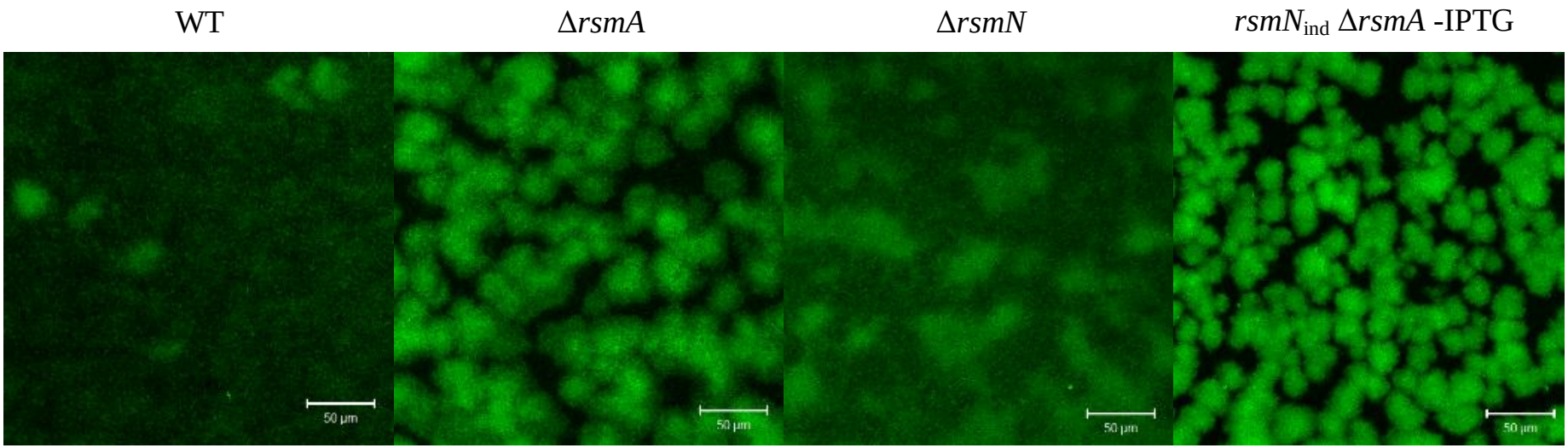


**Figure 3.19. Z-stack images demonstrating the effect of *rsmA* and/or *rsmN* deletions on the biofilm formation of *P. aeruginosa* PAO1 cultivated in 10% LB under continuous shear flow (0.5 dyn/cm$^2$) at 37°C**

The Δ*rsmA* and *rsmN*$_{ind}$ Δ*rsmA* mutants form many microcolonies (latter forming smaller microcolonies compared with the former) and void spaces are detectable between microcolonies. The WT strain forms only a few microcolonies and mostly spreads flat on the surface. The Δ*rsmN* mutant forms more microcolonies than the WT, but less than the Δ*rsmA* and *rsmN*$_{ind}$ Δ*rsmA* strains. Furthermore, spaces between the Δ*rsmN* microcolonies reveal flat undifferentiated cells on the surface. The scale bar represents 50 µm. Images were taken under 20x objective magnification using a Zeiss confocal microscope.

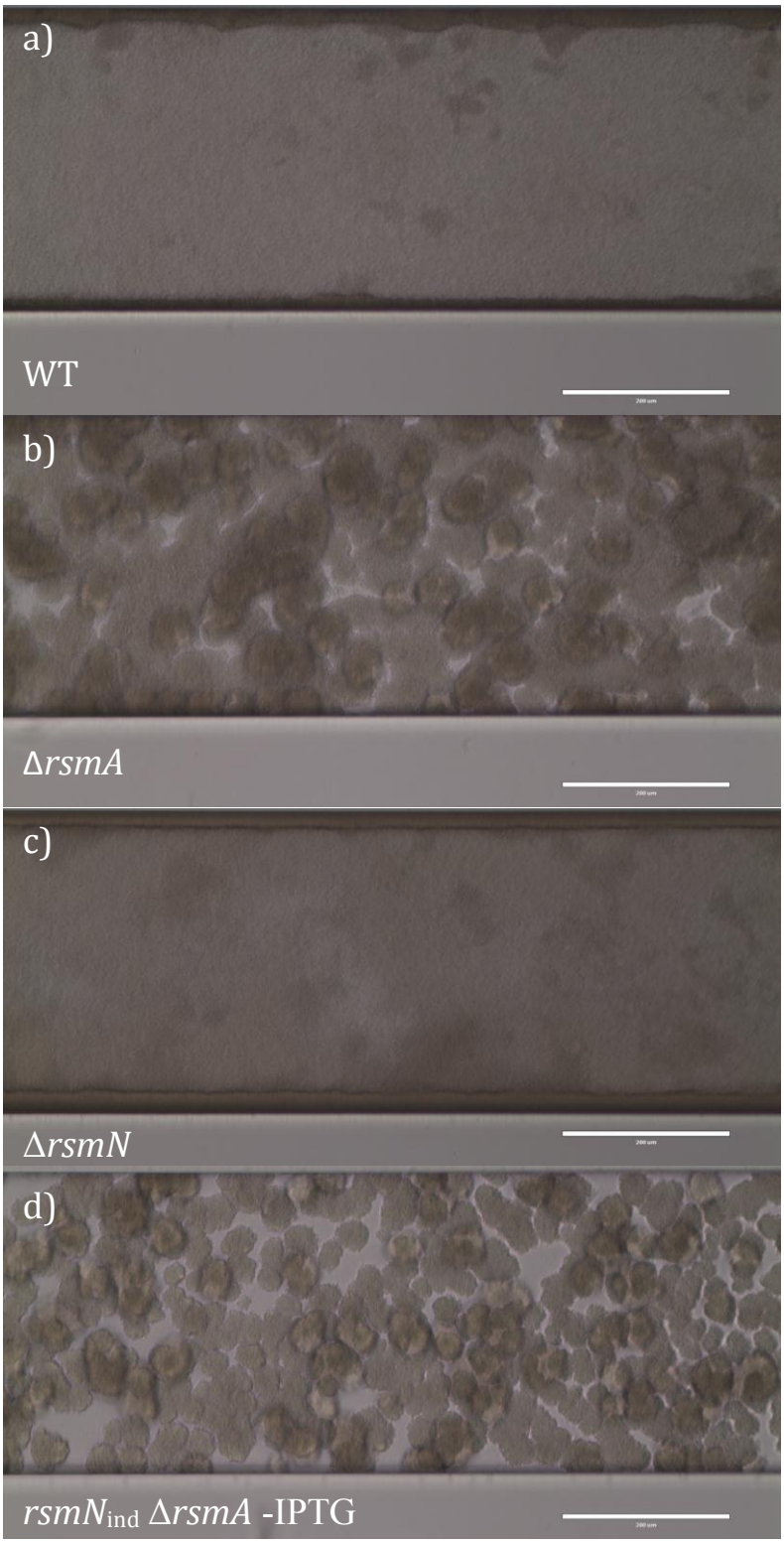


**Figure 3.20. 2D images (14 h post-inoculation) of the WT, Δ*rsmA*, Δ*rsmN* and *rsmN*$_{ind}$ Δ*rsmA* biofilms cultivated in 10% LB under continuous shear flow (0.5 dyn/cm$^2$) at 37°C**
In comparison with the Δ*rsmA* and *rsmN*$_{ind}$ Δ*rsmA* mutants (panels b and d), the WT and Δ*rsmN* strains form fewer microcolonies and cells attach to the walls of the microfluidic chamber (panels a and c). Void spaces are detectable between Δ*rsmA* and *rsmN*$_{ind}$ Δ*rsmA* microcolonies. The scale bar represents 200 µm. Images were taken under 20x objective magnification using an EVOS light microscope.

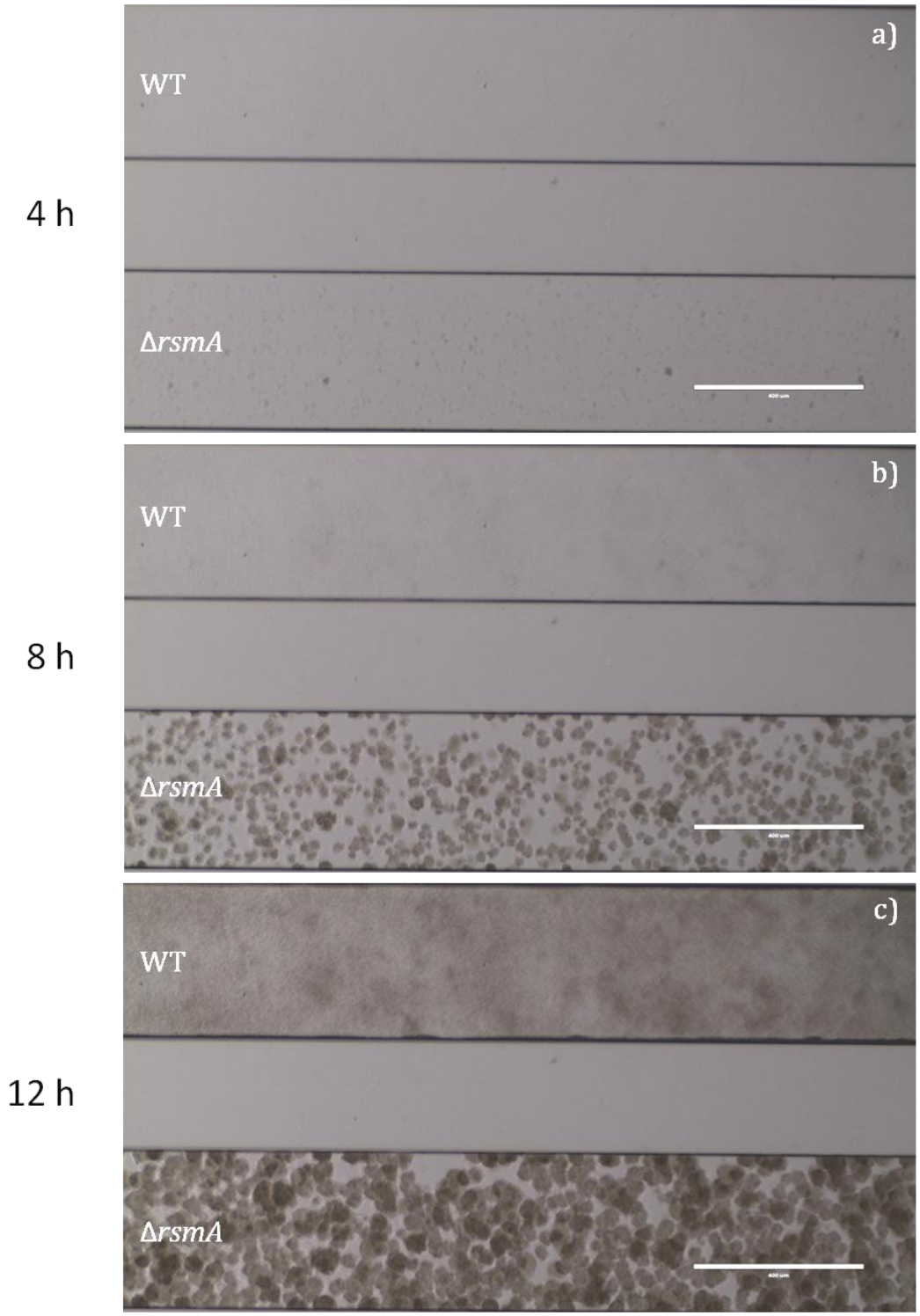


**Figure 3.21. Microscopic images 4 h (panel a), 8 h (panel b), and 12 h (panel c) post-inoculation of WT and Δ*rsmA* biofilms cultivated in 10% LB under continuous shear flow (0.5 dyn/cm$^2$) at 37°C**

Small microcolonies formed by the Δ*rsmA* mutant are detectable as early as 4 h post-inoculation and get larger in time. In comparison, the few microcolonies formed by the WT strain are not observed until ~ 12 h. The scale bar represents 400 µm. Images were taken at 10x objective magnification using EVOS light microscope.

The robust microcolony formation was another Δ*rsmA* phenotype that the multicopy expression of *rsmN* could complement (Figure 3.22). Individual cells of the WT/pME6000 strain could be detected in a flat biofilm. Similarly, Δ*rsmA*/pHS2 cells also formed a flat undifferentiated biofilm, whereas the Δ*rsmA*/pME6000 biofilm mainly consisted of microcolonies. The Δ*rsmN*/pME6000 mutant displayed an intermediate biofilm phenotype to that of WT/pME6000 and Δ*rsmA*/pME6000 biofilm phenotypes. On the other hand, RsmNR62A failed to complement robust microcolony formation by the Δ*rsmA*/pME6000 mutant (Figure 3.22). A comparison of Figures 3.19 and 3.22 reveals that *P. aeruginosa* cells transformed with multicopy plasmids make better biofilms compared with the same strains without plasmids.

### 3.2.7 Colony morphologies of the single and double Δ*rsmA* and Δ*rsmN* deletion mutants

The consequence of *rsmA* and *rsmN* deletions on the colony biofilm morphology was investigated using a protocol described in Dietrich *et al.* [216] with minor modifications (see section 2.4.7.5.2). The WT, Δ*rsmA* and Δ*rsmN* strains grew as smooth colonies on Congo red-tryptone agar (Figure 3.23, first three columns, left & right panels). Strains without a functional RsmA and RsmN, the inducible double deletion mutants grown without IPTG (last two columns, left panel), had a rough colony morphology. The $rsmA_{ind}$ Δ*rsmN* strain grown without IPTG (left panel) showed a smooth ring around the rough centre pointing out to a leaky expression of *rsmA*. Plaque-like clearance zones could be detected on top of the double mutant colonies grown without IPTG. Expression of *rsmA* in the $rsmA_{ind}$ Δ*rsmN* strain resulted in a smooth colony morphology and relieved the surface dryness while *rsmN* expression in the $rsmN_{ind}$ Δ*rsmA* strain did not change the colony morphology (Figure 3.23, right panel, last two columns). However, putative plaques observed on the surface of the inducible double deletion mutants grown without IPTG disappeared after *rsmA* or *rsmN* expression. All colonies displayed an inner circle at the centre and an outer zone around it.

These results demonstrate that the *P. aeruginosa* PAO1 strain has a rough colony morphology in the absence of both RsmA and RsmN.

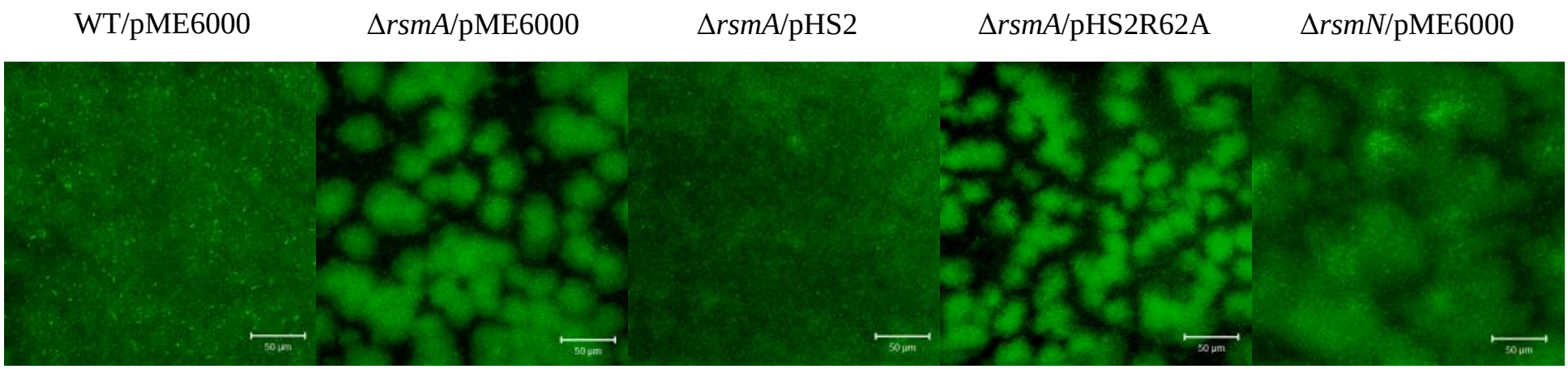


**Figure 3.22. The effect of the multicopy expression of *rsmN* or *rsmN*R62A on the biofilm formation of the Δ*rsmA*/pME6000 strain in comparison with WT/pME6000 and Δ*rsmN*/pME6000 biofilms cultivated in 10% LB under continuous shear flow (0.5 dyn/cm$^2$) at 37°C**

A distinct microcolony phenotype is observed for Δ*rsmA*/pME6000 and Δ*rsmA*/pHS2R62A biofilms whereas the WT/pME6000 and Δ*rsmA*/pHS2 strains form only a few microcolonies and spread out mostly flat. Microcolonies of the Δ*rsmN*/pME6000 strain are diffused in comparison with Δ*rsmA*/pME6000 and Δ*rsmA*/pHS2R62A microcolonies. Multicopy plasmid-encoded *rsmN* complements robust microcolony formation by the Δ*rsmA*/pME6000 mutant but an alanine substitution of the RsmN $Arg_{62}$ results in the loss of the complementary effect. The scale bar represents 50 µm. Images were taken at 20x objective magnification using a Zeiss confocal microscope.

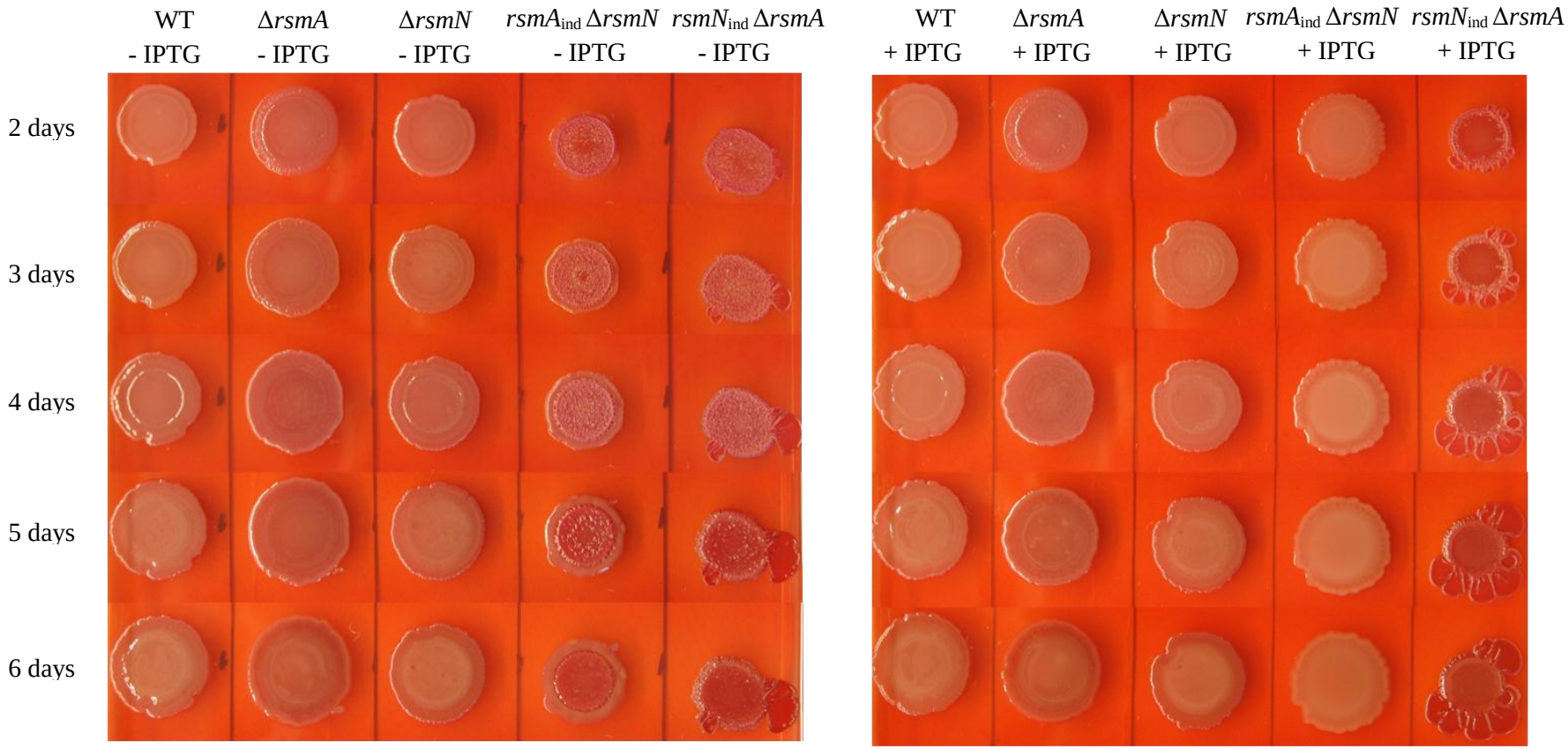


**Figure 3.23. Colony morphologies of the WT, Δ*rsmA*, Δ*rsmN*, *rsmA*$_{ind}$ Δ*rsmN* and *rsmN*$_{ind}$ Δ*rsmA* strains during 2-6 days incubation on Congo red-tryptone agar at room temperature**

While the WT, Δ*rsmA* and Δ*rsmN* strains display smooth colony morphologies, the *rsmA*$_{ind}$ Δ*rsmN* and *rsmN*$_{ind}$ Δ*rsmA* double mutants grow as rough colonies without IPTG and display plaque-like clearance zones on the surface (left panel). Expression of *rsmA* but not *rsmN* in the inducible double deletion mutants results in a smooth colony morphology. However, tiny plaques observed on the rough colony surface of the double mutants disappear after the expression of either *rsmA* or *rsmN* (right panel).

### 3.2.8 *P. aeruginosa* undergoes autolysis in the absence of both RsmA and RsmN

After the observation of tiny plaques on the surface of *rsmA*$_{ind}$ Δ*rsmN* and *rsmN*$_{ind}$ Δ*rsmA* colonies grown without IPTG (Figure 3.23), to determine whether rough colony morphologies of the *rsmA*$_{ind}$ Δ*rsmN* and *rsmN*$_{ind}$ Δ*rsmA* double mutants was due in part to phage-mediated lysis and in particular to prophage Pf4, PAO1B1 and a *Pf4* deletion mutant, PAO1B1Δ*Pf4* strains were employed in the phage plaque assay as described in Rice *et al.* [117] (see section 2.4.7.6). In addition, to investigate whether *rsmA*$_{ind}$ Δ*rsmN* and *rsmN*$_{ind}$ Δ*rsmA* double mutants lysed more readily than the WT, Δ*rsmA* or Δ*rsmN* strains, the presence of the cytosolic protein IscS (cysteine desulfurase) in the respective culture supernatants was checked and the number of colony forming units formed by these strains were compared [232].

A *P. aeruginosa* Δ*pqsL* mutant, characterised by autolysis triggered by the induction of a filamentous bacteriophage by D'Argenio *et al.* [197], was used as a positive control in phage plaque assay. Soft top agar seeded with the PAO1B1 or PAO1B1Δ*Pf4* strains was layered on top of LB agar. 5 µL of cell-free culture supernatants from the PAO1B1, PAO1B1Δ*Pf4*, WT PAO1-N, Δ*rsmA*, Δ*rsmN*, *rsmN*$_{ind}$ Δ*rsmA* and Δ*pqsL* strains were spread across the soft top agar and plates were incubated at 37°C for 18 h.

The left panel of Figure 3.24 displays the control strains according to which phage release from the Δ*rsmA* and Δ*rsmN* deletion mutants could be interpreted. Culture supernatants of the PAO1B1 and Δ*pqsL* strains resulted in plaque formation on a PAO1B1Δ*Pf4* bacterial lawn whereas culture supernatant of the PAO1B1Δ*Pf4* strain devoid of the Pf4 prophage did not lyse PAO1B1Δ*Pf4* cells. PAO1B1 cells were protected against phage-induced lysis. Culture supernatants from all strains tested for phage release resulted in plaque formation on PAO1B1Δ*Pf4* lawn but not on PAO1B1 lawn (right panel of Figure 3.24). Even though this method did not allow quantification of phage released from each strain (due to the spreading method used, plaques merged, making it difficult to count individual plaques), it appears that the highest number of plaques was observed on PAO1B1Δ*Pf4* lawn layered with the *rsmN*$_{ind}$ Δ*rsmA* culture supernatant. However, a more quantifiable assay would be needed to confirm this potential finding.

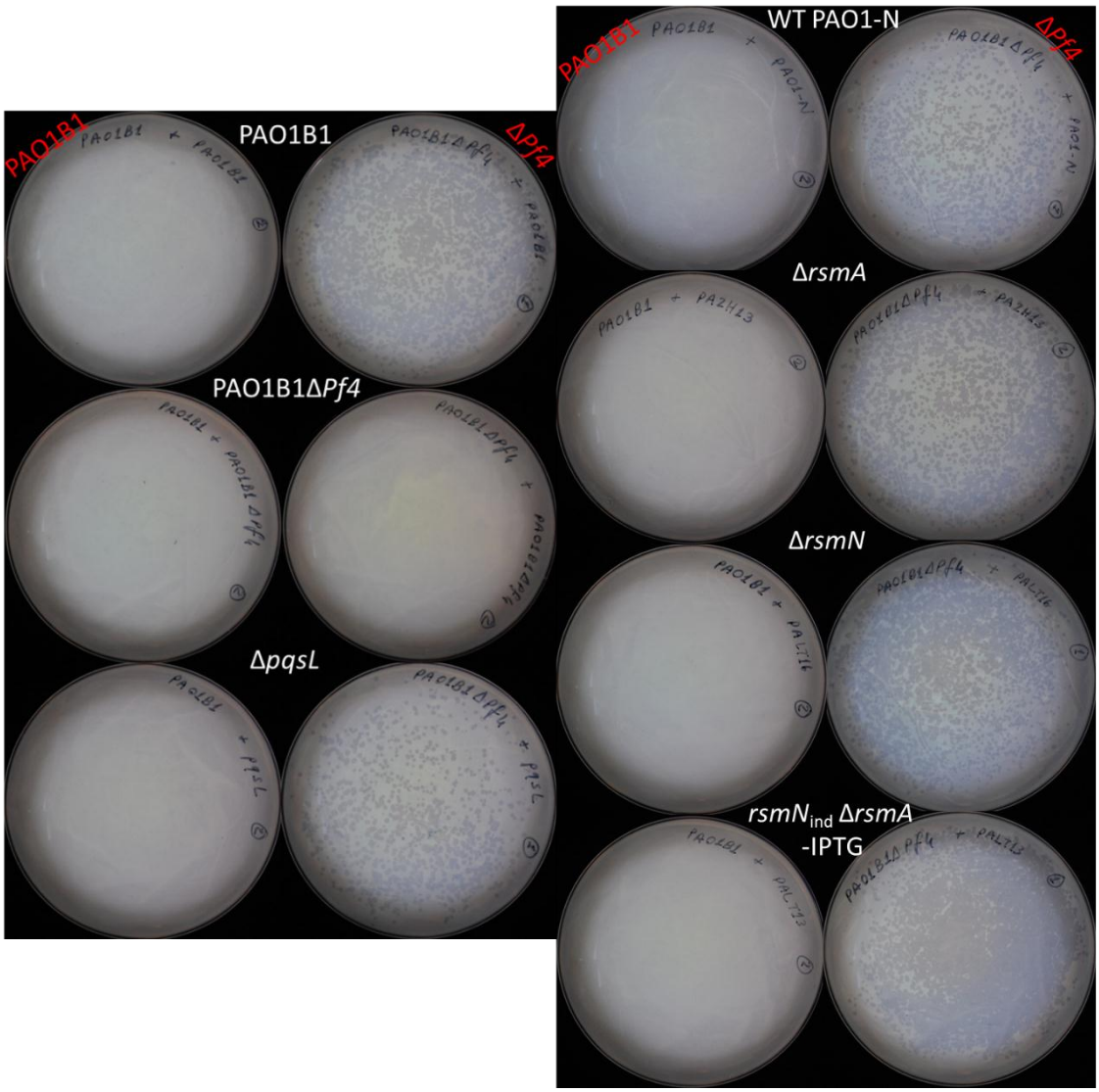


**Figure 3.24. Investigation of phage-induced lysis on the surface of PAO1B1 and PAO1B1Δ*Pf4* soft top agar lawns after spreading culture supernatants of the PAO1B1, PAO1B1Δ*Pf4*, Δ*pqsL*, PAO1-N, Δ*rsmA*, Δ*rsmN* and *rsmN*$_{ind}$ Δ*rsmA* strains**

Left panel: Soft top agar lawns of the positive and negative control strains show that *P. aeruginosa* PAO1B1 cells are resistant to re-infection by phage whereas PAO1B1Δ*Pf4* cells, when exposed to supernatants from phage-harbouring strains (PAO1B1 and Δ*pqsL*), undergo lysis which appears as plaques on a lawn of bacteria.

Right panel: All strains tested on PAO1B1Δ*Pf4* lawns give rise to lytic plaques, whereas PAO1B1 cells are left intact. Although not quantified, it appears that the highest number of phage particles is found in the *rsmN*$_{ind}$ Δ*rsmA* culture supernatant in comparison with culture supernatants of the WT, Δ*rsmA* and Δ*rsmN* strains.

To verify cell lysis, supernatant proteins from 37°C and 34°C overnight cultures of the WT PAO1-N, Δ*rsmA*, Δ*rsmN*, *rsmA*$_{ind}$ Δ*rsmN* and *rsmN*$_{ind}$ Δ*rsmA* (the latter two grown in the absence and presence of 1 mM IPTG) strains were compared and immunoblotted with an antibody to detect the cytoplasmic protein IscS (47 kDa). $OD_{600}$ values of the overnight cultures are listed in Table 3.1. These $OD_{600}$ values show that tested strains except for *rsmA*$_{ind}$ Δ*rsmN* and *rsmN*$_{ind}$ Δ*rsmA* grown without IPTG (optical densities of these cells were slightly less compared with the rest due to the formation of aggregates which did not disperse until ~ 24 h) had similar optical densities at the time of supernatant collection.

**Table 3.1. $OD_{600}$ of bacterial strains during supernatant collection for supernatant protein profiling**

| Strains | $OD_{600}$ 37°C | $OD_{600}$ 34°C |
|---|---|---|
| **WT** | 3.59 | 3.85 |
| **Δ*rsmA*** | 3.68 | 3.85 |
| **Δ*rsmN*** | 3.36 | 3.74 |
| ***rsmA*$_{ind}$ Δ*rsmN* -IPTG** | 2.90 | 2.94 |
| ***rsmA*$_{ind}$ Δ*rsmN* +IPTG** | 3.59 | 3.87 |
| ***rsmN*$_{ind}$ Δ*rsmA* -IPTG** | 2.82 | 2.86 |
| ***rsmN*$_{ind}$ Δ*rsmA* +IPTG** | 3.48 | 3.03 |

Figure 3.25 shows supernatant protein profiles of the WT and mutant strains. To observe as many proteins as possible from each strain, samples were not diluted, therefore, lanes where supernatant proteins of the inducible double deletion mutants were loaded, are overloaded (except for the *rsmA*$_{ind}$ Δ*rsmN* +IPTG sample, the right side of the marker). Supernatant protein profiles of the WT, Δ*rsmA* and Δ*rsmN* strains looked similar, but detected proteins were less abundant in the 34°C culture supernatant of the Δ*rsmA* mutant. The expression of *rsmA* in the *rsmA*$_{ind}$ Δ*rsmN* strain both at 37°C and 34°C reduced the abundance of supernatant proteins. On the other hand, *rsmN* expression reduced the abundance of *rsmN*$_{ind}$ Δ*rsmA* supernatant proteins only at 34°C.

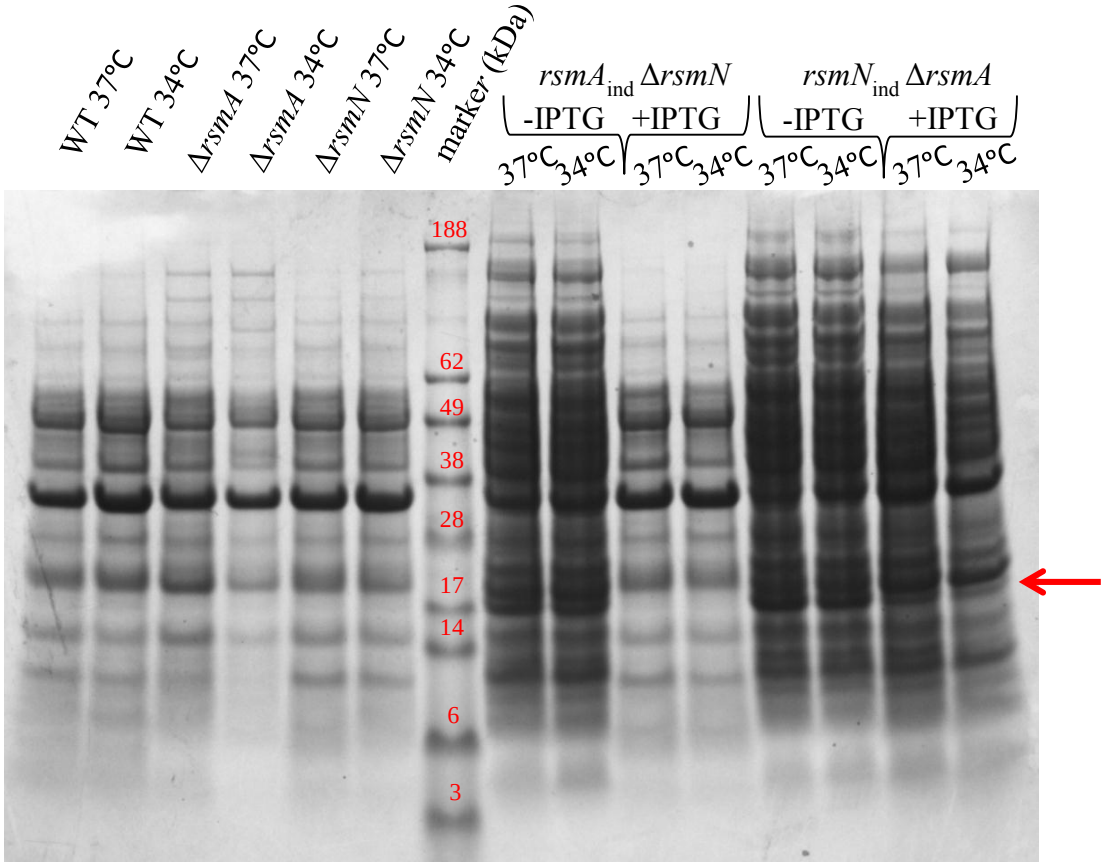


**Figure 3.25. Supernatant protein profiling of the WT, Δ*rsmA*, Δ*rsmN*, *rsmA*$_{ind}$ Δ*rsmN*, and *rsmN*$_{ind}$ Δ*rsmA* strains (the latter two grown with/without IPTG) at 37°C and 34°C**
The obvious difference between supernatant profiles of the tested strains is the high abundance of proteins in the supernatants of the inducible double deletion mutants grown without IPTG. The expression of *rsmA* both at 37°C and 34°C and *rsmN* at 34°C in the respective inducible double deletion mutant reduces the abundance of supernatant proteins. The protein indicated by the red arrow is highly abundant in culture supernatants of the double mutants; however, it is not found in the culture supernatant when *rsmA* is expressed either at 37°C or 34°C and decreased in abundance upon *rsmN* expression at 34°C.

Given that cells were harvested at similar $OD_{600}$, overloaded protein profiles of the inducible double deletion mutants, especially in the absence of IPTG, indicate that a greater level of autolysis occurred when cells lacked both Rsm proteins. This hypothesis was further investigated by immunoblotting the supernatant proteins with α-IscS antisera (Figure 3.26).

Figure 3.26 depicts that IscS was present in culture supernatants of the *rsmA*$_{ind}$ Δ*rsmN* and *rsmN*$_{ind}$ Δ*rsmA* strains grown at 37°C or 34°C without IPTG and the *rsmN*$_{ind}$ Δ*rsmA* strain grown at 37°C with IPTG. A faint band was also detected in the WT

34°C and Δ*rsmN* 37°C cultures. After *rsmA* expression, IscS was not among supernatant proteins of the *rsmA*$_{ind}$ Δ*rsmN* mutant at 34°C and was hardly detectable at 37°C. Furthermore, the abundance of IscS in the 34°C culture supernatant of the *rsmN*$_{ind}$ Δ*rsmA* strain decreased greatly after *rsmN* expression. These results suggest that *P. aeruginosa* PAO1 cells undergo autolysis in the absence of both RsmA and RsmN, and either *rsmA* or *rsmN* expression can prevent the autolysis of a double mutant.

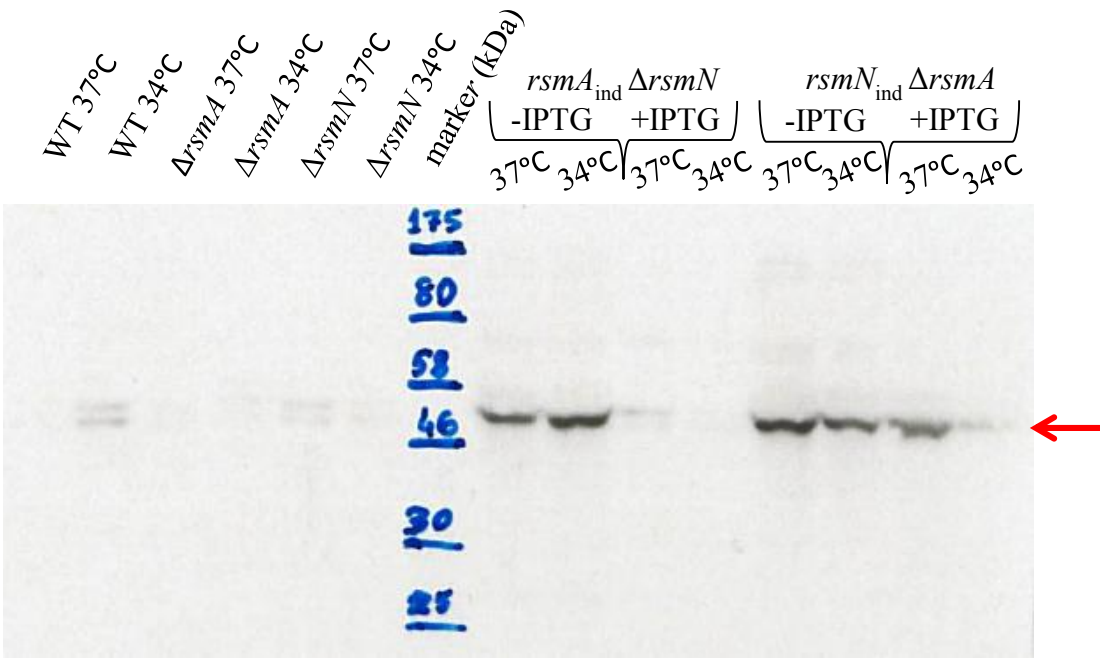


**Figure 3.26. Investigation of cell lysis in the WT, Δ*rsmA*, Δ*rsmN*, *rsmA*$_{ind}$ Δ*rsmN* and *rsmN*$_{ind}$ Δ*rsmA* strains (the latter two grown with/without IPTG) by detection of the cytosolic protein IscS (47 kDa) among secreted proteins**

IscS, indicated by the red arrow, is detected in culture supernatants of the *rsmA*$_{ind}$ Δ*rsmN* and *rsmN*$_{ind}$ Δ*rsmA* strains grown at 37°C or 34°C without IPTG. The expression of *rsmA* in the inducible double deletion mutant prevents IscS release to the culture supernatant at both temperatures whereas IscS is still detected in the supernatant after *rsmN* expression at 37°C.

D'Argenio *et al.* [197] demonstrated that the deletion of *pqsL* results in the autolysis of *P. aeruginosa*, therefore during quantification of autolysis levels in the absence of RsmA and RsmN, the Δ*pqsL* mutant was used as a positive control. 5 mL of soft top agar was seeded with 5 µL of o/n cultures ($OD_{600}$ adjusted to 1.0) of the WT, Δ*rsmA*, Δ*rsmN*, *rsmN*$_{ind}$ Δ*rsmA* and Δ*pqsL* strains and spread on top of LB agar (Supplementary Figure 6). To study the influence of the double deletion of *rsmA* and *rsmN* on autolysis, only the *rsmN*$_{ind}$ Δ*rsmA* mutant was used due to a leaky expression from the *rsmA*$_{ind}$ Δ*rsmN* strain.

Autolysis of the Δ*pqsL* mutant could be seen in the form of plaques (Supplementary Figure 6). From the transparent color of the agar which was seeded with *rsmN*$_{ind}$ Δ*rsmA* cells, it could be speculated that *rsmN*$_{ind}$ Δ*rsmA* cells underwent lysis. Serial dilutions of the o/n cultures were needed to quantify the results. $10^{-1}$, $10^{-2}$, $10^{-3}$, $10^{-4}$, and $10^{-5}$ dilutions of the $OD_{600}$-adjusted cultures were prepared and seeded in soft top agar and colony forming units were counted the following day.

$10^{-5}$ dilution gave the most reliable results as none of the colonies merged with each other; therefore, the experiment was repeated with $10^{-5}$-diluted overnight cultures. Table 3.2 shows the average number of c.f.u. from six independent experiments.

The WT strain and the Δ*rsmN* mutant formed an equal number of c.f.u. The number of *rsmN*$_{ind}$ Δ*rsmA* c.f.u. was 5-fold and Δ*rsmA* c.f.u. was ~ 1,5-fold less than the number of c.f.u. formed by the WT and Δ*rsmN* strains. The Δ*pqsL* mutant formed less c.f.u. than the WT and Δ*rsmN* strains but more than the Δ*rsmA* strain. Based on these results, it can be concluded that the double deletion of *rsmA* and *rsmN* triggers autolysis of *P. aeruginosa*.

**Table 3.2. Quantification of cell lysis in the WT, Δ*rsmA*, Δ*rsmN*, *rsmN*$_{ind}$ Δ*rsmA* and Δ*pqsL* strains by c.f.u. count**

Numbers listed need to be multiplied by $10^3$ to get the actual number of c.f.u. The number of c.f.u. formed by the *rsmN*$_{ind}$ Δ*rsmA* strain is 5-fold less than the number of c.f.u. formed by the WT and Δ*rsmN* strains, and Δ*rsmA* c.f.u. is half the number of c.f.u. formed by the WT and Δ*rsmN* strains.

| Strain | c.f.u. (*$10^3$) |
|---|---|
| **WT PAO1-N** | 1367 ± 339 |
| **Δ*rsmA*** | 733 ± 186 |
| **Δ*rsmN*** | 1383 ± 538 |
| ***rsmN*$_{ind}$ Δ*rsmA* -IPTG** | 267 ± 137 |
| **Δ*pqsL*** | 1017 ± 271 |

A preliminary study investigating the effect of HHQ/PQS accumulation on cell lysis was carried out by Giordano Rampioni using the PAO1-N Δ*pqsL* and Δ*pqsH* Δ*pqsL* mutants. After the discovery of 30-fold and 800-fold increase in Pf4 levels of the Δ*pqsL* and Δ*pqsH* Δ*pqsL* mutants in comparison with the WT strain, lysis and HHQ accumulation in the Δ*pqsL* mutant were linked to the induction of the lytic lifestyle of Pf4 prophage (unpublished data).

Based on this preliminary data, the contribution of PQS and HHQ accumulation to the increased autolysis, hence the rough colony morphotype observed in the absence of Rsm proteins was investigated by exogenous addition of 10, 20 and 40 µM of synthetic PQS and HHQ to Congo red-tryptone agar. There was not much difference between colony morphologies of tested strains on the control plate and plates supplemented with 10 or 20 µM PQS or HHQ. Therefore, only the WT, Δ*rsmA*, Δ*rsmN* and *rsmN*$_{\text{ind}}$ Δ*rsmA* colonies grown on Congo red-tryptone agar supplemented with 40 µM PQS (panel a) and 40 µM HHQ (panel b) are depicted in Figure 3.27. 3 days post-inoculation, the WT, Δ*rsmA* and Δ*rsmN* strains had smooth colony morphologies whereas the *rsmN*$_{\text{ind}}$ Δ*rsmA* strain grew as rough colonies both on control agar and on agar supplemented with 40 µM PQS (panel a). Numerous tendrils originated from the inner circle of the Δ*rsmA* colony on agar supplemented with 40 µM HHQ whereas the WT, Δ*rsmN*, and *rsmN*$_{\text{ind}}$ Δ*rsmA* colonies looked the same with or without the addition of exogenous HHQ (panel b) or PQS (panel a).

Colony morphologies of the wild-type PAO1-N, *rsmN*$_{\text{ind}}$ Δ*rsmA*, Δ*pqsL*, Δ*pqsH*, and Δ*pqsH* Δ*pqsL* strains were also compared 2 days and 6 days post-inoculation (Figure 3.28, top and bottom panels respectively). It has been illustrated that the Δ*pqsH* Δ*pqsL* strain (c) had a rough colony morphology similar to the *rsmN*$_{\text{ind}}$ Δ*rsmA* (b) morphotype and plaques formed in the centre of the Δ*pqsL* (e) and Δ*pqsH* (d) colonies 2 days post-inoculation (top panel). Plaque formation in the centre of the Δ*pqsL* (e) mutant was still detectable 6 days post-inoculation (bottom panel). On the other hand, the PAO1-N strain (a), which is the genetic background of the tested mutants, had smooth colony morphology and no putative plaques were observed on the PAO1-N colony even after 6 days post-inoculation (bottom panel). The WT, Δ*pqsH* and Δ*pqsL* colonies (a, d, e) had yellow inner circles and the *rsmN*$_{\text{ind}}$ Δ*rsmA*, Δ*pqsH* Δ*pqsL*, Δ*pqsL* and WT colonies

(b, c, e, a) had smooth surfaces 6 days post-inoculation. In contrast, the Δ*pqsH* (d) colony had a fragmented and dry surface.

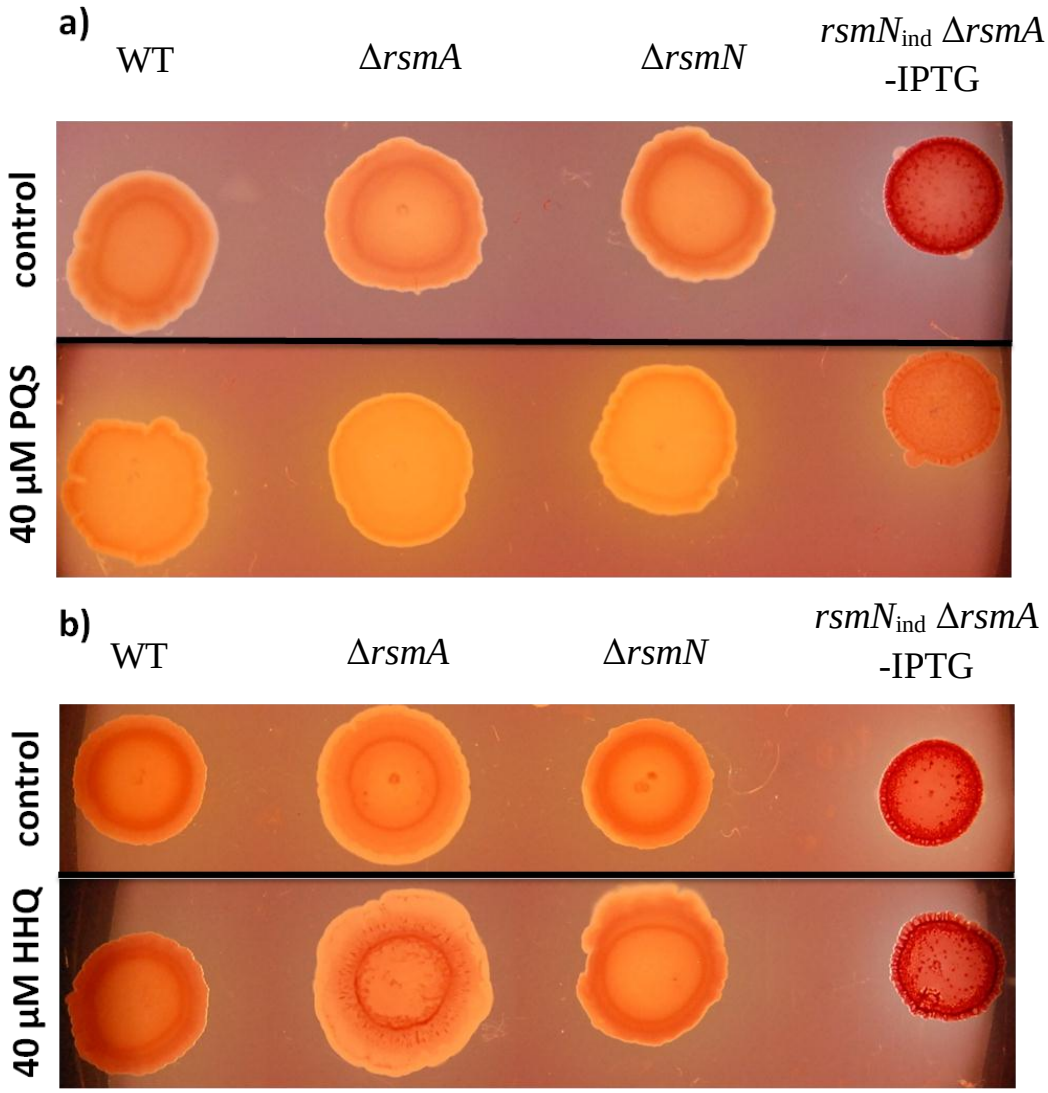


**Figure 3.27. Exogenous addition of HHQ but not PQS results in a lytic colony morphology of the Δ*rsmA* mutant grown on Congo red-tryptone agar at room temperature for 3 days**

PQS addition does not result in any difference in colony morphologies (same on the control and 40 µM PQS supplemented plates) of the WT, Δ*rsmA*, Δ*rsmN* and *rsmN*$_{ind}$ Δ*rsmA* strains whereas HHQ addition results in a lytic morphology of the Δ*rsmA* mutant (tendrils originating from the inner circle) 3 days post-inoculation.

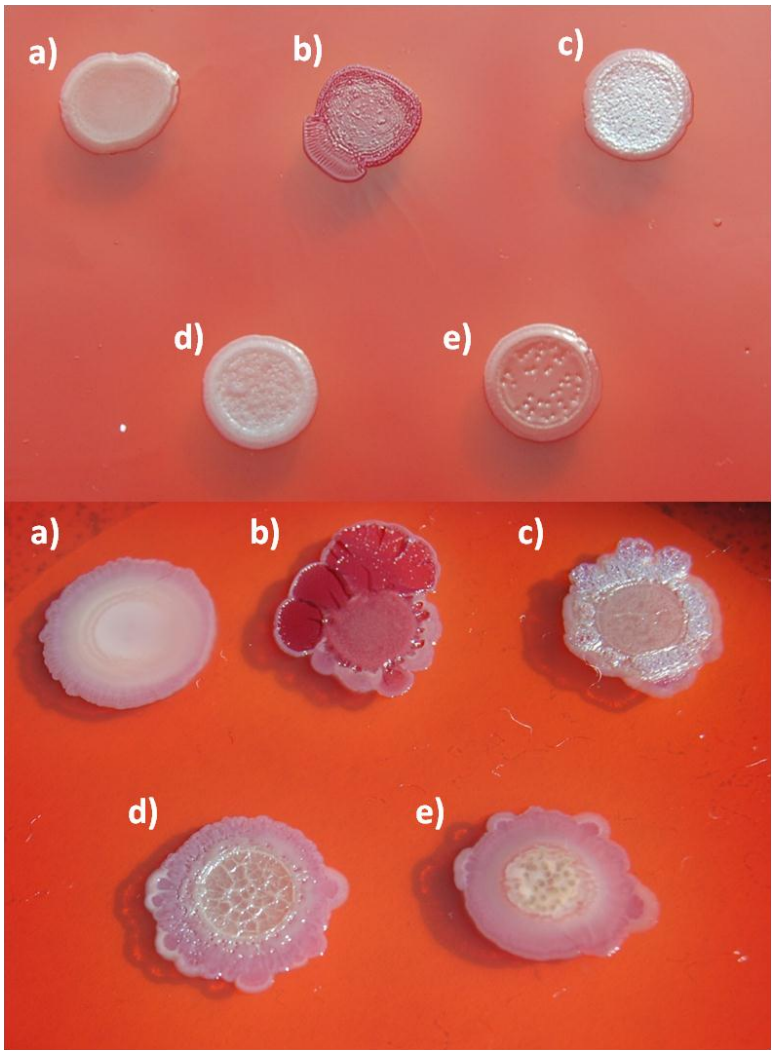


**Figure 3.28. Colony morphologies of the WT PAO1-N (a), *rsmN*$_{ind}$ Δ*rsmA* (b), Δ*pqsH* Δ*pqsL* (c), Δ*pqsH* (d), and Δ*pqsL* (e) strains on Congo red-tryptone agar at room temperature 2 days (top panel) and 6 days post-inoculation (bottom panel)**
Colonies of the *rsmN*$_{ind}$ Δ*rsmA* (b) and Δ*pqsH* Δ*pqsL* (c) strains are characterised by a rough appearance whereas Δ*pqsH* (d) and Δ*pqsL* (e) colonies display plaque formation. On the other hand, the WT (a) strain has a smooth colony morphology.

After investigating autolysis by the *rsmN*$_{ind}$ Δ*rsmA* mutant, the protein highlighted by the red arrow in Figure 3.25 was identified. This protein was not present in culture supernatants of the *rsmA*$_{ind}$ Δ*rsmN* strain grown with IPTG either at 37°C or 34°C. It was detectable in culture supernatants of the *rsmN*$_{ind}$ Δ*rsmA* strain, but less predominant upon IPTG induction, especially at 34°C. Since *rsmN* expression affected the abundance of this protein, it was considered as a direct or indirect target of RsmN and sent to be sequenced.

80 probable proteins were listed after liquid chromatography-mass spectrometry analysis. Some of the listed proteins (40) were at a higher molecular weight than the marker band (17 kDa, Figure 3.25) the protein of interest matched, therefore, they were removed. After elimination of larger proteins, comparison of the percent coverages and total spectrum counts revealed that the sequenced protein might be Hcp1 (hemolysin coregulated protein), a T6SS effector protein (Figure 3.29). Hcp1 secretion was previously shown to be upregulated in a Δ*rsmA* Δ*rsmF* mutant by Marden *et al*. [206].

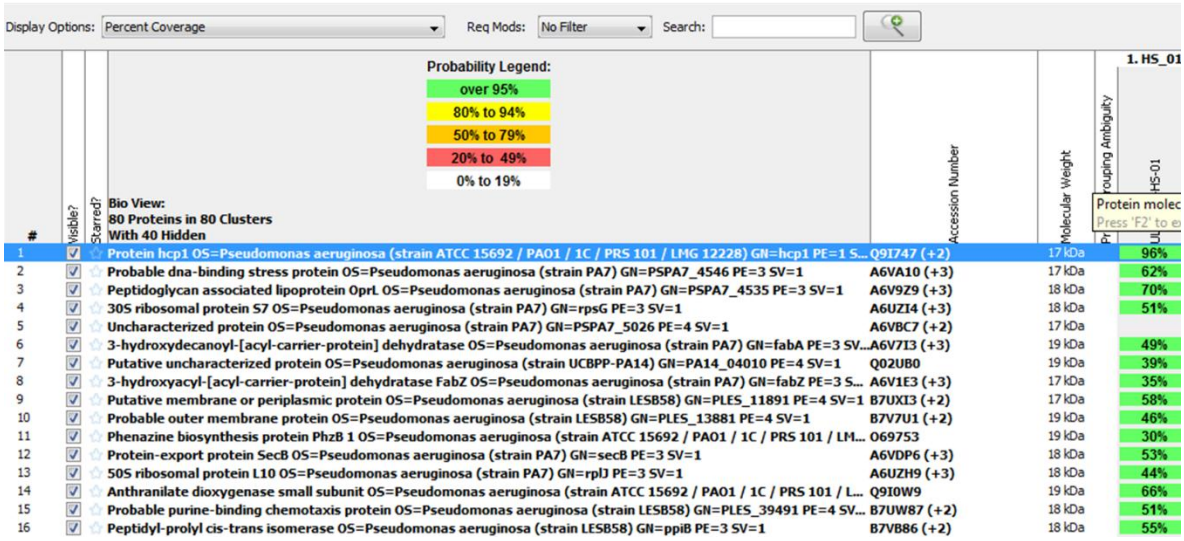


**Figure 3.29. Snapshot of the percent coverages of probable proteins (identified in the 17 kDa region) released to the culture supernatants of the *rsmA*$_{ind}$ Δ*rsmN* and *rsmN*$_{ind}$ Δ*rsmA* strains**

Out of the 80 proteins listed after the LC-MS/MS analysis, 40 with a higher molecular weight than the 17 kDa marker band were eliminated. Among the rest of the probable proteins, Hcp1 had the highest percent coverage and total spectrum count (not shown).

### 3.2.9 Repression of glycogen accumulation in *E. coli* TR1-5 cells by RsmA but not RsmN

RsmA can complement a Δ*csrA* isogenic mutation which results in glycogen overproduction by the *E. coli* TR1-5 cells [44, 204]. Heeb *et al*. [53] showed that TR1-5/pRsmAR44A transformants overproduced glycogen, confirming the loss of biological function of RsmA as a result of the R44A mutation. The ability of RsmN and RsmNR62A, the mutant equivalent to RsmAR44A, to repress glycogen accumulation in *E. coli* TR1-5 strain was investigated by iodine staining of the *E. coli* cells transformed with *rsmN* or *rsmN*R62A expression plasmids on Kornberg medium. The *E. coli* DH5α strain was used as a negative control and the *E. coli* TR1-5 and TR1-5/pME6000 strains were used as positive controls. Iodine staining of the DH5α, TR1-5, TR1-5/pME6000, TR1-5/pRsmA, TR1-5/pHS2 and TR1-5/pHS2R62A strains demonstrates that even though RsmN complemented certain Δ*rsmA* phenotypes, unlike *rsmA*, *rsmN* could not complement the Δ*csrA* mutation in *E. coli* (Figure 3.30). Glycogen accumulation was not repressed in TR1-5/pHS2 or TR1-5/pHS2R62A transformants whereas the yellow color of the TR1-5/pRsmA strain on Kornberg medium indicated the breakdown of glycogen.

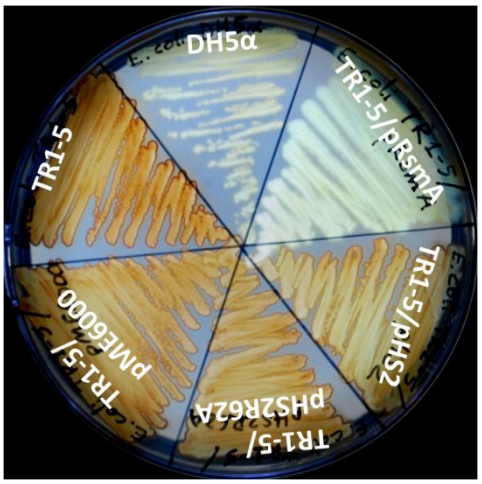


**Figure 3.30. Repression of glycogen accumulation in the *E. coli* Δ*csrA* mutant TR1-5 by *P. aeruginosa* RsmA but not RsmN or RsmNR62A**

The TR1-5, TR1-5/pME6000, TR1-5/pHS2 and TR1-5/pHS2R62A strains turn brown which indicates glycogen accumulation upon iodine staining. On the other hand, the TR1-5/pRsmA and DH5α strains, the latter used as a negative control, stain yellow which is an indication of glycogen breakdown.

### 3.2.10 The contribution of RsmA and RsmN to virulence in a mouse chronic infection model

As RsmA regulates the production of various virulence factors, T3SS and T6SS; and RsmN has been found to contribute to the regulation of motility, microcolony formation, production of exoproducts such as proteases and possibly T6SS as demonstrated in previous sections, it has been hypothesised that *P. aeruginosa* would be less virulent *in vivo* when cells lacked both Rsm proteins. Based on this hypothesis, the WT strain PAO1-N and the *rsmN*$_{ind}$ Δ*rsmA* double mutant were administered in mouse chronic wound infections (done in triplicates) in the laboratory of Professor Rumbaugh at Texas Tech University Health Sciences Centre, Lubbock, U.S.A. The bacterial load, calculated as the ratio of the number of c.f.u. and weight gain in grams, of each strain was checked 4 days post-infection. Table 3.3 outlines bacterial loads of the WT and *rsmN*$_{ind}$ Δ*rsmA* strains 4 days post-infection.

**Table 3.3. Bacterial loads, calculated as the ratio of the c.f.u. and weight gain (g), of the WT PAO1-N and *rsmN*$_{ind}$ Δ*rsmA* strains in mouse chronic wound infections 4 days post-infection**

| Bacterial load | | | | | | | |
|---|---|---|---|---|---|---|---|
| PAO1-N | | | | *rsmN*$_{ind}$ Δ*rsmA* -IPTG | | | |
| | c.f.u. | g | c.f.u./g | | c.f.u. | g | c.f.u./g |
| **Mouse 1** | 1.00 x10$^4$ | 0.085 | 1.18 x10$^5$ | **Mouse 1** | 2.00 x10$^4$ | 0.120 | 1.67 x10$^5$ |
| **Mouse 2** | 4.00 x10$^3$ | 0.062 | 6.45 x10$^4$ | **Mouse 2** | 1.00 x10$^4$ | 0.094 | 1.06 x10$^5$ |
| **Mouse 3** | 2.00 x10$^5$ | 0.093 | 2.15 x10$^6$ | **Mouse 3** | 4.00 x10$^5$ | 0.140 | 2.86 x10$^6$ |
| | | Average | 7.78 x10$^5$ | | | Average | 1.04 x10$^6$ |

These results show that even though the number of *rsmN*$_{ind}$ Δ*rsmA* c.f.u. was ~ 2.5-fold higher, due to a higher increase in mice weight in comparison with the weight of mice infected with the WT strain, there was not a significant difference between bacterial loads of the WT and *rsmN*$_{ind}$ Δ*rsmA* strains *in vivo* 4 days post-infection in a chronic infection model.

### 3.2.11 The contribution of expression from the $P_{rsmN}$, $P_{rsmF}$ and $P_{nmsR}$ promoters on the regulation of swarming motility and production of secondary metabolites

Putative transcriptional start sites of *rsmN*, *rsmF* and *nmsR* were identified previously. Subsequently, expression from the *rsmN* sense promoter $P_{rsmN}$ and the predicted antisense promoter $P_{nmsR}$ was validated using a bioreporter (see section 3.1). The multicopy expression plasmid of *rsmN*, pHS2 (Figure 2.1, panel c) included both $P_{rsmN}$ and $P_{nmsR}$ sequences and the corresponding TSSs. The contribution of the predicted antisense transcript *nmsR* to the regulation of swarming motility, exoprotease, elastase and PYO production was investigated using a construct (pMR1, Figure 3.31) where $P_{nmsR}$ and $P_{rsmN}$ sequences have been removed and *rsmN* expression was induced only by the *lac* promoter ($P_{lac}$) of the backbone vector pME6000. Expression vector pMR1 was obtained by cloning the *rsmN* sequence in a PCR reaction and inserting in pME6000 using 2PRsmNF and 2PRsmNR primers (see Table 2.3) which introduce restriction sites prior to *rsmN* TSS and after the *rsmN* stop codon respectively.

The expression of *rsmN* via pMR1 which lacks the $P_{nmsR}$, $P_{rsmN}$ and $P_{rsmF}$ promoters failed to complement total proteolytic and elastinolytic activities (Supplementary Figure 7); however, it restored swarming motility of the Δ*rsmA* mutant fully (Figure 3.36). Moreover, PYO production by the Δ*rsmA*/pMR1 transformant was significantly increased in comparison with the Δ*rsmA*/pME6000 transformant (Supplementary Figure 8). To further investigate the role of the antisense transcript *nmsR*, another construct where the *rsmN* sequence was reverse complemented and placed after the *nmsR* TSS was prepared using the pUCP18 vector as a backbone (pMR11, Figure 3.31).

While this analysis was taking place, Marden *et al.* [206] identified an *rsmF* TSS upstream of the detected *rsmN* TSS (Figure 3.2). Cloned *rsmN* sequences were reanalysed taking the *rsmF* TSS into consideration and a new construct (pMR12, Figure 3.31) that included both $P_{rsmN}$ and $P_{rsmF}$ promoter sequences and TSSs but excluded the *nmsR* sequence was made. The difference between the pHS2 and pMR12 constructs is the lack of *nmsR* transcription in strains transformed with the latter.

The multicopy *rsmN* expression plasmid pHS2, the derivatives of pHS2 depicted in Figure 3.31 and the background vector pME6000 were transformed into the inducible *rsmN*$_{ind}$ Δ*rsmA* double mutant to check RsmN control on growth, swarming motility, total proteolytic and elastinolytic activities, PYO production and colony morphology (Figures 3.32-3.35) in the absence of both native Rsm proteins (no IPTG was supplied to the culture) and with or without the synthesis of the predicted antisense transcript.

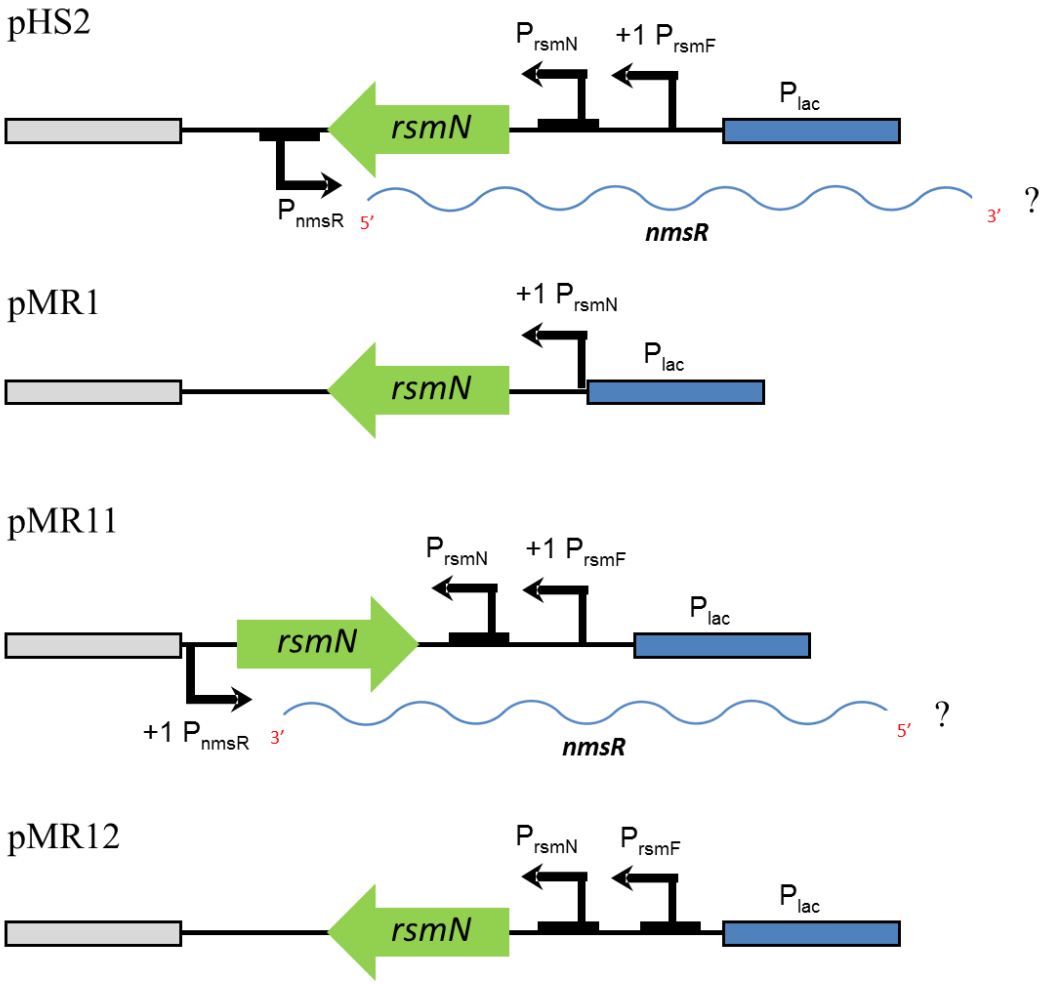


**Figure 3.31. Diagrammatic representation of TSSs and promoter sequences in the pHS2 derivatives**

The antisense *nmsR* transcript, indicated as an RNA strand below the construct diagrams, is produced in pHS2 and pMR11 transformants, whereas it is not produced in pMR1 and pMR12 transformants due to the lack of the $P_{nmsR}$ promoter or the *nmsR* TSS. The *rsmN* sequence was reverse complemented and cloned in pME6000 to obtain pMR11, for this reason, the *nmsR* transcript is illustrated in the 3'-5' orientation below pMR11. The cloned fragment in pMR1 excludes the $P_{rsmN}$ and $P_{rsmF}$ promoter sequences and the *rsmF* TSS in comparison with the pMR12 construct. The pMR11 vector is pUCP18-based whereas all the other constructs are pME6000-based. Both pUCP18 and pME6000 have the *lac* promoter, $P_{lac}$ (depicted in blue, right).

Figure 3.32 illustrates growth curves of the *rsmN*$_{ind}$ Δ*rsmA*/pME6000, *rsmN*$_{ind}$ Δ*rsmA*/pHS2, *rsmN*$_{ind}$ Δ*rsmA*/pMR1, *rsmN*$_{ind}$ Δ*rsmA*/pMR11 and *rsmN*$_{ind}$ Δ*rsmA*/pMR12 strains cultivated without IPTG at 37°C. The generation times of the *rsmN*$_{ind}$ Δ*rsmA*/pHS2, *rsmN*$_{ind}$ Δ*rsmA*/pMR11 and *rsmN*$_{ind}$ Δ*rsmA*/pMR12 strains were almost identical (~ 39, 43 and 43 min. respectively) and shorter than the generation times of the *rsmN*$_{ind}$ Δ*rsmA*/pME6000 and *rsmN*$_{ind}$ Δ*rsmA*/pMR1 strains (~ 67 and 85 min.). At the end of 24 h, all strains had similar optical densities.

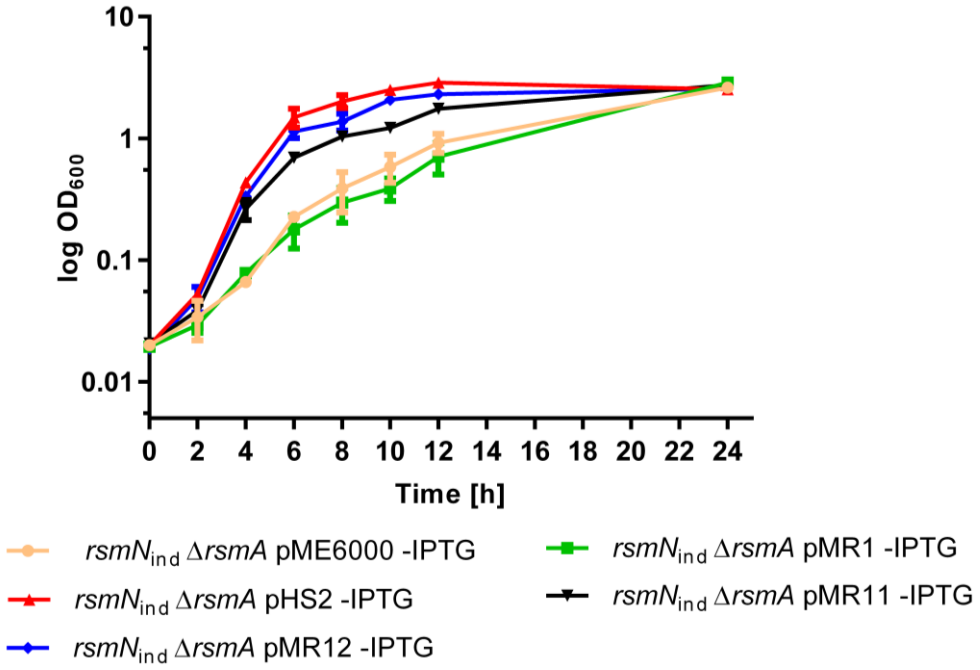


**Figure 3.32. Transcription of the predicted *nmsR* RNA does not influence the growth of the *rsmN*$_{ind}$ Δ*rsmA*/pME6000 double mutant in LB at 37°C**
Although pMR12 lacks the P$_{nmsR}$ promoter to transcribe the *nmsR* RNA, growth curves of the *rsmN*$_{ind}$ Δ*rsmA*/pHS2, *rsmN*$_{ind}$ Δ*rsmA*/pMR11, and *rsmN*$_{ind}$ Δ*rsmA*/pMR12 strains are similar. On the other hand, growth curves of the *rsmN*$_{ind}$ Δ*rsmA*/pME6000 and *rsmN*$_{ind}$ Δ*rsmA*/pMR1 strains are alike. The former three strains reach the stationary phase of growth earlier (after ~ 6 h) than the latter two. All strains have similar population densities at the end of 24 h.

Figure 3.33 illustrates that non-swarming phenotype of the *rsmN*$_{ind}$ Δ*rsmA* mutant could be partially complemented in the presence of P$_{rsmN}$ by multicopy expression of *rsmN* with or without *nmsR* transcription such as in the *rsmN*$_{ind}$ Δ*rsmA*/pHS2, *rsmN*$_{ind}$ Δ*rsmA*/pMR11 and *rsmN*$_{ind}$ Δ*rsmA*/pMR12 transformants. Within 24 h, *rsmN*$_{ind}$ Δ*rsmA*/pHS2 cells swarmed slightly more compared with the *rsmN*$_{ind}$ Δ*rsmA*/pMR11 and *rsmN*$_{ind}$ Δ*rsmA*/pMR12 strains. In contrast, P$_{lac}$-induced expression of *rsmN* via pMR1 failed to restore the motility of the *rsmN*$_{ind}$ Δ*rsmA* cells.

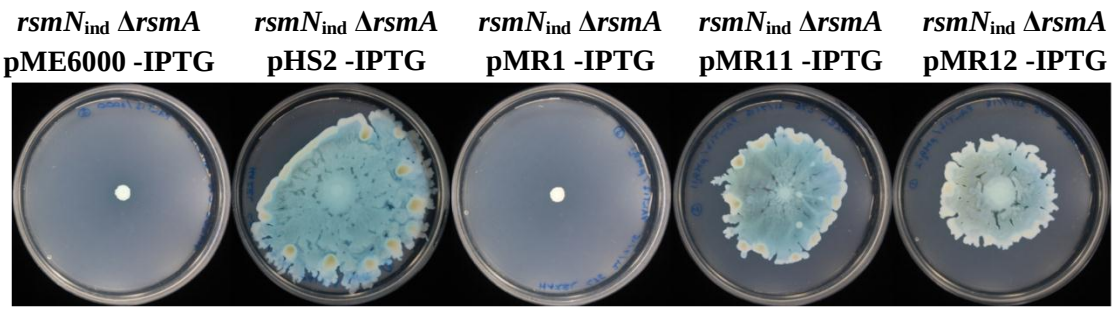


**Figure 3.33. Investigating the influence of *nmsR* transcription on the swarming motility of the *rsmN*ind Δ*rsmA*/pME6000 double mutant on nutrient broth agar (0.5% w/v) at 37°C**
The *rsmN*ind Δ*rsmA*/pME6000 mutant is deficient in swarming motility. Expression of *rsmN* with or without *nmsR* transcription but when the $P_{rsmN}$ sequence is present in the cloned insert restores swarming motility in the *rsmN*ind Δ*rsmA*/pME6000 mutant whereas $P_{lac}$-induced expression of *rsmN* does not.

When grown without the induction of *rsmA* or *rsmN* expression, total proteolytic activity of the *rsmN*ind Δ*rsmA*/pME6000 strain was really low; proteolytic activity of the *rsmN*ind Δ*rsmA*/pMR1 strain was also at a basal level (Figure 3.34, panel a). Proteolytic activities of the *rsmN*ind Δ*rsmA*/pHS2, *rsmN*ind Δ*rsmA*/pMR11 and *rsmN*ind Δ*rsmA*/pMR12 transformants were significantly higher than the *rsmN*ind Δ*rsmA*/pME6000 mutant. Elastinolytic activities of the *rsmN*ind Δ*rsmA*/pHS2, *rsmN*ind Δ*rsmA*/pMR11 and *rsmN*ind Δ*rsmA*/pMR12 transformants (Figure 3.34, panel b) were ~ 3-fold higher than the *rsmN*ind Δ*rsmA*/pME6000 and *rsmN*ind Δ*rsmA*/pMR1 strains. In addition, PYO production by the *rsmN*ind Δ*rsmA*/pHS2, *rsmN*ind Δ*rsmA*/pMR12 and *rsmN*ind Δ*rsmA*/pMR11 transformants was increased ~ 2-fold in comparison with the *rsmN*ind Δ*rsmA*/pME6000 strain. There was not a significant difference between PYO levels of the *rsmN*ind Δ*rsmA*/pME6000 and *rsmN*ind Δ*rsmA*/pMR1 strains.

The rough colony morphotype of the *rsmN*ind Δ*rsmA* mutant (illustrated in section 3.2.7) could be altered by the $P_{rsmN}$-induced expression of *rsmN* with or without the synthesis of the *nmsR* transcript (see *rsmN*ind Δ*rsmA*/pHS2, *rsmN*ind Δ*rsmA*/pMR11 and *rsmN*ind Δ*rsmA*/pMR12 colonies depicted in Figure 3.35). On the contrary, long tendrils started to form around the inner circle of the *rsmN*ind Δ*rsmA*/pMR1 colony 2 days post-inoculation and a wrinkly colony morphology was observed after a few days.

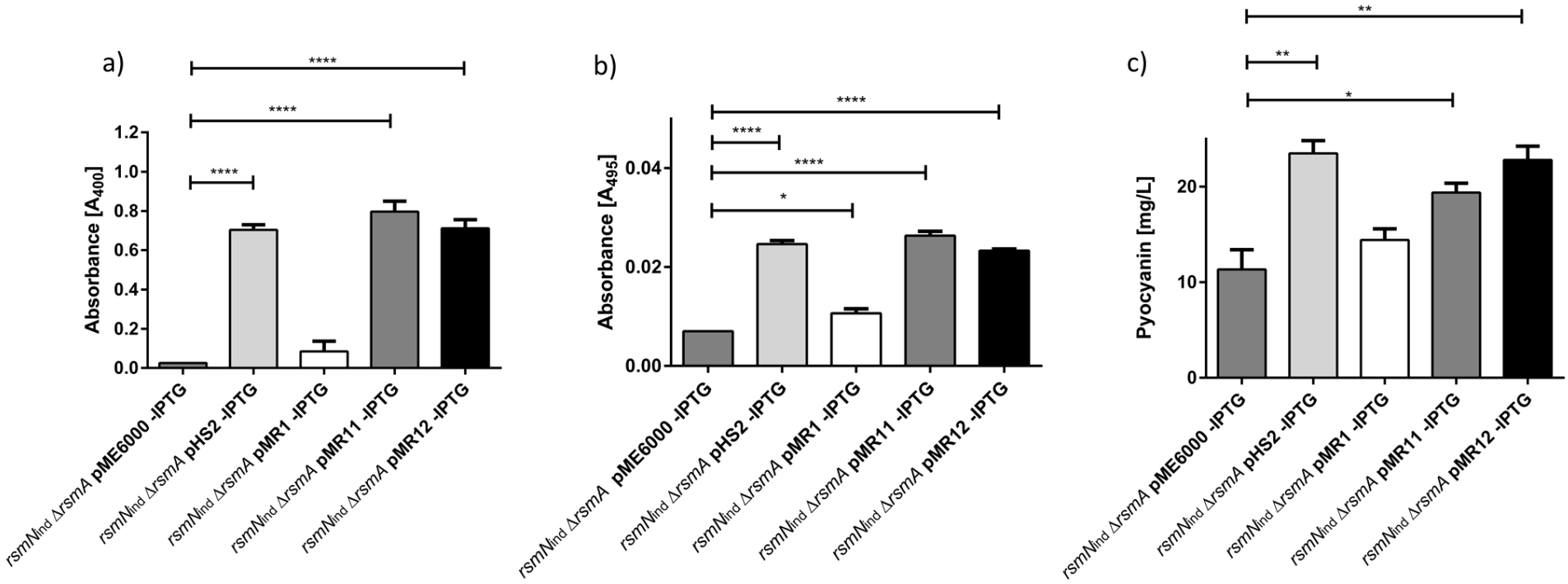


**Figure 3.34. The effect of the multicopy expression of *rsmN* with or without *nmsR* transcription on the exoprotease (panel a), elastase (panel b) and PYO (panel c) levels of the *rsmN*$_{ind}$ Δ*rsmA*/pME6000 mutant grown in LB at 37°C**

The multicopy expression of *rsmN* in the presence of its native promoter (via pHS2, pMR11 and pMR12 constructs) increases exoprotease, elastase and PYO production by the *rsmN*$_{ind}$ Δ*rsmA*/pME6000 mutant. The presence or absence of the *nmsR* transcript does not result in significant changes. $P_{lac}$-induced expression of *rsmN* (via pMR1) increases only the elastinolytic activity significantly. Data represents averages of three independent measurements. Error bars represent standard error of the mean. Statistical differences were determined by ANOVA analysis, followed by Tukey multiple comparisons test; * $p < 0.05$, ** $p < 0.01$, **** $p < 0.0001$.

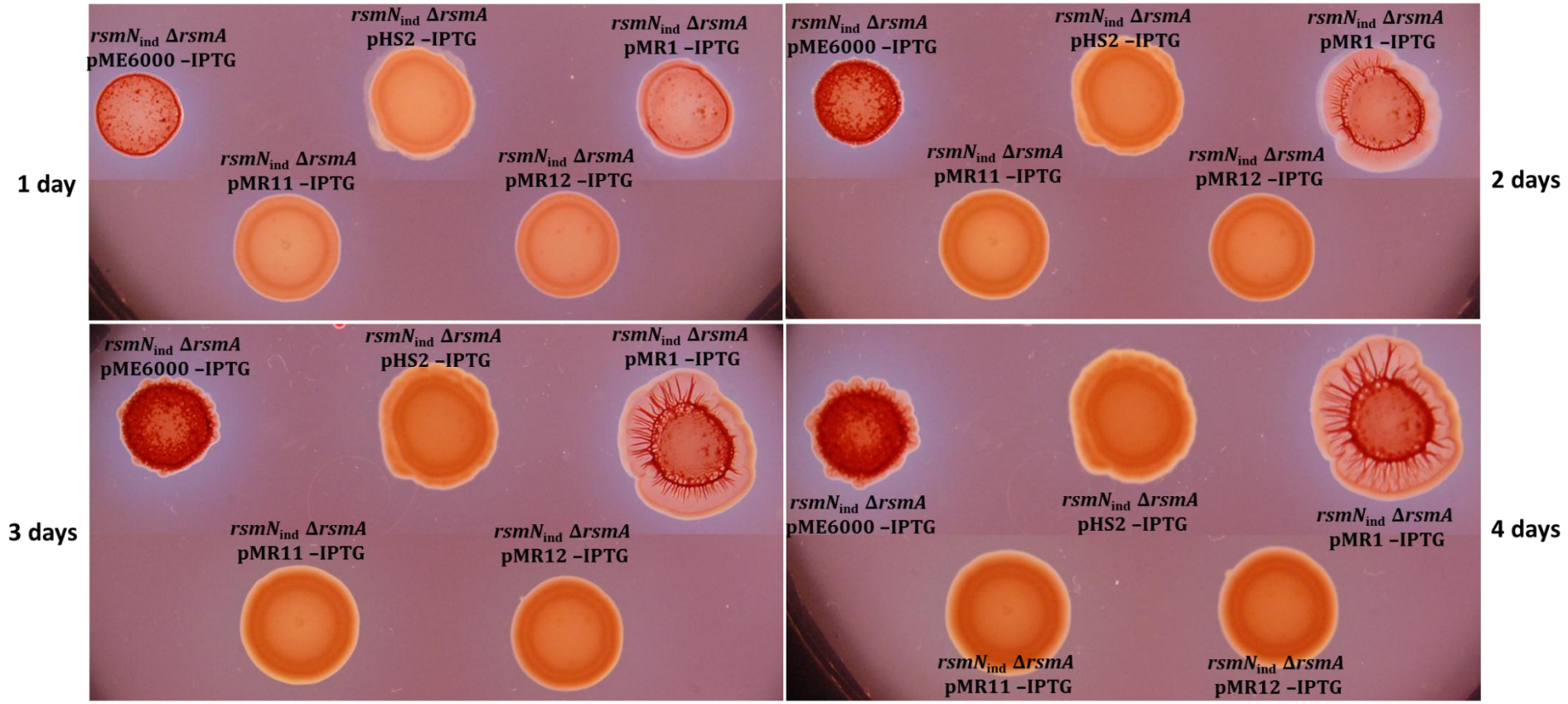


**Figure 3.35. Colony morphologies of the *rsmN*$_{ind}$ Δ*rsmA*/pME6000, *rsmN*$_{ind}$ Δ*rsmA*/pHS2, *rsmN*$_{ind}$ Δ*rsmA*/pMR1, *rsmN*$_{ind}$ Δ*rsmA*/pMR11 and *rsmN*$_{ind}$ Δ*rsmA*/pMR12 strains on Congo red-tryptone agar up to 4 days post-inoculation at room temperature**

The *rsmN*$_{ind}$ Δ*rsmA*/pME6000 colony has a rough morphology. Plasmid-induced *rsmN* expression results in smooth colony formation (*rsmN*$_{ind}$ Δ*rsmA*/pHS2, *rsmN*$_{ind}$ Δ*rsmA*/pMR11 and *rsmN*$_{ind}$ Δ*rsmA*/pMR12 colonies) when the native promoter of *rsmN* is present. On the other hand, *rsmN* expression induced by only the $P_{lac}$ promoter (via pMR1) causes cells to grow 'in wrinkles' outwards the inner circle 2 days post-inoculation.

In addition to the investigation of the effect of the *nmsR* transcript on RsmN-mediated regulation in the *rsmN*$_{ind}$ Δ*rsmA* mutant, plasmids outlined in Figure 3.31 were transformed into the WT, Δ*rsmA*, and Δ*rsmN* strains to elaborate on the reduction of swarming motilities of the WT and Δ*rsmN* strains when *rsmN* is expressed via the multicopy expression plasmid pHS2 at 37°C as depicted in Figure 3.9.

Figure 3.36 displays swarming motilities of the WT, Δ*rsmA*, and Δ*rsmN* strains transformed with pME6000 (backbone), pHS2, pMR1, pMR11 and pMR12 vectors. As shown before, the WT/pHS2 and Δ*rsmN*/pHS2 transformants failed to swarm at 37°C and swarming of the Δ*rsmA*/pME6000 mutant was not complemented by *rsmN* expression at 37°C. Lowering the temperature to 34°C eliminated the reduction of swarming motilities of the WT and Δ*rsmN* strains by *rsmN* expression. Interestingly, expression of *rsmN* by the $P_{lac}$ promoter and in the absence of the $P_{rsmN}$ or $P_{nmsR}$ promoters (via pMR1) also hindered swarming of the WT/pME6000 and Δ*rsmN*/pME6000 strains, however, restored swarming of the Δ*rsmA*/pME6000 mutant fully at 37°C. Furthermore, considering that the difference between pHS2 and pMR12 constructs is mainly the presence of the $P_{nmsR}$ promoter and *nmsR* TSS in the former, it was interesting that the WT/pMR12, Δ*rsmA*/pMR12 and Δ*rsmN*/pMR12 strains swarmed whereas the WT/pHS2, Δ*rsmA*/pHS2 and Δ*rsmN*/pHS2 strains did not swarm at 37°C. On the other hand, swarming phenotypes of the pMR12 and pHS2 transformants of the WT, Δ*rsmA* and Δ*rsmN* strains looked similar at 34°C. Expression of reverse complemented *rsmN* by the pMR11 construct resulted in a swarming phenotype of all tested strains at both temperatures, but, Δ*rsmA* swarming was only partially restored.

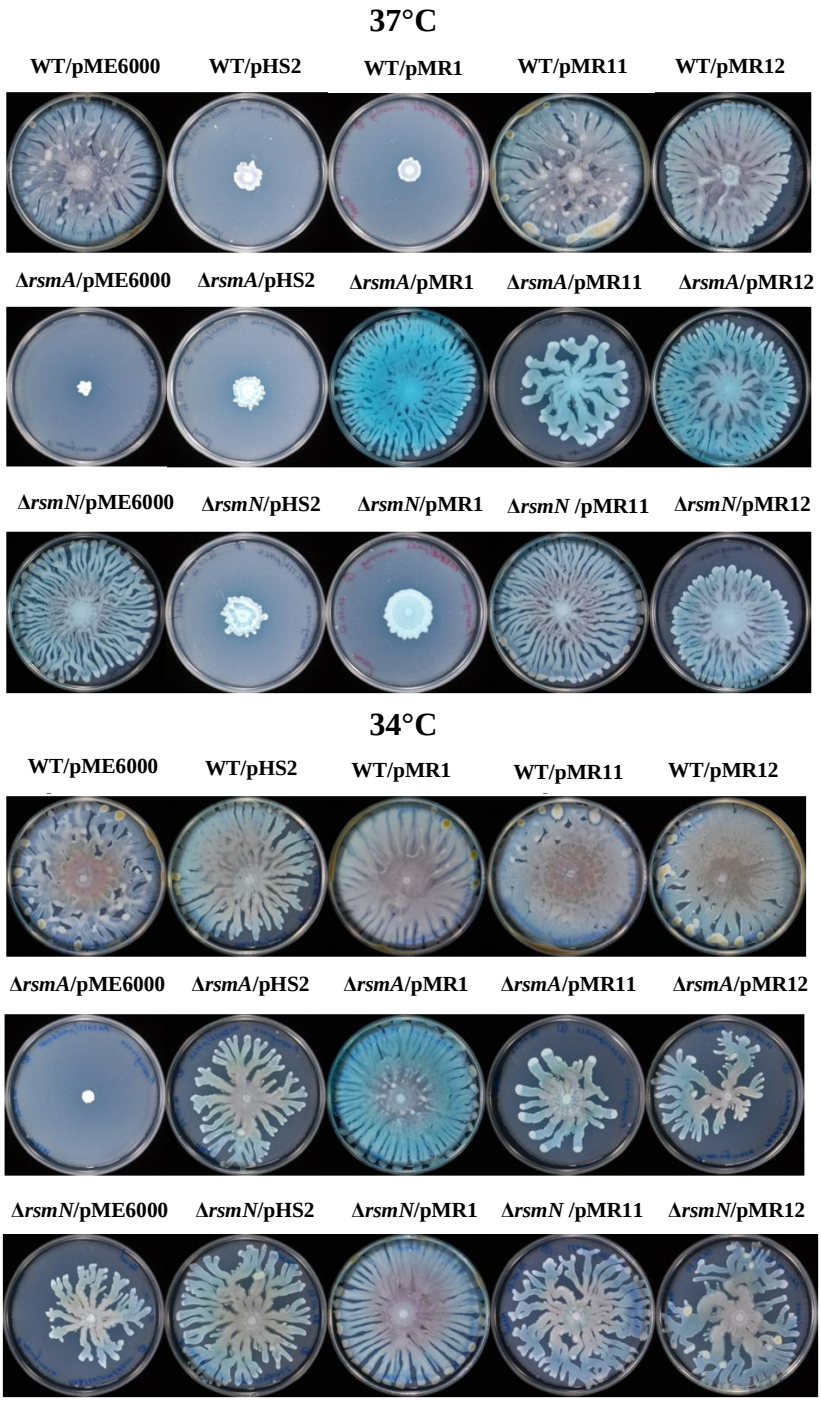


**Figure 3.36. The impact of the multicopy expression of *rsmN* in the presence or absence of the *nmsR* transcript on swarming motilities of the WT, Δ*rsmA* and Δ*rsmN* strains at 37°C and 34°C on nutrient broth agar (0.5% w/v)**

At 37°C and 34°C, the WT/pME6000 and Δ*rsmN*/pME6000 strains both swarm whereas the Δ*rsmA*/pME6000 strain is deficient in swarming motility. Swarming of the Δ*rsmA*/pME6000 and Δ*rsmN*/pME6000 strains increase whereas WT swarming does not change much upon multicopy expression of *rsmN* at 34°C. However, expression of *rsmN* without the $P_{rsmN}$ and *rsmF* TSS sequences (pHS2 and pMR1 constructs) suppresses swarming of the WT and Δ*rsmN* strains at 37°C. Swarming motility of the Δ*rsmA*/pME6000 mutant is restored in the absence of the $P_{nmsR}$ promoter at 37°C whereas *rsmN* expression via any of the constructs restores Δ*rsmA*/pME6000 swarming at 34°C.

Next, possible mechanisms 1) negative regulation by the antisense transcript *nmsR*, 2) cross-regulation between the Rsm proteins, 3) hairpin loop formation (depicted in Figure 3.37) in the near vicinity of the *rsmN* TSS, and 4) cell lysis behind the swarming reduction of the WT/pHS2, WT/pMR1, Δ*rsmN*/pHS2 and Δ*rsmN*/pMR1 strains at 37°C were investigated.

Alteration of codons is another form of regulation/adaptation to the environmental conditions, nutrient levels, stress, and other types of stimuli in bacteria. Codon usage can vary within the whole genome of an organism as well as within a single gene. The mutational bias in the *P. aeruginosa* PAO1 genome, demonstrated by an average genome codon index (GCI) of ~ 0.6 where GCI is described as 'a measure of the synonymous codon bias of a particular gene compared with the average codon bias in all chromosomal genes' has been revealed in Kiewitz *et al*. [224]. Previously, GCI of RsmA, calculated as the ratio of the observed GCI (geometric mean of the RSCU values of each codon used by *P. aeruginosa*) and the maximum GCI possible, was calculated as 0.455 (S. Heeb, personal communication) based on the formula highlighted in Kiewitz *et al*. [224]. Use of a synonymous codon instead of the one with the maximum RSCU value might be advantageous under circumstances where secondary structures might alter translation initiation by disrupting the binding motif recognised by a transcriptional or post-transcriptional regulator. Alternatively, secondary structure formation might expose recognition motifs for the small RNAs or regulatory proteins. In this study, GCI of RsmN was calculated as 0.522. These low GCI values of the Rsm proteins are thought to be due to favouring secondary structures such as stem-loops and hairpins [250, 251].

Analysis of secondary structures in the *rsmN* sequence revealed that there is a hairpin loop formation (5'-AGGGGCCGGTTTGCCCCT-3') in the 5'-UTR region of *rsmN* (Figure 3.37) mostly due to G-C base pairing. Based on this discovery and the following observations i) swarming motility of the Δ*rsmA* mutant is restored in the absence of the $P_{nmsR}$ promoter at 37°C and ii) swarming motilities of the WT and Δ*rsmN* strains is derepressed when *rsmN* expression is induced in the absence of $P_{nmsR}$ at 37°C, a synthetic *rsmN* construct (*NasIrsmN*) was prepared. Original codons of *rsmN* were modified as described in section 2.3.4 with the goal of minimizing secondary structure formation. With this approach of codon optimisation, separating

the protein coding function of *rsmN* from the sRNA function of *nmsR* was aimed to be achieved.



**Figure 3.37. Depiction of the hairpin loop formation between the *rsmN* TSS and translation start site**
Base pairing G-C nucleotides are highlighted in yellow and orange. A-T nucleotides are depicted in green. Formation of this hairpin loop might be an outcome of codon variation within the *rsmN* sequence.

Original codons of RsmN were modified as described in section 2.3.4 and synthetic *NasIrsmN* and native *rsmN* inserts were cloned in the backbone vector pME6000 to obtain pHS4 and pHS5 vectors respectively. Afterwards, colony morphologies, swarming motilities, PYO levels and supernatant protein profiles of the pHS4 and pHS5 transformants of the WT, Δ*rsmA* and Δ*rsmN* strains were compared. The multicopy expression of *rsmN* (via pHS5) or *NasIrsmN* (via pHS4) resulted in similar phenotypes. Bacterial cultures of the Δ*rsmA*/pME6000 strain had a darker green color indicating more PYO production compared with the WT/pME6000 and Δ*rsmN*/pME6000 cultures whereas the expression of *NasIrsmN* or *rsmN* in these strains did not alter PYO levels. Supernatant protein profiles of the WT/pME6000, Δ*rsmA*/pME6000 and Δ*rsmN*/pME6000 strains compared with the corresponding pHS4 and pHS5 transformants were identical both at 34°C and 37°C. Colonies of all tested strains had a smooth surface, the only difference being the darker color of the Δ*rsmA*/pME6000 and Δ*rsmN*/pME6000 strains in comparison with the rest (data not

shown). The WT, Δ*rsmA* and Δ*rsmN* strains transformed with pHS4 or pHS5 vectors all swarmed at 34°C and 37°C. However, swarming motilities of the WT/pME6000 and Δ*rsmN*/pME6000 strains that carry the background vector without any insert were slightly reduced upon the expression of *NasIrsmN* at 37°C. Swarming motility of the Δ*rsmA*/pHS5 strain was slightly less than swarming motility of the Δ*rsmA*/pHS4 both at 34°C and 37°C (data not shown). These results indicate that it is unlikely that the predicted *nmsR* transcript acts as a sRNA and autoregulates *rsmN* translation.

It was noted that swarming was affected negatively after the multicopy expression of *rsmN* in strains with an intact copy of RsmA (the WT and Δ*rsmN* strains) at 37°C. To check if this was due to a cross-regulation between the RsmA and RsmN proteins, swarming motility was investigated in a mutant (*rsmA*$_{ind}$/pMR6) where *rsmA* expression was induced by the $P_{tac}$ promoter upon IPTG addition and *rsmN* expression was induced by the $P_{BAD}$ promoter upon arabinose addition to the medium. The pMR6 vector was constructed from pMR1 by cloning *rsmN* in the pHERD30t vector using the PMR6F and PMR6R primers in a PCR reaction. Different concentrations of IPTG and arabinose (62.5 µM, 125 µM, 250 µM, 500 µM and 1000 µM; 0.025 %, 0.05 %, 0.1 %, and 0.2 % respectively) were used to modulate the expression levels of *rsmA* and *rsmN*. Both *rsmA* and *rsmN* expression in the *rsmA*$_{ind}$/pMR6 strain increased swarming motility independently of each other even with the lowest concentrations of IPTG and arabinose. However, induction of both *rsmA* and *rsmN* expression did not suppress swarming (data not shown). After examination of the 5'-UTR of *rsmF* (*rsmN*), Marden *et al*. [206] reported a putative RsmA binding site (GCAAGGACGC) which overlaps the SD sequence of *rsmF*. Based on this finding, RBS of *rsmN* was replaced with the *lac* RBS to construct pHS2RBSLac multicopy expression plasmid for the investigation of cross-regulation between the RsmA and RsmN proteins. When swarming assay was repeated with the WT, Δ*rsmA* and Δ*rsmN* strains transformed with pHS2 vs. pHS2RBSLac vectors at 37°C, it was seen that replacement of the native *rsmN* RBS with the *lac* RBS results in the restoration of swarming (data not shown).

After observing swarming of the WT/pMR1 and Δ*rsmN*/pMR1 strains at 34°C but not at 37°C (Figure 3.36), a possible conformational change in the protein structure at 34°C was postulated to split the hairpin forming nucleotides (Figure 3.37) in the pMR1 construct. Therefore, derivatives of the pMR1 vector, pMR8 and pMR9 where two

guanine nucleotides were replaced with cytosines to avoid the hairpin loop formation in the former and the nucleotide sequence folding into a hairpin loop was completely removed in the latter, were cloned by PCR using the PMR8F and PMR9F primers together with 2PRsmNR (M. Romero, personal communication, see Table 2.3). Figure 3.38 displays a comparison of the swarming phenotypes of the WT, Δ*rsmA* and Δ*rsmN* strains transformed with the pME6000 (backbone vector), pMR1, pMR8 and pMR9 vectors at 37°C. Even though the hairpin loop formation was hindered (Figure 3.38, WT/pMR8 and WT/pMR9 strains), non-swarming phenotype of the WT/pMR1 transformant was not reverted back to the swarming phenotype of the WT/pME6000 strain. However, blocking the hairpin loop formation derepressed the swarming motility of the Δ*rsmN*/pMR1 strain and abolished full complementation of Δ*rsmA*/pME6000 swarming by multicopy expression of *rsmN*.

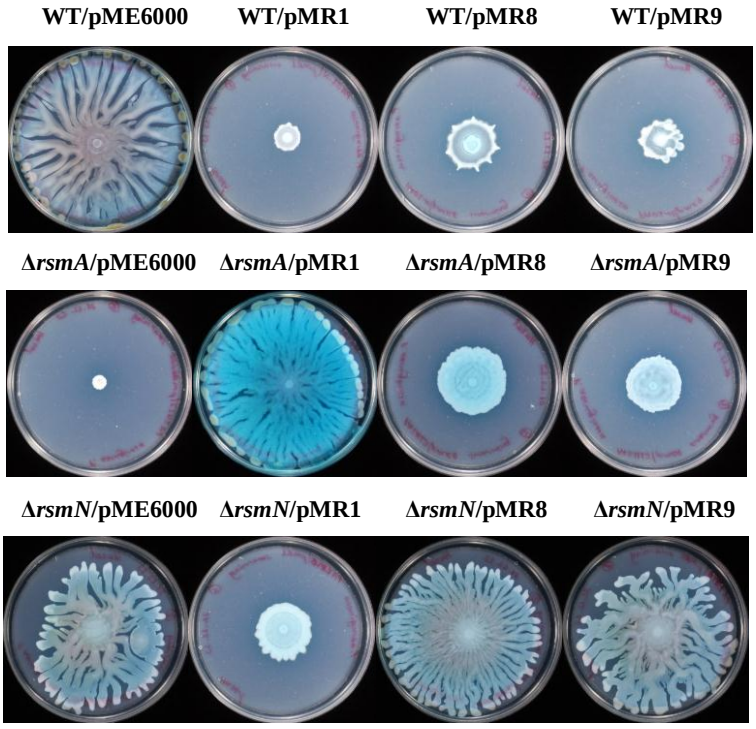


**Figure 3.38. The influence of the hairpin loop located near the *rsmN* TSS on the suppression of WT and Δ*rsmN* swarming motilities and complementation of Δ*rsmA* swarming on nutrient broth agar (0.5% w/v) at 37°C**

Preventing the formation of the hairpin loop near the *rsmN* TSS derepresses swarming motility of the Δ*rsmN*/pMR1 cells and abolishes complementation of Δ*rsmA*/pME6000 swarming. Swarming motility of the WT strain is suppressed in the WT/pMR1, WT/pMR8 and WT/pMR9 transformants.

Additionally, to check if cell lysis caused the reduction in swarming motilities of the WT/pHS2, WT/pMR1, Δ*rsmN*/pHS2 and Δ*rsmN*/pMR1 strains at 37°C, supernatant proteins of the WT/pME6000, WT/pHS2, Δ*rsmA*/pME6000, Δ*rsmA*/pHS2, Δ*rsmA*/pMR1, Δ*rsmA*/pMR11, Δ*rsmA*/pMR12, Δ*rsmN*/pME6000 and Δ*rsmN*/pHS2 strains grown at 37°C and 34°C were separated and immunoblotted with α-IscS (cysteine desulfurase, 47 kDa) antisera as demonstrated in section 3.2.8. Figure 3.39 illustrates that IscS was present in culture supernatants of the WT/pHS2, Δ*rsmA*/pME6000, Δ*rsmA*/pHS2, Δ*rsmA*/pMR1, Δ*rsmA*/pMR12 and Δ*rsmN*/pHS2 strains whereas it was not released to the culture supernatants of the WT/pME6000, Δ*rsmA*/pMR11 and Δ*rsmN*/pME6000 strains at 37°C. It was found in higher abundance in supernatants of the WT/pHS2 and Δ*rsmA*/pHS2 strains compared with the Δ*rsmA*/pME6000, Δ*rsmA*/pMR1 and Δ*rsmA*/pMR12 strains and was not detected in the supernatants of cultures grown at 34°C (data not shown).

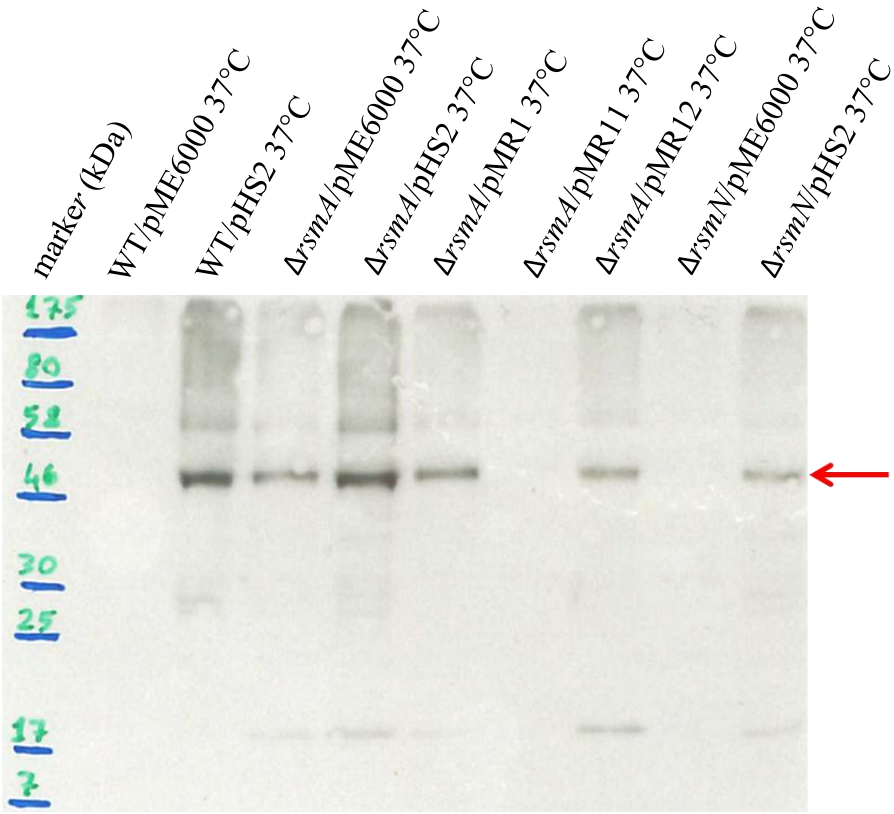


**Figure 3.39. Investigation of cell lysis in the WT/pME6000, Δ*rsmA*/pME6000 and Δ*rsmN*/pME6000 strains upon *rsmN* expression by detection of the cytosolic protein IscS (47 kDa) among secreted proteins**

IscS (pointed by the red arrow) was detected in high abundance in the supernatants of the WT/pHS2 and Δ*rsmA*/pHS2 strains. It was also detected among the extracellular proteins of the Δ*rsmA*/pME6000, Δ*rsmA*/pMR1, Δ*rsmA*/pMR12 and Δ*rsmN*/pHS2 strains cultured in LB for 18 h at 37°C.

## 3.3 Discussion

The biological function, the importance of the $Arg_{62}$ residue and the predicted autoregulatory mechanism of RsmN were investigated in phenotypic assays in this chapter. Based on known Δ*rsmA* phenotypes, the contribution of RsmN to the regulation of motility, biofilm formation and the production of some virulence determinants of *P. aeruginosa* in the presence and absence of RsmA was studied using single deletion mutants of *rsmA* and *rsmN*, inducible double deletion mutants ($rsmA_{ind}$ Δ*rsmN* and $rsmN_{ind}$ Δ*rsmA*) and multicopy *rsmN* expression plasmids. Furthermore, roles of the $Arg_{62}$, a conserved residue among the Rsm proteins of *P. aeruginosa* [53], and the predicted antisense transcript *nmsR* on the biological function of RsmN were explored.

Initially, the effect of *rsmN* deletion on the growth of *P. aeruginosa* was checked. Even though the single deletion of *rsmN* did not alter growth, the double deletion of *rsmA* and *rsmN*, mimicked by growing the $rsmN_{ind}$ Δ*rsmA* strain without IPTG, resulted in an extended lag phase (Figure 3.3). The Δ*rsmA* mutant also had an extended lag phase in comparison with the WT and Δ*rsmN* strains. The multicopy expression of *rsmN* (via pHS2) in the $rsmN_{ind}$ Δ*rsmA*/pME6000 mutant (Figure 3.32) resulted in faster growth (generation times of 39 min. vs. 67 min. respectively).

Both the Δ*rsmA* and inducible $rsmA_{ind}$ Δ*rsmN* and $rsmN_{ind}$ Δ*rsmA* strains formed aggregates (Figure 3.4, highlighted by red arrows) during growth. The clumping phenotype of the Δ*rsmA* mutant has been reported by Heurlier *et al*. [121] and Burrowes *et al*. [183]. Schleheck *et al*. [115] demonstrated aggregate formation by the PAO1 cells in different growth phases and detected aggregate dispersal upon starvation. Extended lag phases of the Δ*rsmA* and $rsmN_{ind}$ Δ*rsmA* strains might be due to extensive aggregate formation, and the dispersal of bacterial clumps after 24 h upon starvation might give rise to $OD_{600}$ values similar to the $OD_{600}$ values of the WT and Δ*rsmN* strains. Although inducing *rsmN* expression in the $rsmN_{ind}$ Δ*rsmA* inducible double deletion mutant did not prevent the formation of cellular aggregates (Figure 3.4), it has been demonstrated that plasmid-induced expression of *rsmN* prevents aggregate formation by the Δ*rsmA*/pME6000 mutant in Figure 3.5. It is likely that at 37°C, *P. aeruginosa* transcribes *rsmA* at a higher level than *rsmN*, hence, neither the single deletion of *rsmN* nor induction of *rsmN* expression by the $P_{tac}$ promoter cloned

in the *rsmN*$_{ind}$ Δ*rsmA* construct leads to any phenotypic changes. However, the influence of *rsmN* expression on tested traits of *P. aeruginosa* becomes apparent when *rsmN* is expressed at multicopy numbers, 20-30 copies per cell, using the pME6000 vector [242]. The clumping phenotype of either the *rsmA*$_{ind}$ Δ*rsmN* or the *rsmN*$_{ind}$ Δ*rsmA* double mutant transformed with a multicopy *rsmN* expression plasmid was not explored; however, higher $OD_{600}$ values obtained for the *rsmN*$_{ind}$ Δ*rsmA*/pHS2 transformant in comparison with the *rsmN*$_{ind}$ Δ*rsmA*/pME6000 mutant until 12 h post-inoculation might be due to the lack of aggregate formation in the former. Burrowes *et al.* [183] demonstrated that expression of *cupA2* which has been linked to cellular clumping by Vallet *et al.* [252] and *cupC3* genes encoding fimbrial chaperone and usher proteins respectively was downregulated in the PAO1 Δ*rsmA* mutant. Therefore, it has been suggested that reduced expression of the *cup* genes might cause the Δ*rsmA* mutant to clump [183]. The factors that cause extensive clumping of the *rsmA*$_{ind}$ Δ*rsmN* and *rsmN*$_{ind}$ Δ*rsmA* strains need to be investigated in more detail.

In the motility assays, twitching assay results could not be reproduced and a swarming-swimming intermediate motility (Figure 3.11) was detected on 0.3% nutrient broth agar instead of swimming. Therefore, swimming and twitching assays need to be repeated. On the other hand, the deletion of *rsmN* resulted in a slight reduction in swarming motility (Figure 3.6 and Supplementary Figure 5) at 37°C. Lowering the temperature from 37°C to environmental temperatures resulted in a significant decrease in the swarming motility of the Δ*rsmN* mutant whereas swarming of the WT strain decreased only slightly (Figure 3.8). Furthermore, plasmid-induced *rsmN* expression suppressed swarming of the WT and Δ*rsmN* strains and did not complement swarming of the Δ*rsmA* mutant at 37°C (Figure 3.9). On the other hand, *rsmN* expression decreased WT swarming only slightly, increased Δ*rsmN* swarming and complemented abolished swarming of the Δ*rsmA* mutant at 34°C. Hockett *et al.* [253] reported that swarming and swimming motilities of *P. syringae* are suppressed at 30°C compared with 20°C. In the follow-up experiments, the authors found that the expression of *fliC* which encodes the major flagellin protein and *syfA* which encodes the non-ribosomal polypeptide synthase needed for the production of the surfactant syringafactin decreased with increasing temperature. Suppression of motility might be a temperature-dependent adaptation in *Pseudomonas* species and swarming results illustrated in this chapter indicate that when expressed at multicopy levels at 37°C,

*rsmN* plays a role in temperature-dependent suppression of swarming motility. It is possible that the positive control of swarming motility by RsmA or RsmN is blocked by a cross-interaction between one of the Rsm proteins and the RNA of the other one at 37°C when *rsmN* is overexpressed in strains that have a functional RsmA i.e. WT and Δ*rsmN*. However, as mentioned in p. 119, inducing *rsmA* and *rsmN* in the $rsmA_{ind}$/pMR6 strain at the same time did not suppress swarming whereas alteration of the RsmA binding site in the 5'-UTR of *rsmN* relieved swarming suppression in the pHS2 transformants of the WT and Δ*rsmN* strains.

Employing pHS2 and pMR12 (Figure 3.31), it has been shown that *rsmN* expression in the absence of the $P_{nmsR}$ promoter (pMR12 construct) does not suppress swarming motilities of the WT and Δ*rsmN* strains and complements Δ*rsmA* swarming at 37°C (Figure 3.36) suggesting negative modulation of swarming motility in the presence of the *nmsR* antisense transcript. In contrast, having the $P_{nmsR}$ sequence included in cloned fragments and thus allowing *nmsR* transcription did not alter the $rsmN_{ind}$ Δ*rsmA* mutant phenotype in the assays tested (section 3.2.11). For this reason, a synthetic construct, pHS4, (a multicopy plasmid to express *NasIrsmN*) was produced by codon optimisation of *rsmN* to further investigate the regulation of RsmN function by the *nmsR* transcript. PYO levels and supernatant protein profiles of the pHS4 and pHS5 transformants of the WT, Δ*rsmA*, and Δ*rsmN* strains were similar. In addition, colony morphologies and swarming motilities did not significantly differ from each other (data not shown), leading to the conclusion that following the codon optimisation technique described in 2.3.4, the predicted antisense transcript *nmsR* does not influence RsmN function under the experimental conditions tested here.

Detection of the IscS protein in the 37°C culture supernatants of the WT/pHS2, Δ*rsmA*/pHS2 and Δ*rsmN*/pHS2 strains (Figure 3.39) indicate cell lysis which might cause the suppression of motility. Furthermore, temperature-dependent suppression of the swarming motility might be linked to the PhrX sRNA rather than an antisense transcript of *rsmN*. The *rsmN* ORF, $P_{nmsR}$, and terminator sequences overlap the *phrX* gene (Figure 3.1), therefore, any modification done in the downstream region of or within the *rsmN* sequence might alter the *phrX* sequence. PhrX was detected by Sonnleitner *et al*. [237] however, no work demonstrating the regulatory role of PhrX has been published so far.

PYO overproduction at 37°C by the Δ*rsmA* mutant compared with the wild-type PAO1 strain has been shown in previous studies [53, 204]. Both of these studies report 5-fold more PYO production by the Δ*rsmA* mutant in comparison with the WT strain. Here, probably due to the use of a different growth medium (LB), no significant increase in PYO production by the Δ*rsmA* mutant was observed at 37°C. Burrowes *et al*. [183] demonstrated that cell cultivation in different media changes PYO production; the Δ*rsmA* mutant produced less PYO compared with the WT strain when grown in LB, whereas when grown in glycerol-alanine rich medium, PYO production by the Δ*rsmA* mutant was 5-fold higher than the WT strain in line with the findings by Pessi *et al.* [204]. In this study, PYO production was increased ~ 2-fold in the Δ*rsmA*, $rsmA_{ind}$ Δ*rsmN* and $rsmN_{ind}$ Δ*rsmA* strains cultured in LB compared with the WT strain at 34°C.

Differences in PYO levels and total proteolytic and elastinolytic activities of the WT and Δ*rsmN* strains were negligible (Figure 3.13, Figures 3.17 and 3.18 panel a), however, total proteolytic and elastinolytic activities of the inducible $rsmA_{ind}$ Δ*rsmN* and $rsmN_{ind}$ Δ*rsmA* mutants were greatly reduced when neither *rsmA* nor *rsmN* expression was induced (represented by the absorbance values close to zero in Figures 3.17 and 3.18, panel a). A possible explanation for this might be the collaborative regulation of exoprotease and elastase levels by RsmA and RsmN. The deletion of *rsmA* resulted in a decrease in total proteolytic and elastinolytic activities, indicating positive regulation by RsmA. Although the single deletion of *rsmN* did not alter the activities, the difference between proteolytic and elastinolytic activities of the Δ*rsmA* and $rsmN_{ind}$ Δ*rsmA* (-IPTG) strains was significant, indicating positive regulation of protease and elastase production also by RsmN, but in the absence of RsmA. Moreover, total proteolytic and elastinolytic activities were partially restored in the $rsmN_{ind}$ Δ*rsmA* mutant by inducing *rsmN* expression in a temperature-dependent manner (at 34°C, Figure 3.17 panel a and at 34°C and 37°C, Figure 3.18 panel a). Additionally, plasmid-induced expression of *rsmN* in the Δ*rsmA* mutant partially restored the proteolytic and elastinolytic activities at 37°C (Figures 3.17 and 3.18, panel b). These results demonstrate positive regulation of exoprotease and elastase production both by RsmA and RsmN. Overproduction of exoproteases at lower temperatures has been observed for *P. fluorescens* [254, 255] and a comparison of the

left (34°C) and right sides (37°C) of Figure 3.17 panels a) and b) shows that exoprotease production by *P. aeruginosa* also increases as the temperature decreases.

There are a few studies where the effect of growth temperature on the virulence factor production of *P. aeruginosa* was investigated. Kropinski *et al*. [256] observed changes in phospholipid, lipopolysaccharide, and outer membrane protein compositions when *P. aeruginosa* PAO1 was grown at 15°C vs. 45°C. Wurtzel and co-workers [257] presented RNASeq data demonstrating that *P. aeruginosa* PA14 genes related to protein secretion and phenazine and alginate biosyntheses were upregulated at 37°C whereas the ribosomal protein genes, histidine catabolic genes, and catechol-related genes were upregulated at 28°C. In PA14 strain, the RsmN orthologue is PA14_68470 [238] and this transcriptomic analysis [257] also demonstrated a 2.2 fold increase in *rsmN* expression at 28°C in comparison with 37°C. Hence, this finding links the detection of RsmN activity at temperatures below 37°C to increased *rsmN* transcription at lower temperatures.

Irie *et al*. [207] demonstrated that RsmA post-transcriptionally regulates the production of the biofilm polysaccharide Psl thus the Δ*rsmA* mutant forms robust biofilms. The Δ*rsmN* mutant had a biofilm phenotype intermediate to the WT (flat and undifferentiated) and Δ*rsmA* mutant (microcolony) phenotypes (Figure 3.19). Formation of large microcolonies by the Δ*rsmA*/pME6000 mutant was prevented by the multicopy expression of *rsmN* and the Δ*rsmA*/pHS2 strain formed biofilms similar to the WT/pME6000 biofilms (Figure 3.22). A comparison of alginate, Pel and Psl production [258] by the WT and Δ*rsmN* strains would be essential to narrow down the factors behind the WT-Δ*rsmA* intermediate biofilm phenotype of the Δ*rsmN* mutant. Dietrich *et al*. [216] elaborated on the roles of phenazines and redox balance in biofilm thickness and colony morphogenesis and demonstrated that colony wrinkling occurs at lower oxygen concentrations and phenazine mutants exhibit the same wrinkly phenotype on Congo red-tryptone agar. Based on these experimental findings, authors concluded that morphogenesis is greatly influenced by the availability of electron acceptors. To check whether the observed Δ*rsmN* biofilm phenotype was due to the downregulation of electron acceptors or formation of an anoxic environment, colony morphologies of the WT, Δ*rsmA*, Δ*rsmN* and inducible $rsmA_{ind}$ Δ*rsmN* and $rsmN_{ind}$ Δ*rsmA* mutants were checked on Congo red-tryptone agar. Aggregate formation in

liquid cultures and Congo red-binding on agar are indicators of increased polysaccharide synthesis in a variety of bacterial species [258]. Although the Δ*rsmA* mutant formed aggregates in the overnight cultures and grew large microcolonies under a constant flow of growth medium for 14 h, colony morphology of the Δ*rsmA* mutant was not different from the WT and Δ*rsmN* strains. However, the inducible *rsmA*$_{ind}$ Δ*rsmN* and *rsmN*$_{ind}$ Δ*rsmA* mutants grew as rough colonies and appeared red indicating increased extracellular polysaccharide production compared with the WT, Δ*rsmA* and Δ*rsmN* strains.

In a previous study, G. Rampioni demonstrated a link between HHQ accumulation and lytic plaque formation on colony biofilms (section 3.2.8). Figure 3.27 illustrates that the exogenous addition of 40 µM HHQ resulted in tendril formation and a lytic centre in a Δ*rsmA* colony. Hence, it was speculated that the lytic phenotype of the *rsmN*$_{ind}$ Δ*rsmA* mutant might be a consequence of cumulative HHQ accumulation due to the deletion of both *rsmA* and *rsmN* as Δ*rsmA*/Δ*rsmN* single deletion mutants grew as smooth colonies. Therefore, colony morphologies of the *rsmN*$_{ind}$ Δ*rsmA* and Δ*pqsH* Δ*pqsL* strains, the latter producing 3.5-fold higher levels of HHQ in comparison with the WT strain (unpublished data, G. Rampioni) were also compared 2 days post-inoculation and morphologies were similar (Figure 3.28, top panel). Nevertheless, a comparison of HHQ levels of the WT, Δ*rsmA*, Δ*rsmN*, *rsmA*$_{ind}$ Δ*rsmN* and *rsmN*$_{ind}$ Δ*rsmA* strains is required to establish a link between *rsmN*$_{ind}$ Δ*rsmA* autolysis and HHQ accumulation. Detection of increased HHQ production in *P. aeruginosa* cells which lack both Rsm proteins would shed light on the mechanism of autolysis and indicate negative regulation of a component of the AQ-dependent QS system by RsmA and RsmN.

The colony morphologies of the *rsmA*$_{ind}$ Δ*rsmN* and *rsmN*$_{ind}$ Δ*rsmA* mutants grown without IPTG on Congo red-tryptone agar also resembled the colony morphology of a *wspF10* mutant grown on swimming agar for 48 h at 23°C (Figure 3.40). The WspF protein plays a role in the chemotaxis of *P. aeruginosa*. A mutation in *wspF* causes hypermethylation of the WspA protein, activating the Wsp pathway. D'Argenio *et al*. [197] found that a mutation in *wspR* which codes the response regulator protein converted the wrinkly colony morphology of the *wspF* mutant to the smooth colony morphology of the WT strain and restored swarming and swimming motilities. In the

same study, authors also noted that autoaggregation required WspR. According to this data, the Wsp pathway might offer a connection between the clumping and rough colony phenotypes of the *rsmN*$_{ind}$ Δ*rsmA* and *rsmA*$_{ind}$ Δ*rsmN* mutants when these strains are cultured without IPTG. In fact, reduced swarming motility, increased cell aggregation/biofilm formation and wrinkly colony morphology was observed in the *P. aeruginosa* PAO1 strain at high c-di-GMP levels as a consequence of *wspF* deletion in a previous study [210].

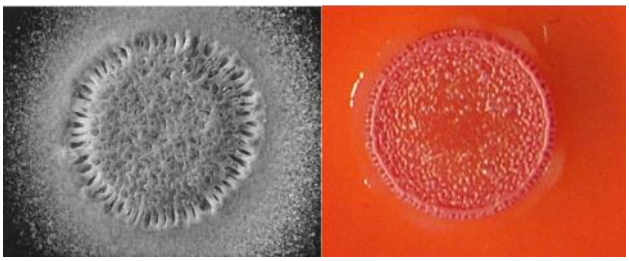

**Figure 3.40. Colony morphologies of a *P. aeruginosa wspF10* mutant grown on swimming agar (left) and an *rsmA*$_{ind}$ Δ*rsmN* mutant grown on Congo red-tryptone agar (right) after 2 days of incubation at room temperature**

Rough colony morphologies of the *rsmA*$_{ind}$ Δ*rsmN* and *rsmN*$_{ind}$ Δ*rsmA* mutants grown without IPTG resemble the wrinkly colony morphology of the *wspF10* mutant. The left figure is taken from D'Argenio *et al*. [197].

Upon detection of plaque formation in the middle of the *rsmN*$_{ind}$ Δ*rsmA* and *rsmA*$_{ind}$ Δ*rsmN* colonies (Figure 3.23, left panel), the impact of *rsmA* and *rsmN* deletions on cell lysis was investigated in a number of assays. Autolysis is mediated by multiple mechanisms such as the QS network, induction of the Pf4 phage of PAO1, motility elements and PYO production [116, 259, 260]. A phage plaque assay was conducted to see if the *rsmN*$_{ind}$ Δ*rsmA* mutant had elevated levels of filamentous phage Pf4 which has been linked to HHQ accumulation in the preliminary study conducted by G. Rampioni. Cell-free supernatants of the WT, Δ*rsmA*, Δ*rsmN* and *rsmN*$_{ind}$ Δ*rsmA* strains all led to the lysis of the PAO1B1Δ*Pf4* cells on soft top agar, resulting in plaque formation (Figure 3.24). The largest clearance zone was obtained when the *rsmN*$_{ind}$ Δ*rsmA* culture supernatant was used. Furthermore, detection of a cytosolic protein (IscS) in the -IPTG culture supernatants of the *rsmN*$_{ind}$ Δ*rsmA* and *rsmA*$_{ind}$ Δ*rsmN* mutants indicated increased autolysis in the absence of both RsmA and RsmN (Figure 3.26). Autolysis of the *rsmN*$_{ind}$ Δ*rsmA* mutant was quantified by c.f.u. count and it has been found that the *rsmN*$_{ind}$ Δ*rsmA* mutant forms 5-fold less c.f.u. than the WT strain (Table 3.2).

The negative regulation of T6SS by *P. aeruginosa* RsmA both at transcriptional and post-transcriptional levels has been demonstrated in previous studies [206, 236]. The identification of the Hcp1 protein of T6SS (Figure 3.29) in culture supernatants of the *rsmA*$_{ind}$ Δ*rsmN* and *rsmN*$_{ind}$ Δ*rsmA* strains and the reduction in Hcp1 abundance upon *rsmA* (both at 37°C and 34°C) and *rsmN* expression (at 34°C) in the double mutant background (Figure 3.25) might be the indication that T6SS is regulated by both Rsm proteins in *P. aeruginosa*. In accordance with these findings, Marden *et al.* [206] demonstrated high levels of Hcp1 in a Δ*rsmA* Δ*rsmF* double mutant and plasmid-based expression of *rsmA* or *rsmF* in the Δ*rsmA* Δ*rsmF* double mutant reduced Hcp1 accumulation. Furthermore, using transcriptional and translational reporters, authors showed that both RsmA and RsmF (RsmN) control *tssa1* expression.

Mulcahy *et al.* [261] showed that the deletion of *rsmA* affects colonization and dissemination of *P. aeruginosa* in an acute pneumonia model negatively while favouring persistence in a mouse model of chronic infection. More recently, Turner *et al.* [262] performed RNASeq to look at the expression of *P. aeruginosa* genes in both chronic and acute mouse infection models and run TnSeq to identify genes essential for bacterial fitness. It has been found that *rsmA* is not required for fitness in either infection model. Based on the relevant information published [206, 261] and results of the phenotypic assays conducted in this study, bacterial loads of the *rsmN*$_{ind}$ Δ*rsmA* and WT strains were monitored in a mouse chronic infection model. However, no difference was observed in bacterial loads even after 4 days post-infection (Table 3.3). Therefore, RsmA and RsmN control on the chronic mode of infection requires further investigation *in vivo*.

The multicopy expression of *rsmN* complemented several Δ*rsmA* phenotypes such as clumping, microcolony formation, proteolytic and elastinolytic activities at 37°C and swarming motility at temperatures below 37°C. Mutation of the RsmNR62 residue abolished complementation of these Δ*rsmA* phenotypes by RsmN, therefore, it can be concluded that Arg$_{62}$ is important for the biological function of RsmN. In contrast, although *rsmN* expression via pHS2 did not change, the expression of *rsmN*R62A decreased PYO production by the Δ*rsmA*/pME6000 mutant significantly (Figure 3.15). Similarly, the expression of *rsmN*R62A decreased proteolytic and elastinolytic

activities in the Δ*rsmA*/pME6000 mutant significantly at 34°C (Figures 3.17 and 3.18, panel b). These observations suggest that mutant RsmNR62A may form homodimers with the native RsmN protein and decrease the efficiency of target-binding.

Observation of phenotypes unique to the $rsmA_{ind}$ Δ*rsmN* and $rsmN_{ind}$ Δ*rsmA* double mutants raise the question about the regulation of RsmN by RsmA since the effect of *rsmN* deletion is only apparent in the absence of RsmA. Marden *et al*. [206] demonstrated that RsmA inhibits the translation of *rsmF* (*rsmN*) which explains why the Δ*rsmN* phenotypes and wild-type phenotypes are similar. A comparison of the *rsmA* and *rsmN* transcript levels would clarify why RsmN control on tested phenotypes is detected after the expression of *rsmN* via a multicopy plasmid or in the absence of RsmA. Total RNA was collected from PAO1-N cultures cultivated at 37°C and 34°C until the early stationary phase ($OD_{600}$ ~ 1.7-1.9), and *rsmA* and *rsmN*-specific primers were ordered to compare the transcript levels; however, qRT-PCR could not be carried out due to time limitations.

In conclusion, it is evident from the results demonstrated in this chapter that RsmA and RsmN have overlapping (positive regulation of protease and elastase activities, swarming motility, negative regulation of microcolony formation and Hcp1 secretion) as well as distinct functions (different control on the PYO production of *P. aeruginosa*, and restoration of glycogen accumulation in *E. coli*). The RsmN-mediated positive control on Δ*rsmA* swarming motility (Figure 3.8) at temperatures below 37°C and complementation of the $rsmN_{ind}$ Δ*rsmA* proteolytic activity by *rsmN* induction at 34°C but not at 37°C (Figure 3.17 panel a) suggest that RsmN operates better at temperatures below 37°C. Additionally, the cross-regulation between RsmA and RsmN masks Δ*rsmN* phenotypes and the regulatory roles of RsmN are only detected in the absence of RsmA or when *rsmN* is expressed at multicopy levels.

# 4 Genome-wide Identification of RsmN Targets

## 4.1 Introduction

In Chapter 3, the biological function of RsmN was explored in phenotypic assays that revealed upregulation or downregulation of some virulence determinants of *P. aeruginosa* by RsmA. Complementation of a few Δ*rsmA* phenotypes such as the robust microcolony formation (Figure 3.19) and reduced proteolytic and elastinolytic activities (Figures 3.17 & 3.18) was achieved by expression of *rsmN* from a multicopy plasmid. However, RsmN did not decrease PYO production by the Δ*rsmA* mutant (Figure 3.15) and glycogen accumulation by the *E. coli* TR1-5 mutant characterised by a *csrA* deletion (Figure 3.30). Positive regulation of swarming motility by RsmN was discovered at temperatures below 37°C (section 3.2.3.1, Figure 3.8). Furthermore, total proteolytic activity of the $rsmN_{\text{ind}}$ Δ*rsmA* mutant could be restored by *rsmN* induction at 34°C but not at 37°C (section 3.2.5, Figure 3.17 panel a). The multicopy expression of *rsmN* in the $rsmN_{\text{ind}}$ Δ*rsmA* strain complemented the swarming motility (Figure 3.33) and total proteolytic activity (Figure 3.34) at 37°C. Altogether, these results suggest that regulation by RsmN is more evident at lower temperatures and when *rsmN* is overexpressed, and RsmA and RsmN target common as well as distinct transcripts.

Direct targets of the CsrA/RsmA family of proteins have been identified in previous studies [183, 236, 263] using transcriptomic analyses. In *E. coli*, CsrA has been shown to regulate the expression of various genes involved in carbon metabolism, energy production, stringent response, transport and cell wall biogenesis [263]. Through comparison of transcriptomic profiles of the wild-type strain and the Δ*rsmA* mutant, mRNAs with an altered abundance were identified in microarray analyses [183, 236]. Burrowes *et al*. [183] reported increased expression of iron acquisition genes and genes coding the MexEF-OprN pump and decreased expression of motility and PQS synthesis genes in the Δ*rsmA* mutant. Furthermore, expression of T3SS genes and genes linked to alginate production was downregulated in the Δ*rsmA* mutant of the PAO1 strain. Brencic and Lory [236] demonstrated decreased expression of T3SS and motility genes and increased expression of T6SS genes in a Δ*rsmA* mutant of the PAK strain. Transcriptomic studies based on microarrays rely on discrete oligonucleotide

probes that are essentially directed against annotated ORFs, hence do not account for mRNAs of unannotated ORFs or ncRNAs. Therefore, in an alternative approach, Brencic and Lory [236] also carried out an RNA-RsmA co-purification experiment using a C-terminally $His_6$-tagged RsmA. Edwards *et al*. [263] also used the co-purification method to identify direct targets of CsrA in *E. coli*.

In a previous study, RNA-binding of RsmN was investigated at a molecular level by Elizabeth Morris [241]. Performing analytical gel filtration chromatography, 2D NMR spectroscopy (using $^{15}N$-labelled $His_6$-tagged RsmN and saturating amounts of RNA) and isothermal titration calorimetry (ITC), binding between a CrcZ 12-mer and $His_6$-tagged RsmN or $His_6$-tagged RsmA was tested. The $K_D$ values of ~ 725 nM and 990 nM were obtained respectively, revealing high-affinity binding of RsmN and RsmA to CrcZ. In addition, the same study revealed that RsmN binds to GGA-motif containing hairpins of the RsmY and RsmZ sRNAs with high affinity ($K_D$ ~ 276 nM and 526 nM). Furthermore, Marden *et al*. [206] demonstrated RsmF (RsmN) binding to the RsmY and RsmZ sRNAs using a $His_6$-tagged RsmF and radiolabeled RNAs in an electrophoretic mobility shift assay (EMSA). The RsmF-RsmY binding affinity was 245-fold lower than the RsmA-RsmY binding affinity ($K_{eq}$ of 49 nM vs. 0.2 nM), and the RsmF-RsmZ binding affinity was 58-fold lower than the RsmA-RsmZ binding affinity ($K_{eq}$ of 23 nM vs. 0.4 nM). Despite these binding results, after testing transcriptional and translational reporter activities using $P_{exsD\text{-}lacZ}$ and $P_{tssa1'\text{-}'lacZ}$ constructs in the Δ*rsmA* and Δ*rsmA* Δ*rsmY* Δ*rsmZ* mutants, it has been concluded that RsmY and RsmZ do not play a major role on the RsmF activity *in vivo*.

A systematic approach was essential to identify and characterise direct targets of RsmN as some phenotypes investigated in Chapter 3 such as swarming are complex and do not depend on a single gene. Also, conflicting results have been published regarding RsmY and RsmZ control on RsmN previously [206, 241]. In this study, RNASeq (see Figure 4.1), a next generation sequencing technique that has many advantages such as indiscriminate detection of mRNA quantities at the nucleotide level, enhanced sensitivity and dynamic range compared to techniques such as qRT-PCR, Northern blotting or microarrays [257, 264] was chosen to identify target transcripts of RsmN as accurately as possible and carried out as described in section 2.4.10. RNASeq was carried out and RsmN targets were reported in a previous study

[212]. However, due to an unforeseen problem with the construct (pRsmN) used to purify RsmN, the validity of this experiment was questioned and RNASeq had to be repeated with the previously used PAO1-L strain of *P. aeruginosa* transformed with a novel construct (pMR4) expressing $His_6$-tagged RsmN in this study. The pME6032-based pMR4 vector was obtained from the pLT27 [212] construct by PCR using the PMR4F and PMR4R primers (M. Romero, personal communication) to introduce a $His_6$-tag at the amino (N)-terminus of RsmN for co-purification of RsmN and bound RNAs using Ni-NTA matrices.

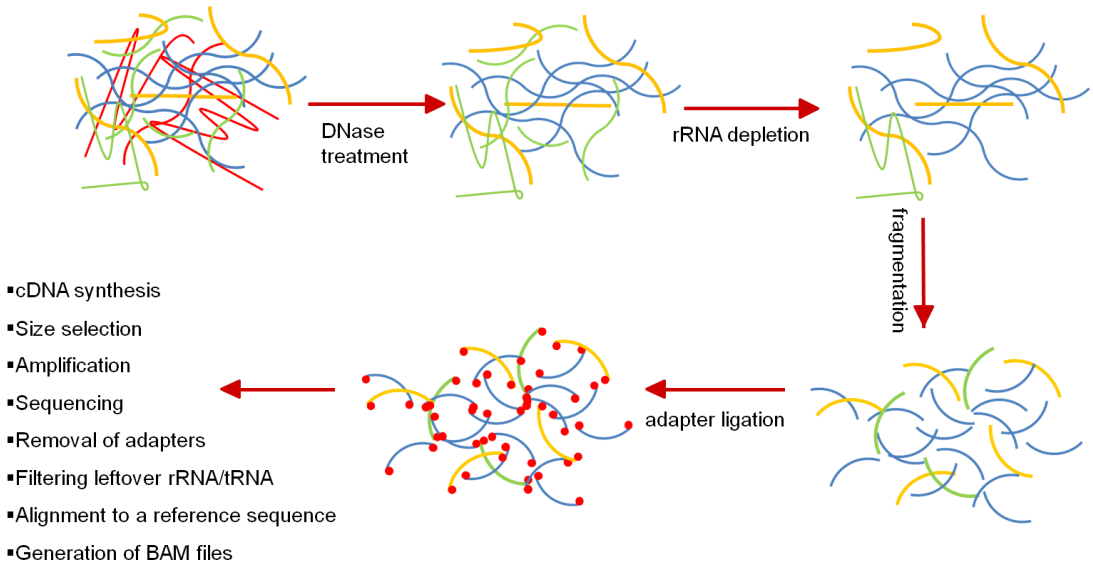


**Figure 4.1. RNASeq workflow**
Following RNA purification, any DNA (red lines, top left) contaminating the RNA samples is removed by DNase treatment. RNA samples further go through the rRNA (green lines) depletion, fragmentation and adapter (depicted as red circles) ligation steps prior to cDNA library preparation. The remaining steps of RNASeq, as listed on the bottom left are cDNA synthesis, size selection and amplification of cDNAs, sequencing, removal of adapters, filtering of the remaining rRNA (green lines) and tRNA (yellow lines), alignment of reads to a reference genome and generation of BAM files. The mRNA strands are depicted as blue lines.

RsmN-bound and total RNA samples from cultures grown at 37°C were obtained by Manuel Romero previously. RNASeq was repeated with RsmN-bound RNAs and total RNA purified from cultures grown at 34°C in this study. Moreover, to identify unique RsmN targets, RsmA RNASeq results obtained in a previous study [212] were reanalysed and compared. RsmN-bound RNA profiles at 34°C and 37°C were also compared.

## 4.2 Results

After co-purification, elution fractions of the 37°C culture had the following RsmN and RNA concentrations (personal communication with M. Romero): E1 → RsmN 0.69 mg/mL, RNA 20.91 ng/µL; E2 → RsmN 0.24 mg/mL, RNA 7.32 ng/µL; E3 → RsmN 0.04 mg/mL, RNA 2.9 ng/µL. Due to the low amount of protein and RNA in elution fraction E3, it was discarded, E1 and E2 fractions were concentrated and split into two aliquots (E1A/B and E2A/B). Concentrations of RsmN and RsmN-bound RNA in elution fractions of the 34°C culture were as follows: Sample I → E1 RsmN 0.97 mg/mL, RNA 48.9 ng/µL; E2 RsmN 0.50 mg/mL, RNA 27.0 ng/µL; E3 RsmN N/A, RNA 5 ng/µL; Sample II → E1 RsmN 0.96 mg/mL, RNA 68.9 ng/µL; E2 RsmN 0.30 mg/mL, RNA 20.5 ng/µL; E3 RsmN N/A, RNA 3.3 ng/µL. Final concentrations of the RsmN-bound RNA sent for cDNA library preparation were 34.43 ng/µL (E1A), 36.91 ng/µL (E1B), and 14.26 ng/µL (E2A) for 37°C samples and 132.0 ng/µL (Sample I) and 132.2 ng/µL (Sample II) for 34°C samples. Concentrations of the total RNA purified from the 37°C and 34°C cultures were 291.45 ng/µL, 361.50 ng/µL and 384.38 ng/µL for triplicates at 37°C and 122.7 ng/µL and 125.5 ng/µL for duplicates at 34°C.

After sequencing, removal of adapters and remaining rRNA and tRNA strands, raw read data files of RNASeq were obtained in `.fastq` format. These files were uploaded on Galaxy web-based tool and reads were mapped to the reference genome `NC_002516.inverted.RGP42insertion.fasta`, a sequence derived by Hardeep Naghra from the PAO1-UW genome taking into account the known 2.2 Mb *rrnA*/*rrnB* chromosomal inversion [110] and the 12 kb inclusion of the region of genome plasticity RGP42 which contains phage genes encoding integrase and coat proteins and serine/threonine phosphotransferases [265] using the Bowtie 2 tool. The output was obtained in `.bam` format (binary version of SAM (`.sam`), a tab-delimited text file that contains sequence alignment data). BAM files were converted to strand-specific `.wig` files which list the number of times that each nucleotide on the chromosome has been read. In total, 28 `.wig` files were generated by deep sequencing of RNAs bound to RsmA at 37°C (n = 4), RsmN at 37°C (n = 6) and RsmN at 34°C (n = 4) and the corresponding total RNAs (n = 14) at the time of sampling, as listed in Table 4.1.

**Table 4.1. Strand-specific RNASeq starting files processed in this study**

E and WT are abbreviations for 'eluted' and 'whole transcripts' and refer to the 37°C RsmN-bound RNA and total RNA samples respectively. E1A and E1B are aliquots of the same elution fraction. E2A is another elution fraction from the same RsmN purification step. In the rest of the files, total RNA samples have been referred to as 'total', RsmA-bound RNA samples as mRNA_RsmA and RsmN-bound RNA samples as 'RSM'. Due to the loss of strand specificity for 34°C RsmN samples, instead of _neg. and _pos., files were grouped as 'a' and 'b'.

| | File | Description | Reference |
|---|---|---|---|
| **RsmA 37°C** | 1. `Laura_5_mRNA_RsmA_neg.wig` | Duplicate of 7, negative strand | L. Lovelock |
| | 2. `Laura_5_mRNA_RsmA_pos.wig` | Duplicate of 7, positive strand | |
| | 3. `Laura_6_total_RsmA_neg.wig` | Duplicate of 8, negative strand | |
| | 4. `Laura_6_total_RsmA_pos.wig` | Duplicate of 8, positive strand | |
| | 5. `Laura_7_mRNA_RsmA_neg.wig` | Duplicate of 5, negative strand | |
| | 6. `Laura_7_mRNA_RsmA_pos.wig` | Duplicate of 5, positive strand | |
| | 7. `Laura_8_total_RsmA_neg.wig` | Duplicate of 6, negative strand | |
| | 8. `Laura_8_total_RsmA_pos.wig` | Duplicate of 6, positive strand | |
| **RsmN 37°C** | 9. `E1A_S2_neg1.wig` | Duplicate of E1B and E2A | M. Romero |
| | 10. `E1A_S2_pos1.wig` | Duplicate of E1B and E2A | |
| | 11. `E1B_S5_neg1.wig` | Duplicate of E1A and E2A | |
| | 12. `E1B_S5_pos1.wig` | Duplicate of E1A and E2A | |
| | 13. `E2A_S3_neg1.wig` | Duplicate of E1x | |
| | 14. `E2A_S3_pos1.wig` | Duplicate of E1x | |
| | 15. `WT1_S6_neg1.wig` | Triplicate of WT2 and WT3 | |
| | 16. `WT1_S6_pos1.wig` | Triplicate of WT2 and WT3 | |
| | 17. `WT2_S1_neg1.wig` | Triplicate of WT1 and WT3 | |
| | 18. `WT2_S1_pos1.wig` | Triplicate of WT1 and WT3 | |
| | 19. `WT3_S4_neg1.wig` | Triplicate of WT1 and WT2 | |
| | 20. `WT3_S4_pos1.wig` | Triplicate of WT1 and WT2 | |
| **RsmN 34°C** | 21. `RSM_LIB1_S5.cut.a.wig` | Duplicate of LIB2 | This study |
| | 22. `RSM_LIB1_S5.cut.b.wig` | Duplicate of LIB2 | |
| | 23. `RSM_LIB2_S6.cut.a.wig` | Duplicate of LIB1 | |
| | 24. `RSM_LIB2_S6.cut.b.wig` | Duplicate of LIB1 | |
| | 25. `TOTAL_LIB1_S3.cut.a.wig` | Duplicate of LIB2 | |
| | 26. `TOTAL_LIB1_S3.cut.b.wig` | Duplicate of LIB2 | |
| | 27. `TOTAL_LIB2_S4.cut.a.wig` | Duplicate of LIB1 | |
| | 28. `TOTAL_LIB2_S4.cut.b.wig` | Duplicate of LIB1 | |

### 4.2.1 Raw data analysis

Initial `.wig` files (Table 4.1) were checked on Artemis annotation tool and were found to contain usable data. Consistency within the replicates was found to be very high, although values varied in their ranges (Figure 4.2), reflecting the robustness of RNASeq technology but revealing the need to normalise the data. The 34°C RsmN data was found to lack strand specificity (Figure 4.2, panel c). After investigation, it was found that this resulted from a supplementary adapter ligation and cDNA amplification step carried out in Malaysia to achieve the minimum quantities required for sequencing.

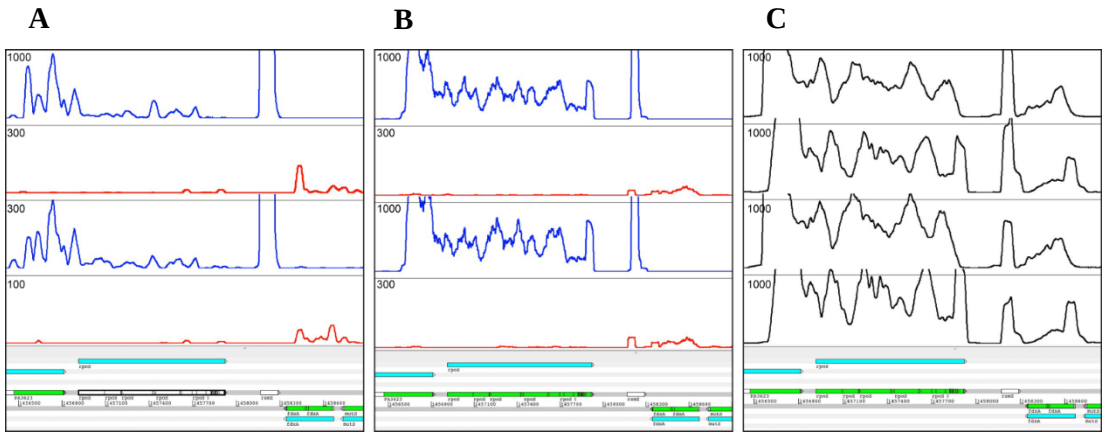


**Figure 4.2. Raw data and replicate robustness**
Data from the initial files was plotted with Artemis against the PAO1-L annotated genomic sequence to verify for consistency. Examples are given for the *rpoS-rsmZ-fdxA* region for (A) total RNA data from the RsmA-bound RNA experiment; (B) equivalent total RNA data from the RsmN-bound RNA at 37°C; and (C) total RNA data from the RsmN-bound RNA at 34°C. Vertical axis: `.wig` values, or number of reads per nucleotide. Note the difference in scales. Colour codes: blue, positive strand; red, negative strand; black, no strand information.

As replicates were considered homogenous, the data was merged by adding the values of the corresponding `.wig` files (Table 4.1), resulting in 10 new files. Files `Laura_5` and `Laura_7` (RsmA-bound RNA), as well as `Laura_6` and `Laura_8` (total RNA) were combined keeping the strand separation (`.neg`/`.pos`), to give four files: 1) `Laura_RsmA_neg.wig`, 2) `Laura_RsmA_pos.wig`,
3) `Laura_Total_neg.wig` and 4) `Laura_Total_pos.wig`. For the 37°C RsmN data, files `E1A`, `E1B` and `E2A` (RsmN-bound RNA) as well as `WT1`, `WT2` and `WT3` (total RNA) were merged keeping strand separation, to produce the following

four files: 1) `Hazel_RsmN37_neg.wig`, 2) `Hazel_RsmN37_pos.wig`, 3) `Hazel_Total37_neg.wig` and
4) `Hazel_Total37_pos.wig`. As the 34°C RsmN `.wig` files lacked strand specificity, all `RSM_LIB` (RsmN-bound RNA) files were merged to produce `Hazel_RsmN34.wig` file and all `TOTAL_LIB` (total RNA) files were combined to produce `Hazel_Total34.wig`.

Every file of this analysis is associated with a `.stats` file that contains some basic statistical information that may be of use, notably the average of all the read values and the position of the maximum value observed.

#### 4.2.1.1 Ribosomal RNA read removal

Examination of the averages and maximum values within each of the 10 `.wig` files followed by visualisation with Artemis tool revealed the presence of very strong read signals corresponding to ribosomal RNA operons, with boundaries (start and end points of reads) not always limited to the coordinates of the genes. As this would affect the subsequent analysis, each file was processed to zero the values of any nucleotide corresponding to *rrn* operons A, B, C and D according to coordinates empirically determined by data examination (Table 4.2).

**Table 4.2. Exclusion boundaries for reads corresponding to ribosomal RNAs**

| Operon | Gene No. | Nt start | Nt end | Basis |
|---|---|---|---|---|
| *rrnA* | PA0668.1-PA4280.1 | 721775 | 727262 | read boundaries |
| *rrnB* | PA4280.5-PA0668.5 | 4788574 | 4793732 | gene coordinates; a few internal reads |
| *rrnC* | PA4690.1-PA4690.5 | 5276152 | 5281666 | read boundaries |
| *rrnD* | PA5369.1-PA5369.5 | 6051627 | 6057275 | read boundaries |

The resulting files were saved with the suffix `.rskip` added to each file and reanalysed as before. The averages changed very variably with reductions between 0.2% and 78.7% depending on the experiment (Table 4.3), however, the highest values remained the same for all but one file: `Laura_RsmA_neg.wig`. Genes having produced each of these resulting maximal values were analysed and found to be of ncRNAs, including RsmZ (Table 4.3). tRNA genes were also verified for interference

with the analysis, but as the values for these were comparatively low, it was decided not to further exclude any reads other than those corresponding to rRNAs.

To facilitate the comparison of the results obtained from RsmN-bound RNAs at 37°C and at 34°C, the latter of which lacks strand information, two supplementary files were created by merging the `.neg` and `.pos` files of the 37°C experiment: `Hazel_RsmN37.rskip.wig` and `Hazel_Total37.rskip.wig`.

**Table 4.3. Changes in the RNASeq data after excluding rRNAs**

[1] Average of reads and [2] the maximum number of reads per nucleotide in raw `.wig` files or after excluding data corresponding to rRNA (-rRNA). [3] Percentage of reduction in the average values resulting from the exclusion of the rRNA data. [4] Maximal values found in `.wig` files divided by 1,000. [5] Position on the PAO1-L genomic sequence, in kb. *nc*, no change, UN, unknown.

| | **Average[1]** | | | **Raw[2]** | | | **-rRNA[2]** | | |
|---|---|---|---|---|---|---|---|---|---|
| | Raw | -rRNA | Red. (%)[3] | Max.[4] | Pos.[5] | Gene | Max.[4] | Pos.[5] | Gene |
| Laura_Total_neg | 70.3 | 21.9 | 68.9 | 1,672 | 4,957 | *rnpB* | *nc* | *nc* | *nc* |
| Laura_Total_pos | 47.8 | 23.5 | 51.0 | 957 | 1,458 | *rsmZ* | *nc* | *nc* | *nc* |
| Laura_RsmA_neg | 61.0 | 13.0 | 78.7 | 471 | 6,052 | *rrnD* | 91 | 1,001 | UN |
| Laura_RsmA_pos | 88.4 | 63.9 | 27.6 | 3,668 | 1,458 | *rsmZ* | *nc* | *nc* | *nc* |
| Hazel_Total37_neg | 31.6 | 31.5 | 0.6 | 127 | 4,956 | *rnpB* | *nc* | *nc* | *nc* |
| Hazel_Total37_pos | 35.2 | 35.1 | 0.2 | 399 | 4,614 | *tmRNA* | *nc* | *nc* | *nc* |
| Hazel_RsmN37_neg | 38.5 | 36.1 | 6.2 | 359 | 4,957 | *rnpB* | *nc* | *nc* | *nc* |
| Hazel_RsmN37_pos | 31.9 | 31.0 | 3.0 | 218 | 5,321 | *crcZ* | *nc* | *nc* | *nc* |
| Hazel_Total34 | 493.5 | 492.1 | 0.3 | 1,858 | 4,614 | *tmRNA* | *nc* | *nc* | *nc* |
| Hazel_RsmN34 | 269.0 | 265.8 | 1.2 | 1,422 | 5,321 | *crcZ* | *nc* | *nc* | *nc* |

The values of each '`.rskip`' file were divided by their corresponding average to create '`.normalised`' files that could be compared with each other. By dividing the normalised read values of Rsm-bound RNAs with the normalised read values of total RNAs, an "enrichment index" could be generated. To facilitate the visualisation of this data, the logarithm of the ratio values for each nucleotide multiplied by an arbitrary factor (100) were saved into five final '`Ratio_`' files applying the equation below:

$$ratio = log_{10}\left(100 \cdot \frac{\mathrm{RNA}_{Rsm}}{\mathrm{RNA}_{Total}}\right)$$

In the resulting data files, any value above 2 would correspond to that of a nucleotide belonging to an Rsm-bound RNA, an example of which is illustrated in Figure 4.3. An exception occurs when there are no reads for a given nucleotide in the total RNA set, in which case the ratio cannot be determined and is therefore given a fixed value of 0. Targets were considered to be enriched if an enrichment index of 1, a logarithmic value of 2, was obtained for the majority of the nucleotides in an open reading frame.

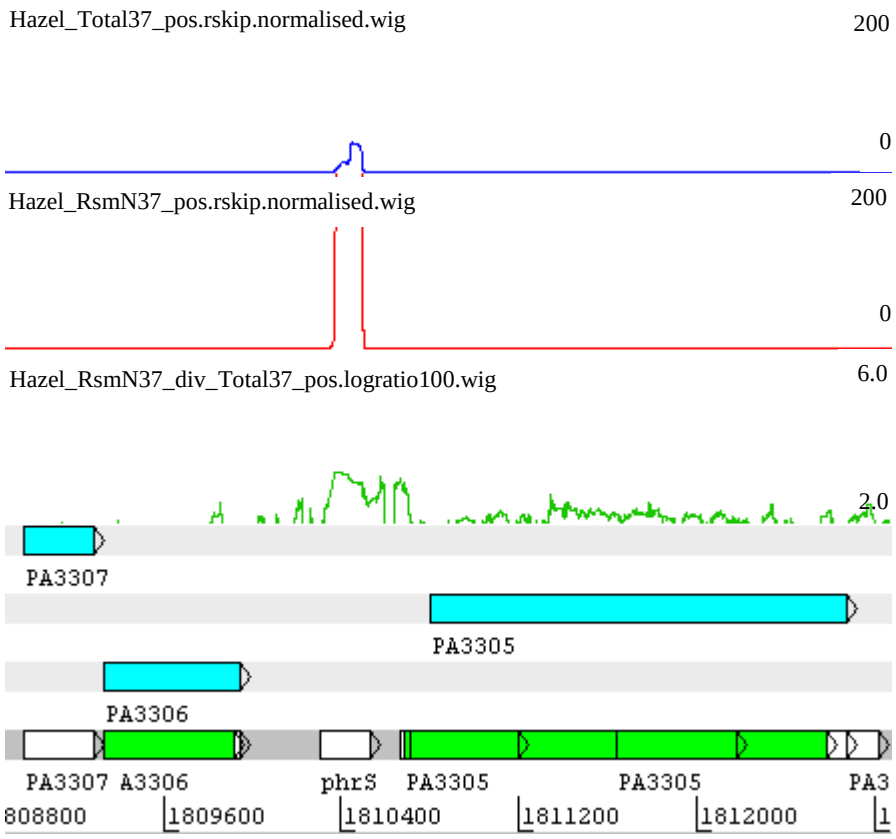


**Figure 4.3. RsmN-enrichment, indicated by an enrichment index greater than 2.0, of PhrS at 37°C**

Data from the normalised `.wig` files of total RNA (top), RsmN-bound RNA (middle) and the corresponding ratio file (bottom) illustrating the target enrichment index plotted against the PAO1-L annotated genomic sequence on the Artemis tool. Detection of an enrichment index > 2.0 and a peak corresponding to higher levels of *phrS* transcription in the RsmN-bound RNA sample compared to the total RNA sample indicate that *phrS* is an RsmN-enriched target. Vertical axis: position on the PAO1-L genomic sequence in base pairs and gene numbers. Note the difference in scales. Colour codes of the plot: blue, total RNA; red, RsmN-bound RNA; green, enrichment index. _pos. indicates that the investigated open reading frame is in 'sense' orientation in the genome.

### 4.2.2 RsmN-only targets and targets in common with RsmA

Target transcripts where the majority of nucleotides in an ORF had a logarithmic enrichment index of 2.0 or above were identified as 'RsmN-enriched' targets and were grouped as 'RsmN-only' and 'common with RsmA' based on the comparison of corresponding enrichment indexes. Tables 4.4 and 4.5 illustrate RsmN-only targets and RsmN-RsmA common targets (including intergenic regions but excluding hypothetical proteins) respectively. Genomic locations of some targets are altered due to an inversion of the region between *PA0668* and *PA4280.5* open reading frames in the PAO1-UW genome.

RsmN-enriched targets (Tables 4.4 and 4.5) relate to diverse systems such as secretion/transport (*fha1*, *tssa1*, *tssb1*, *tssc1*, *hcp1*, *exoT*, *oprM*, *oprI*, *oprF*, *oprG*, *popD*, *popB*, *xcpZ*, *exbD1*, *kdpA*, *braG*), heat shock (*ibpA*, *htpX*, *htpG*, *grpE*, *hslV*), carbon metabolism (*crc*, *adhA*, *ackA*, *gcd*), denitrification (*nirQ*, *nirC*, *nirM*, *nirS*, *norC*, *norB*, *norD*, *napE*), aerobic respiration (*PA4571*, *ccpR*, *ccoN2*, *ccoP2*, *PA0521*), oxidative stress response (*trxB2*, *ahpB*, *katB*, *ahpC*), and regulatory two-component systems (*PA0179*, *PA2571*, *pprB*, *creC*, *narL*, *mifR*). Transcripts such as *hflC*, *pasP*, *clpB*, *asrA* and *aprX* of a few proteases were also identified. Transcripts of numerous transcriptional regulators among which *dnr*, *prtR*, *mvaT*, *nosR* and *psrA* were previously characterised and *rnpB*, *rsmY*, *rgsA*, *crcZ* and *phrS* sRNAs were also among RsmN-enriched targets.

RsmN enrichment index was greater than 2.0 also in some intergenic regions. In previous studies, the presence of a Rho-independent transcription terminator has been considered as an indication of ncRNAs [266, 267]. A Rho-independent transcription terminator, TERM 1377, is found in the intergenic region between *PA1870* and *PA1869* ORFs. Another Rho-independent transcription terminator, TERM 4239 and the binding site of AlgU, the sigma factor controlling alginate production [268], are found in between *PA5492* and *PA5493* ORFs. It is likely that these intergenic regions are enriched by RsmN because uncharacterised ncRNAs are transcribed from these sites.

**Table 4.4. RsmN-enriched targets at 37°C**

| Gene No. | Gene name | Strand | Product |
|---|---|---|---|
| PA0082-PA0083-PA0084 | *tssa1-tssb1-tssc1* | sense | Tssa1-Tssb1-Tssc1 |
| PA0169 | *siaD* | antisense | diguanylate cyclase, SiaD |
| PA0173 | | antisense | probable methylesterase |
| PA0195-PA0195.1-PA0196 | *pntAA-pntAB-pntB* | sense | putative NAD(P) transhydrogenase, alpha subunit parts 1 & 2 - pyridine nucleotide transhydrogenase, beta subunit |
| PA0208-PA0214 | *mdcA-PA0209-mdcC-mcdD-mdcE-* | sense | malonate decarboxylase, alpha subunit-conserved hypothetical protein-malonate decarboxylase, delta, beta, gamma subunits-hypothetical protein-probable acyl transferase |
| PA0423 | *pasP* | sense | small protease, PASP |
| PA0427 | *oprM* | sense | multiple antibiotic resistance efflux protein |
| PA0456 | | sense | probable cold shock protein |
| PA0464 | *creC* | sense | two-component sensor, CreC |
| PA0506 | | sense | probable acyl-CoA dehydrogenase |
| PA0520-PA0521 | *nirQ-* | sense | regulatory protein NirQ-probable cytochrome c oxidase subunit |
| PA0523-PA0524-PA0525 | *norC-norB-norD* | sense | nitric oxide reductase subunit C-nitric oxide reductase subunit B-probable denitrification protein, NorD |
| PA4251-PA4250 | *rplE-rpsN* | sense | 50S ribosomal protein L5-30S ribosomal protein S14 |
| PA4237 | *rplQ* | sense | 50S ribosomal protein L17 |
| PA4114 | | sense | lysine decarboxylase |
| PA3721 | *nalC* | antisense | repressor of the *PA3720-armR* operon, NalC |
| PA3594 | | antisense | probable transcriptional regulator |
| PA3458 | | sense | probable transcriptional regulator |
| PA3450 | | sense | probable antioxidant protein |
| PA3391 | *nosR* | antisense | transcriptional regulator of NosZ, NosR protein |
| PA3337 | *rfaD* | sense | ADP-L-glycero-D-mannoheptose 6-epimerase |
| PA3305.1-PA3305-PA3304 | *phrS-* | sense | sRNA PhrS-beta-*N*-acetyl-D-glucosaminidase-5-methylthioadenosine phosphorylase MtnP |
| PA3181 | | sense | 2-keto-3-deoxy-6-phosphogluconate aldolase |
| PA3126 | *ibpA* | sense | heat shock protein, IbpA |
| PA3106 | | sense | probable short-chain dehydrogenase |
| PA3095 | *xcpZ* | sense | general secretion pathway protein M |
| PA3006 | *psrA* | sense | transcriptional regulator, PsrA |
| PA2853 | *oprI* | antisense | outer membrane lipoprotein OprI precursor |
| intergenic PA2850/PA2849 | | | |

| | | | |
|---|---|---|---|
| intergenic PA2827/PA2826 | | | (OspR binding site) |
| PA2297 | | sense | probable ferredoxin |
| PA2290 | *gcd* | sense | glucose dehydrogenase |
| PA2119 | | sense | alcohol dehydrogenase (Zn-dependent) |
| PA2053-PA2052 | *cynT-cynS* | sense | carbonate dehydratase-cyanate lyase |
| PA2024 | | sense | probable ring-cleaving dioxygenase |
| PA1777 | *oprF* | antisense | major porin and structural outer membrane porin OprF precursor |
| PA1633 | *kdpA* | antisense | potassium-transporting ATPase, A chain |
| PA1561 | *aer* | sense | aerotaxis receptor, Aer |
| PA1557-PA1554 | *ccoN2-ccoP2* | sense | $cbb_3$-type cytochrome *c* oxidase subunits |
| PA1429 | | antisense | probable cation-transporting P-type ATPase |
| PA1070 | *braG* | sense | branched-chain amino acid transport protein, BraG |
| PA0849-PA0848 | *trxB2-ahpB* | antisense | thioredoxin reductase 2-alkyl hydroperoxide reductase |
| PA0836 | *ackA* | sense | acetate kinase |
| PA0730 | | sense | probable transferase |
| PA4296 | *pprB* | sense | two-component response regulator PprB |
| PA4358 | | antisense | probable ferrous iron transport protein |
| PA4421.1 | *rnpB* | sense | RNA component of RNase P, RnpB |
| PA4571 | | sense | probable cytochrome *c* |
| PA4587 | *ccpR* | sense | cytochrome $c_{551}$ peroxidase precursor |
| PA4613 | *katB* | antisense | catalase |
| PA4673.13 | | antisense | RPG42 similar to PA0717 (hypothetical protein of bacteriophage Pf1) |
| PA4704 | *cbpA* | sense | cAMP-binding protein A |
| PA4810 | *fdnI* | antisense | nitrate-inducible formate dehydrogenase, gamma subunit |
| PA5157-PA5160 | | sense | probable transcriptional regulator-probable outer membrane protein precursor-multidrug resistance protein-drug efflux transporter |
| PA5297 | *poxB* | sense | pyruvate dehydrogenase (cytochrome) |
| PA5332 | *crc* | sense | catabolite repression control protein |
| PA5346 | *sadB* | sense | cytoplasmic signal transduction protein, SadB |
| PA5399 | *dgcB* | sense | dimethylglycine catabolism protein, DgcB |
| PA5418-PA5421 | *soxA-fdhA* | sense | sarcosine oxidase subunits-formyltetrahydrofolate deformylase-glutathione-independent formaldehyde dehydrogenase |
| PA5427 | *adhA* | sense | alcohol dehydrogenase |
| intergenic PA5429/PA5430 | | | (Rho-independent transcription terminator) |
| PA5440 | | sense | probable peptidase |
| PA5495 | *thrB* | sense | homoserine kinase |
| PA5553 | *atpC* | antisense | ATP synthase, epsilon chain |

**Table 4.5. RsmN-RsmA common targets**

| Gene No. | Gene name | Strand | Product |
|---|---|---|---|
| PA0004 | *gyrB* | sense | DNA gyrase subunit B |
| intergenic PA0039/PA0040 | | | |
| PA0044 | *exoT* | sense | exoenzyme T |
| PA0081 | *fha1* | antisense | Fha domain protein |
| PA0085 | *hcp1* | sense | Hcp1 protein |
| PA0139 | *ahpC* | sense | alkyl hydroperoxide reductase subunit C |
| PA0179 | | antisense | probable two-component response regulator |
| PA0199 | *exbD1* | sense | transport protein, ExbD |
| PA0366 | | antisense | probable aldehyde dehydrogenase |
| PA0436 | | sense | probable transcriptional regulator |
| PA0517-PA0518-PA0519 | *nirC-nirM-nirS* | antisense | probable *c*-type cytochrome precursor-cytochrome $c_{551}$ precursor-nitrite reductase precursor |
| PA0527 | *dnr* | antisense | transcriptional regulator, Dnr |
| PA0527.1 | *rsmY* | sense | sRNA antagonist to RsmA |
| PA0605 | *agtC* | sense | ABC transporter permease |
| PA0611 | *prtR* | antisense | transcriptional regulator, PrtR |
| PA4280 | *birA* | sense | bifunctional ligase/repressor, BirA |
| intergenic PA4237/PA4236 | | | |
| PA4067 | *oprG* | antisense | outer membrane protein OprG precursor |
| PA4061 | | antisense | probable thioredoxin |
| intergenic PA4034/PA4033 | intergenic *aqpZ/mucE* | | |
| PA3879 | *narL* | antisense | two-component response regulator, NarL |
| PA3769 | *guaA* | sense | guanosine monophosphate synthase |
| intergenic PA3739/PA3738 | | | |
| PA3692 | *lptF* | antisense | lipotoxin F |
| PA3531 | *bfrB* | antisense | bacterioferritin B |
| PA3482 | *metG* | antisense | methionyl-tRNA synthetase |
| PA3013 | *foaB* | sense | fatty acid oxidation complex, beta subunit |
| PA2958.1 | *rgsA* | antisense | sRNA, RgsA |
| PA2888 | *atuC* | antisense | geranyl-CoA carboxylase, beta subunit |
| PA2867 | | antisense | probable chemotaxis transducer |
| PA2830 | *htpX* | antisense | heat shock protein, HtpX |
| PA2571 | | sense | probable two-component sensor |
| PA2550 | | sense | probable acyl-CoA dehydrogenase |
| PA2396 | *pvdF* | sense | pyoverdine synthetase F |
| PA2376 | | antisense | probable transcriptional regulator |
| PA2127 | *cgrA* | sense | *cupA* gene regulator A, CgrA |
| intergenic PA2042/PA2041 | | | |
| intergenic PA1870/PA1869 | | | (Rho-independent transcription terminator, TERM 1377) |

| | | | |
|---|---|---|---|
| intergenic PA1736/PA1735 | | | |
| PA1709-PA1708 | *popD-popB* | antisense | translocator outer membrane protein PopD precursor-translocator protein, PopB |
| PA1596 | *htpG* | antisense | heat shock protein, HtpG |
| PA1546 | *hemN* | sense | oxygen-independent coproporphyrinogen III oxidase |
| PA1245 | *aprX* | antisense | alkaline protease, AprX |
| PA1177 | *napE* | sense | periplasmic nitrate reductase protein, NapE |
| PA0962 | *dps* | sense | DNA-binding protein from starved cells, Dps |
| PA0905 | *rsmA* | antisense | RNA-binding protein, RsmA |
| PA0840 | | antisense | probable oxidoreductase |
| PA0779 | *asrA* | sense | ATP-dependent protease, AsrA |
| PA0763 | *mucA* | antisense | negative regulator of alginate biosynthesis |
| PA4284 | *recB* | antisense | exodeoxyribonuclease V, beta chain |
| PA4315 | *mvaT* | sense | transcriptional regulator MvaT, P16 subunit |
| PA4385 | *groEL* | antisense | heat shock chaperonin, GroEL |
| PA4428 | *sspA* | antisense | stringent starvation protein A |
| PA4542 | *clpB* | antisense | ATP-binding subunit of Clp protease |
| PA4595 | | antisense | probable ATP-binding component of the ABC transporter |
| PA4726.11 | *crcZ* | sense | sRNA, CrcZ |
| PA4761-PA4762 | *dnaK-grpE* | antisense | chaperone-heat shock protein, GrpE |
| PA4941 | *hflC* | antisense | protease subunit |
| PA5053 | *hslV* | sense | heat shock protein, HslV |
| intergenic PA5057/PA5058 | | | |
| PA5173 | *arcC* | sense | carbamate kinase |
| PA5435-PA5436 | | antisense | probable transcarboxylase subunits |
| intergenic PA5492/PA5493 | | | (Rho-independent transcription terminator, TERM 4239 and AlgU binding site) |
| PA5511 | *mifR* | antisense | response regulator of the MifS/MifR two-component system |

### 4.2.3 RsmA and RsmN both regulate CrcZ

RNASeq results showed that *crcZ* is a common target of RsmA and RsmN whereas *crc* was detected as a target of RsmN only. CrcZ sequesters Crc proteins in a similar mechanism to the sequestration of RsmA proteins by RsmY and relieves catabolite repression exerted by Crc in the presence of less-preferred carbon sources. Sonnleitner *et al*. [68] demonstrated that a *crcZ* deletion mutant of *P. aeruginosa* was unable to grow on acetamide supplemented minimal medium (BSM, see section 2.1). To check for RsmA and RsmN control of CrcZ, the growth of the WT strain, Δ*rsmA* and Δ*rsmN* single and inducible double deletion mutants were tested on BSM agar along with the Δ*crcZ* mutant. Plates were incubated at 37°C overnight and pictures were taken the next day.

Figure 4.4, panel a) illustrates that PAO1 cells that lack only RsmA or RsmN were able to grow on acetamide supplemented BSM agar plates like WT cells, but without RsmA and RsmN ($rsmN_{ind}$ Δ*rsmA* -IPTG), there was no growth, resembling the Δ*crcZ* phenotype. In a control plate without any acetamide provided, none of the strains grew (panel b). The lack of growth in both $rsmN_{ind}$ Δ*rsmA* and Δ*crcZ* mutants indicates a positive control of *crcZ* translation by RsmA and RsmN.

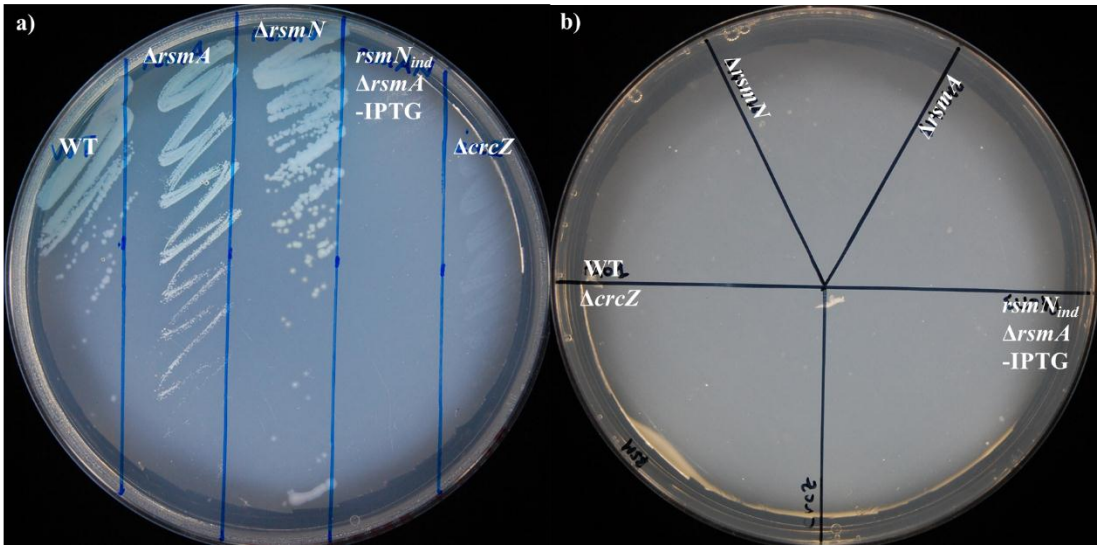


**Figure 4.4. The double deletion of *rsmA* and *rsmN*, like the deletion of *crcZ*, prevents the growth of PAO1 on acetamide supplemented BSM agar (a), none of the strains grow on BSM agar without any acetamide (b) at 37°C**

### 4.2.4 The double deletion of *rsmA* and *rsmN* might lead to carbon starvation

Transcripts of *dps*, coding a DNA-binding protein from starved cells and *sspA* stringent starvation protein were listed among common targets of RsmA and RsmN. To be able to establish a link between starvation and regulation by the Rsm proteins, *P. aeruginosa* cells were grown in minimal medium instead of the rich LB medium. The growth of the WT, Δ*rsmA*, Δ*rsmN* and *rsmN*$_{ind}$ Δ*rsmA* (-IPTG) strains was checked in liquid or on solid minimal media (CDM or BSM, see section 2.1) supplemented with TCA cycle intermediates (citrate, malate, fumarate and succinate). Concentrations of the carbon sources used were adjusted based on the number of carbons the molecule has (citrate 6C vs. succinate, fumarate and malate 4C) so that the total mass of carbons provided in the medium would be equal.

Takeuchi *et al*. [99] concluded that oxaloacetate was a poor substrate for the growth of *P. fluorescens* CHA0 cells in minimal medium. Oxaloacetate proved to be a poor growth substrate for *P. aeruginosa* cells as well in this study, hence, results of growth on oxaloacetate are excluded from this section. Takeuchi *et al*. [99] also reported the difficulty of growth measurements in liquid minimal medium due to cell clumping and a solid medium was preferred to grow bacteria. Cell clumping (see section 3.2.2, Figure 3.4) also made OD measurements from liquid minimal medium cultures difficult in this study. For this reason, duplicate and triplicate measurements were not taken. Figure 4.5 depicts growth curves plotted from single $OD_{600}$ measurements. Growth was checked in triplicates on minimal medium (BSM) agar supplemented with TCA cycle intermediates instead.

Figure 4.5 illustrates growth curves of the WT, Δ*rsmA*, Δ*rsmN* and *rsmN*$_{ind}$ Δ*rsmA* strains in CDM supplemented with citrate (panel A), malate (panel B), fumarate (panel C) and succinate (panel D). With malate (panel B), all tested strains started growing exponentially (WT and Δ*rsmN* strains after ~ 2 h, Δ*rsmA* and *rsmN*$_{ind}$ Δ*rsmA* strains after ~ 4 h) at earlier time points compared with growth in the presence of citrate, fumarate or succinate. In the presence of succinate or fumarate as the single carbon source, *rsmN*$_{ind}$ Δ*rsmA* cells had a lag phase of 8 h, with citrate lag phase was elongated to 10 h. The lag phase of the *rsmN*$_{ind}$ Δ*rsmA* mutant was longer than other strains in all TCA cycle intermediates tested, however, the same optical density as the rest of the

strains was reached by the end of 24 h in fumarate, succinate, and malate supplemented CDM. The Δ*rsmA* strain started to grow exponentially after a lag phase of 6 h in fumarate and succinate supplemented CDM, and 8 h in citrate supplemented CDM. The Δ*rsmN* deletion mutant did not display a growth pattern much different than the WT strain. The WT and Δ*rsmN* strains reached stationary phase 12-14 h post-inoculation in citrate, fumarate and succinate supplemented CDM and after 6 h in malate supplemented CDM. The Δ*rsmA* mutant reached stationary phase a bit later than the WT and Δ*rsmN* strains; ~ 14-16 h post-inoculation in citrate, fumarate and succinate and ~ 10 h post-inoculation in malate supplemented CDM. The $rsmN_{ind}$ Δ*rsmA* mutant reached stationary phase around 16 h post-inoculation in fumarate and malate, and 22 h in succinate supplemented CDM.

Figure 4.6 illustrates that the $rsmN_{ind}$ Δ*rsmA* mutant grew poorly on BSM agar supplemented with citrate (20 mM), fumarate (30 mM) and succinate (30 mM) in comparison with WT, Δ*rsmA* and Δ*rsmN* strains. Furthermore, the $rsmN_{ind}$ Δ*rsmA* mutant did not display the characteristic green colour of *P. aeruginosa*. The extended lag phases in liquid (Figure 4.5) and poor growth on solid (Figure 4.6) minimal media supplemented with TCA cycle intermediates in comparison with LB (Figure 3.3) reflect that the $rsmN_{ind}$ Δ*rsmA* mutant is not able to utilise TCA cycle intermediates as good as the WT, Δ*rsmA* or Δ*rsmN* strains. Therefore, it can be suggested that deletion of both *rsmA* and *rsmN* leads to carbon starvation.

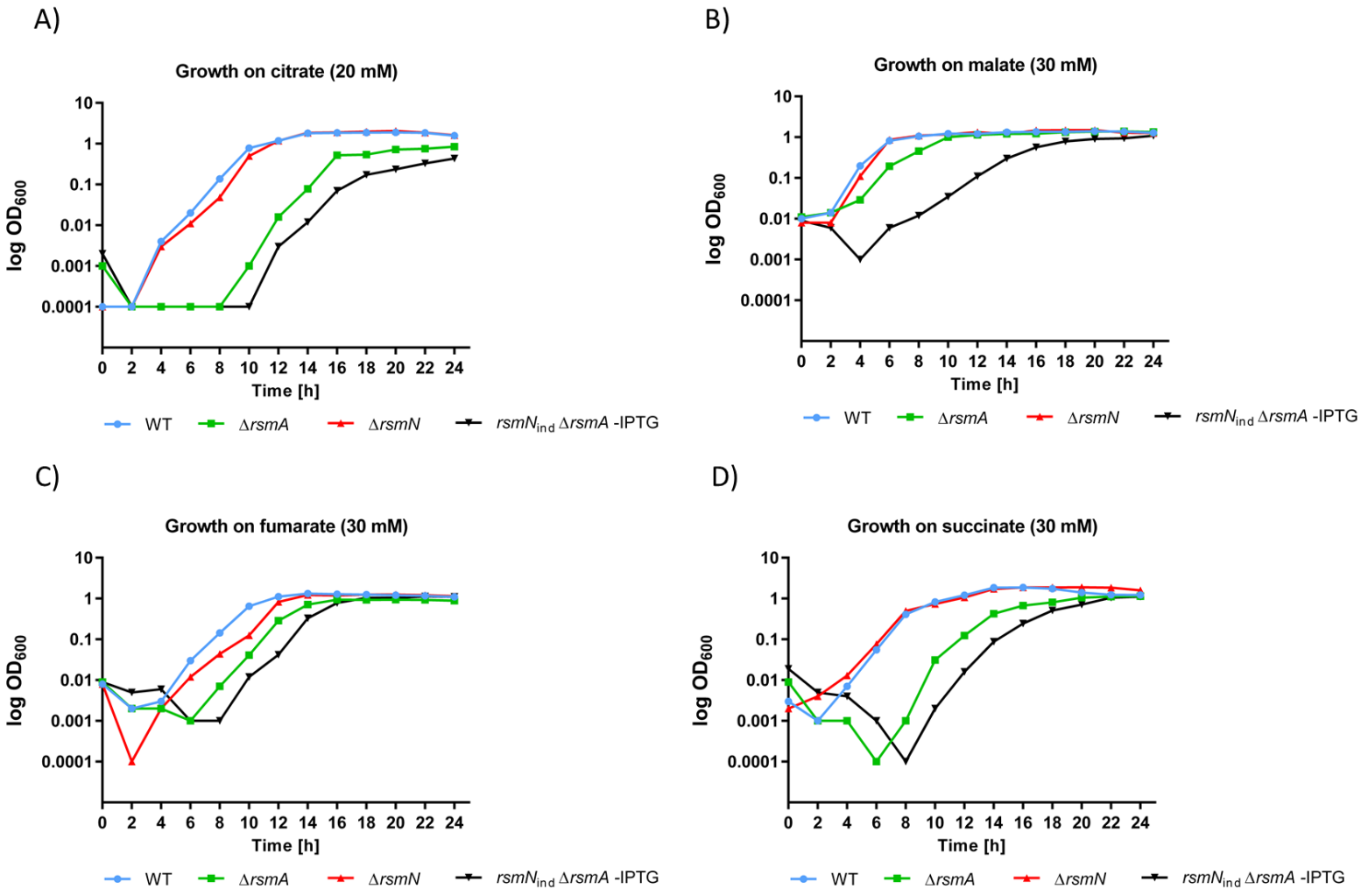


**Figure 4.5. The influence of *rsmA* and *rsmN* mutations on the growth of *P. aeruginosa* in chemically defined minimal medium (CDM) supplemented with citrate (A), malate (B), fumarate (C) and succinate (D) at 37°C**

The single deletion of *rsmA* and the double deletion of *rsmA* and *rsmN* cause *P. aeruginosa* cells to have extended lag phases. In succinate (D) and citrate (A) supplemented CDM, the Δ*rsmA* and $rsmN_{ind}$ Δ*rsmA* strains have longer lag phases than in fumarate (C) and malate (B) supplemented CDM. The single deletion of *rsmN* does not alter the growth of *P. aeruginosa* in minimal medium.

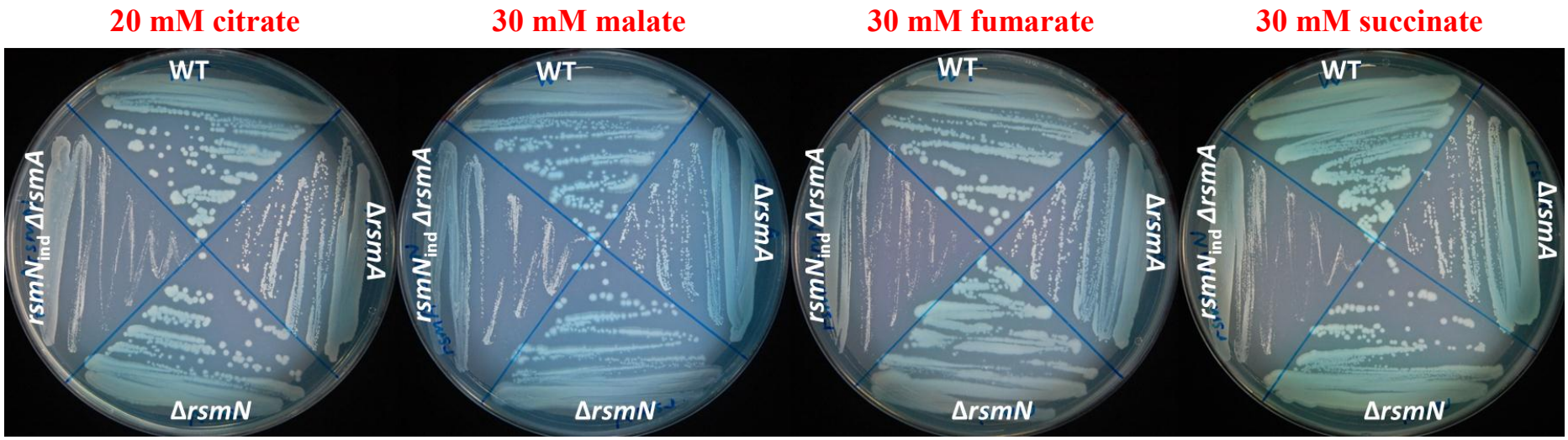


**Figure 4.6. The influence of *rsmA* and *rsmN* mutations on the growth of *P. aeruginosa* on basal salts minimal agar supplemented with citrate, malate, fumarate and succinate**

In the absence of both RsmA and RsmN, *P. aeruginosa* cells grow poorly on citrate, succinate and fumarate supplemented minimal medium agar and are not green. On malate supplemented minimal medium, the lawn of *rsmN*$_{ind}$ Δ*rsmA* mutant appears green, but cells grow poorly when compared with the Δ*rsmA* and Δ*rsmN* deletion mutants and the wild-type strain. The single deletion of *rsmA* or *rsmN* does not affect growth on solid medium, however, smaller colonies of the Δ*rsmA* are observed. Concentrations of carbon sources were adjusted to equalise the total mass of carbons provided in the growth media.

### 4.2.5 RsmN-RNA interaction at 34°C

During the extraction of RNA from cultures grown at 34°C for the RNASeq analysis, it was discovered that 200 mL culture of PAO1-L/pMR4 cells grown at 34°C yielded less RsmN-bound RNA in comparison with 200 mL culture of PAO1-L/pMR4 cells grown at 37°C although the amount of the purified protein was similar. Hence, protein purification was repeated using exactly the same amount of bacterial culture (250 mL), and quantities of the protein and RNA extracted from cultures grown to early stationary phase ($OD_{600}$ 2.155 and 1.965 respectively) at 34°C and 37°C were compared. After protein purification, RsmN concentrations were nearly the same: 7.62 mg/mL (34°C) and 7.61 mg/mL (37°C) in ~ 120 µL (after concentration of three elution fractions, see section 2.4.8.5) HPLC-grade water.

Figure 4.7 depicts the protein content in each purification fraction and the abundance of RsmN in concentrated elution fractions. Lysis and flow through fractions had the highest abundance of proteins. In the first wash step, a portion of these proteins was washed away, however, some were co-purified with RsmN.

The concentrations of RNA bound to 7.62 mg/mL (34°C) and 7.61 mg/mL (37°C) of RsmN were 287.5 ng/µL vs. 294.4 ng/µL respectively. After purification, following RNA concentrations were obtained: 192.4 ng/µL (34°C) and 257.9 ng/µL (37°C). This outcome might reflect that RsmN binds to less RNA transcripts at 34°C in comparison with at 37°C.

After repetition of RNASeq with total RNA and RsmN-bound RNA purified from 34°C cultures of the PAO1-L/pMR4 strain, a small set of ORFs, outlined in Table 4.6, were identified as RsmN-enriched targets only at 34°C. Furthermore, it was noted that transcripts such as *grpE* and *hslV* of the heat shock proteins, of the *tss* operon coding T6SS components (Figure 4.8), of the outer membrane proteins OprI, OprG and OprM, of the denitrification pathway components and *rsmA* were enriched by RsmN only at 37°C. The number of targets enriched by RsmN only at 34°C (listed in Table 4.6) is less than the number of targets enriched by RsmN only at 37°C (Table 4.4).

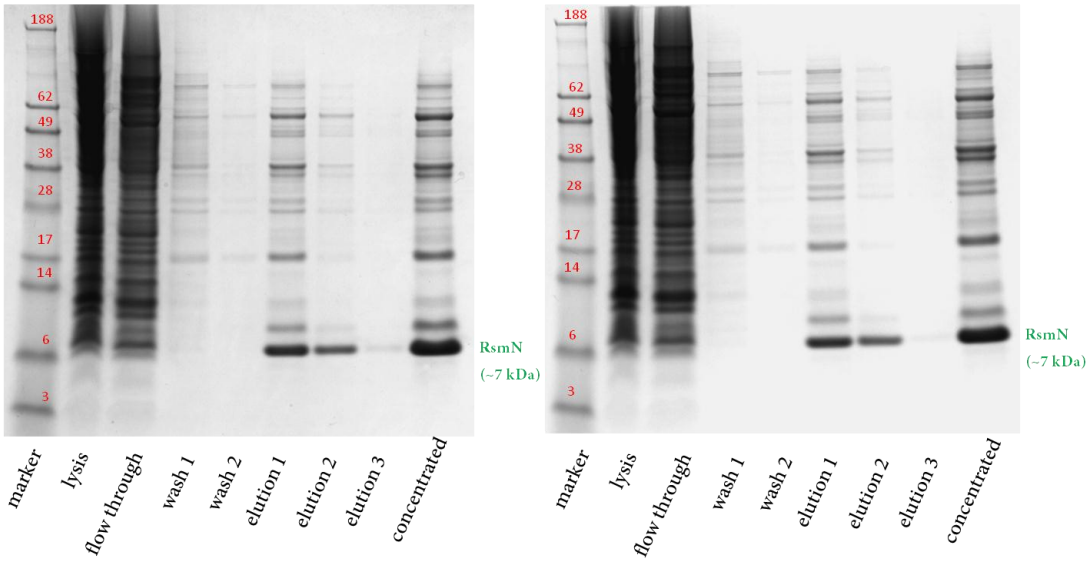


**Figure 4.7. Protein profiles of each fraction during purification of RsmN from the 34°C (left) and 37°C (right) cultures of the PAO1-L/pMR4 strain**

*Left panel* Protein profiles at each step (lysis, flow through, wash 1, wash 2, elution 1, elution 2, elution 3, and concentration in centrifugal filters) of RsmN purification from a 34°C culture of the PAO1-L/pMR4 strain. *Right panel* Protein profiles at each step of RsmN purification from a 37°C culture of the PAO1-L/pMR4 strain. The band corresponding to $His_6$-tagged RsmN (~ 7 kDa) in the concentrated elution fraction is labelled in green. Although the majority of cellular proteins are discarded and washed away in flow through and wash steps, pooled and concentrated elution fractions include a few other proteins co-purified with RsmN.

**Table 4.6. RsmN-enriched targets only at 34°C**

| Gene No. | Gene name | Strand | Product |
|---|---|---|---|
| PA0102-PA0103 | | sense | probable carbonic anhydrase-probable sulfate transporter |
| intergenic PA0185/PA0186 | | | |
| PA3924 | | | probable medium-chain acyl-CoA ligase |
| PA3724 | *lasB* | sense | elastase LasB |
| intergenic PA3065/PA3064 | | | |
| PA2634 | *aceA* | antisense | isocitrate lyase, AceA |
| PA2514-PA2513-PA2512 | *antC-antB-antA* | antisense | anthranilate dioxygenase reductase-anthranilate dioxygenase small subunit-anthranilate dioxygenase large subunit |
| PA2511 | *antR* | sense | transcriptional regulator, AntR |
| PA2426 | *pvdS* | antisense | sigma factor, PvdS |
| PA1282 | | sense | probable major facilitator superfamily (MFS) transporter |
| PA0694 | *exbD2* | antisense | transport protein, ExbD |
| PA0675 | *vreI* | antisense | ECF sigma factor, VreI |
| intergenic PA0672/PA0671 | | | |
| PA5556 | *atpA* | antisense | ATP synthase alpha chain |

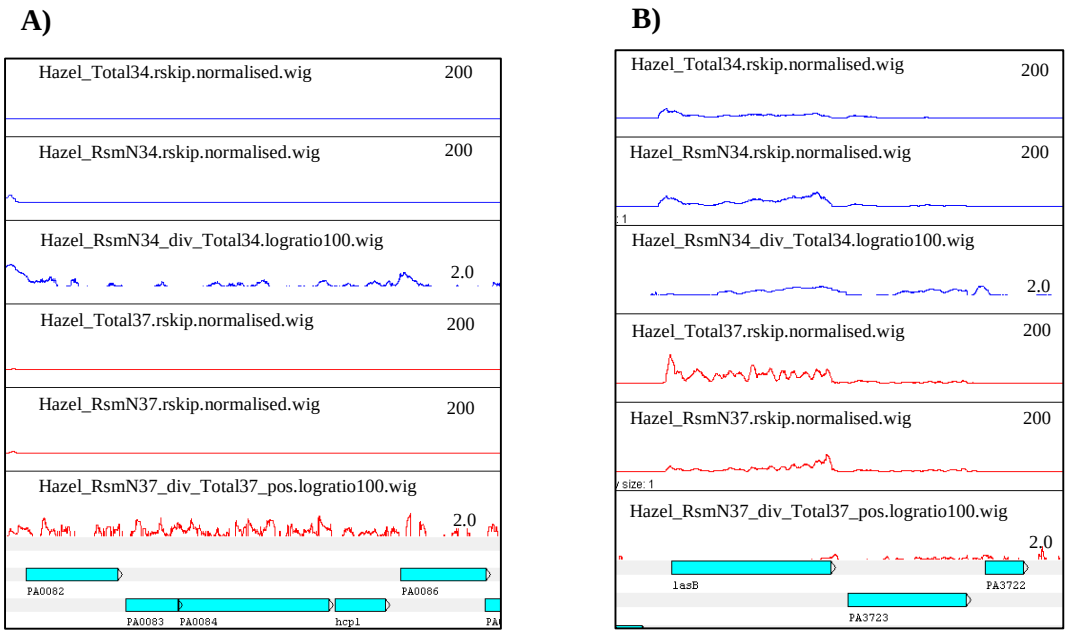


**Figure 4.8. The *tss* operon as an RsmN target only at 37°C (A) and *lasB* as an RsmN target only at 34°C (B)**

Data from the 34°C normalised `.wig` files of total RNA, RsmN-bound RNA and the corresponding ratio file (blue) plotted in comparison with the data from the 37°C `.wig` files of total RNA, RsmN-bound RNA and the strand-specific ratio file (red) on Artemis tool against the PAO1-L annotated genomic sequence. An enrichment index greater than 2.0 is detected for the *tss* operon (*PA0082-PA0083-PA0084*) only at 37°C (A) and for *lasB* gene only at 34°C (B).

Table 4.6 lists the transcripts of genes (*antABC* operon and *antR*) linked to the degradation of anthranilate and the transcriptional activator, AntR, of anthranilate degradation [269], of *lasB* coding elastase (Figure 4.8), of a few transporter coding genes, of the *pvdS* and *vreI* sigma factor genes and *aceA* coding the isocitrate lyase AceA, enriched by RsmN only at 34°C.

## 4.3 Discussion

Direct regulation by RsmA in *P. aeruginosa* was first demonstrated by Pessi *et al.* [204] for the *hcnA* transcript. More potential targets of RsmA were identified in microarray analyses (see section 4.1) performed by Burrowes *et al.* [183] and Brencic and Lory [236]. However, these transcriptomic approaches did not allow the distinction of primary from secondary Rsm targets and relied on Affymetrix chips made of discrete oligonucleotide probes that are directed only against annotated open reading frames. Therefore, target transcripts of RsmN were identified on a genome-

wide basis using RNASeq which is a powerful method to map and quantify RNA levels in biological samples.

Results analysed in this study indicate that replicates (Table 4.1) appear to be robust enough to pool the data into simplified files. Although this verification was done visually (Figure 4.2), recently released computer programs such as the BEDTools suite [270] are now available to statistically compare the `.wig` files, and these could validate the merging approach used in this study. RNASeq is still an emerging technology, notably to use with samples of bacterial origin, and even though new software to analyse the data is regularly being released, there is not any currently available that would process the kind of protein-bound RNA data as that produced in this study.

The capability of RNASeq to generate strand-specific information and independently of any genome annotation is of great value in the context of suspected unannotated genes belonging, for example, to still uncharacterised ncRNAs. However, to generate correct strand-specific data, it is crucial that the correct genomic sequence applying to the strains from which the samples are taken is used. The reference sequence of *P. aeruginosa* PAO1 is based on the subline PAO1-UW, and this is known to have a large chromosomal inversion between the ribosomal operons *rrnA* and *rrnB* [110] and lacks the region of genome plasticity RGP42 [265], unlike many other laboratory sublines including the PAO1-L strain used in this study. For this reason, RNASeq reads were mapped to the genomic sequence of PAO1-L (H. Naghra, in preparation) and not against the usual reference corresponding to PAO1-UW.

Initial analysis of the `.wig` files resulting from the mapping revealed the presence of significant signals corresponding to rRNAs, despite the samples having undergone a physical ribodepletion step before cDNA library preparation. This ribodepletion was not complete for any of the samples, a contamination which was not unexpected given that the vast majority of RNA in growing bacterial cells consists of rRNA. Boundaries of signals originating from rRNAs were determined by visually examining the data on Artemis annotation tool around the four *rrn* operons present in *P. aeruginosa* and determining the precise coordinates of the regions to exclude (Table 4.2). These coordinates were then used to change all the corresponding values to 0 in all the `.wig`

files. This exclusion altered the average reads per nucleotide at variable levels, from a 0.2% to a 78.7% reduction, depending on the file and experiments. The greatest reductions in averages were seen for the data of the RsmA-bound RNA which resulted from an experiment carried out a few years before the others. It is possible that the ribodepletion kit used at the time was different than the one used for the more recent samples, or a mistake or a defect in the kit prevented a comparable ribodepletion. In any case, the contamination was not problematic enough to mask the mapping of all the other RNAs, which were those of interest.

After the removal of the data corresponding to rRNAs from the `.wig` files, these were analysed again for the highest values observed, and to identify the genes causing such strong signals. For all but one file (`Laura_RsmA_neg.wig`) these values did not change and corresponded to known sRNAs, including RsmZ. Because of their small size, these would not affect the average reads per nucleotide greatly and were therefore left in the datasets. For one file, the highest value initially corresponded to rRNA that was mapped to *rrnD*. Once this data was removed, another maximal value appeared at another location, which corresponded to an unannotated intergenic region. It is possible that this is an uncharacterised ncRNA and was therefore not excluded from the study.

Once data from each `.wig` file was normalised with respect to its average, a ratio, a value corresponding to an 'enrichment index', was calculated between Rsm-bound RNA and total RNA signals. A value of 1 would mean that a nucleotide has been read, proportionally, at the same level in both samples. Values greater than 1 would correspond to RNAs preferentially enriched in the Rsm-bound RNA fraction and would, therefore, indicate the proximity of an active Rsm-binding site. To facilitate the visualisation of these results, the ratio was multiplied by 100 and the logarithm of the resulting values was taken. Therefore, any ORF where the majority of the nucleotides have an enrichment index logarithmic value of 2.0 and above was considered to code a target of RsmN (Figure 4.3).

Co-purification of RNAs bound to a $His_6$-tagged protein is a low-resolution approach especially when the protein of interest cannot be purified alone (see Figure 4.7) and the obtained RNA profile is based on the assumption that none of the co-purified

proteins is also an RNA-binding protein. Therefore, some of the listed target RNAs might be artefacts. For example, in some cases, the target ORF was not transcribed at detectable levels neither in the total RNA sample nor in the RsmN-bound RNA sample in experimental conditions chosen in this study, however, a logarithmic value greater than 2.0 was obtained as the enrichment index (Figure 4.8, panel A). Another disadvantage of using the co-purification method with RNA-binding proteins is that RBPs may strengthen RNA stability by blocking RNase binding, thus, binding to Rsm proteins might indirectly alter transcript levels of RNA targets in comparison with the unbound RNAs. Because of these limitations, validation of the RNASeq data by complementary methods such as RNA electrophoretic mobility shift assay or Northern Blot is required. Furthermore, algorithms that enable the comparison of different RNASeq data sets using a computer software could be refined to maximise the reliability of RNASeq results.

It has been demonstrated that the deletion of *rsmA* results in reduced expression of T3SS genes and increased expression of T6SS genes in Burrowes *et al*. [183] and Brencic and Lory [236]. Furthermore, Mulcahy *et al.* [205] reported that *rsmA* deletion results in decreased expression of genes such as *exsA*, *exsC, cyaB* and *vfr* linked to the T3SS. RNASeq results of this study show that transcripts of *exoT* coding one of the cytotoxins secreted by T3SS [271] and *popB*/*popD* which are both essential for pore formation in T3SS were enriched by both RsmA and RsmN. Brencic and Lory [236] demonstrated a 3.3-fold decrease in *exoT* expression as a result of *rsmA* deletion in the PAK strain. It is likely that RsmA and RsmN regulate the translation of *exoT*, *popB* and *popD* in the PAO1 strain positively, this can be further investigated by constructing translational fusions. On the other hand, *hcp1* (*PA0085*) coding the hemolysin-coregulated protein Hcp1 was enriched by both RsmA and RsmN (Table 4.5). Furthermore, transcripts of the T6SS gene cluster *PA0081-PA0085* were enriched by RsmN (Table 4.4). Downregulation of Hcp1 secretion by RsmA and RsmN was deduced from the supernatant protein profiles investigated in Chapter 3 (Figures 3.25 and 3.29). Phosphorylation of the Fha1 domain protein by PpkA, a membrane-spanning threonine kinase post-translationally activates the T6SS of *P. aeruginosa* and triggers secretion of the Hcp1 protein which makes up the secretion tube for the export of effector proteins [154, 158]. Based on RNASeq results, *fha1* is a common target of RsmA and RsmN, hence, it can be suggested that Rsm proteins of *P. aeruginosa*

suppress Hcp1 secretion under T6SS by downregulating *fha1* translation (illustrated as a diagram in Figure 4.9). RsmN control on Fha1 is currently being investigated by Manuel Romero using a reporter with *fha1'-'lacZ* translational fusion (unpublished data). Moreover, in support of these findings, Marden *et al.* [206] demonstrated that *tssa1* (*PA0082*) is translationally derepressed 2.2-fold in the Δ*rsmA* mutant and 18.3-fold in the Δ*rsmA* Δ*rsmF* mutant. Additionally, Hcp1 secretion was significantly increased in the Δ*rsmA* Δ*rsmF* mutant. Based on these findings altogether, it can be suggested that RsmA and RsmN regulate T3SS positively and T6SS negatively.

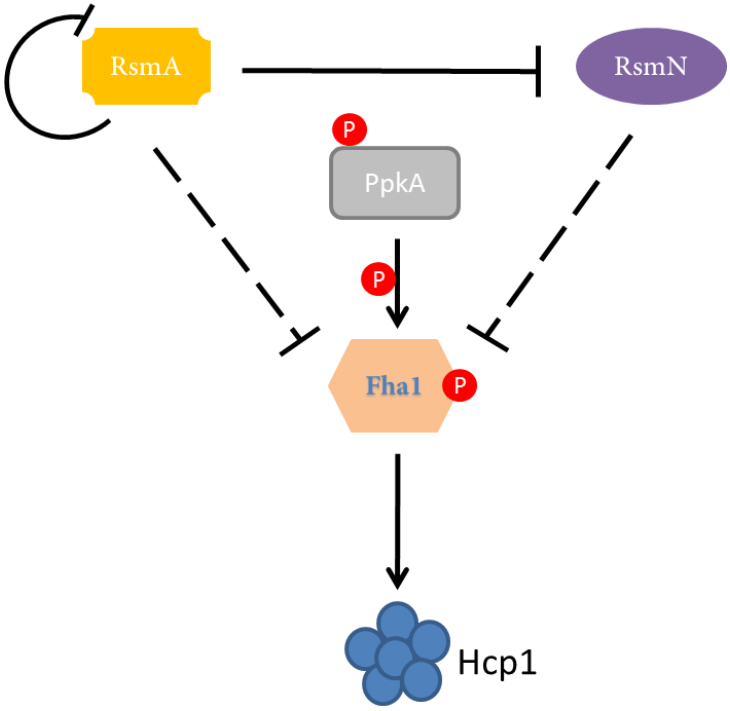


**Figure 4.9. Predicted regulatory roles of the Rsm proteins on the T6SS of *P. aeruginosa***
RsmA represses its own translation as well as *rsmN* translation (Rsm proteins function as homodimers, one monomer of each protein is omitted from the figure for simplicity). T6SS of *P. aeruginosa* is activated through phosphorylation (phosphate group illustrated in red) of Fha1 by PpkA, a serine-threonine kinase, upon receiving appropriate environmental signals (not depicted) [154]. According to RNAseq results, *fha1* is a common target of RsmA and RsmN and supernatant protein profiling indicates that Hcp1 proteins (depicted in hexamers) are secreted into the culture supernatant excessively when cells lack both RmA and RsmN. Based on these results, RsmA and RsmN are predicted (indicated by dashed lines) to downregulate *fha1* translation which results in reduced Hcp1 secretion.

Sharma and Storz [272] listed small regulatory RNAs (PhrS, PrrF1, PrrF2, PrrH, RsmY, RsmZ, CrcZ, RgsA and PhrD) characterised in *P. aeruginosa*. Transcripts of *phrS*, *crcZ*, *rgsA*, *rsmY* and *rnpB* small RNAs are detected among RsmN-enriched targets in this study (Tables 4.4 and 4.5).

It has been demonstrated that at high cell densities where RsmA protein is in high numbers, the GacA/GacS TCS induces transcription of the RsmY and RsmZ sRNAs which sequester RsmA away from target mRNAs, for instance, reversing the negative control over the *rhl* system and virulence determinants such as elastase, PYO and HCN [20, 121, 204]. Based on RNASeq results, *rsmY* is an RsmA-RsmN common target. Marden *et al*. [206] demonstrated RsmF (RsmN)-RsmY and RsmF-RsmZ binding in an EMSA. However, after checking *exsD* and *tssa1* transcriptional and translational reporter activities in the Δ*rsmA* and Δ*rsmA* Δ*rsmY* Δ*rsmZ* mutants they concluded that RsmY and RsmZ do not control RsmF activity *in vivo*. Whereas *rsmZ* was enriched by RsmA (data not shown), it was not among RsmN-enriched transcripts in this study. Contrarily, E. Morris demonstrated that RsmN binds to GGA-motif containing hairpins from RsmY and RsmZ with high affinity in a previous study [241]. After constructing transcriptional and translational reporters using an RsmN-only target outlined in Table 4.4, a comparison of reporter activities in the Δ*rsmA*, Δ*rsmA* Δ*rsmY*, Δ*rsmA* Δ*rsmZ* and Δ*rsmA* Δ*rsmY* Δ*rsmZ* mutants would provide more information on the regulation of RsmN by RsmY and RsmZ assuming that the Rsm system is limited to the RsmA and RsmN proteins and the RsmY and RsmZ sRNAs in *P. aeruginosa*. If RsmY or RsmZ controlled RsmN, transcriptional or translational reporter activities of the chosen RsmN target would be altered in the Δ*rsmA* Δ*rsmY*, Δ*rsmA* Δ*rsmZ* or Δ*rsmA* Δ*rsmY* Δ*rsmZ* mutants when compared with the reporter activities in the Δ*rsmA* mutant. Checking reporter activities in a Δ*rsmA* background is crucial as there is a cross-regulation between RsmA and RsmN as demonstrated both in Chapter 3 of this study and in Marden *et al.* [206].

RgsA (regulation by GacA and stress) sRNA was discovered by Livny and colleagues [58] following a combination of computational methods and was investigated further by Gonzalez *et al*. [273]. A single ANGGA-binding motif which is typical for Rsm-regulating sRNAs was found in an unpaired region of *P. fluorescens* CHA0 RgsA, however, overexpressed RgsA failed to relieve the translation repression exerted by

the Rsm proteins. Gonzalez *et al.* [273] demonstrated that RpoS is essential for *rgsA* expression both in *P. aeruginosa* and *P. fluorescens*. Table 4.4 shows that although *rpoS* is not, *psrA* coding the transcriptional activator of *rpoS* [274] is enriched by RsmN.

CrcZ, antagonist sRNA to the catabolite repression control protein Crc, is also a common target of RsmA and RsmN. Evidence of RsmN/RsmA-CrcZ interaction was provided in a previous study [241]. Figure 4.4 in section 4.2.3 illustrates that deletion of both *rsmA* and *rsmN* prevents the growth of *P. aeruginosa* on acetamide supplemented minimal medium in parallel with the Δ*crcZ* mutant, suggesting positive modulation of CrcZ by RsmA and RsmN. An EMSA is currently carried out by Manuel Romero to demonstrate RsmN-CrcZ binding (unpublished data). In addition, the *crc* transcript is also enriched by RsmN. These results establish a link between RsmN and catabolite repression in *P. aeruginosa*.

PhrS is among RsmN-only targets (Table 4.4). PhrS is not controlled by a TCS; its transcription requires the anaerobic regulator ANR [272]. In a study by Sonnleitner *et al*. [19], PhrS was detected at higher levels as cells reached the stationary phase of growth and oxygen started to become limiting. Overexpression of *phrS* led to increased transcription of the *phzA-G* operon and *phzS*, both required for PYO production, as well as the *pqsABCDE* operon and *phnAB* genes which are essential for PQS synthesis. After Deziel *et al.* [275] showed regulation of PYO and PQS synthesis by PqsR, Sonnleitner *et al.* [19] demonstrated a regulatory link between PhrS and PqsR. PhrS was found to regulate *pqsR* translation positively by activating a translationally-coupled upstream ORF, resulting in increased HHQ and PQS production. Assessment of PYO production after the multicopy expression of *rsmN* in the $rsmN_{ind}$ Δ*rsmA* strain (section 3.2.11, Figure 3.34) showed that on the contrary to RsmA, RsmN positively regulates PYO synthesis. As the *phz* operon is not among RsmN targets, this positive control might be linked to the positive modulation of PhrS by RsmN. Sonnleitner *et al*. [237] demonstrated that the expression of *groEL* coding a heat shock chaperonin [276] and *oprD* coding the outer membrane protein OprD [277, 278] was upregulated by PhrS. Both *groEL* and *oprD* are among RsmN-enriched targets. It is possible that RsmN was bound to the *phrS* transcript when this sRNA was in a complex with the

*groEL* and *oprD* transcripts under the experimental conditions RNASeq was carried out in this study.

A comparison of RsmN targets at 37°C and 34°C revealed that *rsmA* was enriched by RsmN only at 37°C. The cross-regulation between RsmA and RsmN has been shown in phenotypic assays outlined in Chapter 3 of this study and the inhibition of *rsmF* (*rsmN*) translation by RsmA has been reported by Marden *et al*. [206]. When *rsmN* expression was induced, swarming motilities of the WT and Δ*rsmN* strains were completely suppressed at 37°C but not at 34°C (Figure 3.36). The suppression of swarming is likely to be due to the cross-regulation between RsmA and RsmN at 37°C. It can be hypothesised that when both proteins are present, they negatively regulate each other and the positive control over swarming motility is completely lost. Also, assuming that *rsmA* transcript levels are higher than *rsmN* transcript levels at 37°C, it is possible that RsmA titrates some transcripts which are potentially also RsmN targets but cannot be co-purified with RsmN due to RsmA-binding. For this reason, performing RNASeq using a Δ*rsmA* Δ*rsmN* mutant would minimise the interference of cross-regulation between the two proteins on RNASeq results.

The *lasB* transcript coding elastase, a major protease of *P. aeruginosa*, appeared to be enriched by RsmN only at 34°C (Table 4.6). RNASeq results show that *lasB* is also enriched by RsmA (data not shown). Negative control of RsmA on elastase production was demonstrated by Pessi *et al*. [204] previously, however, in this study RsmA was found to control elastase production positively (Chapter 3, Figure 3.18). Elastinolytic activity was drastically reduced when both *rsmA* and *rsmN* were deleted. Inducing *rsmN* expression in the $rsmN_{ind}$ Δ*rsmA* strain partially restored elastinolytic activity (Figure 3.18, panel a). Furthermore, multicopy expression of *rsmN* increased elastinolytic activity in the Δ*rsmA* mutant (Figure 3.18, panel b). Hence, it can be suggested that RsmN upregulates elastinolytic activity by regulating *lasB* translation positively but RsmN control on *lasA* which is required for the staphylolytic activity [279] remains to be investigated.

RNASeq results revealed that transcripts of *mvaT* which codes the negative regulator of *cup* gene clusters [280] and *cgrA* which codes the *cupA* gene regulator A [281] are among common targets of RsmA and RsmN. In section 3.3, reduced expression of the

*cup* genes has been suggested as a factor causing the Δ*rsmA* cells to clump. The *cupA* gene cluster is required for the assembly of fimbrial structures which have a role in cell adhesion [252]. In the PAO1 Δ*rsmA* mutant, the expression of *cupA2* was reduced ninefold [183]. Based on this microarray data and the RNASeq data of this study, it can be proposed that RsmA and RsmN repress *mvaT* translation and enhance *cgrA* translation to increase *cupA* expression. Thus, it can be suggested that decreased *cupA* expression contributes to the clumping and microcolony biofilm phenotypes of the Δ*rsmA* and *rsmN*$_{ind}$ Δ*rsmA* (-IPTG) mutants.

In the CF lung where microaerobic conditions prevail, in addition to aerobic respiration, arginine fermentation and denitrification are also important to ensure bacterial survival [282]. A large number of transcripts coding the components of the denitrification pathway and the *dnr* transcript coding the transcriptional regulator of the denitrification genes were enriched by RsmN. Denitrification is a multistep process where nitrate ($NO_3^-$) is reduced to dinitrogen ($N_2$) by nitrate reductase (Nar), nitrite reductase (Nir), nitric oxide reductase (Nor) and nitrous oxide reductase (Nos) activities respectively [283]. NirM and NirC, transcripts enriched by RsmN, transfer electrons from the cytochrome $bc_1$ complex to nitrite reductase [282]. It has also been demonstrated that OprF, enriched by RsmN, might function as a permease for the $NO_3^-$ /$NO_2^-$ uptake [284]. The *napE* transcript encoding the periplasmic nitrate reductase protein was enriched by both RsmN and RsmA. Furthermore, *PA1546* which encodes HemN, an oxygen-independent coproporphyrinogen III oxidase involved in heme biosynthesis [105], *ccoN2* and *ccoP2* encoding the CcoN and CcoP subunits of the $cbb_3$-type cytochrome c oxidase [285] and *arcC* encoding carbamate kinase of the arginine fermentation pathway are also among enriched transcripts of RsmN. Dietrich *et al.* [216] demonstrated that *P. aeruginosa* maintains redox homoeostasis by undergoing morphological changes and forming wrinkly colonies to expand the surface area in the absence of nitrate or phenazines. Hence, downregulation of denitrification enzymes and a decrease in nitrate reduction might be the underlying mechanism of rough colony formation by the *rsmA*$_{ind}$ Δ*rsmN* and *rsmN*$_{ind}$ Δ*rsmA* mutants. Alternatively, as mentioned in section 3.3, increased c-di-GMP levels also result in a wrinkly colony morphotype and *siaD* encoding a diguanylate cyclase is among RsmN-enriched transcripts (Table 4.4). Additionally, the *mucA* transcript and the intergenic region *PA5492*/*PA5493* where an AlgU binding site is located were

enriched by both RsmA and RsmN. The MucA and MucB proteins of *P. aeruginosa* control alginate production, hence, the conversion to mucoidy phenotype negatively by blocking the sigma factor AlgU [286]. If the Rsm proteins controlled translation of *mucA* or *siaD*, this regulation is likely to be negative, increasing alginate production in the case of the former and reducing c-di-GMP levels via downregulating diguanylate cyclase in the latter. In the absence of RsmA and RsmN, increased c-di-GMP levels and decreased alginate production could promote rough colony formation by the *rsmA*$_{ind}$ Δ*rsmN* and *rsmN*$_{ind}$ Δ*rsmA* mutants (Figure 3.23, left panel).

Hauser A.R. [287] demonstrated that a pore-mediated increase in membrane permeability might trigger cell death and cause leakage of the supernatant proteins into the cytosol which is observed in the case of the *rsmA*$_{ind}$ Δ*rsmN* and *rsmN*$_{ind}$ Δ*rsmA* strains grown without IPTG (Figure 3.25). RNASeq results presented here illustrate that *oprM*, coding a multiple antibiotic resistance efflux protein, *oprF* coding the major membrane porin, and *oprI* and *oprG* coding outer membrane proteins were enriched by RsmA and/or RsmN. Therefore, it can be speculated that RsmA and RsmN have a role in membrane permeability.

Initially, Zinser and Kolter [288], later Pernestig *et al.* [56] reported that autolysis occurs in bacterial cells that cannot maintain essential activities due to insufficient supply of carbon. Under such conditions, remaining cells are supplied by carbon in the form of free amino acids released from lysed cells. Upon detection of *dps* and *sspA* transcripts (coding a DNA-binding protein from starved cells and the stringent starvation protein A respectively) among common targets of RsmA and RsmN, the growth of the *rsmA* and *rsmN* deletion mutants was checked on minimal medium supplemented with a single carbon source. The *rsmN*$_{ind}$ Δ*rsmA* strain could not grow on acetamide, and grew poorly on tricarboxylic acid supplemented minimal media. The most elongated lag phases were observed when the Δ*rsmA* and *rsmN*$_{ind}$ Δ*rsmA* strains were grown in chemically defined minimal medium with citrate (Figure 4.5, panel A). On BSM agar plates supplemented with citrate, the *rsmN*$_{ind}$ Δ*rsmA* inoculum was dried up and very little growth was observed (Figure 4.6). With malate, fumarate, or succinate supplementation (Figure 4.5, panels B, C and D), lag phases of the Δ*rsmA* and *rsmN*$_{ind}$ Δ*rsmA* strains were still longer than lag phases of the WT and Δ*rsmN* strains, however, similar optical densities were obtained in comparison with the WT

strain at the end of 24 h. Schleheck *et al*. [115] reported dispersal of *P. aeruginosa* PAO1 aggregates upon carbon, nitrogen or oxygen limitation. Based on this, it can be suggested that dispersal of the clumped Δ*rsmA* or *rsmN*$_{ind}$ Δ*rsmA* cells is increasing the optical density by the end of the 24 h incubation. These results suggest that survival of the *rsmN*$_{ind}$ Δ*rsmA* bacterial population under carbon starvation conditions might be supported by cell death of a portion of the population.

Alternatively, cell death might be triggered by aggregation of misfolded proteins [289]. Protein misfolding is common under severe heat conditions. Bacterial cells cope with heat stress by triggering transcription of the *hsp* genes, controlled by the sigma factor RpoH, and synthesise chaperones and proteases either to aid in accurate folding or degradation of misfolded proteins. RsmN-only target *ibpA* codes the inclusion body-associated protein A (IbpA) that belongs to the α-crystalline-type small Hsps which prevent the aggregation of misfolded proteins under heat stress conditions [290]. In addition to *ibpA*, transcripts such as *htpX*, *htpG*, *dnaK*, *grpE*, *hslV*, and *groEL* of a few heat shock proteins and of a few proteases (*hflC*, *clpB*, and *aprX*) were also enriched by RsmN at 37°C. ClpB ATPase with DnaK, DnaK with DnaJ and GrpE cochaperones, and GroEL with GroES assist misfolded and aggregated proteins to refold [289]. Assuming a positive control on the translation of the *clpB*, *dnaK*, *grpE*, and *groEL* transcripts by RsmA and RsmN, it can be proposed that increased autolysis which occurs as a result of *rsmA* and *rsmN* double deletion might alternatively be associated with the accumulation of misfolded proteins due to decreased levels of cellular chaperones.

Identification of outer membrane proteins, chaperones, components of the T3SS and T6SS, terminal oxidases, denitrification and arginine fermentation enzymes, CrcZ and Crc among targets of RsmA and RsmN by RNASeq, considered in parallel with increased cellular lysis and rough colony formation, diminished proteolytic and elastinolytic activities and poor growth on minimal medium in the absence of both RsmA and RsmN suggest that Rsm proteins act as cellular checkpoints influencing the growth and virulence of *P. aeruginosa*.

# 5 General Conclusions and Future Directions

Alternative methods are sought to fight against pathogenic superbugs such as *P. aeruginosa* which gains resistance to the available antimicrobials rapidly. In addition to the QS systems, the TCSs that bacteria use to regulate gene expression according to changing environmental conditions are also targeted for antivirulence therapy as they are absent in humans [74].

The GacS/GacA TCS along with the RetS and LadS sensors and the Rsm system which consists of the RNA-binding protein RsmA and the regulatory sRNAs RsmY and RsmZ control virulence through regulation of QS, motility, biofilm formation and production of secondary metabolites in *P. aeruginosa* [112, 186]. The RsmA/CsrA family of RNA-binding proteins are highly conserved across different species of bacteria and multiple copies exist in some species. In a previous study [210], a *P. aeruginosa* RsmA homologue named RsmN was discovered. Negative regulation of the production of HCN, PYO, PA-IL lectin and AHL molecules and positive regulation of swarming motility, lipase and rhamnolipid production by RsmA have been demonstrated [121, 204]. Furthermore, the importance of the $Arg_{44}$ residue for the RNA-binding and biological function of RsmA was elucidated [53, 241]. Being an RsmA homologue, it was speculated that RsmN carries out overlapping roles with RsmA. Chapter 3 of this study establishes a regulatory network where RsmN controls the swarming motility, proteolytic and elastinolytic activities positively, and microcolony formation and Hcp1 secretion negatively.

The single deletion of *rsmN* affected swarming motility negatively and microcolony formation positively, however, the effect of *rsmN* deletion on other biological processes was masked due to the presence of an intact copy of RsmA which falls in line with the finding that RsmA controls *rsmF* (*rsmN*) translation in Marden *et al.* [206]. Nevertheless, the multicopy expression of *rsmN* restored the tested Δ*rsmA* phenotypes partially with the exception of PYO production. On the other hand, the multicopy expression of R62A mutant of *rsmN*, *rsmA*R44A equivalent, resulted in the loss of RsmN control over these biological processes, demonstrating the importance of the $Arg_{62}$ residue for the protein function. RNA-binding experiments elucidating the

role of $Arg_{62}$ for target binding of RsmN were conducted in a previous study [241], and it was concluded that like RsmAR44, RsmNR62 is also essential for RNA-binding. Distinct from the Δ*rsmA* phenotypes, the lack of both RsmA and RsmN resulted in excessive autolysis, rough colony morphology, elevated levels of the Hcp1 protein (required for the assembly of the secretion tube in T6SS) and a significant reduction in proteolytic and elastinolytic activities. Although the IPTG-induced expression of *rsmN* from the chromosomally inserted *tac* promoter only restored the total proteolytic and elastinolytic activities partially, plasmid-induced constitutive expression of *rsmN* complemented the swarming motility, proteolytic and elastinolytic activities, rough colony morphology of the $rsmN_{ind}$ Δ*rsmA* mutant and increased PYO production.

The total proteolytic activity in the $rsmN_{ind}$ Δ*rsmA* mutant was not restored by IPTG-induced *rsmN* expression at 37°C but it was partially restored at 34°C. Furthermore, positive modulation of the Δ*rsmA* swarming motility by multicopy expression of *rsmN* was not observed at 37°C but it was detected at temperatures below 37°C. It was also noted that the single deletion of *rsmN* led to a reduction in swarming motility as temperature decreased gradually from 37°C to 28°C. Based on these results it can be suggested that there is increased RsmN activity at lower temperatures. In an evolutionary approach, *rsmA* and *rsmN* might be transcribed by *P. aeruginosa* differentially at different temperatures. For instance, RsmA may be functionally dominant at 37°C and higher temperatures due to higher transcript levels in comparison with RsmN. In contrast, RsmN functions might become apparent at temperatures below 37°C due to a decrease in *rsmA* transcript levels and an increase in *rsmN* transcript levels both of which relieve the negative control of RsmA over RsmN. Detection of a 2.2 fold increase in *PA14_68470* (the *rsmN* orthologue in the PA14 strain) expression at 28°C compared to 37°C is in support of this theory [257]. Running qRT-PCR at a range of temperatures such as 25°C, 34°C, 37°C, and 42°C would provide evidence to the differential expression of *rsmA* and *rsmN* in a temperature dependent manner. Additionally, transcriptome profiles of the WT and Δ*rsmN* strains or the WT and *rsmN*-overexpressing strains of *P. aeruginosa* could be compared at environmental temperatures vs. host-associated temperatures.

The temperature dependence of RsmN regulation might also be due to conformational changes that alter protein folding and hence, affect target binding. A reduced amount

of RNA was co-purified with RsmN from a 34°C bacterial culture than a 37°C culture; this could be the outcome of conformational changes which mask the RNA-binding pocket slightly at 34°C. The influence of temperature on target binding of RsmN can be investigated in an isothermal titration calorimetry assay [291] or using small angle X-ray scattering (SAXS) [292]. Another possibility is that temperature change leads to the modification of the *phrX* transcript as it was concluded that the predicted transcription of *nmsR* does not influence RsmN regulation in Chapter 3. The *rsmN* gene overlaps the *phrX* gene and expression from the $P_{nmsR}$ promoter might influence *phrX* expression. RT-PCR can be used to check expression levels of *phrX* in samples with different levels of $P_{nmsR}$ induction to test this hypothesis. It is also possible that *phrX* acts as a thermosensor and due to the overlap between *rsmN* and *phrX* open reading frames, this thermosensor function is perceived as the temperature dependence of RsmN regulation.

As most phenotypes such as the reduced swarming motility and rough colony morphology investigated in this study reflect complex biological processes, RsmN targets were also identified in a genome-wide approach using RNASeq. Furthermore, RsmA RNASeq results obtained previously [212] were reanalysed. As outlined in Chapter 4, under the conditions chosen for RNASeq, RsmN had distinct as well as common targets with RsmA. RNASeq results supported by phenotypic data presented in both results chapters indicate indirect positive regulation of *cupA* expression, direct positive regulation of proteolytic activity, *lasB* and *crcZ* translation and negative regulation of T6SS by RsmA and RsmN; and downregulation of *rsmN* translation by RsmA (Figure 5.1). Further investigation by constructing transcriptional and translational reporter fusions is required to confirm these findings and to discover whether RsmN control on other target transcripts is positive or negative. RNASeq technique applied here can be improved by a) overexpressing *rsmN* in a Δ*rsmA* Δ*rsmN* mutant to minimise the effect of cross-regulation between RsmA and RsmN on co-purification of target transcripts b) optimising protein purification e.g. purifying RsmN from a Δ*rsmA* mutant by size exclusion chromatography and c) developing algorithms which quantify the enrichment data from the `.wig` files according to the number of enriched nucleotides and the length of an open reading frame. In addition, assessment of *rsmN* transcript levels by qRT-PCR in a cell-density-dependent manner may allow detection of more suitable conditions for RNASeq sampling in future analyses.

While i) comparison of the supernatant protein profiles and the number of c.f.u. formed by the *rsmN*$_{ind}$ Δ*rsmA* mutant with the WT strain, ii) detection of the cytosolic protein IscS in the *rsmA*$_{ind}$ Δ*rsmN* and *rsmN*$_{ind}$ Δ*rsmA* culture supernatants, and iii) rough colony morphologies of the *rsmA*$_{ind}$ Δ*rsmN* and *rsmN*$_{ind}$ Δ*rsmA* strains grown without IPTG provided pieces of evidence to the increased autolysis in the absence of both Rsm proteins, there were gaps in knowledge in terms of the mechanism involved. The *Pf4* prophage of PAO1, PQS/HHQ accumulation and carbon starvation have been linked to cellular lysis [56, 116, 117, 197] and, initially it has been speculated that rough colony morphologies of the *rsmA*$_{ind}$ Δ*rsmN* and *rsmN*$_{ind}$ Δ*rsmA* strains are due to PQS/HHQ accumulation or increased Pf4 prophage release. For this reason, colony morphologies of the WT, Δ*rsmA*, Δ*rsmN*, and *rsmN*$_{ind}$ Δ*rsmA* strains were compared with and without exogenous PQS/HHQ addition to the growth medium. Tendrils resembling wrinkles formed at the centre of the Δ*rsmA* colony with exogenous addition of 40 µM HHQ, however, the obtained colony morphology was not similar to the rough colony morphology of the *rsmN*$_{ind}$ Δ*rsmA* mutant. Therefore, a comparison of the PQS/HHQ levels of the WT, Δ*rsmA*, Δ*rsmN*, and *rsmN*$_{ind}$ Δ*rsmA* strains (-IPTG) is essential to reach a conclusion. On the other hand, a phage plaque assay performed with the same set of strains indicated higher levels of Pf4 release into the *rsmN*$_{ind}$ Δ*rsmA* culture supernatant, however, this finding requires quantification. Phage particles can be purified from single and double *rsmA* and *rsmN* deletion mutants and characterised in a PCR reaction using *Pf4*-specific primers and a control primer to check for interference by the chromosomal DNA.

Targets identified in RNASeq also offered possibilities such as the downregulation of denitrification enzymes, increased c-di-GMP levels, carbon starvation, increased membrane permeability and accumulation of aggregated proteins for the mechanism behind the autolysis of the *rsmN*$_{ind}$ Δ*rsmA* (-IPTG) mutant (Figure 5.1). Investigation of outer membrane protein profiles and intracellular redox state in single and double *rsmA* and *rsmN* deletion mutants, testing the growth of the *rsmN*$_{ind}$ Δ*rsmA* mutant on more carbon sources in minimal medium and under anaerobic conditions with and without $KNO_3$ and measurement of c-di-GMP levels in the *rsmN*$_{ind}$ Δ*rsmA* and WT strains are also necessary to narrow down the possible mechanisms behind *rsmN*$_{ind}$ Δ*rsmA* autolysis.

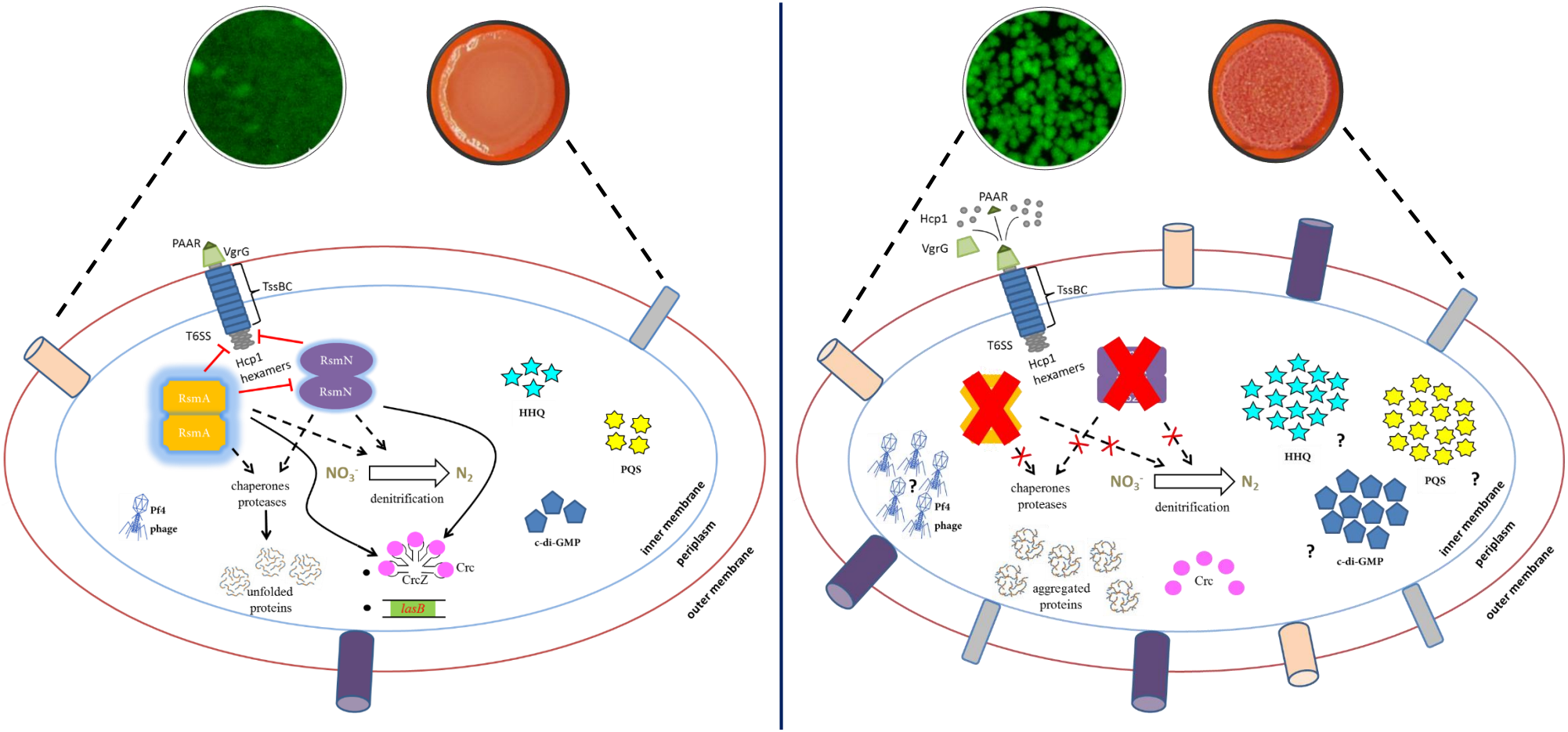
WT
rsmNind ΔrsmA -IPTG
PAAR
VgrG
TssBC
T6SS
Hcp1
hexamers
RsmN
RsmN
RsmA
RsmA
HHQ
PQS
chaperones
proteases
NO3-
N2
denitrification
Pf4
phage
c-di-GMP
CrcZ
Crc
unfolded
proteins
lasB
inner membrane
periplasm
outer membrane
aggregated
proteins

**Figure 5.1. A cellular diagram illustrating (left panel) the proposed negative regulation of T6SS, positive regulation of protease/chaperone levels, *crcZ* and *lasB* translation and the denitrification pathway by RsmA and RsmN, and the negative control by RsmA on *rsmN* in the WT strain characterised by a smooth colony morphology and flat undifferentiated biofilm phenotype, and (right panel) the possible mechanisms behind the excessive autolysis of the *rsmN*$_{ind}$ Δ*rsmA* mutant (-IPTG) characterised by a rough colony morphology and microcolony biofilm phenotype**

The Rsm proteins function as homodimers and research outlined in this study suggests that RsmN is less active than RsmA at 37°C (portrayed with a thin blue shadow around the RsmN dimer compared with RsmA). Experimental results of the current study, supported by related studies suggest that RsmA blocks *rsmN* translation and both Rsm proteins regulate T6SS negatively (red lines in the left panel). In *P. aeruginosa* T6SS, the secretion tube is made up of Hcp1 hexamers and the outer sheath is coded by *tssb-tssc*. Once T6SS is activated, the Hcp1, PAAR, and VgrG proteins are secreted outside (right panel) [294]. RsmA and RsmN upregulate translation of the *crcZ* and *lasB* transcripts coding the CrcZ sRNA antagonist to the Crc protein and a major protease, elastase, respectively (left panel). This connection between the Rsm proteins and the carbon metabolism via CrcZ-Crc suggests that carbon starvation is one of the factors enhancing *rsmN*$_{ind}$ Δ*rsmA* autolysis. It is also proposed that RsmA and RsmN regulate the synthesis of chaperones and proteases positively -aiding in refolding or cleavage of misfolded proteins- and outer membrane proteins (depicted as purple, beige and grey cylinders) negatively. Therefore, the double deletion of *rsmA* and *rsmN* might cause protein aggregation or increased membrane permeability. Additionally, in the absence of RsmA and RsmN, the intracellular redox state of the cell may be imbalanced due to a decrease in nitrate reduction (right panel). A comparison of left and right-hand sides of this diagram further illustrates that excessive autolysis of the *rsmN*$_{ind}$ Δ*rsmA* mutant might alternatively be caused by any of the following: elevated levels of the HHQ/PQS/c-di-GMP signalling molecules or the lytic Pf4 prophage.

Research presented in this thesis provides an evolutionary perspective on the Rsm system of *P. aeruginosa*. This study demonstrates that RsmN can function as an RsmA homologue biologically, however, conditions that promote maximal RsmN activity are distinctive and remain to be investigated in more detail. Experiments conducted so far suggest a differential expression of *rsmA* and *rsmN* at different temperatures and demonstrate a cross-regulation between the two proteins. Keeping the versatility of this opportunistic pathogen in mind, it can be proposed that RsmN has evolved to regulate the metabolism and virulence of *P. aeruginosa* when RsmA cannot fulfil its function. Nevertheless, targeting the Rsm system of *P. aeruginosa* for antivirulence therapy requires many more questions such as ‘which conditions stimulate the on/off switches of RsmA and RsmN?’, ‘is RsmN activity antagonised by the Rsm sRNAs and does RsmN control their translation?’, ‘in addition to robust microcolony formation, which mechanisms promote the survival of the *P. aeruginosa* cells lacking both Rsm proteins?’ to be answered.

## Supplementary Figures

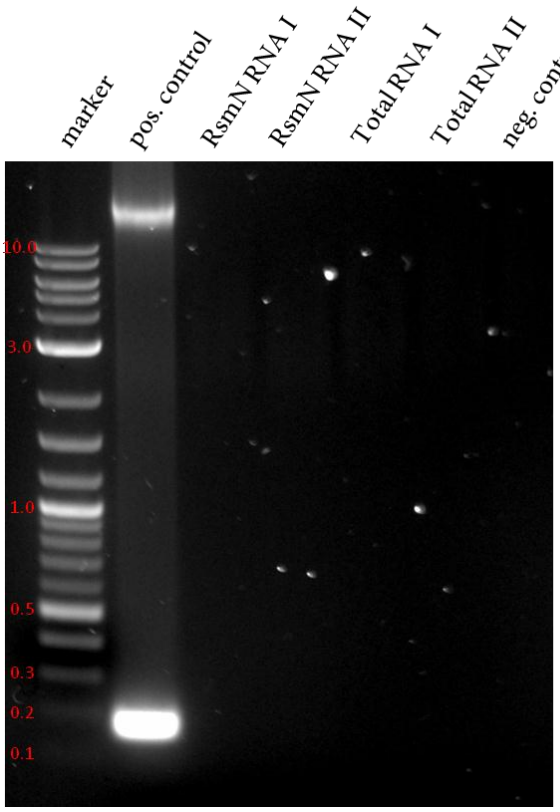


**Supplementary Figure 1. Genomic DNA removal from the RNA samples using Turbo DNase**

45 min. digestion with Turbo DNase removed the residual genomic DNA from the RsmN-bound and total RNA samples, demonstrated by the empty lanes to the right side of the positive control. As a positive control, PCR reaction was run with a wild-type PAO1-N colony using *rsmA* primers and the reaction mixture without any RNA template was included as a negative control. Quick-Load 2-Log DNA ladder (NEB) was used as the marker. Molecular weights (kb) of a few marker bands are shown in red (left).

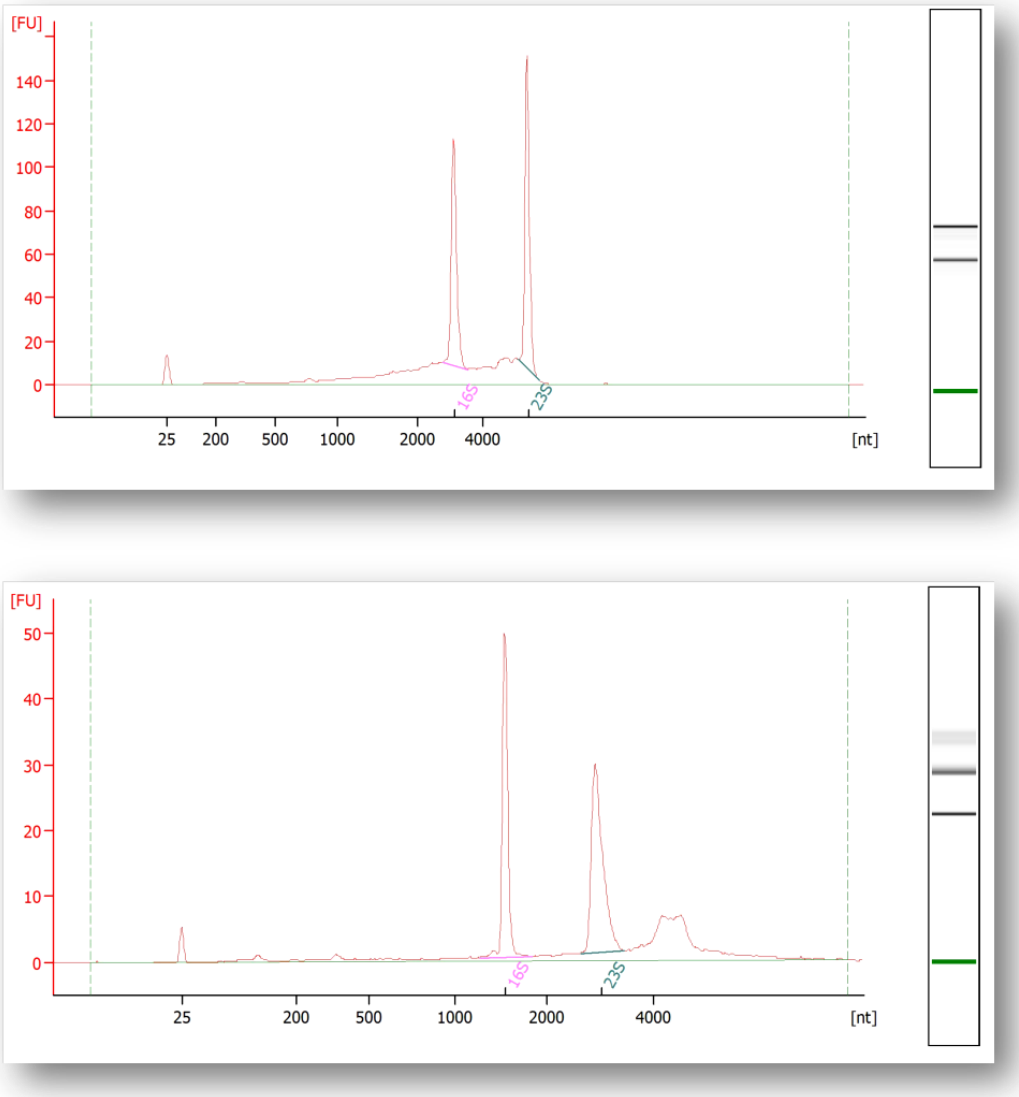


**Supplementary Figure 2. Agilent bioanalyzer electrograms of the total RNA purified from the PAO1-L/pMR4 strain cultured at 37°C (top panel) and 34°C (bottom panel)** Both RNA samples display clear peaks for the 16S (peak at 1536 nt) and 23S (peak at 2891 nt) rRNAs. The peak at 25 nt corresponds to the marker. The peak beyond 4000 nt (bottom panel) is suspected to be due to the use of SUPERase (Ambion®) during DNase treatment. The three prominent gel bands correspond to ~ 25 nt, 1700 nt and 3000 nt from bottom to top. *Top panel* RNA Area 458.7; RNA concentration: 124 ng/µL; rRNA ratio [23S/16S]: 1.0; RNA integrity number (RIN): 8.0 *Bottom panel* RNA Area 163.6; RNA concentration: 87 ng/µL; rRNA ratio [23S/16S]: 1.2; RIN: 9.5.

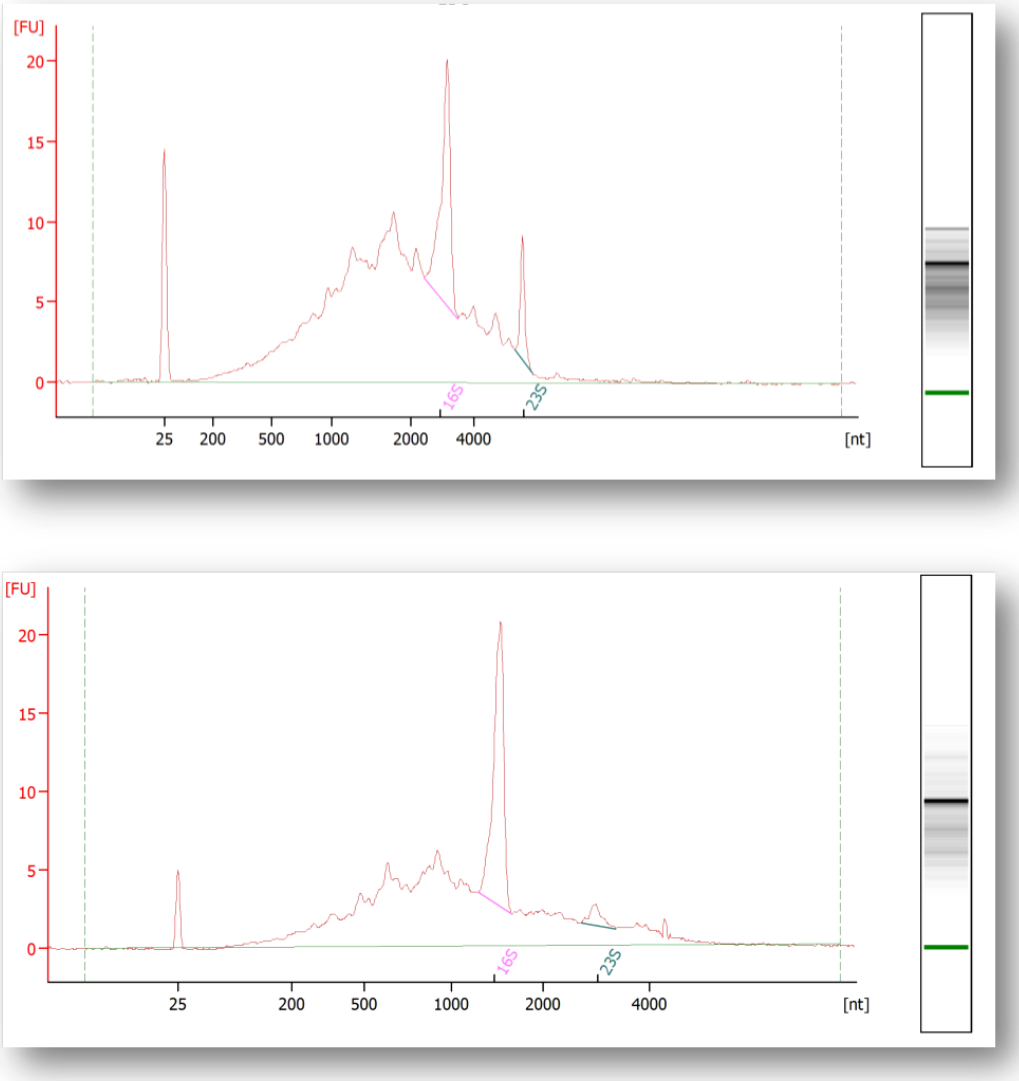


**Supplementary Figure 3. Agilent bioanalyzer electrograms of the RsmN-bound RNAs purified from the PAO1-L/pMR4 strain cultured at 37°C (top panel) and 34°C (bottom panel)**

The peak at 25 nt corresponds to the marker. The 16S rRNA (peak at 1536 nt) is detected for both samples, however, the 23S rRNA (peak at 2891 nt) is not prominent in the 34°C RNA sample (bottom panel). The peak beyond 4000 nt (bottom panel) is suspected to be due to the use of SUPERase (Ambion®) during DNase treatment. The spikes before the 16S rRNA peak reflect impurity of the RNA samples. The three prominent gel bands correspond to ~ 25 nt, 1700 nt and 3000 nt from bottom to top. *Top panel* RNA Area 277.2; RNA concentration: 75 ng/µL; rRNA ratio [23S/16S]: 0.2; RIN: 5.3 *Bottom panel* RNA Area 186.1; RNA concentration: 99 ng/µL; rRNA ratio [23S/16S]: 0.1; RIN: 5.5.

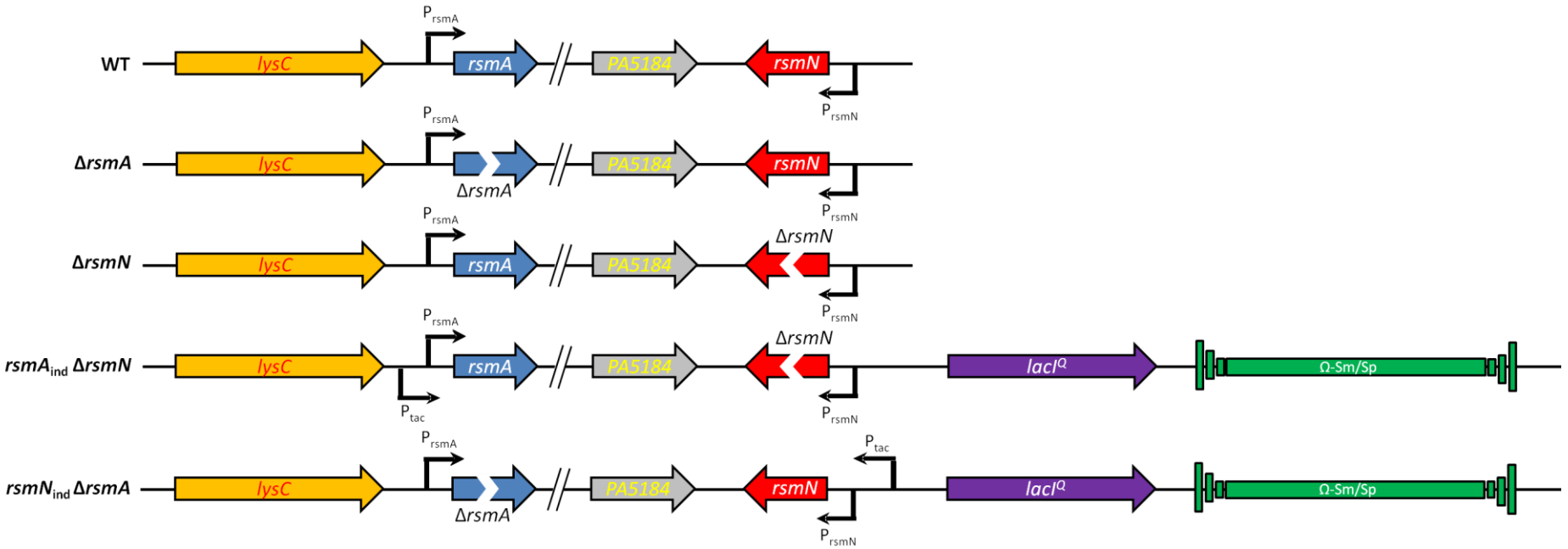


**Supplementary Figure 4. *P. aeruginosa* strains used in this study and their characteristics**

Deletion mutants were constructed using suicide plasmids. Illustrated are: *lysC* (orange), *rsmA* (blue), *PA5184* (grey), *rsmN* (red), *lacI*$^{Q}$ (purple) and Ω-cassette disruption/streptomycin-spectinomycin resistance (green). Mutated genes are depicted as disrupted arrows. Promoters of the *rsmA* and *rsmN* genes and *tac* promoter are represented by arrows upstream of the genes. In the case of inducible double deletion mutants, *rsmA* or *rsmN* expression was induced by the *tac* promoter. The figure is adapted from Lovelock L. [212].

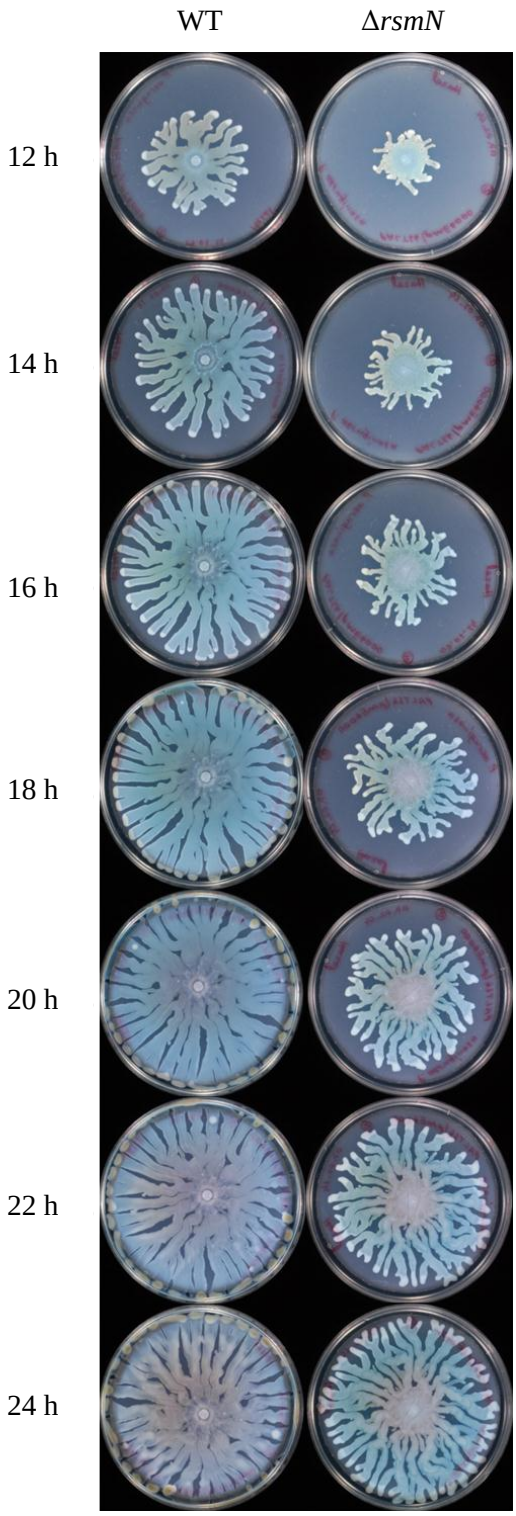


**Supplementary Figure 5. Swarming motilities of the WT and Δ*rsmN* strains on nutrient broth agar (0.5% w/v) monitored in a time-dependent manner at 37°C**
Swarmer cells of the WT strain reach to the edge of the petri dish 16 h post-inoculation. During this time, the Δ*rsmN* mutant spreads only halfway across the petri dish and reaches to the edge of the petri dish 24 h post-inoculation.

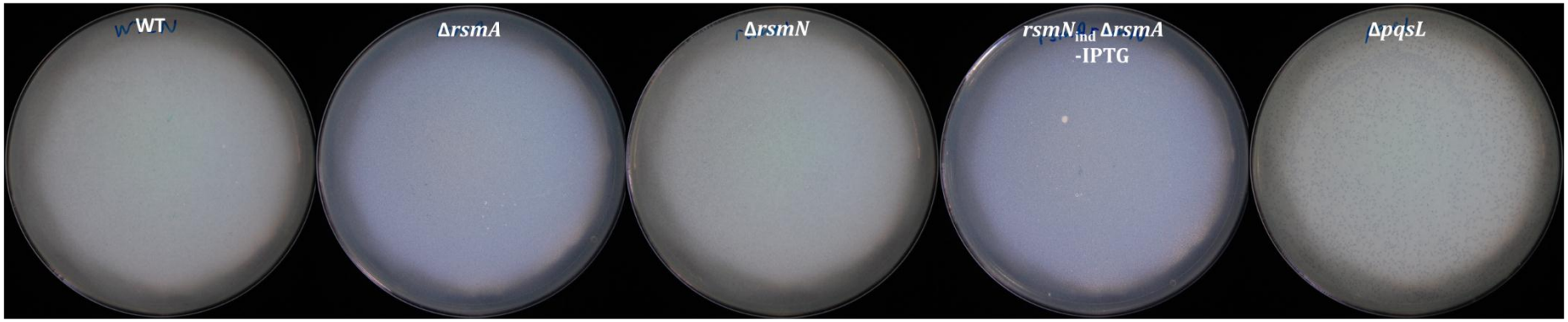


**Supplementary Figure 6. Surface of the soft top agar after spreading undiluted cell-free supernatants from the WT PAO1-N, Δ*rsmA*, Δ*rsmN*, *rsmN*$_{ind}$ Δ*rsmA* and Δ*pqsL* strains**

Plaque-like lysis zones are detected on the surface of the agar inoculated with the Δ*pqsL* strain which was included as a positive control. For the remaining strains, it was difficult to identify individual plaques. However, the transparency of the soft top agar inoculated with the Δ*rsmA* and *rsmN*$_{ind}$ Δ*rsmA* strains is an indication of increased autolysis.

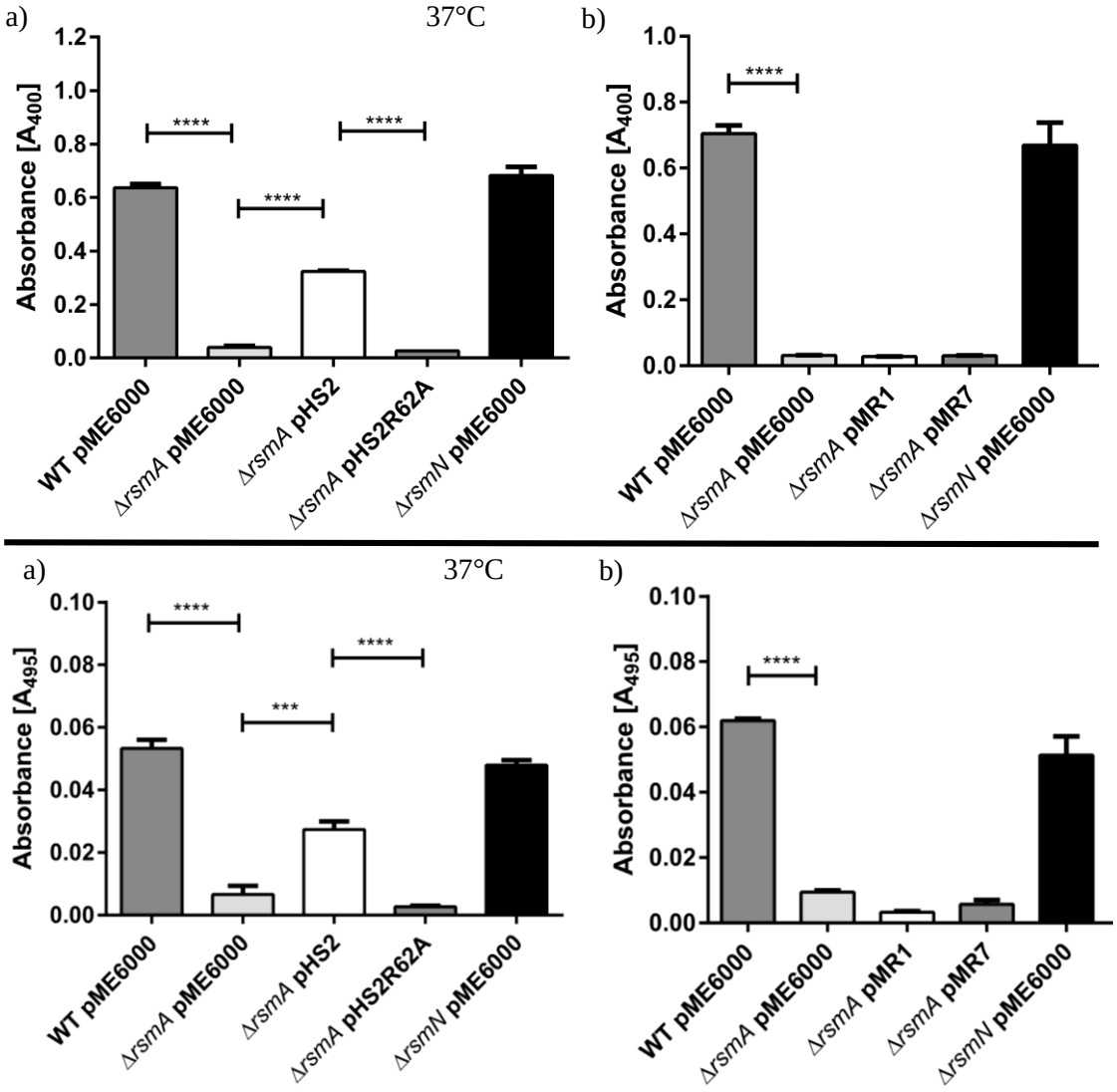


**Supplementary Figure 7. The effect of *rsmN* or *rsmN*R62A expression induced in the presence (a) or absence (b) of the $P_{rsmN}$ and $P_{nmsR}$ promoters on total proteolytic (top) and elastinolytic (bottom) activities of the Δ*rsmA*/pME6000 mutant at 37°C**

The deletion of *rsmN* does not, but the deletion of *rsmA* decreases proteolytic and elastinolytic activities significantly at 37°C. Expression of *rsmN* in the presence of the $P_{rsmN}$ and $P_{nmsR}$ promoters (via pHS2) increases the proteolytic and elastinolytic activities of the Δ*rsmA*/pME6000 mutant significantly, this complementary effect is lost with the R62A mutation of *rsmN* (pHS2R62A). Expression of *rsmN* via pMR1 which lacks the $P_{rsmN}$ and $P_{nmsR}$ promoters fails to complement the proteolytic and elastinolytic activities. The pMR7 vector (obtained by PCR using 2PRsmNF and PMR7R primers, see Table 2.3) is a derivative of pMR1 where *rsmN* is replaced by *rsmN*R62A. The proteolytic and elastinolytic activities of the Δ*rsmA*/pME6000 mutant are also not influenced by *rsmN*R62A expression (via pMR7) in the absence of the $P_{rsmN}$ and $P_{nmsR}$ promoters. Data represents averages of three independent absorbance measurements of the reaction buffer containing fractionated azocasein (protease assay)/Elastin-Congo red (elastase assay) and culture (grown in LB for 18 h) supernatants. Error bars represent standard error of the mean. Statistical differences were determined by ANOVA analysis, followed by Tukey multiple comparisons test; *** $p < 0.001$, **** $p < 0.0001$.

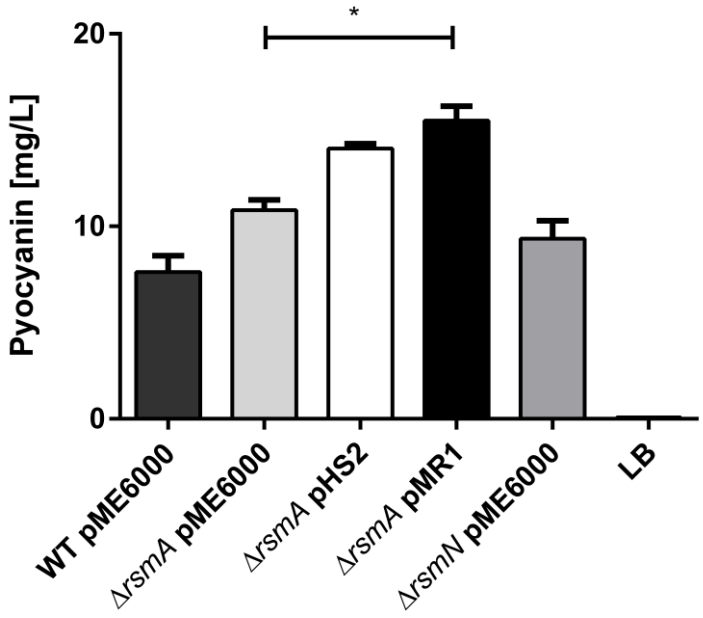


**Supplementary Figure 8. The effect of *rsmN* expression induced in the presence of the $P_{lac}$, $P_{rsmN}$ and $P_{nmsR}$ promoters (via pHS2) or the $P_{lac}$ promoter (pMR1) on PYO production of the Δ*rsmA*/pME6000 mutant in LB at 37°C**

The deletion of *rsmA* or *rsmN* does not influence PYO production at 37°C. Furthermore, the multicopy expression of *rsmN* in the presence of the $P_{rsmN}$ and $P_{nmsR}$ promoters (via pHS2) in the Δ*rsmA*/pME6000 strain does not affect PYO production significantly. On the other hand, the multicopy expression of *rsmN* induced by $P_{lac}$ in the absence of the $P_{rsmN}$ and $P_{nmsR}$ promoters (via pMR1) increases PYO production by the Δ*rsmA*/pME6000 strain significantly. Data represents averages of three independent extractions from cultures grown in LB for 18 h. Error bars represent standard error of the mean. Statistical differences were determined by ANOVA analysis, followed by Tukey multiple comparisons test; * $p < 0.05$.

# References


1. Beceiro A, Tomas M, Bou G: **Antimicrobial resistance and virulence: a successful or deleterious association in the bacterial world?** *Clin Microbiol Rev* 2013, **26**(2):185-230.
2. Tubby S, Wilson M, Nair SP: **Inactivation of staphylococcal virulence factors using a light-activated antimicrobial agent**. *BMC Microbiol* 2009, **9**:211.
3. Wu H, Song Z, Givskov M, Doring G, Worlitzsch D, Mathee K, Rygaard J, Hoiby N: ***Pseudomonas aeruginosa* mutations in *lasI* and *rhlI* quorum sensing systems result in milder chronic lung infection**. *Microbiology* 2001, **147**(Pt 5):1105-1113.
4. Russell AB, Hood RD, Bui NK, LeRoux M, Vollmer W, Mougous JD: **Type VI secretion delivers bacteriolytic effectors to target cells**. *Nature* 2011, **475**(7356):343-347.
5. Vora T, Hottes AK, Tavazoie S: **Protein occupancy landscape of a bacterial genome**. *Mol Cell* 2009, **35**(2):247-253.
6. Balleza E, Lopez-Bojorquez LN, Martinez-Antonio A, Resendis-Antonio O, Lozada-Chavez I, Balderas-Martinez YI, Encarnacion S, Collado-Vides J: **Regulation by transcription factors in bacteria: beyond description**. *FEMS Microbiol Rev* 2009, **33**(1):133-151.
7. Baumberg S: **Prokaryotic gene expression**. Oxford: Oxford University Press; 1999.
8. Van Assche E, Van Puyvelde S, Vanderleyden J, Steenackers HP: **RNA-binding proteins involved in post-transcriptional regulation in bacteria**. *Front Microbiol* 2015, **6**:141.
9. Timmermans J, Van Melderen L: **Post-transcriptional global regulation by CsrA in bacteria**. *Cell Mol Life Sci* 2010, **67**(17):2897-2908.
10. Lapouge K, Schubert M, Allain FH, Haas D: **Gac/Rsm signal transduction pathway of gamma-proteobacteria: from RNA recognition to regulation of social behaviour**. *Mol Microbiol* 2008, **67**(2):241-253.
11. Lehninger AL, Nelson DL, Cox MM: **Lehninger principles of biochemistry**, 4th edn. New York: W.H. Freeman; 2005.
12. Desnoyers G, Bouchard MP, Masse E: **New insights into small RNA-dependent translational regulation in prokaryotes**. *Trends Genet* 2013, **29**(2):92-98.
13. Shimoni Y, Friedlander G, Hetzroni G, Niv G, Altuvia S, Biham O, Margalit H: **Regulation of gene expression by small non-coding RNAs: a quantitative view**. *Mol Syst Biol* 2007, **3**:138.
14. Caldelari I, Chao Y, Romby P, Vogel J: **RNA-mediated regulation in pathogenic bacteria**. *Cold Spring Harb Perspect Med* 2013, **3**(9):a010298.
15. Richards GR, Vanderpool CK: **Molecular call and response: the physiology of bacterial small RNAs**. *Biochim Biophys Acta* 2011, **1809**(10):525-531.
16. Waters LS, Storz G: **Regulatory RNAs in bacteria**. *Cell* 2009, **136**(4):615-628.
17. Sonnleitner E, Haas D: **Small RNAs as regulators of primary and secondary metabolism in *Pseudomonas* species**. *Appl Microbiol Biotechnol* 2011, **91**(1):63-79.
18. Storz G, Vogel J, Wassarman KM: **Regulation by small RNAs in bacteria: expanding frontiers**. *Mol Cell* 2011, **43**(6):880-891.
19. Sonnleitner E, Gonzalez N, Sorger-Domenigg T, Heeb S, Richter AS, Backofen R, Williams P, Huttenhofer A, Haas D, Blasi U: **The small RNA PhrS stimulates synthesis of the *Pseudomonas aeruginosa* quinolone signal**. *Mol Microbiol* 2011, **80**(4):868-885.
20. Kay E, Humair B, Denervaud V, Riedel K, Spahr S, Eberl L, Valverde C, Haas D: **Two GacA-dependent small RNAs modulate the quorum-sensing response in *Pseudomonas aeruginosa***. *J Bacteriol* 2006, **188**(16):6026-6033.

21. Bejerano-Sagie M, Xavier KB: **The role of small RNAs in quorum sensing**. *Curr Opin Microbiol* 2007, **10**(2):189-198.
22. Hoe CH, Raabe CA, Rozhdestvensky TS, Tang TH: **Bacterial sRNAs: regulation in stress**. *Int J Med Microbiol* 2013, **303**(5):217-229.
23. Darfeuille F, Unoson C, Vogel J, Wagner EG: **An antisense RNA inhibits translation by competing with standby ribosomes**. *Mol Cell* 2007, **26**(3):381-392.
24. Brantl S: **Regulatory mechanisms employed by *cis*-encoded antisense RNAs**. *Curr Opin Microbiol* 2007, **10**(2):102-109.
25. Opdyke JA, Kang JG, Storz G: **GadY, a small-RNA regulator of acid response genes in *Escherichia coli***. *J Bacteriol* 2004, **186**(20):6698-6705.
26. Georg J, Hess WR: ***cis*-antisense RNA, another level of gene regulation in bacteria**. *Microbiol Mol Biol Rev* 2011, **75**(2):286-300.
27. Weaver KE: **Emerging plasmid-encoded antisense RNA regulated systems**. *Curr Opin Microbiol* 2007, **10**(2):110-116.
28. Gerdes K, Wagner EG: **RNA antitoxins**. *Curr Opin Microbiol* 2007, **10**(2):117-124.
29. Beisel CL, Storz G: **Base pairing small RNAs and their roles in global regulatory networks**. *FEMS Microbiol Rev* 2010, **34**(5):866-882.
30. Winkler WC, Breaker RR: **Regulation of bacterial gene expression by riboswitches**. *Annu Rev Microbiol* 2005, **59**:487-517.
31. Coppins RL, Hall KB, Groisman EA: **The intricate world of riboswitches**. *Curr Opin Microbiol* 2007, **10**(2):176-181.
32. Nudler E, Mironov AS: **The riboswitch control of bacterial metabolism**. *Trends Biochem Sci* 2004, **29**(1):11-17.
33. Henkin TM: **Riboswitch RNAs: using RNA to sense cellular metabolism**. *Genes Dev* 2008, **22**(24):3383-3390.
34. Mandal M, Breaker RR: **Gene regulation by riboswitches**. *Nat Rev Mol Cell Biol* 2004, **5**(6):451-463.
35. Krajewski SS, Narberhaus F: **Temperature-driven differential gene expression by RNA thermosensors**. *Biochim Biophys Acta* 2014, **1839**(10):978-988.
36. Waldminghaus T, Gaubig LC, Narberhaus F: **Genome-wide bioinformatic prediction and experimental evaluation of potential RNA thermometers**. *Mol Genet Genomics* 2007, **278**(5):555-564.
37. Grosso-Becerra MV, Croda-Garcia G, Merino E, Servin-Gonzalez L, Mojica-Espinosa R, Soberon-Chavez G: **Regulation of *Pseudomonas aeruginosa* virulence factors by two novel RNA thermometers**. *Proc Natl Acad Sci U S A* 2014, **111**(43):15562-15567.
38. Johansson J, Mandin P, Renzoni A, Chiaruttini C, Springer M, Cossart P: **An RNA thermosensor controls expression of virulence genes in *Listeria monocytogenes***. *Cell* 2002, **110**(5):551-561.
39. Bohme K, Steinmann R, Kortmann J, Seekircher S, Heroven AK, Berger E, Pisano F, Thiermann T, Wolf-Watz H, Narberhaus F *et al*: **Concerted actions of a thermo-labile regulator and a unique intergenic RNA thermosensor control *Yersinia* virulence**. *PLoS Pathog* 2012, **8**(2):e1002518.
40. Valverde R, Edwards L, Regan L: **Structure and function of KH domains**. *Febs J* 2008, **275**(11):2712-2726.
41. Chang KY, Ramos A: **The double-stranded RNA-binding motif, a versatile macromolecular docking platform**. *Febs J* 2005, **272**(9):2109-2117.
42. Clery A, Blatter M, Allain FH: **RNA recognition motifs: boring? Not quite**. *Curr Opin Struct Biol* 2008, **18**(3):290-298.
43. Maris C, Dominguez C, Allain FH: **The RNA recognition motif, a plastic RNA-binding platform to regulate post-transcriptional gene expression**. *Febs J* 2005, **272**(9):2118-2131.

44. Romeo T, Gong M, Liu MY, Brun-Zinkernagel AM: **Identification and molecular characterization of *csrA*, a pleiotropic gene from *Escherichia coli* that affects glycogen biosynthesis, gluconeogenesis, cell size, and surface properties**. *J Bacteriol* 1993, **175**(15):4744-4755.
45. Babitzke P, Baker CS, Romeo T: **Regulation of translation initiation by RNA binding proteins**. *Annu Rev Microbiol* 2009, **63**:27-44.
46. Heroven AK, Bohme K, Dersch P: **The Csr/Rsm system of *Yersinia* and related pathogens: a post-transcriptional strategy for managing virulence**. *RNA Biol* 2012, **9**(4):379-391.
47. Gutierrez P, Li Y, Osborne MJ, Pomerantseva E, Liu Q, Gehring K: **Solution structure of the carbon storage regulator protein CsrA from *Escherichia coli***. *J Bacteriol* 2005, **187**(10):3496-3501.
48. Romeo T, Vakulskas CA, Babitzke P: **Post-transcriptional regulation on a global scale: form and function of Csr/Rsm systems**. *Environ Microbiol* 2013, **15**(2):313-324.
49. Lucchetti-Miganeh C, Burrowes E, Baysse C, Ermel G: **The post-transcriptional regulator CsrA plays a central role in the adaptation of bacterial pathogens to different stages of infection in animal hosts**. *Microbiology* 2008, **154**(Pt 1):16-29.
50. Altier C, Suyemoto M, Lawhon SD: **Regulation of *Salmonella enterica* serovar typhimurium invasion genes by *csrA***. *Infect Immun* 2000, **68**(12):6790-6797.
51. Cui Y, Chatterjee A, Liu Y, Dumenyo CK, Chatterjee AK: **Identification of a global repressor gene, *rsmA*, of *Erwinia carotovora* subsp. *carotovora* that controls extracellular enzymes, *N*-(3-oxohexanoyl)-L-homoserine lactone, and pathogenicity in soft-rotting *Erwinia* spp**. *J Bacteriol* 1995, **177**(17):5108-5115.
52. Liu MY, Yang H, Romeo T: **The product of the pleiotropic *Escherichia coli* gene *csrA* modulates glycogen biosynthesis via effects on mRNA stability**. *J Bacteriol* 1995, **177**(10):2663-2672.
53. Heeb S, Kuehne SA, Bycroft M, Crivii S, Allen MD, Haas D, Camara M, Williams P: **Functional analysis of the post-transcriptional regulator RsmA reveals a novel RNA-binding site**. *J Mol Biol* 2006, **355**(5):1026-1036.
54. Figueroa-Bossi N, Schwartz A, Guillemardet B, D'Heygere F, Bossi L, Boudvillain M: **RNA remodeling by bacterial global regulator CsrA promotes Rho-dependent transcription termination**. *Genes Dev* 2014, **28**(11):1239-1251.
55. Schubert M, Lapouge K, Duss O, Oberstrass FC, Jelesarov I, Haas D, Allain FH: **Molecular basis of messenger RNA recognition by the specific bacterial repressing clamp RsmA/CsrA**. *Nat Struct Mol Biol* 2007, **14**(9):807-813.
56. Pernestig AK, Georgellis D, Romeo T, Suzuki K, Tomenius H, Normark S, Melefors O: **The *Escherichia coli* BarA-UvrY two-component system is needed for efficient switching between glycolytic and gluconeogenic carbon sources**. *J Bacteriol* 2003, **185**(3):843-853.
57. Vogel J, Luisi BF: **Hfq and its constellation of RNA**. *Nat Rev Microbiol* 2011, **9**(8):578-589.
58. Livny J, Brencic A, Lory S, Waldor MK: **Identification of 17 *Pseudomonas aeruginosa* sRNAs and prediction of sRNA-encoding genes in 10 diverse pathogens using the bioinformatic tool sRNAPredict2**. *Nucleic Acids Res* 2006, **34**(12):3484-3493.
59. Nogueira T, Springer M: **Post-transcriptional control by global regulators of gene expression in bacteria**. *Curr Opin Microbiol* 2000, **3**(2):154-158.
60. Gottesman S, Storz G: **Bacterial small RNA regulators: versatile roles and rapidly evolving variations**. *Cold Spring Harb Perspect Biol* 2011, **3**(12).
61. Fender A, Elf J, Hampel K, Zimmermann B, Wagner EG: **RNAs actively cycle on the Sm-like protein Hfq**. *Genes Dev* 2010, **24**(23):2621-2626.

62. Bruckner R, Titgemeyer F: **Carbon catabolite repression in bacteria: choice of the carbon source and autoregulatory limitation of sugar utilization**. *FEMS Microbiol Lett* 2002, **209**(2):141-148.
63. Gorke B, Stulke J: **Carbon catabolite repression in bacteria: many ways to make the most out of nutrients**. *Nat Rev Microbiol* 2008, **6**(8):613-624.
64. Collier DN, Hager PW, Phibbs PV, Jr.: **Catabolite repression control in the *Pseudomonads***. *Res Microbiol* 1996, **147**(6-7):551-561.
65. Wolff JA, MacGregor CH, Eisenberg RC, Phibbs PV, Jr.: **Isolation and characterization of catabolite repression control mutants of *Pseudomonas aeruginosa* PAO**. *J Bacteriol* 1991, **173**(15):4700-4706.
66. MacGregor CH, Wolff JA, Arora SK, Phibbs PV, Jr.: **Cloning of a catabolite repression control (*crc*) gene from *Pseudomonas aeruginosa*, expression of the gene in *Escherichia coli*, and identification of the gene product in *Pseudomonas aeruginosa***. *J Bacteriol* 1991, **173**(22):7204-7212.
67. Linares JF, Moreno R, Fajardo A, Martinez-Solano L, Escalante R, Rojo F, Martinez JL: **The global regulator Crc modulates metabolism, susceptibility to antibiotics and virulence in *Pseudomonas aeruginosa***. *Environ Microbiol* 2010, **12**(12):3196-3212.
68. Sonnleitner E, Abdou L, Haas D: **Small RNA as global regulator of carbon catabolite repression in *Pseudomonas aeruginosa***. *Proc Natl Acad Sci U S A* 2009, **106**(51):21866-21871.
69. O'Toole GA, Gibbs KA, Hager PW, Phibbs PV, Jr., Kolter R: **The global carbon metabolism regulator Crc is a component of a signal transduction pathway required for biofilm development by *Pseudomonas aeruginosa***. *J Bacteriol* 2000, **182**(2):425-431.
70. Wadhams GH, Armitage JP: **Making sense of it all: bacterial chemotaxis**. *Nat Rev Mol Cell Biol* 2004, **5**(12):1024-1037.
71. Stock AM, Robinson VL, Goudreau PN: **Two-component signal transduction**. *Annu Rev Biochem* 2000, **69**:183-215.
72. Paterson GK, Blue CE, Mitchell TJ: **Role of two-component systems in the virulence of *Streptococcus pneumoniae***. *J Med Microbiol* 2006, **55**(Pt 4):355-363.
73. Rodrigue A, Quentin Y, Lazdunski A, Mejean V, Foglino M: **Two-component systems in *Pseudomonas aeruginosa*: why so many?** *Trends Microbiol* 2000, **8**(11):498-504.
74. Gotoh Y, Eguchi Y, Watanabe T, Okamoto S, Doi A, Utsumi R: **Two-component signal transduction as potential drug targets in pathogenic bacteria**. *Curr Opin Microbiol* 2010, **13**(2):232-239.
75. Capra EJ, Laub MT: **Evolution of two-component signal transduction systems**. *Annu Rev Microbiol* 2012, **66**:325-347.
76. Pirrung MC: **Histidine kinases and two-component signal transduction systems**. *Chem Biol* 1999, **6**(6):R167-175.
77. Konkel ME, Tilly K: **Temperature-regulated expression of bacterial virulence genes**. *Microbes Infect* 2000, **2**(2):157-166.
78. Alm E, Huang K, Arkin A: **The evolution of two-component systems in bacteria reveals different strategies for niche adaptation**. *PLoS Comput Biol* 2006, **2**(11):e143.
79. Mondragon V, Franco B, Jonas K, Suzuki K, Romeo T, Melefors O, Georgellis D: **pH-dependent activation of the BarA-UvrY two-component system in *Escherichia coli***. *J Bacteriol* 2006, **188**(23):8303-8306.
80. Herren CD, Mitra A, Palaniyandi SK, Coleman A, Elankumaran S, Mukhopadhyay S: **The BarA-UvrY two-component system regulates virulence in avian pathogenic *Escherichia coli* O78:K80:H9**. *Infect Immun* 2006, **74**(8):4900-4909.

81. Mukhopadhyay S, Schellhorn HE: **Identification and characterization of hydrogen peroxide-sensitive mutants of *Escherichia coli*: genes that require OxyR for expression**. *J Bacteriol* 1997, **179**(2):330-338.
82. Pernestig AK, Melefors O, Georgellis D: **Identification of UvrY as the cognate response regulator for the BarA sensor kinase in *Escherichia coli***. *J Biol Chem* 2001, **276**(1):225-231.
83. Vakulskas CA, Potts AH, Babitzke P, Ahmer BM, Romeo T: **Regulation of bacterial virulence by Csr (Rsm) systems**. *Microbiol Mol Biol Rev* 2015, **79**(2):193-224.
84. Zhang JP, Normark S: **Induction of gene expression in *Escherichia coli* after pilus-mediated adherence**. *Science* 1996, **273**(5279):1234-1236.
85. Suzuki K, Wang X, Weilbacher T, Pernestig AK, Melefors O, Georgellis D, Babitzke P, Romeo T: **Regulatory circuitry of the CsrA/CsrB and BarA/UvrY systems of *Escherichia coli***. *J Bacteriol* 2002, **184**(18):5130-5140.
86. Chavez RG, Alvarez AF, Romeo T, Georgellis D: **The physiological stimulus for the BarA sensor kinase**. *J Bacteriol* 2010, **192**(7):2009-2012.
87. Palaniyandi S, Mitra A, Herren CD, Lockatell CV, Johnson DE, Zhu X, Mukhopadhyay S: **BarA-UvrY two-component system regulates virulence of uropathogenic *E. coli* CFT073**. *PLoS One* 2012, **7**(2):e31348.
88. Nishijyo T, Haas D, Itoh Y: **The CbrA-CbrB two-component regulatory system controls the utilization of multiple carbon and nitrogen sources in *Pseudomonas aeruginosa***. *Mol Microbiol* 2001, **40**(4):917-931.
89. Li W, Lu CD: **Regulation of carbon and nitrogen utilization by CbrAB and NtrBC two-component systems in *Pseudomonas aeruginosa***. *J Bacteriol* 2007, **189**(15):5413-5420.
90. Abdou L, Chou HT, Haas D, Lu CD: **Promoter recognition and activation by the global response regulator CbrB in *Pseudomonas aeruginosa***. *J Bacteriol* 2011, **193**(11):2784-2792.
91. Sonnleitner E, Valentini M, Wenner N, Haichar FZ, Haas D, Lapouge K: **Novel targets of the CbrAB/Crc carbon catabolite control system revealed by transcript abundance in *Pseudomonas aeruginosa***. *PLoS One* 2012, **7**(10):e44637.
92. Zhang XX, Rainey PB: **Dual involvement of CbrAB and NtrBC in the regulation of histidine utilization in *Pseudomonas fluorescens* SBW25**. *Genetics* 2008, **178**(1):185-195.
93. Gerth ML, Ferla MP, Rainey PB: **The origin and ecological significance of multiple branches for histidine utilization in *Pseudomonas aeruginosa* PAO1**. *Environ Microbiol* 2012, **14**(8):1929-1940.
94. Itoh Y: **Cloning and characterization of the *aru* genes encoding enzymes of the catabolic arginine succinyltransferase pathway in *Pseudomonas aeruginosa***. *J Bacteriol* 1997, **179**(23):7280-7290.
95. Humair B, Gonzalez N, Mossialos D, Reimmann C, Haas D: **Temperature-responsive sensing regulates biocontrol factor expression in *Pseudomonas fluorescens* CHA0**. *Isme J* 2009, **3**(8):955-965.
96. Workentine ML, Chang L, Ceri H, Turner RJ: **The GacS-GacA two-component regulatory system of *Pseudomonas fluorescens*: a bacterial two-hybrid analysis**. *FEMS Microbiol Lett* 2009, **292**(1):50-56.
97. Heeb S, Blumer C, Haas D: **Regulatory RNA as mediator in GacA/RsmA-dependent global control of exoproduct formation in *Pseudomonas fluorescens* CHA0**. *J Bacteriol* 2002, **184**(4):1046-1056.
98. Lapouge K, Sineva E, Lindell M, Starke K, Baker CS, Babitzke P, Haas D: **Mechanism of *hcnA* mRNA recognition in the Gac/Rsm signal transduction pathway of *Pseudomonas fluorescens***. *Mol Microbiol* 2007, **66**(2):341-356.

99. Takeuchi K, Kiefer P, Reimmann C, Keel C, Dubuis C, Rolli J, Vorholt JA, Haas D: **Small RNA-dependent expression of secondary metabolism is controlled by Krebs cycle function in *Pseudomonas fluorescens***. *J Biol Chem* 2009, **284**(50):34976-34985.
100. Seaton SC, Silby MW, Levy SB: **Pleiotropic effects of GacA on *Pseudomonas fluorescens* Pf0-1 *in vitro* and in soil**. *Appl Environ Microbiol* 2013, **79**(17):5405-5410.
101. Cooley M, Chhabra SR, Williams P: ***N*-acylhomoserine lactone-mediated quorum sensing: a twist in the tail and a blow for host immunity**. *Chem Biol* 2008, **15**(11):1141-1147.
102. Finch RG, Pritchard DI, Bycroft BW, Williams P, Stewart GS: **Quorum sensing: a novel target for anti-infective therapy**. *J Antimicrob Chemother* 1998, **42**(5):569-571.
103. de Kievit TR, Iglewski BH: **Bacterial quorum sensing in pathogenic relationships**. *Infect Immun* 2000, **68**(9):4839-4849.
104. Ramos J-L, Goldberg JB, Filloux A: ***Pseudomonas*, vol. 7.** New York: Kluwer Academic/Plenum Publishers; 2015.
105. Filiatrault MJ, Picardo KF, Ngai H, Passador L, Iglewski BH: **Identification of *Pseudomonas aeruginosa* genes involved in virulence and anaerobic growth**. *Infect Immun* 2006, **74**(7):4237-4245.
106. Van Alst NE, Sherrill LA, Iglewski BH, Haidaris CG: **Compensatory periplasmic nitrate reductase activity supports anaerobic growth of *Pseudomonas aeruginosa* PAO1 in the absence of membrane nitrate reductase**. *Can J Microbiol* 2009, **55**(10):1133-1144.
107. Overhage J, Bains M, Brazas MD, Hancock RE: **Swarming of *Pseudomonas aeruginosa* is a complex adaptation leading to increased production of virulence factors and antibiotic resistance**. *J Bacteriol* 2008, **190**(8):2671-2679.
108. Yeung AT, Torfs EC, Jamshidi F, Bains M, Wiegand I, Hancock RE, Overhage J: **Swarming of *Pseudomonas aeruginosa* is controlled by a broad spectrum of transcriptional regulators, including MetR**. *J Bacteriol* 2009, **191**(18):5592-5602.
109. Williams P, Winzer K, Chan WC, Camara M: **Look who's talking: communication and quorum sensing in the bacterial world**. *Philos Trans R Soc Lond B Biol Sci* 2007, **362**(1483):1119-1134.
110. Stover CK, Pham XQ, Erwin AL, Mizoguchi SD, Warrener P, Hickey MJ, Brinkman FS, Hufnagle WO, Kowalik DJ, Lagrou M *et al*: **Complete genome sequence of *Pseudomonas aeruginosa* PAO1, an opportunistic pathogen**. *Nature* 2000, **406**(6799):959-964.
111. Antunes LC, Ferreira RB, Buckner MM, Finlay BB: **Quorum sensing in bacterial virulence**. *Microbiology* 2010, **156**(Pt 8):2271-2282.
112. Jimenez PN, Koch G, Thompson JA, Xavier KB, Cool RH, Quax WJ: **The multiple signaling systems regulating virulence in *Pseudomonas aeruginosa***. *Microbiol Mol Biol Rev* 2012, **76**(1):46-65.
113. Shrout JD, Chopp DL, Just CL, Hentzer M, Givskov M, Parsek MR: **The impact of quorum sensing and swarming motility on *Pseudomonas aeruginosa* biofilm formation is nutritionally conditional**. *Mol Microbiol* 2006, **62**(5):1264-1277.
114. Donlan RM, Costerton JW: **Biofilms: survival mechanisms of clinically relevant microorganisms**. *Clin Microbiol Rev* 2002, **15**(2):167-193.
115. Schleheck D, Barraud N, Klebensberger J, Webb JS, McDougald D, Rice SA, Kjelleberg S: ***Pseudomonas aeruginosa* PAO1 preferentially grows as aggregates in liquid batch cultures and disperses upon starvation**. *PLoS One* 2009, **4**(5):e5513.
116. Webb JS, Thompson LS, James S, Charlton T, Tolker-Nielsen T, Koch B, Givskov M, Kjelleberg S: **Cell death in *Pseudomonas aeruginosa* biofilm development**. *J Bacteriol* 2003, **185**(15):4585-4592.

117. Rice SA, Tan CH, Mikkelsen PJ, Kung V, Woo J, Tay M, Hauser A, McDougald D, Webb JS, Kjelleberg S: **The biofilm life cycle and virulence of *Pseudomonas aeruginosa* are dependent on a filamentous prophage**. *Isme J* 2009, **3**(3):271-282.
118. Morris JD, Hewitt JL, Wolfe LG, Kamatkar NG, Chapman SM, Diener JM, Courtney AJ, Leevy WM, Shrout JD: **Imaging and analysis of *Pseudomonas aeruginosa* swarming and rhamnolipid production**. *Appl Environ Microbiol* 2011, **77**(23):8310-8317.
119. Tremblay J, Deziel E: **Gene expression in *Pseudomonas aeruginosa* swarming motility**. *BMC Genomics* 2010, **11**:587.
120. Kearns DB: **A field guide to bacterial swarming motility**. *Nat Rev Microbiol* 2010, **8**(9):634-644.
121. Heurlier K, Williams F, Heeb S, Dormond C, Pessi G, Singer D, Camara M, Williams P, Haas D: **Positive control of swarming, rhamnolipid synthesis, and lipase production by the posttranscriptional RsmA/RsmZ system in *Pseudomonas aeruginosa* PAO1**. *J Bacteriol* 2004, **186**(10):2936-2945.
122. Goodman AL, Kulasekara B, Rietsch A, Boyd D, Smith RS, Lory S: **A signaling network reciprocally regulates genes associated with acute infection and chronic persistence in *Pseudomonas aeruginosa***. *Dev Cell* 2004, **7**(5):745-754.
123. Yoon MY, Lee KM, Park Y, Yoon SS: **Contribution of cell elongation to the biofilm formation of *Pseudomonas aeruginosa* during anaerobic respiration**. *PLoS One* 2011, **6**(1):e16105.
124. Li XZ, Livermore DM, Nikaido H: **Role of efflux pump(s) in intrinsic resistance of *Pseudomonas aeruginosa*: resistance to tetracycline, chloramphenicol, and norfloxacin**. *Antimicrob Agents Chemother* 1994, **38**(8):1732-1741.
125. Poole K: ***Pseudomonas aeruginosa*: resistance to the max**. *Front Microbiol* 2011, **2**:65.
126. Poole K: **Multidrug efflux pumps and antimicrobial resistance in *Pseudomonas aeruginosa* and related organisms**. *J Mol Microbiol Biotechnol* 2001, **3**(2):255-264.
127. Livermore DM: **Multiple mechanisms of antimicrobial resistance in *Pseudomonas aeruginosa*: our worst nightmare?** *Clin Infect Dis* 2002, **34**(5):634-640.
128. Lamarche MG, Deziel E: **MexEF-OprN efflux pump exports the *Pseudomonas* quinolone signal (PQS) precursor HHQ (4-hydroxy-2-heptylquinoline)**. *PLoS One* 2011, **6**(9):e24310.
129. Pearson JP, Van Delden C, Iglewski BH: **Active efflux and diffusion are involved in transport of *Pseudomonas aeruginosa* cell-to-cell signals**. *J Bacteriol* 1999, **181**(4):1203-1210.
130. Passador L, Cook JM, Gambello MJ, Rust L, Iglewski BH: **Expression of *Pseudomonas aeruginosa* virulence genes requires cell-to-cell communication**. *Science* 1993, **260**(5111):1127-1130.
131. Van Delden C, Iglewski BH: **Cell-to-cell signaling and *Pseudomonas aeruginosa* infections**. *Emerg Infect Dis* 1998, **4**(4):551-560.
132. Williams P: **Quorum sensing, communication and cross-kingdom signalling in the bacterial world**. *Microbiology* 2007, **153**(Pt 12):3923-3938.
133. Campa M, Bendinelli M, Friedman H: ***Pseudomonas aeruginosa* as an opportunistic pathogen**. New York: Plenum Press; 1993.
134. Huang J, Sonnleitner E, Ren B, Xu Y, Haas D: **Catabolite repression control of pyocyanin biosynthesis at an intersection of primary and secondary metabolism in *Pseudomonas aeruginosa***. *Appl Environ Microbiol* 2012, **78**(14):5016-5020.
135. Priyaja P, Jayesh P, Philip R, Bright Singh IS: **Pyocyanin induced *in vitro* oxidative damage and its toxicity level in human, fish and insect cell lines for its selective biological applications**. *Cytotechnology* 2014.

136. Dietrich LE, Price-Whelan A, Petersen A, Whiteley M, Newman DK: **The phenazine pyocyanin is a terminal signalling factor in the quorum sensing network of *Pseudomonas aeruginosa***. *Mol Microbiol* 2006, **61**(5):1308-1321.
137. Kessler E, Safrin M, Olson JC, Ohman DE: **Secreted LasA of *Pseudomonas aeruginosa* is a staphylolytic protease**. *J Biol Chem* 1993, **268**(10):7503-7508.
138. Filloux A, Ramos J-L: ***Pseudomonas* Methods and Protocols**. Methods in Molecular Biology, 1149. New York: Humana Press; 2014.
139. Liu PV: **Extracellular toxins of *Pseudomonas aeruginosa***. *J Infect Dis* 1974, **130 Suppl**(0):S94-99.
140. Morihara K, Tsuzuki H, Oka T, Inoue H, Ebata M: ***Pseudomonas aeruginosa* Elastase. Isolation, Crystallization, and Preliminary Characterization**. *J Biol Chem* 1965, **240**:3295-3304.
141. Heck LW, Morihara K, Abrahamson DR: **Degradation of soluble laminin and depletion of tissue-associated basement membrane laminin by *Pseudomonas aeruginosa* elastase and alkaline protease**. *Infect Immun* 1986, **54**(1):149-153.
142. Heck LW, Morihara K, McRae WB, Miller EJ: **Specific cleavage of human type III and IV collagens by *Pseudomonas aeruginosa* elastase**. *Infect Immun* 1986, **51**(1):115-118.
143. Schultz DR, Miller KD: **Elastase of *Pseudomonas aeruginosa*: inactivation of complement components and complement-derived chemotactic and phagocytic factors**. *Infect Immun* 1974, **10**(1):128-135.
144. Cowell BA, Twining SS, Hobden JA, Kwong MS, Fleiszig SM: **Mutation of *lasA* and *lasB* reduces *Pseudomonas aeruginosa* invasion of epithelial cells**. *Microbiology* 2003, **149**(Pt 8):2291-2299.
145. Ohman DE, Cryz SJ, Iglewski BH: **Isolation and characterization of *Pseudomonas aeruginosa* PAO mutant that produces altered elastase**. *J Bacteriol* 1980, **142**(3):836-842.
146. Park PW, Pier GB, Preston MJ, Goldberger O, Fitzgerald ML, Bernfield M: **Syndecan-1 shedding is enhanced by LasA, a secreted virulence factor of *Pseudomonas aeruginosa***. *J Biol Chem* 2000, **275**(5):3057-3064.
147. Filloux A: **Protein Secretion Systems in *Pseudomonas aeruginosa*: An Essay on Diversity, Evolution, and Function**. *Front Microbiol* 2011, **2**:155.
148. Wretlind B, Pavlovskis OR: **Genetic mapping and characterization of *Pseudomonas aeruginosa* mutants defective in the formation of extracellular proteins**. *J Bacteriol* 1984, **158**(3):801-808.
149. Tommassen J, Filloux A, Bally M, Murgier M, Lazdunski A: **Protein secretion in *Pseudomonas aeruginosa***. *FEMS Microbiol Rev* 1992, **9**(1):73-90.
150. Ball G, Durand E, Lazdunski A, Filloux A: **A novel type II secretion system in *Pseudomonas aeruginosa***. *Mol Microbiol* 2002, **43**(2):475-485.
151. Guzzo J, Pages JM, Duong F, Lazdunski A, Murgier M: ***Pseudomonas aeruginosa* alkaline protease: evidence for secretion genes and study of secretion mechanism**. *J Bacteriol* 1991, **173**(17):5290-5297.
152. Dacheux D, Goure J, Chabert J, Usson Y, Attree I: **Pore-forming activity of type III system-secreted proteins leads to oncosis of *Pseudomonas aeruginosa*-infected macrophages**. *Mol Microbiol* 2001, **40**(1):76-85.
153. Bladergroen MR, Badelt K, Spaink HP: **Infection-blocking genes of a symbiotic *Rhizobium leguminosarum* strain that are involved in temperature-dependent protein secretion**. *Mol Plant Microbe Interact* 2003, **16**(1):53-64.
154. Mougous JD, Cuff ME, Raunser S, Shen A, Zhou M, Gifford CA, Goodman AL, Joachimiak G, Ordonez CL, Lory S *et al*: **A virulence locus of *Pseudomonas aeruginosa* encodes a protein secretion apparatus**. *Science* 2006, **312**(5779):1526-1530.

155. Filloux A, Hachani A, Bleves S: **The bacterial type VI secretion machine: yet another player for protein transport across membranes**. *Microbiology* 2008, **154**(Pt 6):1570-1583.
156. Leiman PG, Basler M, Ramagopal UA, Bonanno JB, Sauder JM, Pukatzki S, Burley SK, Almo SC, Mekalanos JJ: **Type VI secretion apparatus and phage tail-associated protein complexes share a common evolutionary origin**. *Proc Natl Acad Sci U S A* 2009, **106**(11):4154-4159.
157. Pell LG, Kanelis V, Donaldson LW, Howell PL, Davidson AR: **The phage lambda major tail protein structure reveals a common evolution for long-tailed phages and the type VI bacterial secretion system**. *Proc Natl Acad Sci U S A* 2009, **106**(11):4160-4165.
158. Hood RD, Singh P, Hsu F, Guvener T, Carl MA, Trinidad RR, Silverman JM, Ohlson BB, Hicks KG, Plemel RL *et al*: **A type VI secretion system of *Pseudomonas aeruginosa* targets a toxin to bacteria**. *Cell Host Microbe* 2010, **7**(1):25-37.
159. Schwarz S, Hood RD, Mougous JD: **What is type VI secretion doing in all those bugs?** *Trends Microbiol* 2010, **18**(12):531-537.
160. Filloux A: **The type VI secretion system: a tubular story**. *Embo J* 2009, **28**(4):309-310.
161. Potvin E, Lehoux DE, Kukavica-Ibrulj I, Richard KL, Sanschagrin F, Lau GW, Levesque RC: ***In vivo* functional genomics of *Pseudomonas aeruginosa* for high-throughput screening of new virulence factors and antibacterial targets**. *Environ Microbiol* 2003, **5**(12):1294-1308.
162. Rampioni G, Schuster M, Greenberg EP, Bertani I, Grasso M, Venturi V, Zennaro E, Leoni L: **RsaL provides quorum sensing homeostasis and functions as a global regulator of gene expression in *Pseudomonas aeruginosa***. *Mol Microbiol* 2007, **66**(6):1557-1565.
163. Wright A, Hawkins CH, Anggard EE, Harper DR: **A controlled clinical trial of a therapeutic bacteriophage preparation in chronic otitis due to antibiotic-resistant *Pseudomonas aeruginosa*; a preliminary report of efficacy**. *Clin Otolaryngol* 2009, **34**(4):349-357.
164. Rumbaugh KP, Griswold JA, Iglewski BH, Hamood AN: **Contribution of quorum sensing to the virulence of *Pseudomonas aeruginosa* in burn wound infections**. *Infect Immun* 1999, **67**(11):5854-5862.
165. Moscoso JA, Mikkelsen H, Heeb S, Williams P, Filloux A: **The *Pseudomonas aeruginosa* sensor RetS switches type III and type VI secretion via c-di-GMP signalling**. *Environ Microbiol* 2011, **13**(12):3128-3138.
166. Coggan KA, Wolfgang MC: **Global regulatory pathways and cross-talk control *Pseudomonas aeruginosa* environmental lifestyle and virulence phenotype**. *Curr Issues Mol Biol* 2012, **14**(2):47-70.
167. Sall KM, Casabona MG, Bordi C, Huber P, de Bentzmann S, Attree I, Elsen S: **A *gacS* deletion in *Pseudomonas aeruginosa* cystic fibrosis isolate CHA shapes its virulence**. *PLoS One* 2014, **9**(4):e95936.
168. Miller MB, Bassler BL: **Quorum sensing in bacteria**. *Annu Rev Microbiol* 2001, **55**:165-199.
169. Bassler BL: **Small talk. Cell-to-cell communication in bacteria**. *Cell* 2002, **109**(4):421-424.
170. Williams P, Camara M: **Quorum sensing and environmental adaptation in *Pseudomonas aeruginosa*: a tale of regulatory networks and multifunctional signal molecules**. *Curr Opin Microbiol* 2009, **12**(2):182-191.
171. Rampioni G, Pustelny C, Fletcher MP, Wright VJ, Bruce M, Rumbaugh KP, Heeb S, Camara M, Williams P: **Transcriptomic analysis reveals a global alkyl-quinolone-independent regulatory role for PqsE in facilitating the environmental adaptation**

**of *Pseudomonas aeruginosa* to plant and animal hosts**. *Environ Microbiol* 2010, **12**(6):1659-1673.

172. Seed PC, Passador L, Iglewski BH: **Activation of the *Pseudomonas aeruginosa lasI* gene by LasR and the *Pseudomonas* autoinducer PAI: an autoinduction regulatory hierarchy**. *J Bacteriol* 1995, **177**(3):654-659.
173. Latifi A, Winson MK, Foglino M, Bycroft BW, Stewart GS, Lazdunski A, Williams P: **Multiple homologues of LuxR and LuxI control expression of virulence determinants and secondary metabolites through quorum sensing in *Pseudomonas aeruginosa* PAO1**. *Mol Microbiol* 1995, **17**(2):333-343.
174. Winson MK, Camara M, Latifi A, Foglino M, Chhabra SR, Daykin M, Bally M, Chapon V, Salmond GP, Bycroft BW *et al*: **Multiple *N*-acyl-L-homoserine lactone signal molecules regulate production of virulence determinants and secondary metabolites in *Pseudomonas aeruginosa***. *Proc Natl Acad Sci U S A* 1995, **92**(20):9427-9431.
175. Diggle SP, Winzer K, Chhabra SR, Worrall KE, Camara M, Williams P: **The *Pseudomonas aeruginosa* quinolone signal molecule overcomes the cell density-dependency of the quorum sensing hierarchy, regulates *rhl*-dependent genes at the onset of stationary phase and can be produced in the absence of LasR**. *Mol Microbiol* 2003, **50**(1):29-43.
176. Chugani SA, Whiteley M, Lee KM, D'Argenio D, Manoil C, Greenberg EP: **QscR, a modulator of quorum-sensing signal synthesis and virulence in *Pseudomonas aeruginosa***. *Proc Natl Acad Sci U S A* 2001, **98**(5):2752-2757.
177. Lazdunski AM, Ventre I, Sturgis JN: **Regulatory circuits and communication in Gram-negative bacteria**. *Nat Rev Microbiol* 2004, **2**(7):581-592.
178. Venturi V: **Regulation of quorum sensing in *Pseudomonas***. *FEMS Microbiol Rev* 2006, **30**(2):274-291.
179. Juhas M, Wiehlmann L, Huber B, Jordan D, Lauber J, Salunkhe P, Limpert AS, von Gotz F, Steinmetz I, Eberl L *et al*: **Global regulation of quorum sensing and virulence by VqsR in *Pseudomonas aeruginosa***. *Microbiology* 2004, **150**(Pt 4):831-841.
180. Cornelis P, Aendekerk S: **A new regulator linking quorum sensing and iron uptake in *Pseudomonas aeruginosa***. *Microbiology* 2004, **150**(Pt 4):752-756.
181. Liang H, Deng X, Ji Q, Sun F, Shen T, He C: **The *Pseudomonas* aeruginosa global regulator VqsR directly inhibits QscR to control quorum-sensing and virulence gene expression**. *J Bacteriol* 2012, **194**(12):3098-3108.
182. Ramos J-L, Filloux A: ***Pseudomonas*, vol. 1.** New York: Kluwer Academic / Plenum Publishers; 2004.
183. Burrowes E, Baysse C, Adams C, O'Gara F: **Influence of the regulatory protein RsmA on cellular functions in *Pseudomonas aeruginosa* PAO1, as revealed by transcriptome analysis**. *Microbiology* 2006, **152**(Pt 2):405-418.
184. Albus AM, Pesci EC, Runyen-Janecky LJ, West SE, Iglewski BH: **Vfr controls quorum sensing in *Pseudomonas aeruginosa***. *J Bacteriol* 1997, **179**(12):3928-3935.
185. Rampioni G, Bertani I, Zennaro E, Polticelli F, Venturi V, Leoni L: **The quorum-sensing negative regulator RsaL of *Pseudomonas aeruginosa* binds to the *lasI* promoter**. *J Bacteriol* 2006, **188**(2):815-819.
186. Reimmann C, Beyeler M, Latifi A, Winteler H, Foglino M, Lazdunski A, Haas D: **The global activator GacA of *Pseudomonas aeruginosa* PAO positively controls the production of the autoinducer *N*-butyryl-homoserine lactone and the formation of the virulence factors pyocyanin, cyanide, and lipase**. *Mol Microbiol* 1997, **24**(2):309-319.
187. Whiteley M, Parsek MR, Greenberg EP: **Regulation of quorum sensing by RpoS in *Pseudomonas aeruginosa***. *J Bacteriol* 2000, **182**(15):4356-4360.

188. Diggle SP, Winzer K, Lazdunski A, Williams P, Camara M: **Advancing the quorum in *Pseudomonas aeruginosa*: MvaT and the regulation of *N*-acylhomoserine lactone production and virulence gene expression**. *J Bacteriol* 2002, **184**(10):2576-2586.
189. Wells IC: **Antibiotic substances produced by *Pseudomonas aeruginosa*; syntheses of Pyo Ib, Pyo Ic, and Pyo III**. *J Biol Chem* 1952, **196**(1):331-340.
190. Wade DS, Calfee MW, Rocha ER, Ling EA, Engstrom E, Coleman JP, Pesci EC: **Regulation of *Pseudomonas* quinolone signal synthesis in *Pseudomonas aeruginosa***. *J Bacteriol* 2005, **187**(13):4372-4380.
191. Luckner M, Ritter C: **On the biosynthesis of the 2-*N*-alkyl-4-hydroxyquinolines of *Pseudomonas aeruginosa* (Schroet.) Migula**. *Tetrahedron Lett* 1965, **12**:741-744.
192. Essar DW, Eberly L, Hadero A, Crawford IP: **Identification and characterization of genes for a second anthranilate synthase in *Pseudomonas aeruginosa*: interchangeability of the two anthranilate synthases and evolutionary implications**. *J Bacteriol* 1990, **172**(2):884-900.
193. Schertzer JW, Brown SA, Whiteley M: **Oxygen levels rapidly modulate *Pseudomonas aeruginosa* social behaviours via substrate limitation of PqsH**. *Mol Microbiol* 2010, **77**(6):1527-1538.
194. Gallagher LA, McKnight SL, Kuznetsova MS, Pesci EC, Manoil C: **Functions required for extracellular quinolone signaling by *Pseudomonas aeruginosa***. *J Bacteriol* 2002, **184**(23):6472-6480.
195. McKnight SL, Iglewski BH, Pesci EC: **The *Pseudomonas* quinolone signal regulates *rhl* quorum sensing in *Pseudomonas aeruginosa***. *J Bacteriol* 2000, **182**(10):2702-2708.
196. Reen FJ, Mooij MJ, Holcombe LJ, McSweeney CM, McGlacken GP, Morrissey JP, O'Gara F: **The *Pseudomonas* quinolone signal (PQS), and its precursor HHQ, modulate interspecies and interkingdom behaviour**. *FEMS Microbiol Ecol* 2011, **77**(2):413-428.
197. D'Argenio DA, Calfee MW, Rainey PB, Pesci EC: **Autolysis and autoaggregation in *Pseudomonas aeruginosa* colony morphology mutants**. *J Bacteriol* 2002, **184**(23):6481-6489.
198. Heeb S, Haas D: **Regulatory roles of the GacS/GacA two-component system in plant-associated and other gram-negative bacteria**. *Mol Plant Microbe Interact* 2001, **14**(12):1351-1363.
199. Finck-Barbancon V, Goranson J, Zhu L, Sawa T, Wiener-Kronish JP, Fleiszig SM, Wu C, Mende-Mueller L, Frank DW: **ExoU expression by *Pseudomonas aeruginosa* correlates with acute cytotoxicity and epithelial injury**. *Mol Microbiol* 1997, **25**(3):547-557.
200. Hancock RE, Mutharia LM, Chan L, Darveau RP, Speert DP, Pier GB: ***Pseudomonas aeruginosa* isolates from patients with cystic fibrosis: a class of serum-sensitive, nontypable strains deficient in lipopolysaccharide O side chains**. *Infect Immun* 1983, **42**(1):170-177.
201. Laskowski MA, Osborn E, Kazmierczak BI: **A novel sensor kinase-response regulator hybrid regulates type III secretion and is required for virulence in *Pseudomonas aeruginosa***. *Mol Microbiol* 2004, **54**(4):1090-1103.
202. Goodman AL, Merighi M, Hyodo M, Ventre I, Filloux A, Lory S: **Direct interaction between sensor kinase proteins mediates acute and chronic disease phenotypes in a bacterial pathogen**. *Genes Dev* 2009, **23**(2):249-259.
203. Ventre I, Goodman AL, Vallet-Gely I, Vasseur P, Soscia C, Molin S, Bleves S, Lazdunski A, Lory S, Filloux A: **Multiple sensors control reciprocal expression of *Pseudomonas aeruginosa* regulatory RNA and virulence genes**. *Proc Natl Acad Sci U S A* 2006, **103**(1):171-176.
204. Pessi G, Williams F, Hindle Z, Heurlier K, Holden MT, Camara M, Haas D, Williams P: **The global posttranscriptional regulator RsmA modulates production of virulence**

**determinants and *N*-acylhomoserine lactones in *Pseudomonas aeruginosa***. *J Bacteriol* 2001, **183**(22):6676-6683.
205. Mulcahy H, O'Callaghan J, O'Grady EP, Adams C, O'Gara F: **The posttranscriptional regulator RsmA plays a role in the interaction between *Pseudomonas aeruginosa* and human airway epithelial cells by positively regulating the type III secretion system**. *Infect Immun* 2006, **74**(5):3012-3015.
206. Marden JN, Diaz MR, Walton WG, Gode CJ, Betts L, Urbanowski ML, Redinbo MR, Yahr TL, Wolfgang MC: **An unusual CsrA family member operates in series with RsmA to amplify posttranscriptional responses in *Pseudomonas aeruginosa***. *Proc Natl Acad Sci U S A* 2013, **110**(37):15055-15060.
207. Irie Y, Starkey M, Edwards AN, Wozniak DJ, Romeo T, Parsek MR: ***Pseudomonas aeruginosa* biofilm matrix polysaccharide Psl is regulated transcriptionally by RpoS and post-transcriptionally by RsmA**. *Mol Microbiol* 2010, **78**(1):158-172.
208. Martinez LC, Vadyvaloo V: **Mechanisms of post-transcriptional gene regulation in bacterial biofilms**. *Front Cell Infect Microbiol* 2014, **4**:38.
209. Liu Y: **Understanding chronic inflammatory diseases in the human lung: the cystic fibrosis and idiopathic pulmonary fibrosis paradigms**. PhD thesis. Nottingham: University of Nottingham; 2014.
210. Messina M: **Gene regulation in *Pseudomonas aeruginosa*: from environmental signals to responses via global post-transcriptional control and intracellular messaging**. PhD thesis. Nottingham: University of Nottingham; 2010.
211. Morris ER, Hall G, Li C, Heeb S, Kulkarni RV, Lovelock L, Silistre H, Messina M, Camara M, Emsley J *et al*: **Structural rearrangement in an RsmA/CsrA ortholog of *Pseudomonas aeruginosa* creates a dimeric RNA-binding protein, RsmN**. *Structure* 2013, **21**(9):1659-1671.
212. Lovelock L: **RsmN - a new atypical RsmA homologue in *Pseudomonas aeruginosa***. PhD thesis. Nottingham: University of Nottingham; 2012.
213. Rashid M, Kornberg A: **Inorganic polyphosphate is needed for swimming, swarming, and twitching motilities of *Pseudomonas aeruginosa***. *Proceedings of the National Academy of Sciences of the United States of America* 2000, **97**(9):4885-4890.
214. Hall BG, Acar H, Nandipati A, Barlow M: **Growth rates made easy**. *Mol Biol Evol* 2014, **31**(1):232-238.
215. Gudapaty S, Suzuki K, Wang X, Babitzke P, Romeo T: **Regulatory interactions of Csr components: the RNA binding protein CsrA activates *csrB* transcription in *Escherichia coli***. *J Bacteriol* 2001, **183**(20):6017-6027.
216. Dietrich LE, Okegbe C, Price-Whelan A, Sakhtah H, Hunter RC, Newman DK: **Bacterial community morphogenesis is intimately linked to the intracellular redox state**. *J Bacteriol* 2013, **195**(7):1371-1380.
217. Benoit MR, Conant CG, Ionescu-Zanetti C, Schwartz M, Matin A: **New device for high-throughput viability screening of flow biofilms**. *Appl Environ Microbiol* 2010, **76**(13):4136-4142.
218. Sambrook J, Fritsch EF, Maniatis T: **Molecular cloning : a laboratory manual**, 2nd ed. Cold Spring Harbor, N.Y.: Cold Spring Harbor Laboratory; 1989.
219. Kuehne SA: **RsmA - a global post-transcriptional regulator in *Pseudomonas aeruginosa***. PhD thesis. Nottingham: University of Nottingham; 2008.
220. Maurhofer M, Reimmann C, Schmidli-Sacherer P, Heeb S, Haas D, Defago G: **Salicylic Acid Biosynthetic Genes Expressed in *Pseudomonas fluorescens* Strain P3 Improve the Induction of Systemic Resistance in Tobacco Against Tobacco Necrosis Virus**. *Phytopathology* 1998, **88**(7):678-684.
221. Chhabra SR, Harty C, Hooi DS, Daykin M, Williams P, Telford G, Pritchard DI, Bycroft BW: **Synthetic analogues of the bacterial signal (quorum sensing) molecule *N*-(3-**

**oxododecanoyl)-L-homoserine lactone as immune modulators**. *J Med Chem* 2003, **46**(1):97-104.
222. Westfall LW, Luna AM, San Francisco M, Diggle SP, Worrall KE, Williams P, Camara M, Hamood AN: **The *Pseudomonas aeruginosa* global regulator MvaT specifically binds to the *ptxS* upstream region and enhances *ptxS* expression**. *Microbiology* 2004, **150**(Pt 11):3797-3806.
223. Xu XZ, Liu QP, Fan LJ, Cui XF, Zhou XP: **Analysis of synonymous codon usage and evolution of begomoviruses**. *J Zhejiang Univ Sci B* 2008, **9**(9):667-674.
224. Kiewitz CW, Christian; Tümmler, Burkhard: **Genome Codon Index of *Pseudomonas aeruginosa*: A Codon Index That Utilizes Whole Genome Sequence Data**. In: *Genome Letters.* vol. 1; 2002: 61-70.
225. Saiki RK, Scharf S, Faloona F, Mullis KB, Horn GT, Erlich HA, Arnheim N: **Enzymatic amplification of beta-globin genomic sequences and restriction site analysis for diagnosis of sickle cell anemia**. *Science* 1985, **230**(4732):1350-1354.
226. Corpet F: **Multiple sequence alignment with hierarchical clustering**. *Nucleic Acids Res* 1988, **16**(22):10881-10890.
227. Lazenby JJ, Griffin PE, Kyd J, Whitchurch CB, Cooley MA: **A quadruple knockout of *lasIR* and *rhlIR* of *Pseudomonas aeruginosa* PAO1 that retains wild-type twitching motility has equivalent infectivity and persistence to PAO1 in a mouse model of lung infection**. *PLoS One* 2013, **8**(4):e60973.
228. Tremblay J, Deziel E: **Improving the reproducibility of *Pseudomonas aeruginosa* swarming motility assays**. *J Basic Microb* 2008, **48**(6):509-515.
229. Brock FM, Forsberg CW, Buchanan-Smith JG: **Proteolytic activity of rumen microorganisms and effects of proteinase inhibitors**. *Appl Environ Microbiol* 1982, **44**(3):561-569.
230. Rust L, Messing CR, Iglewski BH: **Elastase assays**. *Methods Enzymol* 1994, **235**:554-562.
231. Caballero AR, Moreau JM, Engel LS, Marquart ME, Hill JM, O'Callaghan RJ: ***Pseudomonas aeruginosa* protease IV enzyme assays and comparison to other *Pseudomonas* proteases**. *Anal Biochem* 2001, **290**(2):330-337.
232. Luckett JC, Darch O, Watters C, Abuoun M, Wright V, Paredes-Osses E, Ward J, Goto H, Heeb S, Pommier S *et al*: **A novel virulence strategy for *Pseudomonas aeruginosa* mediated by an autotransporter with arginine-specific aminopeptidase activity**. *PLoS Pathog* 2012, **8**(8):e1002854.
233. Carver T, Berriman M, Tivey A, Patel C, Bohme U, Barrell BG, Parkhill J, Rajandream MA: **Artemis and ACT: viewing, annotating and comparing sequences stored in a relational database**. *Bioinformatics* 2008, **24**(23):2672-2676.
234. Watters C, DeLeon K, Trivedi U, Griswold JA, Lyte M, Hampel KJ, Wargo MJ, Rumbaugh KP: ***Pseudomonas aeruginosa* biofilms perturb wound resolution and antibiotic tolerance in diabetic mice**. *Med Microbiol Immunol* 2013, **202**(2):131-141.
235. Rutherford ST, Bassler BL: **Bacterial quorum sensing: its role in virulence and possibilities for its control**. *Cold Spring Harb Perspect Med* 2012, **2**(11).
236. Brencic A, Lory S: **Determination of the regulon and identification of novel mRNA targets of *Pseudomonas aeruginosa* RsmA**. *Mol Microbiol* 2009, **72**(3):612-632.
237. Sonnleitner E, Sorger-Domenigg T, Madej MJ, Findeiss S, Hackermuller J, Huttenhofer A, Stadler PF, Blasi U, Moll I: **Detection of small RNAs in *Pseudomonas aeruginosa* by RNomics and structure-based bioinformatic tools**. *Microbiology* 2008, **154**(Pt 10):3175-3187.
238. Winsor GL, Lam DK, Fleming L, Lo R, Whiteside MD, Yu NY, Hancock RE, Brinkman FS: ***Pseudomonas* Genome Database: improved comparative analysis and population genomics capability for *Pseudomonas* genomes**. *Nucleic Acids Res* 2011, **39**(Database issue):D596-600.

239. Vallet-Gely I, Opota O, Boniface A, Novikov A, Lemaitre B: **A secondary metabolite acting as a signalling molecule controls *Pseudomonas entomophila* virulence**. *Cell Microbiol* 2010, **12**(11):1666-1679.
240. Kay E, Dubuis C, Haas D: **Three small RNAs jointly ensure secondary metabolism and biocontrol in *Pseudomonas fluorescens* CHA0**. *Proc Natl Acad Sci U S A* 2005, **102**(47):17136-17141.
241. Morris ER: **Structural and RNA-binding studies of post-transcriptional regulators RsmA and RsmN from *Pseudomonas aeruginosa* strain PAO1**. PhD thesis. Nottingham: University of Nottingham; 2012.
242. Lefebre MD, Valvano MA: **Construction and evaluation of plasmid vectors optimized for constitutive and regulated gene expression in *Burkholderia cepacia* complex isolates**. *Appl Environ Microbiol* 2002, **68**(12):5956-5964.
243. Kingsford CL, Ayanbule K, Salzberg SL: **Rapid, accurate, computational discovery of Rho-independent transcription terminators illuminates their relationship to DNA uptake**. *Genome Biol* 2007, **8**(2):R22.
244. Wang CLJDYT, F.; Zhang, L.: **ARF-TSS: an alternative method for identification of transcription start site in bacteria**. In: *Biotechniques.* 2012: 1-3.
245. Schaefer BC: **Revolutions in rapid amplification of cDNA ends: new strategies for polymerase chain reaction cloning of full-length cDNA ends**. *Anal Biochem* 1995, **227**(2):255-273.
246. Nielsen H: **RNA : methods and protocols**. Totowa, New Jersey: Humana Press; 2011.
247. Higgins S: **Regulation of phenazine biosynthesis by quorum sensing in *Pseudomonas aeruginosa*: a systems biology approach**. PhD thesis. Nottingham: University of Nottingham; 2014.
248. Patrick JE, Kearns DB: **Laboratory strains of *Bacillus subtilis* do not exhibit swarming motility**. *J Bacteriol* 2009, **191**(22):7129-7133.
249. Jones HE, Park RW: **The influence of medium composition on the growth and swarming of *Proteus***. *J Gen Microbiol* 1967, **47**(3):369-378.
250. Plotkin JB, Kudla G: **Synonymous but not the same: the causes and consequences of codon bias**. *Nat Rev Genet* 2011, **12**(1):32-42.
251. Goodman DB, Church GM, Kosuri S: **Causes and effects of N-terminal codon bias in bacterial genes**. *Science* 2013, **342**(6157):475-479.
252. Vallet I, Olson JW, Lory S, Lazdunski A, Filloux A: **The chaperone/usher pathways of *Pseudomonas aeruginosa*: identification of fimbrial gene clusters (*cup*) and their involvement in biofilm formation**. *Proc Natl Acad Sci U S A* 2001, **98**(12):6911-6916.
253. Hockett KL, Burch AY, Lindow SE: **Thermo-regulation of genes mediating motility and plant interactions in *Pseudomonas syringae***. *PLoS One* 2013, **8**(3):e59850.
254. Gugi B, Orange N, Hellio F, Burini JF, Guillou C, Leriche F, Guespin-Michel JF: **Effect of growth temperature on several exported enzyme activities in the psychrotrophic bacterium *Pseudomonas fluorescens***. *J Bacteriol* 1991, **173**(12):3814-3820.
255. Termine E, Michel GP: **Transcriptome and secretome analyses of the adaptive response of *Pseudomonas aeruginosa* to suboptimal growth temperature**. *Int Microbiol* 2009, **12**(1):7-12.
256. Kropinski AM, Lewis V, Berry D: **Effect of growth temperature on the lipids, outer membrane proteins, and lipopolysaccharides of *Pseudomonas aeruginosa* PAO**. *J Bacteriol* 1987, **169**(5):1960-1966.
257. Wurtzel O, Yoder-Himes DR, Han K, Dandekar AA, Edelheit S, Greenberg EP, Sorek R, Lory S: **The single-nucleotide resolution transcriptome of *Pseudomonas aeruginosa* grown in body temperature**. *PLoS Pathog* 2012, **8**(9):e1002945.
258. Colvin KM, Gordon VD, Murakami K, Borlee BR, Wozniak DJ, Wong GC, Parsek MR: **The Pel polysaccharide can serve a structural and protective role in the biofilm matrix of *Pseudomonas aeruginosa***. *PLoS Pathog* 2011, **7**(1):e1001264.

259. Das T, Manefield M: **Pyocyanin promotes extracellular DNA release in *Pseudomonas aeruginosa***. *PLoS One* 2012, **7**(10):e46718.
260. Allesen-Holm M, Barken KB, Yang L, Klausen M, Webb JS, Kjelleberg S, Molin S, Givskov M, Tolker-Nielsen T: **A characterization of DNA release in *Pseudomonas aeruginosa* cultures and biofilms**. *Mol Microbiol* 2006, **59**(4):1114-1128.
261. Mulcahy H, O'Callaghan J, O'Grady EP, Macia MD, Borrell N, Gomez C, Casey PG, Hill C, Adams C, Gahan CG *et al*: ***Pseudomonas aeruginosa* RsmA plays an important role during murine infection by influencing colonization, virulence, persistence, and pulmonary inflammation**. *Infect Immun* 2008, **76**(2):632-638.
262. Turner KH, Everett J, Trivedi U, Rumbaugh KP, Whiteley M: **Requirements for *Pseudomonas aeruginosa* acute burn and chronic surgical wound infection**. *PLoS Genet* 2014, **10**(7):e1004518.
263. Edwards AN, Patterson-Fortin LM, Vakulskas CA, Mercante JW, Potrykus K, Vinella D, Camacho MI, Fields JA, Thompson SA, Georgellis D *et al*: **Circuitry linking the Csr and stringent response global regulatory systems**. *Mol Microbiol* 2011, **80**(6):1561-1580.
264. Croucher NJ, Thomson NR: **Studying bacterial transcriptomes using RNAseq**. *Curr Opin Microbiol* 2010, **13**(5):619-624.
265. Klockgether J, Munder A, Neugebauer J, Davenport CF, Stanke F, Larbig KD, Heeb S, Schock U, Pohl TM, Wiehlmann L *et al*: **Genome diversity of *Pseudomonas aeruginosa* PAO1 laboratory strains**. *J Bacteriol* 2010, **192**(4):1113-1121.
266. Argaman L, Hershberg R, Vogel J, Bejerano G, Wagner EG, Margalit H, Altuvia S: **Novel small RNA-encoding genes in the intergenic regions of *Escherichia coli***. *Curr Biol* 2001, **11**(12):941-950.
267. Lenz DH, Miller MB, Zhu J, Kulkarni RV, Bassler BL: **CsrA and three redundant small RNAs regulate quorum sensing in *Vibrio cholerae***. *Mol Microbiol* 2005, **58**(4):1186-1202.
268. Damron FH, Napper J, Teter MA, Yu HD: **Lipotoxin F of *Pseudomonas aeruginosa* is an AlgU-dependent and alginate-independent outer membrane protein involved in resistance to oxidative stress and adhesion to A549 human lung epithelia**. *Microbiology* 2009, **155**(Pt 4):1028-1038.
269. Kim SK, Im SJ, Yeom DH, Lee JH: **AntR-mediated bidirectional activation of *antA* and *antR*, anthranilate degradative genes in *Pseudomonas aeruginosa***. *Gene* 2012, **505**(1):146-152.
270. Quinlan AR: **BEDTools: The Swiss-Army Tool for Genome Feature Analysis**. *Curr Protoc Bioinformatics* 2014, **47**:11 12 11-11 12 34.
271. Barbieri JT, Sun J: ***Pseudomonas aeruginosa* ExoS and ExoT**. *Rev Physiol Biochem Pharmacol* 2004, **152**:79-92.
272. Sharma CM, Storz G: **Interesting twists on small RNA themes in *Pseudomonas aeruginosa***. *Mol Microbiol* 2011, **80**(4):855-859.
273. Gonzalez N, Heeb S, Valverde C, Kay E, Reimmann C, Junier T, Haas D: **Genome-wide search reveals a novel GacA-regulated small RNA in *Pseudomonas* species**. *BMC Genomics* 2008, **9**:167.
274. Humair B, Wackwitz B, Haas D: **GacA-controlled activation of promoters for small RNA genes in *Pseudomonas fluorescens***. *Appl Environ Microbiol* 2010, **76**(5):1497-1506.
275. Deziel E, Gopalan S, Tampakaki AP, Lepine F, Padfield KE, Saucier M, Xiao G, Rahme LG: **The contribution of MvfR to *Pseudomonas aeruginosa* pathogenesis and quorum sensing circuitry regulation: multiple quorum sensing-regulated genes are modulated without affecting *lasRI*, *rhlRI* or the production of *N*-acyl-L-homoserine lactones**. *Mol Microbiol* 2005, **55**(4):998-1014.
276. Hendrick JP, Hartl FU: **Molecular chaperone functions of heat-shock proteins**. *Annu Rev Biochem* 1993, **62**:349-384.

277. Trias J, Nikaido H: **Outer membrane protein D2 catalyzes facilitated diffusion of carbapenems and penems through the outer membrane of *Pseudomonas aeruginosa***. *Antimicrob Agents Chemother* 1990, **34**(1):52-57.
278. Trias J, Nikaido H: **Protein D2 channel of the *Pseudomonas aeruginosa* outer membrane has a binding site for basic amino acids and peptides**. *J Biol Chem* 1990, **265**(26):15680-15684.
279. Toder DS, Ferrell SJ, Nezezon JL, Rust L, Iglewski BH: ***lasA* and *lasB* genes of *Pseudomonas aeruginosa*: analysis of transcription and gene product activity**. *Infect Immun* 1994, **62**(4):1320-1327.
280. Vallet I, Diggle SP, Stacey RE, Camara M, Ventre I, Lory S, Lazdunski A, Williams P, Filloux A: **Biofilm formation in *Pseudomonas aeruginosa*: fimbrial *cup* gene clusters are controlled by the transcriptional regulator MvaT**. *J Bacteriol* 2004, **186**(9):2880-2890.
281. McManus HR, Dove SL: **The CgrA and CgrC proteins form a complex that positively regulates *cupA* fimbrial gene expression in *Pseudomonas aeruginosa***. *J Bacteriol* 2011, **193**(22):6152-6161.
282. Hogardt M, Heesemann J: **Microevolution of *Pseudomonas aeruginosa* to a chronic pathogen of the cystic fibrosis lung**. *Curr Top Microbiol Immunol* 2013, **358**:91-118.
283. Arai H, Mizutani M, Igarashi Y: **Transcriptional regulation of the *nos* genes for nitrous oxide reductase in *Pseudomonas aeruginosa***. *Microbiology* 2003, **149**(Pt 1):29-36.
284. Yoon SS, Hennigan RF, Hilliard GM, Ochsner UA, Parvatiyar K, Kamani MC, Allen HL, DeKievit TR, Gardner PR, Schwab U *et al*: ***Pseudomonas aeruginosa* anaerobic respiration in biofilms: relationships to cystic fibrosis pathogenesis**. *Dev Cell* 2002, **3**(4):593-603.
285. Xie H, Buschmann S, Langer JD, Ludwig B, Michel H: **Biochemical and biophysical characterization of the two isoforms of *cbb*$_3$-type cytochrome *c* oxidase from *Pseudomonas stutzeri***. *J Bacteriol* 2014, **196**(2):472-482.
286. Martin DW, Schurr MJ, Mudd MH, Deretic V: **Differentiation of *Pseudomonas aeruginosa* into the alginate-producing form: inactivation of *mucB* causes conversion to mucoidy**. *Mol Microbiol* 1993, **9**(3):497-506.
287. Hauser AR: **The type III secretion system of *Pseudomonas aeruginosa*: infection by injection**. *Nat Rev Microbiol* 2009, **7**(9):654-665.
288. Zinser ER, Kolter R: **Mutations enhancing amino acid catabolism confer a growth advantage in stationary phase**. *J Bacteriol* 1999, **181**(18):5800-5807.
289. Weibezahn J, Tessarz P, Schlieker C, Zahn R, Maglica Z, Lee S, Zentgraf H, Weber-Ban EU, Dougan DA, Tsai FT *et al*: **Thermotolerance requires refolding of aggregated proteins by substrate translocation through the central pore of ClpB**. *Cell* 2004, **119**(5):653-665.
290. Krajewski SS, Nagel M, Narberhaus F: **Short ROSE-like RNA thermometers control IbpA synthesis in *Pseudomonas* species**. *PLoS One* 2013, **8**(5):e65168.
291. Freyer MW, Lewis EA: **Isothermal titration calorimetry: experimental design, data analysis, and probing macromolecule/ligand binding and kinetic interactions**. *Methods Cell Biol* 2008, **84**:79-113.
292. Rosenbau.G, Holmes KC, Witz J: **SYNCHROTRON RADIATION AS A SOURCE FOR X-RAY DIFFRACTION**. *Nature* 1971, **230**(5294):434-&.
293. Gupta R, Schuster M: **Quorum sensing modulates colony morphology through alkyl quinolones in *Pseudomonas aeruginosa***. *BMC Microbiol* 2012, **12**:30.
294. Basler M: **Type VI secretion system: secretion by a contractile nanomachine**. *Philos Trans R Soc Lond B Biol Sci* 2015, **370**(1679).